The Getty Conservation Institute

Conservation and Seismic Strengthening of Byzantine Churches in Macedonia

Predrag Gavrilović
William S. Ginell
Veronika Sendova
Lazar Šumanov

GCI Scientific Program Reports

Conservation and Seismic Strengthening of Byzantine Churches in Macedonia

This page intentionally left blank

GCI Scientific Program Reports

Conservation and Seismic Strengthening of Byzantine Churches in Macedonia

Predrag Gavrilović

William S. Ginell

Veronika Sendova

Lazar Šumanov

The Getty Conservation Institute Los Angeles

Getty Conservation Institute
Scientific Reports series

Timothy P. Whalen, *Director, Getty Conservation Institute*
Jeanne Marie Teutonico, *Associate Director, Field Projects and Conservation Science, Getty Conservation Institute*

Getty Publications
1200 Getty Center Drive, Suite 500
Los Angeles, California 90049-1682
www.getty.edu

Chris Hudson, *Publisher*
Mark Greenberg, *Editor in Chief*

Dinah Berland, *Editor*
Leslie Tilley, *Manuscript Editor*
Pamela Heath, *Production Coordinator*
Garland Kirkpatrick, *Cover Designer*
Hespenheide Design, *Designer*

Printed in Canada

The Getty Conservation Institute works internationally to advance conservation and to enhance and encourage the preservation and understanding of the visual arts in all of their dimensions—objects, collections, architecture, and sites. The Institute serves the conservation community through scientific research, education and training, field projects, and the dissemination of the results of both its work and the work of others in the field. In all its endeavors, the Institute is committed to addressing unanswered questions and promoting the highest possible standards of conservation practice.

The Getty Conservation Institute is a program of the J. Paul Getty Trust, an international cultural and philanthropic organization devoted to the visual arts and the humanities that includes an art museum as well as programs for education, scholarship, and conservation.

The GCI Scientific Program Reports series presents current research being conducted under the auspices of the Getty Conservation Institute. Related books in this series include *Planning and Engineering Guidelines for the Seismic Retrofitting of Historic Adobe Structures* (2002), *Seismic Stabilization of Historic Adobe Structures: Final Report of the Getty Seismic Adobe Project* (2000), and *Survey of Damage to Historic Adobe Buildings after the January 1994 Northridge Earthquake* (1996).

All photographs are by the authors unless otherwise indicated.

Library of Congress Cataloging-in-Publication Data
Conservation and seismic strengthening of Byzantine churches in Macedonia / Predrag Gavrilović ... [et al.].
p. cm. — (GCI scientific program reports)
ISBN 0-89236-777-6 (pbk.)
Includes bibliographical references and index.
1. Earthquake resistant design—Macedonia. 2. Church buildings—Earthquake effects—Macedonia. 3. Historic sites—Earthquake effects—Macedonia.
I. Gavrilović, Predrag. II. Series.
TA658.44.C69 2004
690'.65'094956—dc22

2004009818

Contents

	vii	**Foreword**
	ix	**Acknowledgments**
	xi	**Introduction**
Chapter 1	1	**General Considerations Regarding the Conservation of Historic Buildings in Seismic Zones**
	1	Criteria and Objectives
	2	Retrofitting Approaches
Chapter 2	5	**Overview of Byzantine Churches**
	5	Architecture
	6	Frescoes
	7	Types of Byzantine Churches
	12	Structural Characteristics
	15	Surface Characteristics
Chapter 3	19	**Survey of Existing Byzantine Churches in Macedonia**
	19	Present State of Selected Church Buildings—Causes and Level of Damage
	22	Authenticity
	22	Churches Selected for Detailed Investigation
	26	The Church of St. Nikita, Banjani
Chapter 4	37	**Proposed Strengthening Method and Preliminary Analysis of the Retrofitted St. Nikita Church**
	37	Possible Methods for Repair and Strengthening of Historic Structures
	39	Design of the St. Nikita Church Model
	45	Model Construction
	50	Wall Element Tests
Chapter 5	53	**Shaking-Table Tests of the St. Nikita Church Model**
	54	Tests of the Original Church Model
	62	Repair and Strengthening of the Damaged Model
	65	Tests of the Repaired and Strengthened Church Model

Chapter 6	71	**Analytical Modeling of the Dynamic Behavior of Masonry Structures Exposed to Earthquake Motions**
	71	Dynamic Analysis of the Nonlinear Response of an Idealized Single-Degree-of-Freedom System
	72	Dynamic Equations of Motions
	73	Models of Hysteretic Behavior
Chapter 7	79	**Analytical Studies and Correlation of the Behavior of the Two Models**
	80	Original Model
	87	Strengthened Model
	99	The Bearing and Deformability Capacities of the Model Structures at the Design and Maximum Levels of Expected Ground Motion
	100	Capacity Analysis of Masonry Buildings
Chapter 8	103	**Mathematical Model of the Byzantine Church Structure**
	103	Analysis of Structural Walls
	106	Calculation Procedure
	107	Results from the MASAN Program for the Original St. Nikita Model
	108	Results for the Strengthened Church Model
	109	Bearing Capacity of the Church Model Structure
Chapter 9	111	**Capacity Analysis of Existing Byzantine Church Structures**
	111	Analysis of St. Nikita, Banjani
	112	Analysis of St. Bogorodica Zahumska, Trpejca
	114	Analysis of St. Nikola, Psača
	116	Analysis of St. Bogorodica, Matejče
	120	Analysis of St. Gjorgji, Kurbinovo
Chapter 10	123	**Implementation of Methods for Repair and Strengthening of Byzantine Church Structures**
	124	Possible Methods and Techniques for Repair and Strengthening of Historic Byzantine Churches
	126	Repair and Strengthening of Historic Monuments in Accordance with the Experimentally Verified Methodology
	128	Strengthening of the Structures of Three Representative Churches
Chapter 11	139	**Summary, Conclusions, and Recommendations**
Appendix A	141	**List of Churches Surveyed**
Appendix B	143	**Single-Degree-of-Freedom Analysis Flowchart**
Appendix C	145	**Experimental and Analytical Displacement and Acceleration Time History**
Appendix D	153	**Results of Dynamic-Response Analysis of the Existing St. Nikita Church Using the IZIIS Hysteretic Model**
	155	**References**
	157	**Additional Reading**
	159	**Glossary**
	161	**Index**
	173	**About the Authors**

Foreword

The conservation of historic and culturally significant buildings involves not only preserving features that define the character of a structure and repairing existing damage but also implementing measures to prevent and minimize future damage or deterioration. Only recently has serious consideration been given to retrofitting as a means of minimizing the potential catastrophic destruction and loss of life from earthquakes. Incorporating seismic design features in new construction is now accepted worldwide; however, applying these methods to the stabilization of existing structures, especially historic buildings, remains a challenge. Variations in design, building materials, and the extent of deterioration make it extremely difficult to generalize retrofitting technologies. Such generalization is possible, however, for structures that share similar building materials and designs. One example is the historic adobe, or earthen, structures located in the American Southwest and other regions of the world. Retrofitting methods for this class of buildings were developed and tested successfully at the Getty Conservation Institute (GCI) as part of its Getty Seismic Adobe Project.

Some years ago, seismic structural engineers in Yugoslavia, an area subject to frequent and violent earthquakes, identified another class of historic structures for which generalized retrofitting techniques could be applied. These were the churches constructed during the late Byzantine period (ninth through fourteenth century) that had survived in various states of preservation. The Institute for Earthquake Engineering and Engineering Seismology (IZIIS) in Skopje, Macedonia, proposed the development of a retrofitting methodology that could provide seismic stabilization for these culturally important buildings. Under the joint sponsorship of the GCI and IZIIS, a project was initiated to test the methodology. This book is the product of that project and the work carried out between 1991 and 1996.

Conservation and Seismic Strengthening of Byzantine Churches in Macedonia describes the present condition of a number of churches in the Republic of Macedonia, the theoretical basis for the experimental work that was performed to validate the proposed methodology, the results of the study, and the design of possible applications to existing churches. The work, carried out in Skopje, involved the construction of a scaled-down model of a specific church and progressive tests of the model on a computer-controlled shaking table. The results led

to structural modifications designed to provide maximum stabilization with minimal intrusion, as well as to limit changes to the building's appearance and authenticity, all of which are goals of modern conservation practice.

The GCI, through its Science Program, is pleased to have been associated with this project and to have participated with our partner, IZIIS, in demonstrating the efficacy of a method to preserve the dwindling number of historic and culturally significant Byzantine structures. It is our hope that the results of this research will not only help preserve the cultural legacy of Macedonia but also serve the conservation community by providing specialists with a methodology for strengthening similar structures worldwide.

This project and this book would not have been possible without the dedication of William S. Ginell, recently retired senior scientist at the GCI. Bill's knowledge and years of experience have been invaluable to the GCI during its many years of work in conservation. I would also like to thank our partners and colleagues in Macedonia, especially Predrag Gavrilović (principal investigator) and Veronika Sendova at IZIIS, and Lazar Šumanov (now at Macedonia ICOMOS) and his colleagues at the Republic Institute for the Protection of Cultural Monuments (RZZSK). We are grateful for their commitment, expertise, and valuable contributions to this research and publication.

The GCI works to benefit and serve the conservation profession. It is my hope that this book will advance the growing field of seismic retrofitting studies and become a valuable tool for conservation specialists charged with protecting the cultural heritage in earthquake-prone regions around the world.

Timothy P. Whalen
Director, The Getty Conservation Institute

Acknowledgments

This book is a summary of the work of many individuals who contributed their specialized skills and experience to advancing the knowledge of how to protect historic and culturally important structures from earthquake damage. The efforts encompassed project planning and management, field investigations, model construction and testing, instrumentation design and operation, data acquisition and evaluation, computer analysis, laboratory analysis, photographic documentation, report writing, translation, editing, and the many other technical operations required for the successful completion of this complex project. The authors would like to express our profound appreciation to all our colleagues who worked as a team to develop and evaluate the seismic stabilization concepts that formed the basis for the study recorded in this volume. This research would not have been successful without their diligent and professional efforts.

Participants in the studies are listed here, both members of the project and their associates at the Republic Institute for the Protection of Cultural Monuments (RZZSK), the Institute of Earthquake Engineering and Engineering Seismology (IZIIS) of the University "SS. Cyril and Methodius," ADING Ltd., and the Getty Conservation Institute (GCI).

Principal Investigators
Predrag Gavrilović
William S. Ginell
Lazar Šumanov

Investigators
Dusko Aleksovski
Donka Bardzieva
Dime Danailovski
Lidija Krstevska
Zoran Milutinović
Jasminka Nikolić
Dr. Veronika Sendova
Tepi Staniševa
Miroslav Stojković
Ljubomir Taskov
Vasilka Trajkovska
Panče Velkov
Živoin Vinčić

Collaborators
Gorgi Dapčev
Mirakovski Gavril
Jane Jančevski
Gjurgjica Lekovska
Dimće Mamućevski
Blagojce Sojanovski

Other technical collaborators
Angele Gligorov
Vlado Kiprijanovski
Milenko Milojević

Translators from the Macedonian
Vesna Kitanovska
Fanija Stosić

GCI editorial and bibliographic assistance
Cynthia Godlewski
Valerie Greathouse
Gary Mattison
Ford Monel
Monique Stover

Getty Publications staff and consultants
Dinah Berland
Pamela Heath
Hespenheide Design
Karen Stough
Leslie Tilley

We are also grateful to the director of IZIIS, Professor Dr. Dimitar Jurukovski, and to the director of RZZSK, Jovan Ristov, for their support of this study at their respective institutions.

This research project would not have been undertaken were it not for the determination, foresight, and financial support of Luis Monreal, director of the Getty Conservation Institute, who in 1985 recognized the need for the GCI to become involved in the area of disaster planning and, specifically, in efforts to protect historic buildings from earthquake damage. He encouraged one of the authors (Dr. Ginell) to attend an ICCROM/IZIIS seminar on seismic engineering in Skopje, Yugoslavia (now the Republic of Macedonia). This project was a direct result of that seminar, Mr. Monreal's intuitive recognition of the need for research, and the GCI's participation in this important architectural conservation area.

And last, but certainly not least, the authors will always be indebted to Sir Bernard Feilden, whose wise counsel was instrumental in the development of our understanding of the need for consideration of the aesthetic aspects of architectural conservation, in addition to the purely technical stabilization requirements, both of which he has championed for many years.

Predrag Gavrilović
William S. Ginell
Veronika Sendova
Lazar Šumanov

Introduction

This publication summarizes the results of a study to evaluate structural seismic retrofitting concepts that are applicable to the Byzantine churches still in existence in the Republic of Macedonia. The design of repair or strengthening procedures for structures located in seismically active regions depends largely on the earthquake conditions to which they have been exposed in the past, on the expected future ground motions, and on the materials and methods used in church construction. Therefore, it is important that planning for the seismic retrofitting of each of these historic structures include estimates of the expected seismic hazard, the local soil conditions, the dynamic properties of the building's structural systems, the strength and deformability of the structural elements and their materials, and the dynamic response of the structure during earthquake loading.

Most historic buildings in Macedonia are constructed of brittle materials. Their structural elements are heavy, have large cross sections, and are exceptionally rigid, which limits the possibilities for ductility improvement. Therefore, quantitative analytical estimations of the earthquake response of these buildings is limited to the elastic range of structural behavior. This requires that estimates of earthquake ground motions be based not only on amplitudes but also on the frequency content of both local and distant seismic sources and how these two factors are modified by local soil conditions. Other important factors that affect the determination of seismic response are the dynamic properties of the structural system (resonant frequencies, mode shapes, and damping capacity), the strength and deformability of the materials and major structural elements, and the nature of the interaction between local soil and the highly rigid structure. All of these factors determine the earthquake response of historic structures such as the churches in Macedonia.

Seismic analysis of these structures cannot be performed using the seismic design codes developed for modern buildings, which are based on the assumption that the building will behave elastically. Methods and techniques considered for retrofitting to restore and preserve these buildings should be based on improving ductility. This requires detailed studies of the structural system and condition of the building and of all engineering factors that affect the cost-effectiveness of the various possible solutions to the seismic protection problem.

To maintain the authenticity of Macedonian churches, the process of repairing and strengthening the structure must not alter the basic structural system. Methods should be developed that are technically consistent with seismic safety, provide adequate bearing and deformation capacity to prevent serious earthquake damage to the structure, minimize damage to frescoes and other culturally significant architectural aspects of the historic churches, and are economically justified.

An effort to evaluate seismic retrofitting technologies for structures of this type was initiated in 1991 with a research project: Study of the Seismic Strengthening, Conservation, and Restoration of Churches Dating from the Byzantine Period (Ninth to Fourteenth Century) in Macedonia. The principal objective of this project was to design, develop, and test appropriate methods and techniques for the repair of existing earthquake damage and for strengthening the principal structural elements of the buildings. These methods must meet the requirements of minimal invasiveness and significant enhancement of the churches' ability to avoid major structural damage from future earthquakes. Additional objectives were to develop analytical methodologies for evaluation of the potential damage to buildings exposed to regional earthquakes and to evaluate the effectiveness of the retrofitting in stabilizing these structures.

The work was performed by staff of the Institute of Earthquake Engineering and Engineering Seismology (IZIIS), University "SS. Cyril and Methodius," in Skopje, Republic of Macedonia; personnel of the Republic Institute for the Protection of Cultural Monuments (RZZSK), in Skopje; and the Getty Conservation Institute (GCI), in Los Angeles.

The three-year research effort included the following activities:

- study and documentation of the existing state and topology of fifty Byzantine churches in the Republic of Macedonia;
- selection and analysis of four characteristic structural types of churches;
- delineation of repair and strengthening criteria;
- definition of expected future seismic events in Macedonia and their probable parameters;
- experimental studies of the physical and chemical properties and bearing capacities of the Byzantine church materials;
- measurements of the dynamic responses of selected church structures;
- development of repair and strengthening methodologies;
- construction and dynamic testing of a scale model of a Byzantine church on the seismic shaking table at IZIIS;
- data reduction and analytical studies of the observed structural behavior of the model;
- development and application of computational methods for evaluating seismic effects on retrofitted structures; and

- suggested applications of the retrofitting technology to other vulnerable churches in Macedonia.

Included in this volume are brief descriptions of Byzantine church types; detailed information on the church selected as the prototype for testing, the analytical modeling of the church, and the construction and testing of a 1:2.75 scale model of the prototype; an analysis of the test results; and possible applications of the repair and retrofitting methodology to several other churches. Further details of the project, including in-depth characterizations of the structural systems of the fifty churches surveyed during the first phases of the project, their histories and current physical conditions, and further seismic engineering calculations and analyses of the performance of the model during the shaking-table tests, are given in the twelve IZIIS reports listed in the references at the back of this book (see Gavrilović, Šumanov, et al. 1991). These volumes are on deposit at the Information Center of the Getty Conservation Institute in Los Angeles and at both IZIIS and RZZSK in Skopje, Republic of Macedonia.

This page intentionally left blank

Chapter 1

General Considerations Regarding the Conservation of Historic Buildings in Seismic Zones

Several basic conservation principles guide the design of interventions contemplated for historically or culturally significant buildings, regardless of construction materials, design, or location of the buildings (Feilden 1982):

- Develop an understanding of the building following a detailed inspection and review of documents pertaining to the structure.
- Measure actual building parameters that have not been identified.
- Minimize structural and cosmetic interventions.
- Preserve the historic and significant architectural features as well as the physical integrity of the building.

To satisfy these criteria, each building should be examined as a whole, in context, and each of its parts must be assessed individually from archaeological and historic viewpoints to collect information pertinent to future structural interventions. This information should guide the design of minimum interventions to assure the safety of the building's occupants, enhance the strength and capability of the building to survive future earthquakes, and preserve the authenticity of the building.

Criteria and Objectives

The design of structures that can adequately resist dynamic seismic loads is directly related to the site's seismicity, the importance of the structure, and the allowable extent of damage. Three criteria for historic buildings based on earthquake characteristics are as follows:

- For minor earthquakes, the dynamic structural behavior should not damage either the structural or nonstructural elements.
- For moderate earthquakes (the "design" earthquake), small deformations of nonstructural elements are acceptable, but no damage to the main structure is permissible.

- For an earthquake of the maximum severity expected, the stability of the main structure should not be affected. Large deformations of both structural and nonstructural elements are allowed if the entire structure is not damaged beyond repair.

Repair and strengthening methods are directly related to conservation demands; that is, they must include a consideration of restoration ethics with regard to the effects of the proposed structural measures required to achieve the seismic safety of the structure. To arrive at an adequate repair and strengthening concept, it is necessary to perform a detailed structural analysis of the historic building, taking into account the type, condition, and mechanical properties of the masonry materials; the significant architectural elements of the structure, such as ceilings, roofs, and floors; and the historic and artistic aspects of the building that require protection.

Repair and retrofitting methods should increase either the strength of the existing structure or its ductile capacity, but in certain cases both objectives can be realized with proper design. Because the design and materials used in the construction of older historic buildings are quite different from those of more modern ones, the design engineer and architect have fewer options when selecting an adequate repair method. If the load-carrying capacity of the existing structural elements is not sufficient to receive and transfer forces generated during an earthquake, new structural elements must be provided.

The principal goals of a design for the strengthening of structural systems are providing for the integrity of the building at the floor and roof levels, increasing its moment and shear resistance, and providing additional ductility. To attain these goals, it is necessary to consider the existing building condition, possible failure mechanisms, criteria for stability, the seismicity of the region, and information derived from an analysis of the seismic stability of the building.

Retrofitting Approaches

Analysis of damaged massive structures has shown that one of the initial failure modes is wall separation, accompanied by the subsequent deterioration of the structural integrity as a result of the inability of the floor or roof system to withstand tensile forces. Therefore, the principal strengthening objective should be to assure structural integrity by inserting elements that enable the structure to respond as an entity to tensile stresses. Walls should be able to resist shear forces and moments and exhibit ductile behavior. In general, the moment resistance of walls depends on their geometrical characteristics as well as on their capacity to withstand tensile forces. For example, masonry has little tensile strength, but this can be increased by appropriate grouting or by insertion of reinforcements at the ends of the walls.

Masonry structures usually behave rigidly, but shear effects that produce cracks predominate in earthquakes, so the relative danger

to the structure depends to a great extent on masonry strength. The load-carrying capacity of the masonry walls in traditional Byzantine churches was increased during the original construction by incorporating timber ties in the church interiors and placing timber belts in the walls at roof level, at ends of vaults, above wall openings, and at foundation level. Two methods for strengthening these walls would be to (1) replace missing timber belt courses with steel ties and (2) inject modern bonding materials into voids and cracks in the masonry.

To summarize, repair and strengthening of structures such as the Macedonian Byzantine churches can be accomplished using a conservative approach and the following modified classical engineering methods:

- Strengthen the main structural system by providing strong horizontal elements at the roof level, by using steel belts within the walls, and by partial grout injection inside linear elements. Traditional timber ties and belts can be replaced by steel ties, or the more visually acceptable timber ties can be reinforced internally with steel rods or external cables. Masonry bonding can be improved by grouting cracks. These methods are suitable for small, compact churches that have many load-carrying elements and are located in regions of relatively low seismicity.
- To resist tensile forces resulting from overturning moments, insert vertical elements at the ends of walls and around openings, and assure positive connections between the vertical elements and the structure with partial grout injection.

This page intentionally left blank

Chapter 2

Overview of Byzantine Churches

The research project on which this publication is based concerns a portion of the abundant Byzantine cultural heritage in architecture and art, as exemplified in churches that were built during the ninth to fourteenth century in Macedonia. Their condition is of constant concern to preservationists due to damage from natural forces (earthquakes, floods, subsidence, wind) and human factors (war, fire, pollution, vandalism, neglect) that continue to diminish the number of remaining churches.

Architecture

Over the past three millennia, many different peoples have lived in the area of the Balkans now known as the Republic of Macedonia. Invading armies have conquered and occupied the region, and their civilizations and cultures developed, passed through, and sometimes died out. Each left traces that persist and bear evidence of its history, achievements, and culture.

A review of the general characteristics of this area reveals many examples of architectural monuments dating from the period of early human civilization. Remnants of early settlements exist in the form of archaeological sites dating from the ancient Greek and Roman cultures, and architectural structures—fragments, entire buildings, and even complexes—from the time of the Byzantine Empire. Many of these latter structures are of religious character, and these are the subject of this investigation.

In the third and fourth centuries AD, a succession of historical events led to the gradual disintegration of the Roman Empire, the separation of its eastern provinces, and the establishment of the Eastern Roman Empire, which began with the founding of Byzantium (now Constantinople) in the fourth century. During the following eleven centuries, the area now known as the Republic of Macedonia was initially part of the Byzantine Empire and then part of the empire of King Samoil (in the tenth and eleventh centuries). Later it came under the successive jurisdiction of Byzantium (again), Bulgaria, and Serbia. After the arrival of the Turks, in 1453, Macedonia was ruled by the Ottoman Empire. Against this background, the architecture in the region developed in accord with the changing social, economic, and historical climate, and this gave rise to extraordinary architectural examples—many of which have survived to the present.

The development of church architecture and construction techniques during the Byzantine period, between the ninth and fourteenth centuries, reflected the changing needs of the people. Although certain stylistic similarities unite the designs of these structures, the many different architectural solutions resulted in a wide variety of church plans. For example, the early churches were actually large, multipurpose structures. These buildings—in the classic, Roman, three-nave basilica style—were used as marketplaces, sites for public gatherings, and courts for the administration of justice. Only later were they used for religious purposes; at that time, the large space allowed the separation of religious from other activities, and during some periods, the segregation of the sexes.

Eventually, the need for large structures diminished, although some basilicas continued to be built until the tenth century. Instead, smaller, dedicated church buildings began to be built; these provided space for a maximum of 120 persons (segregation was no longer a requirement). At the same time, the changing liturgy of the church affected the allocation of space within the building, resulting in the development of the architectural features of the altar, prothesis, diaconicon, naos, narthex, porch, and chapels, which are common design features of the later churches (see glossary for descriptions).

Frescoes

When the Slavic tribes invaded the Balkan regions in the sixth century, they were exposed to the cultural achievements of the Byzantine Empire, as exemplified by its elaborately ornamented religious structures decorated with mosaics and fresco paintings, and the monumental necropolises and public buildings, which featured marble columns and statues.

Today the creative achievements of the early Slavs in the Macedonian area are known mainly through the remnants of fresco paintings preserved in the ruins of the basilica excavated in the ancient town of Stobi. Only a small portion of those wall paintings have been preserved intact. From their artistic characteristics and style, the frescoes appear to be related to the Byzantine icons preserved from about the same time in the monastery of St. Catherine of Sinai, on the island of Crete. The saints are depicted with wide-open eyes, drawn with strong contours, and colored in lively hues, all of which are hallmarks of works dating from the early Christian period.

The oldest churches in Macedonia that contain well-preserved fresco paintings date from about the eleventh century. The most important of these are in the churches of St. Sofia in the town of Ohrid, and St. Leontije in Vodoča; and in the monastery of St. Bogorodica Eleusa in Veljusa. Mural paintings from the twelfth century in Macedonia are more numerous, and many are in good condition. Among these are the frescoes in the chapel of St. Sofia and in St. Leontije and in the important and complete fresco ensembles in the churches of St. Pantelejmon, Gorno Nerezi, and St. Gjorgji, Kurbinovo. Fourteenth-century frescoes are found in the monasteries of Lesnovo, St. Andreja, and Matejče and in the churches of St. Nikita, Banjani; St. Dimitrija, Markov Monastery, Sušica;

(a)

(b)

Figure 2.1
Basilica-type church, St. Sofia, Ohrid: (a) north facade, (b) west facade.

Figure 2.2
Triconch church, St. Andreja, Matka: south and east facades.

and St. Bogorodica, Treskavec Monastery, Dabnica. Monastic life in these centers promoted the spread of Byzantine culture and, with the changing political conditions initiated under Serbian rule, the Slavic influence spread throughout the region and influenced further church design changes.

Types of Byzantine Churches

In the chronology of the development of the Byzantine period of architecture, four major types of structures can be identified (Bošković 1947; Hoddinott 1963; Mango 1974). The basilica plan, originally developed by the Romans, was the predominant structure at the beginning of this period, that is, from the fifth to tenth century (fig. 2.1). The tri- and

Figure 2.3
Tetraconch church, St. Bogorodica Eleusa, Veljusa: south and east facades.

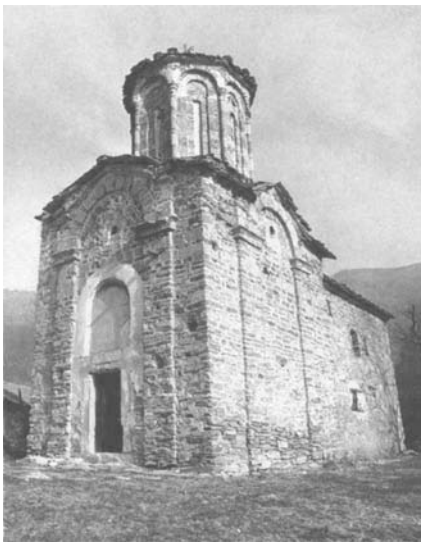

Figure 2.4
Quincunx church, St. Bogorodica, Matejče: north and west facades.

Figure 2.5
Single-nave church, St. Nikola, Šiševo: south and west facades.

tetraconch churches with a single dome (figs. 2.2 and 2.3, respectively) were characteristic of the middle of this period, from the tenth to twelfth century. Single-dome and quincunx churches with developed or narrowed inscribed crosses in a rectangular plan (fig. 2.4), single-nave churches (fig. 2.5), and smaller buildings with more simplified plans prevailed from the twelfth to fourteenth century. These basic types of structures, especially those with an inscribed cross, are found in many variations and modifications.

Basilica-type churches

Basilica-type structures continued to be constructed in Macedonia for many years, continuing the Roman basilica design. The structural system of the basilica is characterized by massive, meter-thick facade walls and two rows of symmetrically placed columns that separate the central nave from the two aisles. Usually, the plan was a three-nave structure with a flat timber roof. An example of this type is the older part of the church of St. Gjorgji, Staro Nagoričane (fig. 2.6). Exceptions exist, however, such as the churches of St. Sofia, Ohrid, and St. Bogorodica, Drenovo, whose naves are surmounted by vaults. In the original structures, the central naves apparently had domes, but these no longer exist. The exterior shapes of the single apses of basilicas are either semicircular or polygonal (fig. 2.7).

Tri- and tetraconch churches

Triconch and tetraconch designs were used for construction of churches of smaller proportions that were part of monastery complexes. These churches belonged to a single monastic order and were intended to accommodate a smaller number of persons. The structural system of conched churches con-

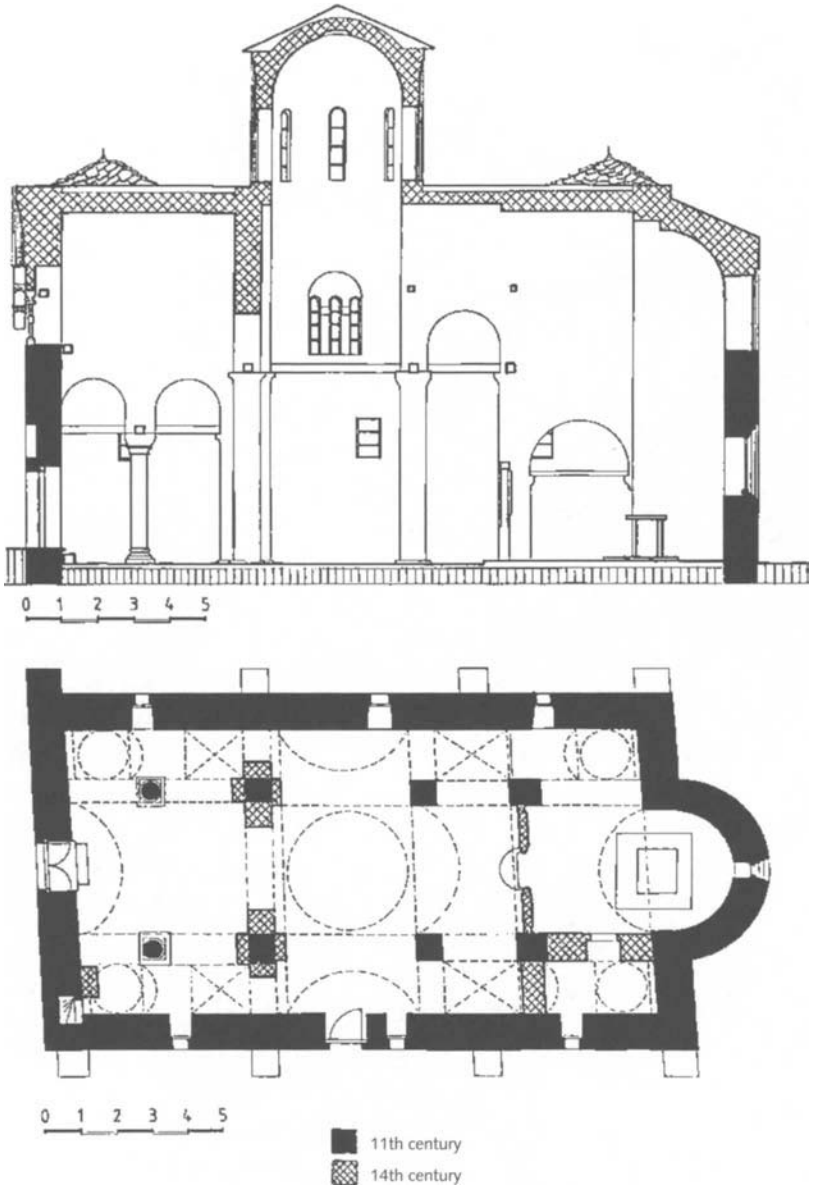

Figure 2.6
St. Gjorgji, Staro Nagoričane: basilica plan and elevation.

Figure 2.7
St. Sofia, Ohrid: east facade and apse.

sisted of massive walls and a central area surmounted by a semicircular dome, which rested on a tambour constructed over the circular spatial architectural element formed by triangular pendentives. The tambour was usually octagonal when viewed from the outside but cylindrical on the inside. In triconch churches, the north, east, and south arms had the form of semicircular conches on the inside and were polygonal on the outside.

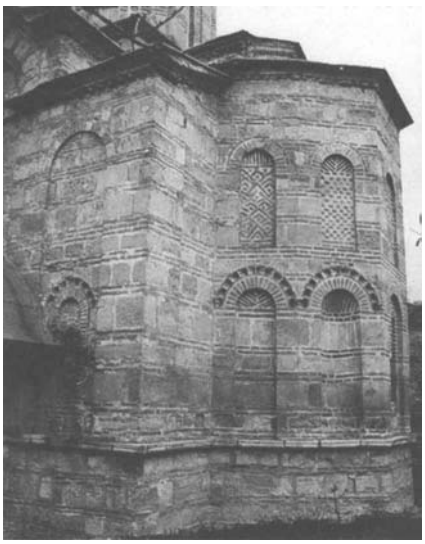

Figure 2.8
St. Dimitrija, Markov Monastery, Sušica: east facade and apse.

Single-dome and quincunx churches

Most of the churches built in Macedonia toward the end of the Byzantine period were of the single-dome or quincunx type. The principal feature of these churches was the inscribed cross formed by the rectangular area at the intersection of the cross arms. The dome that surmounted this area was supported by the tambour and pendentives in the naos and by four freestanding columns; it was generally square or rectangular in cross section. The apse was semicircular on the inside and polygonal on the outside.

In a variation of this design, the dome was supported by corner pilasters, which represent, in fact, wall areas. These churches were usually built without a narthex; that is, there was only an altar area and a naos. The prothesis and the diaconicon were constructed either as separate areas or as two semicircular niches in the east wall. In some cases, the niche was decorated on the outside with semicircular blind niches (fig. 2.8).

The upper portions of quincunx churches feature four main vaults surmounted by a central dome. The corners between the cross arms are lower and covered either by vaults (in single-dome churches) or by smaller domes that are lower than the central dome. The central tambours are usually octagonal or dodecahedral, as in the church of St. Bogorodica, Matejče (see fig. 2.4). The overly large dimensions of the central dome of this quincunx church (in combination with the low narthex, which is separated from the naos by two existing columns and two new columns) creates an unusual interior (fig. 2.9).

The church of St. Gjorgji, Staro Nagoričane (fig. 2.10), was created by renovating a ruined Byzantine basilica. The five-dome plan was incorporated into the old basilica outline, resulting in a combination of a basilica and a quincunx (see fig. 2.10). The side naves of the basilica were incorporated and columns were constructed in the interior.

Smaller, single-nave churches

Many of the churches in Macedonia belong to this architectural group, which is characterized by simple, single-nave designs (figs. 2.11, 2.12). The much smaller, rectangular buildings have barrel vaults or timber-couple roofs and usually have an apse that is semicircular on the inside and polygonal on the outside (figs. 2.13, 2.14).

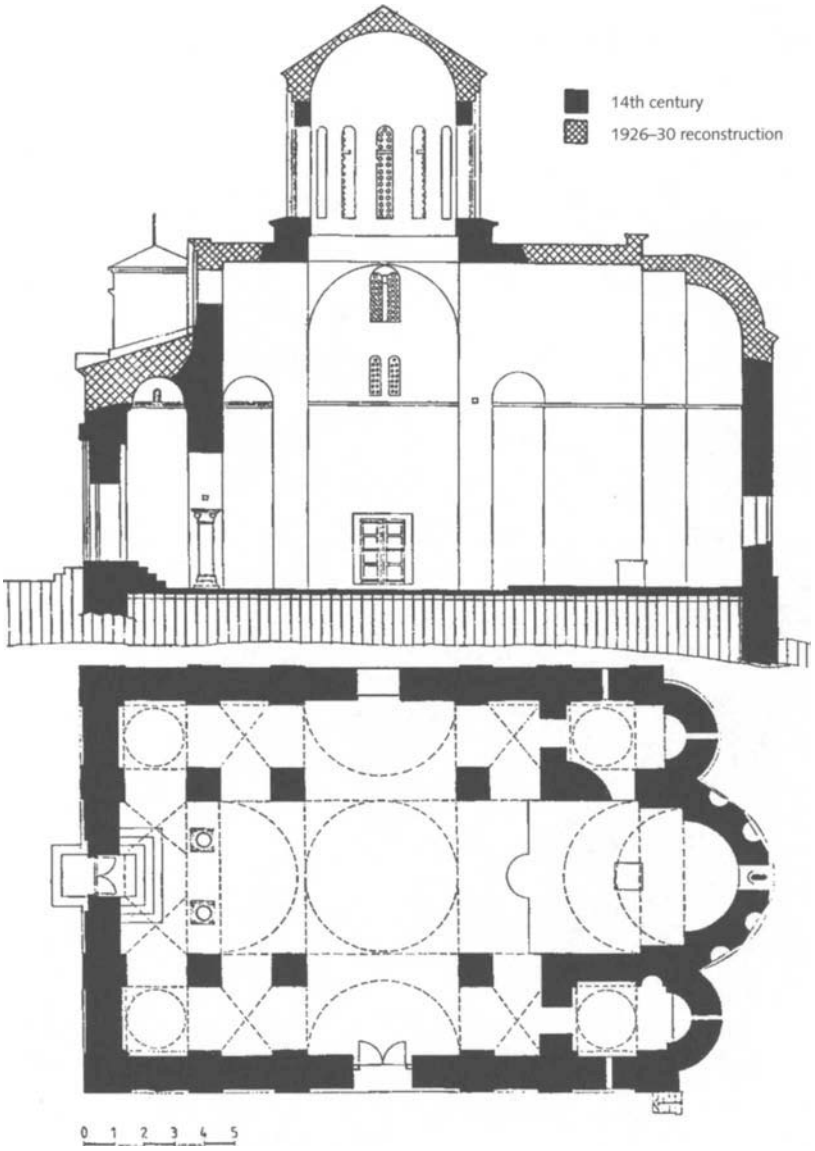

Figure 2.9
St. Bogorodica, Matejče: Quincunx plan and elevation.

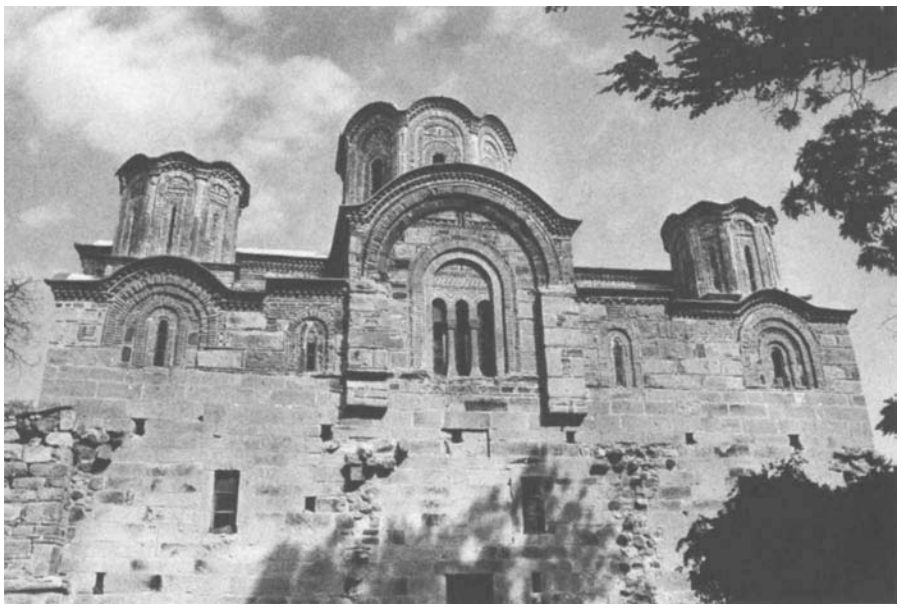

Figure 2.10
St. Gjorgji, Staro Nagoričane: south facade.

Figure 2.11
St. Nikola, Šiševo: single-nave plan and elevation.

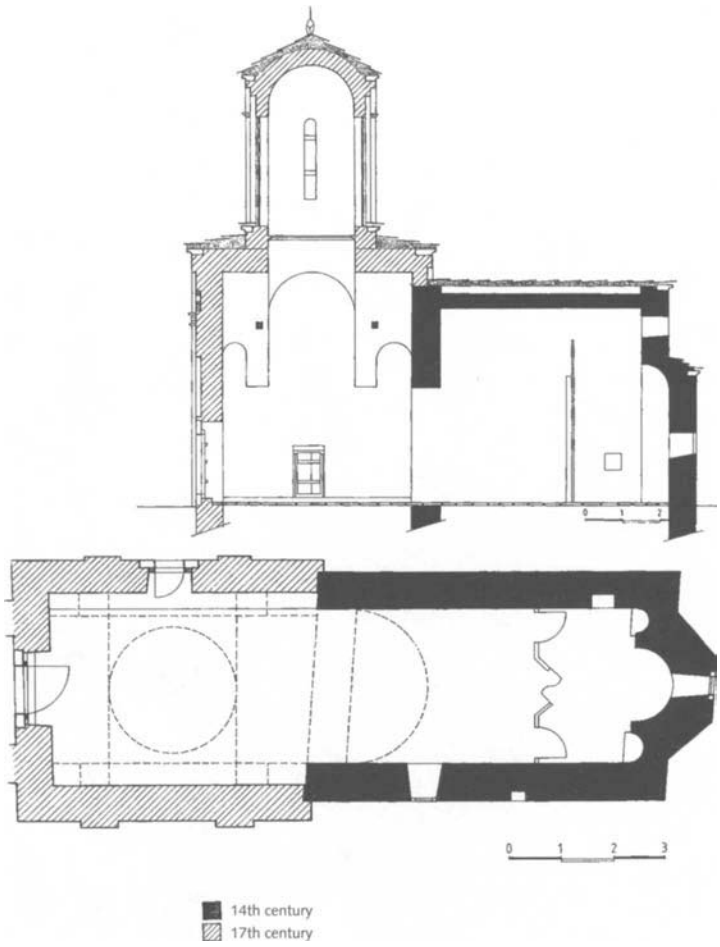

Figure 2.12
St. Jovan, Ohrid.

Structural Characteristics

In general, the structural systems of all churches of this period consisted essentially of walls, columns, and vaults with massive cross sections. Because of their size and geometry, these elements were capable of sustaining the high compressive stresses in the structure resulting from gravity loads.

Byzantine churches were built using natural local materials, wood and stone, in conjunction with manufactured masonry materials, such as brick and lime mortar. Roofs were usually sheathed with sheet lead or protected by clay tiles. The massive peripheral walls were constructed of polished or roughly hewn stone (usually tufa—a porous calcium carbonate—or limestone but occasionally sandstone) or fired brick of various sizes, shapes, and dimensions, or combinations of these materials. The columns were usually monolithic and were fabricated from marble or granite blocks. Standard mortars were composed of slaked lime and sand, or were modified by the addition of crushed brick or brick powder.

Load-carrying Roman walls consisted of two exterior wall faces that were erected first; the space between them was then filled with

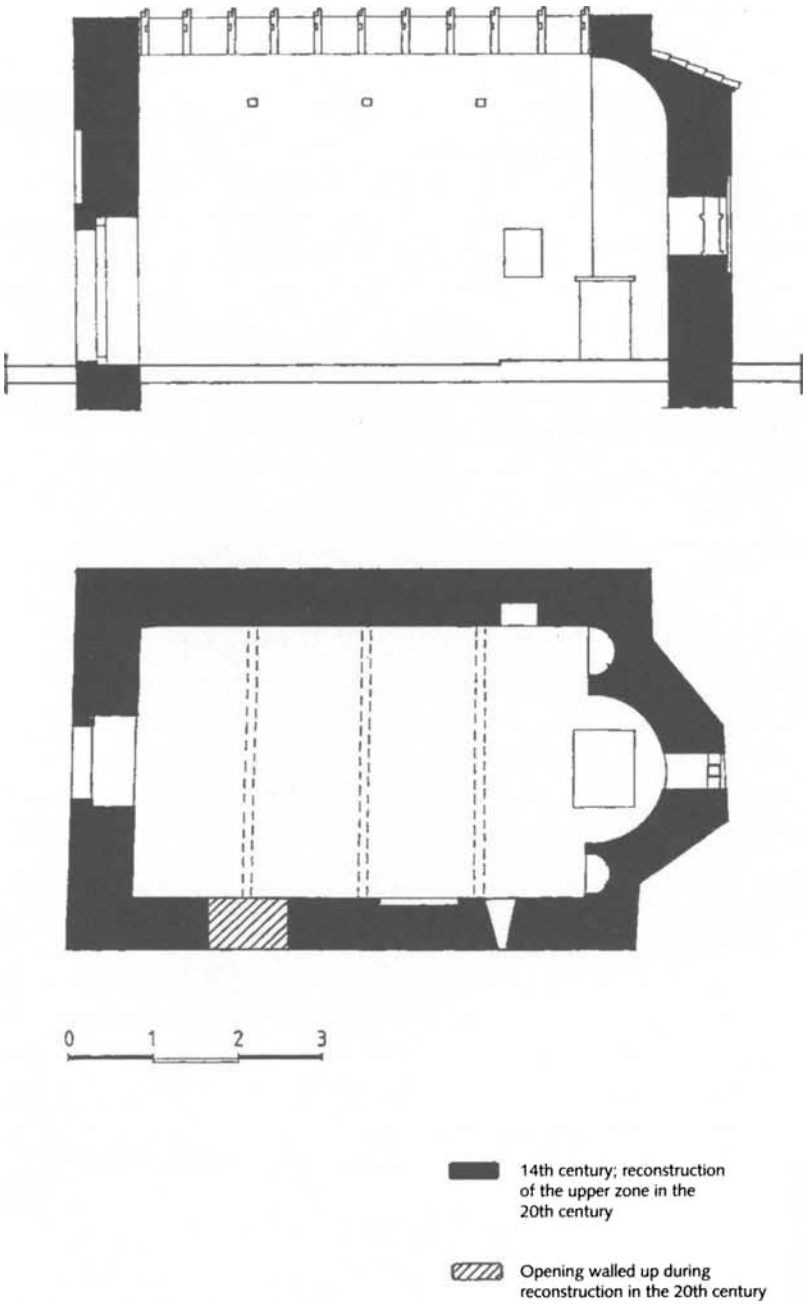

Figure 2.13
St. Vrači Mali, Ohrid: single-nave, couple-roof plan and elevation.

Figure 2.14
St. Vrači Mali, Ohrid: apse.

Roman cement, a mixture of *pozzolana* and lime that became a strong calcified mass after curing. Byzantine walls, however, lack this homogeneous wall core. They generally consist of horizontal brick and stone masonry walls separated by a core of lime mortar and rubble masonry.

The construction process involved placing one, two, three, or more horizontal layers of brick and framing them in with bricks placed horizontally or vertically, which resulted in the polychromatic effect characteristic of Byzantine walls. Occasionally, when framing vertical stone, the mason would place three or four bricks horizontally, as in the church of St. Leontije, Vodoča (figs. 2.15, 2.16). The upper and lower walling formed the so-called cloisonné type of surface. Vaults and arches were usually of the semibarrel type, although groin vaults without flanges

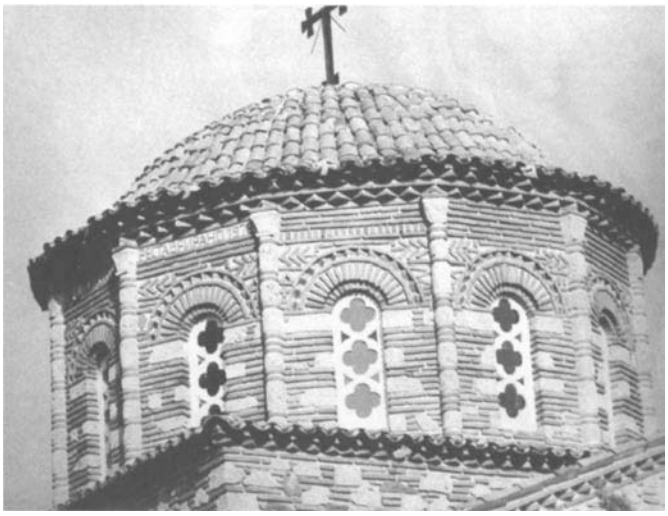

Figure 2.15
St. Leontije, Vodoča: tambour and dome.

Figure 2.16
St. Leontije, Vodoča: north facade.

and tetravaults were also used. The vaults were usually constructed of hewn limestone, a light material that is easily shaped and cut when sufficiently damp, but sometimes vaults, calottes and conches (see glossary), and domes were constructed of brick masonry. Arches terminating in columns were always embedded in the wall mass rather than being supported by pilasters (fig. 2.17).

An important feature of almost all Byzantine churches was the incorporation of visible timber ties placed at several upper levels in the interior of the church (fig. 2.18). These ties sustained the tensile stresses in the structure resulting from differential settlement, wind loads, and seismic effects. To ensure the uniform settlement of buildings during the temporary interruption of construction required by the slow curing of

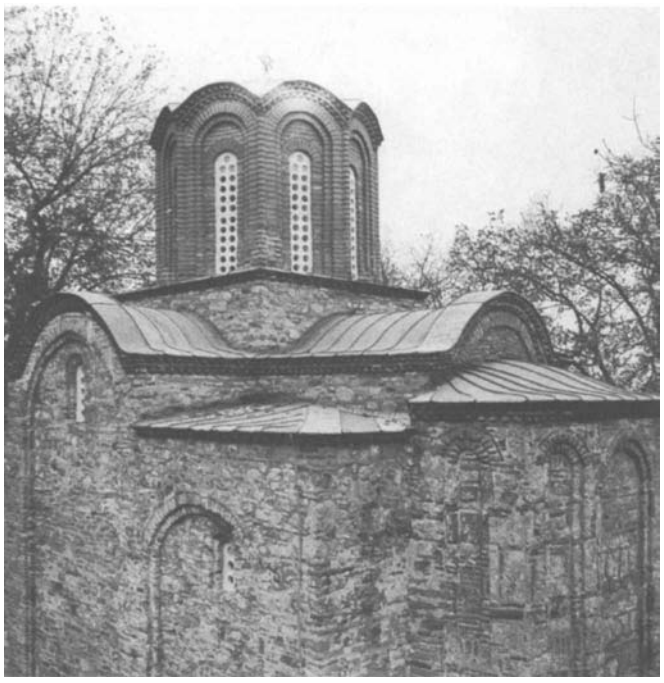

Figure 2.17
St. Stefan, Konče: east and south facades.

Figure 2.18
St. Sophia, Ohrid: interior timber ties.

Figure 2.19
St. Gjorgji, Kurbinovo: fresco
ca. 1191.

Figure 2.20
St. Gjorgji, Kurbinovo: fresco
ca. 1191.

Figure 2.21
St. Bogorodica Perivlepta,
Ohrid: fresco.

Figure 2.22
SS. Elena and Konstantin,
Ohrid: fresco.

lime mortar, dual horizontal timber belts were embedded within the walls at vertical separations of 1.0–1.2 meters. They were connected in the transverse direction every 60–70 centimeters by smaller beams and at the corners of the walls. These wooden elements were the same height as the walls and were connected with wooden ties at the base level of vaults or arches, as well as at the bases of the tambours and domes. The belts served also to stiffen the structure and increase its stability under seismic or other dynamic loads. Over time many of the timber belts in Byzantine-period churches have deteriorated or have been destroyed by insects, so voids now exist at many former belt locations.

Surface Characteristics

The interior wall surfaces of Byzantine churches were completely covered with painted murals depicting biblical scenes, which was in accord with church customs during this period (figs. 2.19–2.22). Byzantine murals are world-renowned and considerable conservation efforts have been made to repair and preserve these remarkable works of art (Djurić 1974). The surfaces on which the murals were painted were always smoothly plastered, and only in a few cases was the expanse of clear walls interrupted by blind niches or windows at the level of the gable walls of the cross arms or vaults. Generally, the foundation level of the church was decorated to mimic the marble used in churches in Byzantium. Floors were moderately finished, often with stone but occasionally with bricks arranged in a mosaic pattern, such as in the churches of St. Bogorodica Eleusa, Veljusa, and St. Sofia, Ohrid.

In contrast to the modest architectural finishing of the interiors of these churches, special attention was given to the finishing of the exterior church facades, which were seldom rendered or covered with

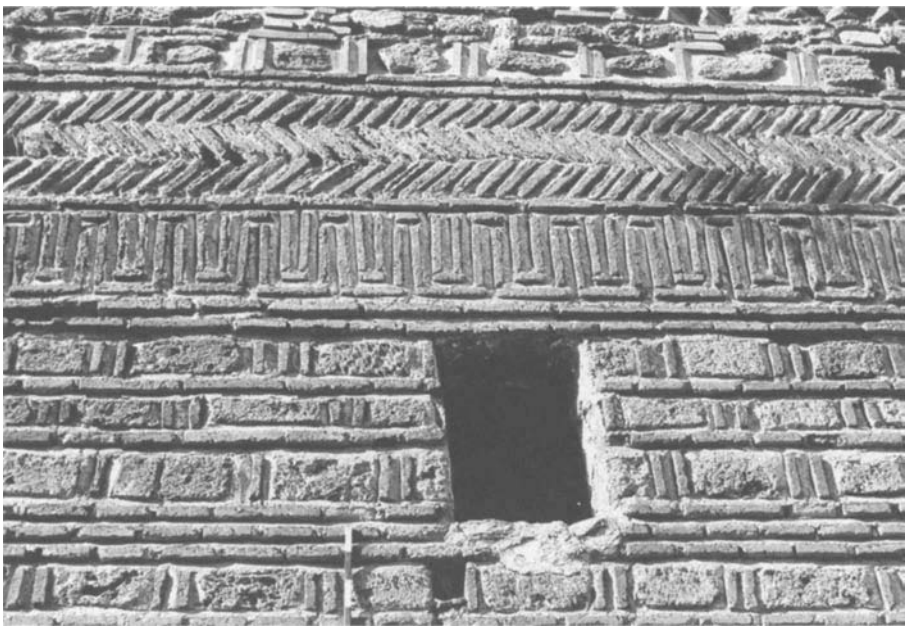

Figure 2.23
St. Dimitrija, Varoš: facade polychromy.

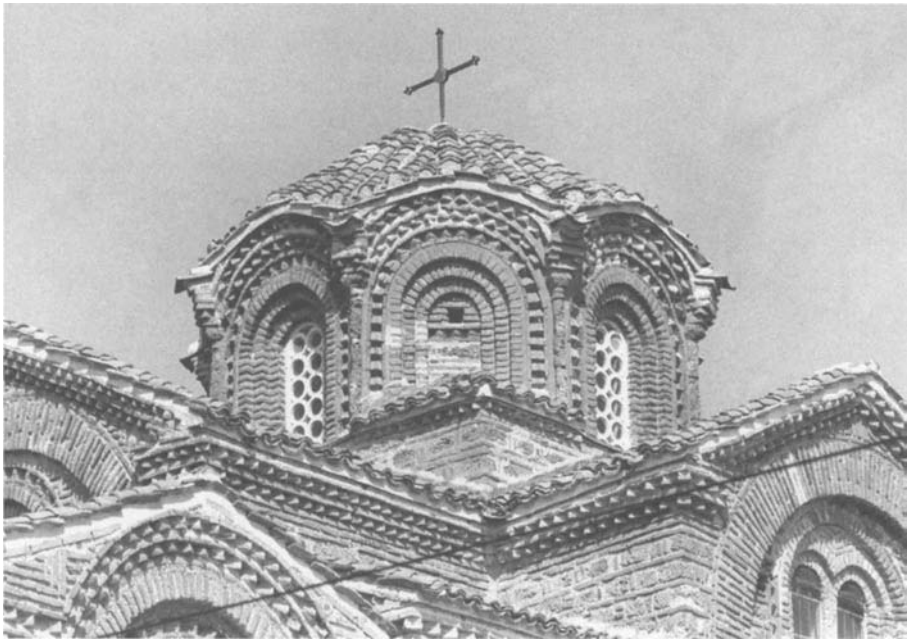

Figure 2.24
St. Bogorodica Perivlepta, Ohrid: elaborate polychromy on tambour and facade.

mortar. Mortar joints were carefully pointed with a thin layer of high-quality lime mortar, which improved the appearance of the structure.

For economic reasons, brick was used most often for church construction, especially in the early and middle Byzantine periods. It was used not only for masonry but also to create the rich ornamentation that covered large wall areas (fig. 2.23). Bricks were placed in several ways—horizontally, vertically, inclined, and flat—creating checkerboard patterns with one field of brick and one of mortar. Bricks set in fishbone or meandering patterns were used for finishing dentilated single or double cornices (fig. 2.24). Brick combined with limestone was used for the construction of decorative arches and for wall inscriptions.

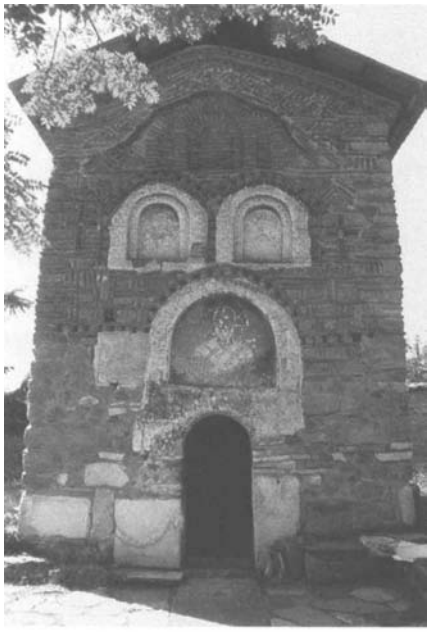

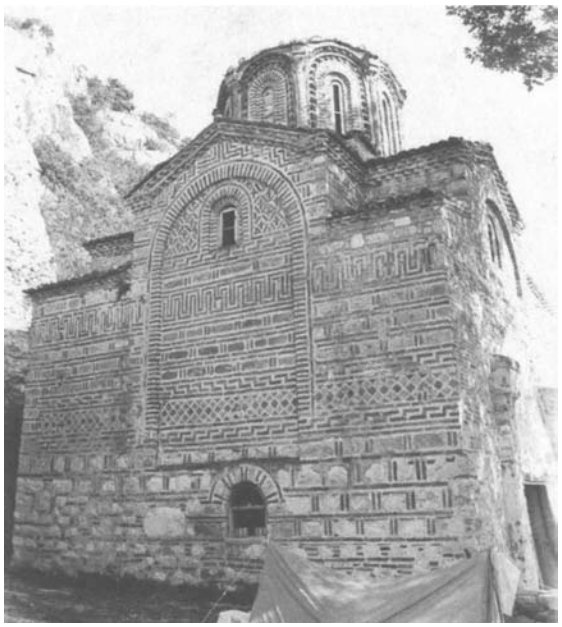

Figure 2.27
St. Dimitrija, Markov Monastery, Sušica: apse.

Figure 2.25
St. Nikola, Varoš: exterior fresco and polychromy.

Figure 2.26
St. Bogorodica Zahumska, Trpejca: west facade.

Multicolored stone was used occasionally, and mortar was available in colors ranging from white to light rose, depending on the composition and quantity of the ground brick or brick powder added to enhance the strength of the mortar. The polychromatic effect obtained in this way is one of the most striking characteristics of Byzantine architecture. Outstanding examples of such polychromy can be seen in the churches of St. Nikola, Varoš (fig. 2.25), and St. Bogorodica Zahumska, Trpejca (fig. 2.26).

Flat wall surfaces were visually enhanced by incorporating pilasters, arches, and niches. Deep semicircular niches in the facade, especially on the east-facing apse, created a particularly dramatic effect. This can be seen, for example, in the churches at St. Bogorodica Eleusa, Veljusa; St. Spas, Kučevište; and St. Dimitrija, Markov Monastery, Sušica (fig. 2.27).

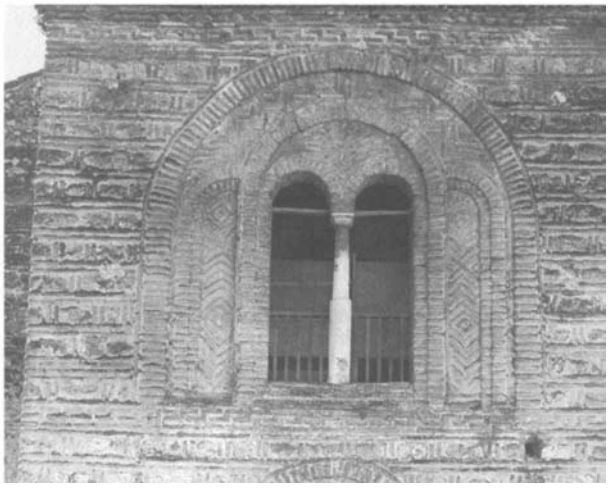

Figure 2.28
St. Gjorgji, Gorni Kozjak: pendentive and interior of tambour.

Figure 2.29
St. Sofia, Ohrid: biforium.

Dome tambours and pendentives (fig. 2.28) were usually made of brick, but in rare cases bricks in combination with tufa stone were used, for example, at St. Bogorodica, Osogovo Monastery, Kriva Palenka; St. Nikola, Šiševo; and St. Dimitrija, Markov Monastery, Sušica (fig. 2.27). Individual windows have special stylistic characteristics, such as one, two, or three openings. Triple windows (triforia) are usually found on the apses of larger churches, and double windows (biforia) are generally seen on the gable walls of cross arms (fig. 2.29).

Chapter 3

Survey of Existing Byzantine Churches in Macedonia

During the first phase of the Seismic Strengthening, Conservation, and Restoration project, fifty churches in the Republic of Macedonia were surveyed and documented extensively by a diverse group of specialists. These data provided a basis for selection of a single prototype church, which would be modeled analytically. Later, in the experimental phase of the project, a scale model of the church would be constructed and tested. The documentation for each church consisted of a survey of its history; a series of photographs of the exterior and interior; descriptions of the architecture, frescoes, structural systems, present condition, and previous conservation work; and measurements of selected physical and chemical characteristics of the masonry and other building materials. Detailed information on the survey is available in Gavrilović, Šumanov, et al. (1991, vols. 2–6). In view of the length of these volumes, only brief illustrative examples are included here. A list of the churches surveyed, with their locations and approximate dates of construction, is given in appendix A.

Present State of Selected Church Buildings—Causes and Level of Damage

Until this work was undertaken, no systematic methodologies for the repair and retrofitting of historic structures (such as Byzantine churches) had been devised based on the type of analytical and experimental engineering studies that would be necessary to ensure the survival of these buildings following the severe—or even moderate-intensity—earthquakes that occur in Macedonia. This project was designed to develop and evaluate methods to strengthen the principal structural systems that would allow these historic buildings to resist serious damage from seismic effects.

The survey of existing churches showed that many were in poor structural condition and that interior frescoes were badly damaged and in need of conservation. These churches included St. Bogorodica Zahumska, Trpejca; St. Kliment Mal, Ohrid; St. Dimitrija, Ohrid; St. Bogorodica, Treskavec Monastery, Dabnica; St. Nikola, Manastir; and St. Arhangel Mihail, Radožda. To ensure their ability to survive the

harsh local environment and future earthquakes, the buildings must be retrofitted and repaired. For St. Bogorodica Zahumska and St. Bogorodica, Treskavec Monastery, extensive repairs will be required.

Damage to these and other buildings has been caused primarily by one or more of the following factors:

- capillary moisture in the walls and salt crystallization damage;
- growth of broad-leaved plants, lichens, or fungi and insect infestation;
- earthquakes and floods, especially in the Skopje and Ohrid regions;
- lack of adequate maintenance, water damage, and vandalism; or
- ineffective or inappropriate methods or materials used during previous conservation efforts.

Although each of these factors can be responsible for continuing damage to these churches, earthquakes (and floods) are of vital concern due to the sudden, violent destruction they produce. Preventive retrofitting and repair measures need to be taken as soon as possible because, as Sir Bernard Feilden so aptly stated, "We must always be aware that we live between two earthquakes" (1987).

Investigations have shown that repair and conservation work have been carried out to some extent at almost every structure included in this study. The detailed investigations found the physical condition of some church buildings to be generally good only because of the conservation and maintenance efforts performed in the past. These included the churches of St. Sofia, Ohrid; St. Nikita, Banjani; St. Dimitrija, Markov Monastery, Sušica; and St. Pantelejmon, Gorno Nerezi. However, these measures were not always performed in accordance with currently accepted conservation principles or recommendations for the treatment of cultural monuments as set forth in the Venice and Burra Charters (US/ICOMOS 1999).

Typical conservation measures and structural changes included removal of enlargements and architectural elements in the churches of St. Jovan Kaneo, Ohrid; St. Bogorodica Eleusa, Veljusa; St. Stefan, Konče; and St. Nikola, Psača. Even entire parts of buildings dating from earlier periods were removed, such as the roofs and domes of St. Stefan, Konče; St. Pantelejmon, Gorno Nerezi; St. Gjorgji, Staro Nagoričane; St. Nikita, Banjani; and St. Andreja, Matka.

Conservation work at the lower zones of the buildings, where the foundation was in contact with the surrounding soil, often included the construction of drainage channels. Although this may have been appropriate at the time the measures were implemented, in some cases these efforts contributed to an increase in the height to which capillary moisture rose in the walls. The drainage channel wall was coated first with cement emulsion and then with one or two layers of hot bitumen.

Both cement and bitumen are impermeable and thus do not allow moisture to evaporate from the wall at the lower level. Because the rising moisture contained soluble salts, evaporation and salt crystallization occurred at the upper reaches of the walls in areas occupied by fresco paintings, resulting in severe damage to the frescoes.

Repair procedures practiced at many of the churches included the use of portland cement mortar for grout injection and for the pointing of brick and stone masonry. Reinforced-concrete belt courses, vaults, columns, and domes were added to the churches of St. Stefan, Konče; St. Leontije, Vodoča; St. Bogorodica, Matejče; St. Bogorodica, Osogovo Monastery, Kriva Palenka; St. Pantelejmon, Gorno Nerezi; and St. Nikola, Radišani. Such additions and the use of portland cement for mortars and concrete can have adverse effects on structures originally built using lime-based masonry products.

- Common cement mortar containing soluble salts is susceptible to salt crystallization damage, and is incompatible with lime mortar, the original bonding element. Cement mortar is stronger and more rigid than lime mortar and is more hygroscopic and impermeable to water.
- The incorporation of reinforced-concrete elements into the original church structure results in a mismatch in the mechanical interaction between the original and the new structural systems. This mismatch can lead to differences in bearing capacities and deformability characteristics, which can result in damage to the structure when it is exposed to earthquake conditions.
- An especially unfavorable effect is ascribed to the attachment of new masonry to the original masonry, either horizontally or vertically, especially at the corners of the buildings, where during the original construction care was taken to assure continuity of the stone or brick walls. This alteration has played a significant role in earthquake damage.
- Incorporation of iron (rather than stainless steel) reinforcements or tie rods in walls resulted in corrosion and damage to aged, carbonated lime mortar and to plastered areas covered by frescoes.

Unfortunately, inappropriate materials were often used for conservation and repair of damage to Byzantine churches in Macedonia. The scope and the nature of earlier conservation activities played a decisive role in the selection of the churches to be studied in detail. They constitute crucial factors that must be considered in defining a methodology for seismic strengthening, conservation, and restoration in accordance with modern principles of conservation and recommendations for the treatment of cultural monuments in seismically active regions.

Authenticity

It is difficult to find Byzantine church structures that have been preserved in their original form and have not been changed in any substantial way over the ages. The extent to which authenticity has been retained varies from structure to structure. Some that retain most of their original features and materials and can thus be considered authentic examples of Byzantine art and architecture are the churches of St. Bogorodica Zahumska, Trpejca; St. Gjorgji, Rečica; St. Bogorodica Perivlepta, Ohrid; St. Arhangel Mihail, Lesnovo; and St. Dimitrija, Markov Monastery, Sušica. Others have undergone extensive reconstruction, including St. Leontije, Vodoča; St. Nikola, Radišani; St. Nikola, Ljuboten; and St. Bogorodica, Matejče. Roofs and the edges of walls, domes, and cornices have also been reconstructed. Usually care was taken to preserve as much as possible the authenticity of the interiors, but conservation efforts were not always completely successful.

Churches Selected for Detailed Investigation

Four churches were selected for more detailed study from the group of fifty churches documented during the initial phases of this investigation. Selection of the four churches was based on consideration of the following criteria:

- architectural design and structure of the buildings;
- present condition of the buildings and causes and extent of damage;
- methods used for earlier repairs, restoration, and strengthening; and
- degree of authenticity of the church.

As described in chapter 2, Byzantine churches from the ninth to fourteenth century can be divided into four main types of architecture: basilicas, tri- and tetraconch churches, single-dome structures with an inscribed cross or its quincunx modification, and single-nave churches. On consideration of these criteria and the survey of the present state of the fifty churches, four churches were selected:

- St. Nikola, Psača;
- St. Nikita, Banjani;
- St. Bogorodica Zahumska, Trpejca; and
- St. Bogorodica, Matejče.

These churches are all single-dome structures of the inscribed-cross type or its quincunx modification, and all date from about the same period (the fourteenth century). The degree of authenticity of the churches with respect to the original design and construction materials ranges from that of the church of St. Bogorodica Zahumska, which is largely original, to

that of the St. Nikita and St. Nikola, which have undergone many changes. Extensive conservation work was performed on St. Nikola, whereas very little was done for St. Bogorodica Zahumska. The church of St. Bogorodica, Matejče, was selected because it is a quincunx-type church with a developed cross and five domes. It was reconstructed extensively in 1926, when all vault and dome areas were rebuilt. During the 1980s, it was strengthened by installation of reinforced concrete elements (columns, belt courses, vaults, and domes), which were incorporated into the previously reconstructed walls. A description of St. Nikita, Banjani—the prototype church studied in this project—appears in chapter 5. (More detailed descriptions of this and the other three churches are given in Gavrilović, Šumanov, et al. 1991, vol. 2.)

To evaluate the stability and vulnerability of the four churches, it was necessary (1) to estimate the probability of occurrence and probable characteristics of future earthquakes, (2) to determine experimentally the static and dynamic properties of the structures, and from these data (3) to estimate the response of the buildings and define the range of parameters to be used during the tests of a scale model of one of the four churches.

Seismic hazard parameters

The territory of the Republic of Macedonia is a part of the Mediterranean seismic region of the Alpine-Himalayan belt, which is characterized by a wide spectrum of intensive and frequent tectonic processes, resulting in severe seismic activities (Hadžievski 1976). More than three thousand earthquakes occurred in this area during the twentieth century. (Except for evidence of the devastating 1555 earthquake in Skopje, few historical records exist of seismic activity before 1900.) A map of the epicenters of known earthquakes in the southern Balkan area (fig. 3.1) shows that several regions of intense seismic activity exist and that the distribution of earthquakes in this region is complex.

Detailed investigations were carried out to determine the seismic characteristics of the area: the spatial, temporal, and energy distribution of earthquakes; earthquake frequency; macro-seismic field characteristics; and the relation between the expected seismic activity and the geological and geophysical properties of the locations (Gavrilović, Šumanov, et al. 1991, vol. 7). These seismic parameters were defined for the four selected church sites. It was shown that the churches had been exposed to earthquakes with magnitudes of MCS ≥ 6 many times during the period from 1900 to 1999.[1] The maximum expected ground accelerations for the four selected churches, expressed as fractions of "g" (acceleration of gravity) for various characteristic earthquake return periods were calculated. The accelerations listed in table 3.1 represent the combined influence of local earthquakes (less than 40 km from the site) and more distant earthquakes (more than 40 km from the site). The table also lists the estimated earthquake intensities expressed as MCS magnitudes. The values calculated for specific regions in Macedonia indicate high seismicities, especially in the areas around Ohrid, Skopje,

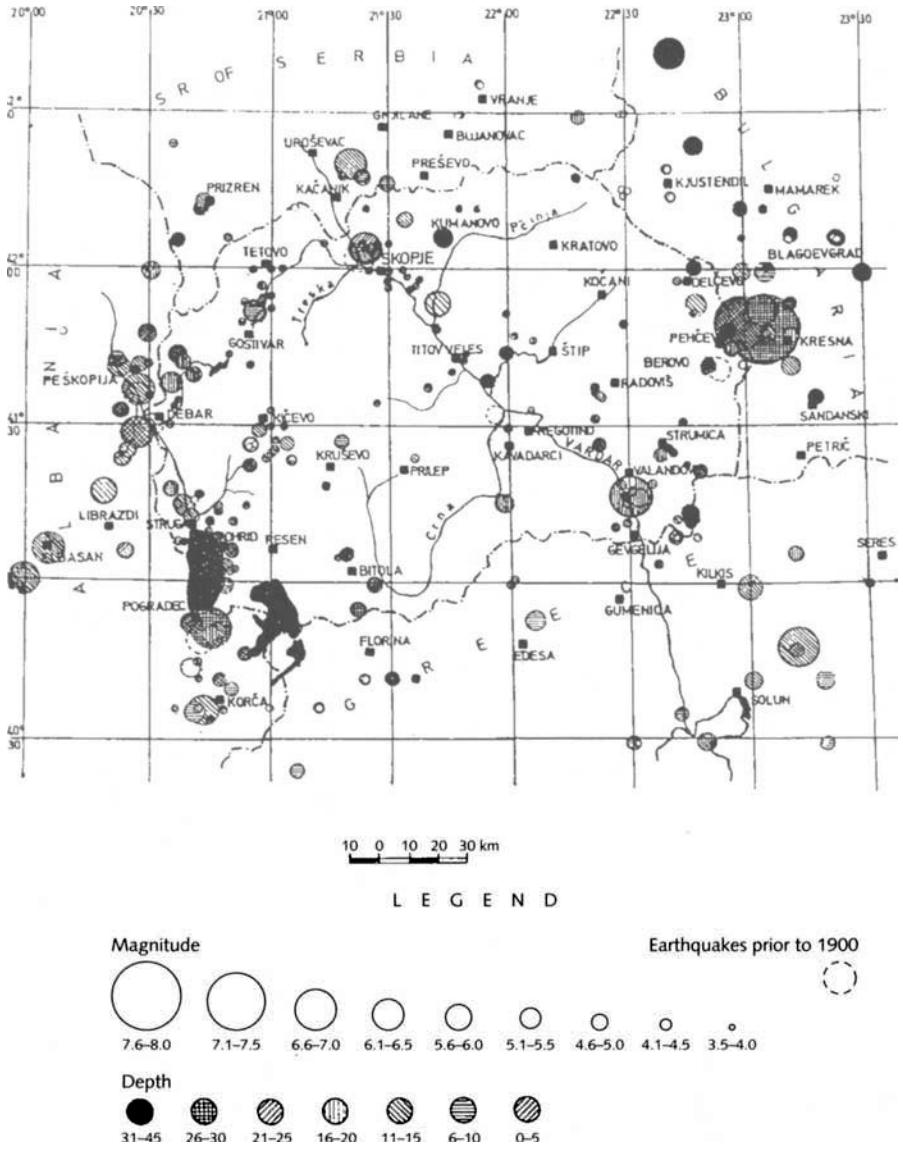

Figure 3.1
Epicenters of known earthquakes in Macedonia.

Table 3.1
Estimated maximum ground accelerations (a_{max}) for the selected churches, the corresponding return periods (t_p), and the estimated MCS magnitude (I)

		Return period, t_p (years)						
Church		**25**	**50**	**100**	**200**	**500**	**1000**	**10,000**
St. Nikita, Banjani	a_{max}	0.093	0.117	0.146	0.198	0.292	0.340	0.360
	I	6.73	7.06	7.36	7.82	8.38	8.60	8.68
St. Bogorodica Zahumska, Trpejca	a_{max}	0.163	0.202	0.235	0.268	0.320	0.344	0.380
	I	7.53	7.84	8.06	8.25	8.51	8.61	8.76
St. Nikola, Psača	a_{max}	0.107	0.143	0.178	0.191	0.204	0.210	0.220
	I	6.93	7.35	7.66	7.76	7.86	7.90	7.97
St. Bogorodica, Matejče	a_{max}	0.121	0.140	0.173	0.233	0.293	0.318	0.350
	I	7.10	7.32	7.62	8.05	8.38	8.50	8.65

Radoviš, and Strumica, areas where many important Byzantine cultural monuments are located.

On the basis of these parameters, it may be concluded that during their long existence (at least six hundred years), most of the Byzantine church structures in Macedonia have probably experienced one or more earthquakes that corresponded to the intensity and ground accelerations of the defined "design" earthquake, which has a return period of 100–200 years. Most of these structures were able to resist serious structural damage to the body of the church, although evidence exists that most of the domes and tambours have been rebuilt. However, no data are available on whether these buildings ever experienced the "maximum expected" seismic effect, which has a return period of 1000 years. Clearly, such a strong earthquake would have caused severe damage to church buildings—or even complete collapse. To provide the proper level of seismic safety for structures exposed to conditions of such high seismic risk (1000-year return period), it was necessary to consider retrofitting measures for the repair and strengthening of these churches.

Dynamic properties of selected churches

The dynamic characteristics are the principal parameters for the analysis of the structural behavior of buildings under any vibrational stress. From a mathematical viewpoint, the mode shapes of the natural frequencies of a single system represent eigen vectors and eigen values of the dynamic matrix consisting of the stiffness and mass matrices. Therefore, any variation in the dynamic characteristics at constant mass can be used to determine the stiffness variation. If the structural response to a random type of excitation is recorded and processed in the frequency domain, the natural frequencies of the system can be distinguished as peak values.

To formulate a mathematical model of a building, in this case a Byzantine church, certain structural parameters need to be known: the church mass, natural vibration frequencies, vibration mode shapes, and damping characteristics. Determination of masses can be done analytically, but the other parameters can only be defined using experimental procedures involving tests of models or by in situ tests directly on the prototype structures. The two prevailing techniques for full-scale, prototype structure tests are the forced-vibration and ambient vibration methods. The latter method was used for testing the four selected church structures (Gavrilović, Šumanov, et al. 1991, vol. 8).

The ambient vibration method for determining the dynamic characteristics of structures is relatively simple and requires only equipment that can be transported easily (Foutch 1976; Jurukovski and Percinkov 1977; Taskov and Petkovski 1991). Such a test can be conducted even while the structure is in use. The theory behind this method rests on the analytical assumption that the exciting force is a stationary stochastic process with a relatively flat frequency spectrum. This theoretical requirement can be fulfilled successfully if the prevailing wind is assumed to be the random exciting force. The natural periods, vibration mode shapes, and damping characteristics of the building can then be determined experimentally. The instruments used in this study were three

Table 3.2
Dynamic characteristics of Byzantine churches obtained using the ambient vibration technique: f = natural frequency; ξ = damping coefficient

	St. Nikita		St. Bogorodica Zahumska		St. Nikola, Psača		St. Bogorodica, Matejče	
Direction	**f (Hz)**	**ξ (%)**	**f (Hz)**	**ξ (%)**	**f (Hz)**	**ξ (%)**	**f (Hz)**	**ξ (%)**
East-west	6.0	3.2	6.0	1.5	5.4	6.5	4.4	2.7
North-south	4.8	4.0	4.6	2.2	4.0	8.3	3.4	4.9
Torsion	8.0	2.1	8.2	2.5	6.4	5.2	5.8	1.5

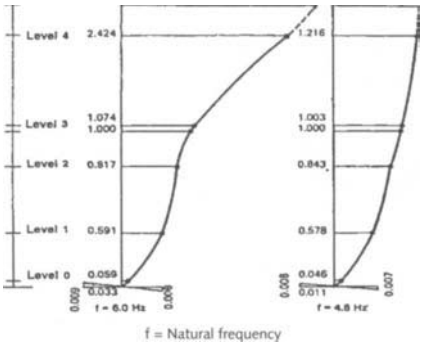

Figure 3.2
Calculated mode shapes for St. Nikita, Banjani.

Kinemetrics seismometers (model SS-1), a Kinemetrics signal conditioner (model SC-1), a Hewlett-Packard tape recorder, and a Hewlett-Packard Fast Fourier Transform Spectrum Analyzer (model 3582A).

Ambient vibration measurements in two orthogonal directions and in torsion were carried out on the four selected churches. The results are shown in table 3.2, and the calculated mode shapes for the church of St. Nikita are given in figure 3.2.

During the field studies on St. Nikita, tests were also performed to determine if the longitudinal timber belts still existed within the perimeter walls. These tests were performed by measuring the velocity of sound in the walls, which would differ depending on whether wood or cavities previously filled with wood were present in the walls. It was found that the timber belts were still present over the doors and below the main vaults but were essentially decayed at other locations.

The Church of St. Nikita, Banjani

Following the studies of the properties of the four churches, the project team selected St. Nikita in the village of Banjani (fig. 3.3) as the prototype for modeling and development of a seismic strengthening methodology, since it was typical of many of the churches in Macedonia.

This fourteenth-century church is part of a monastic complex situated on the slopes of Skopska Crna Gora, a mountain in the village of Banjani, which lies 10 kilometers northwest of Skopje. In plan (fig. 3.4a, b), the church of St. Nikita is a single-dome structure with an inscribed cross. A peculiarity of this church is the pronounced frontal area of the apse and the absence of a narthex.

The walls of the church consist of alternating rows of stone and brick. The stones are framed with bricks, and the width of the joints is nearly the same as the thickness of the bricks. Special emphasis is given to the east facade wall (the apse), which is decorated with brick checkerboard, meander, and other patterns.

No original historic data exist that specify the construction date of this monastic church or the completion date of the extensive fresco paintings. However, indirect data found in documents signed by King Milutin (reigned 1282–1321) clearly indicate that he was the

Figure 3.3
Prototype church, St. Nikita, Banjani: south (with door) and east (with apse) facades.

founder of the church. They also show that this church was a renovation of a ruined structure that may have been built around the fifth or sixth century, during the early period of the Byzantine Empire.

Architecture

The design of St. Nikita is that of an inscribed cross in a rectangular plan; four freestanding rectangular columns support the dome. (Plan views are shown in figure 3.4a, b; elevation views in figure 3.4c, d.) The church contains two clearly defined areas: altar and naos. The altar area includes a diaconicon and prothesis, a semicircular apse with an unusually wide, high monoforium, and two semicircular niches in the east wall. The central naos contains the dome, which surmounts the square space over the intersection of the cross arms and is supported by four massive columns and pendentives. The naos is entered through the central nave from either the west or south side. The areas over the arms of the cross, at the corners, and between the walls and columns are vaulted by semicircular arches and vaults, with a semicalotte over the apse. This plan and the remains of the facade frescoes suggest that an open porch existed at some earlier time.

The central area is surmounted by a semicircular dome, which is supported by an octagonal tambour with its flat sides oriented toward the main cardinal points. Each side of the tambour contains a narrow, high monoforium. In addition to the apsidal monoforium in the interior, other monoforia embellish the north wall, entrance, and altar nave. The absence of a monoforium on the south wall constitutes further evidence for the former existence of a south porch. In the central nave, a biforium appears on both the south and north walls. The building roofs are barrel vaults.

Figure 3.4 (on this and the opposite page) St. Nikita, Banjani: (a) plan, (b) tambour plan, (c) north-south elevation, (d) east-west elevation.

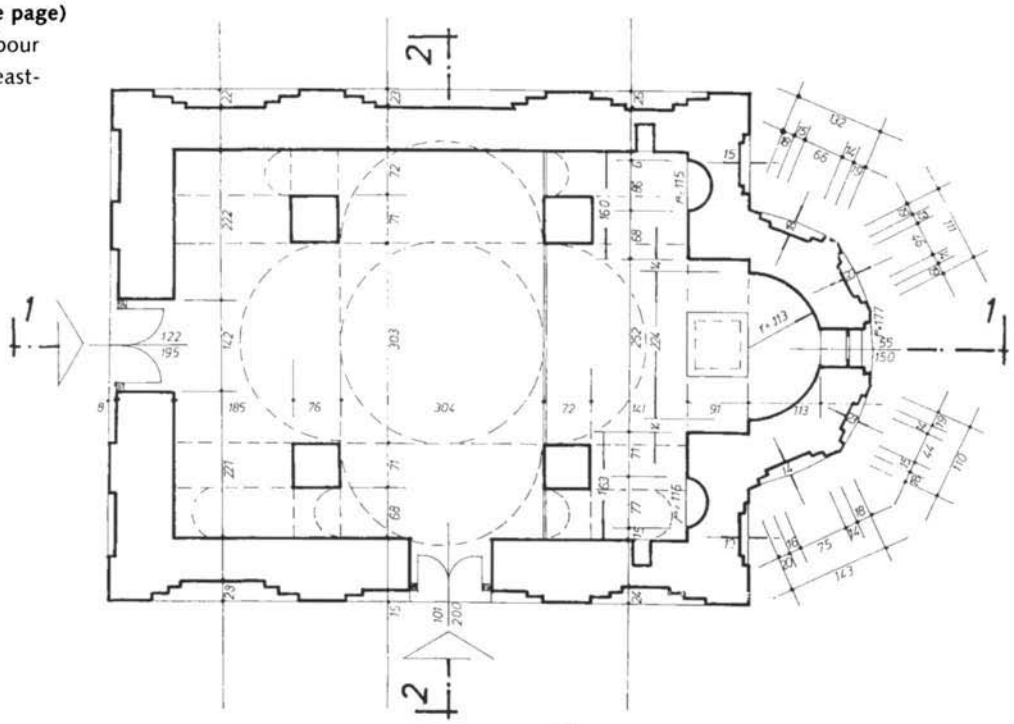

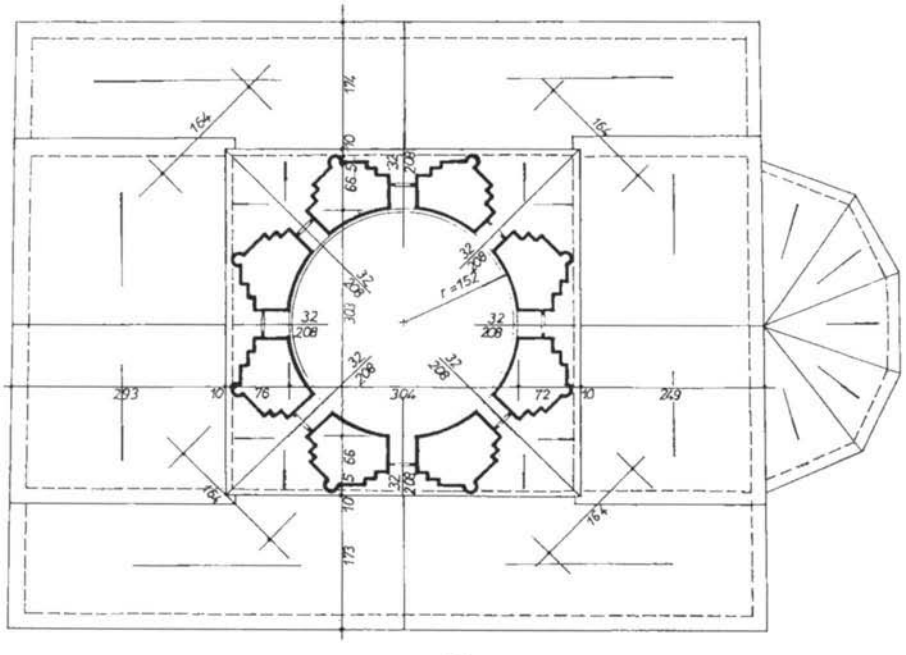

Special attention was paid to the construction of the facades, as is evident from the three-dimensional polychromy, the pronounced horizontal double brick rows, the framing of the dressed and rubble stone, and the visual interruption of the flat areas by shallow niches and pilasters, which are related structurally to the church plan.

The positions of the pilasters on the south, west, and north facades correspond to those of the internal columns, which contribute to the stability of the building (fig. 3.5). Two shallow niches were formed

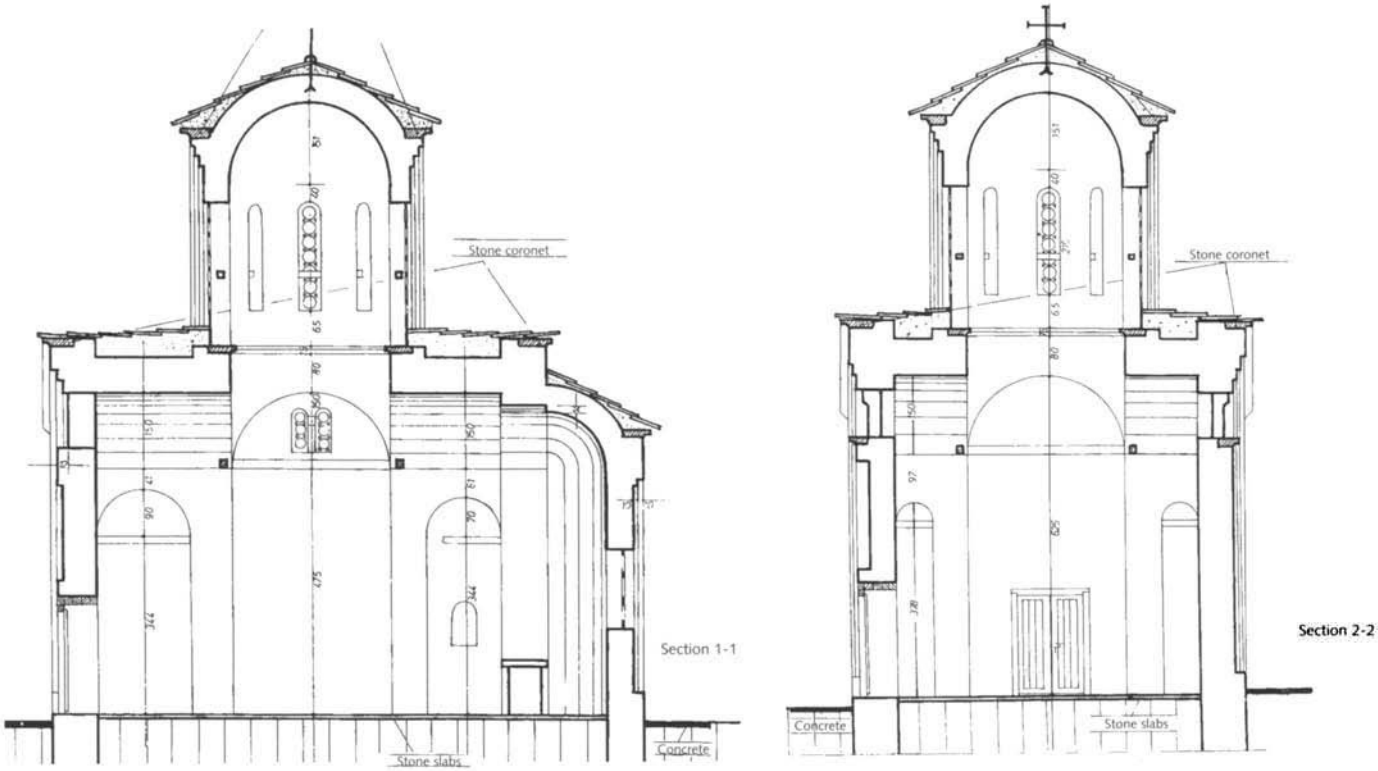

in the gable wall over the west entrance, while the south wall (see fig. 3.3) has a shallow, single niche with a blind arch. All niches on the north facade are triple, with three blind arches constructed of bricks (see fig. 3.5), and a double niche occupies the central part of the south facade (fig. 3.6).

Figure 3.5
St. Nikita: north facade window.

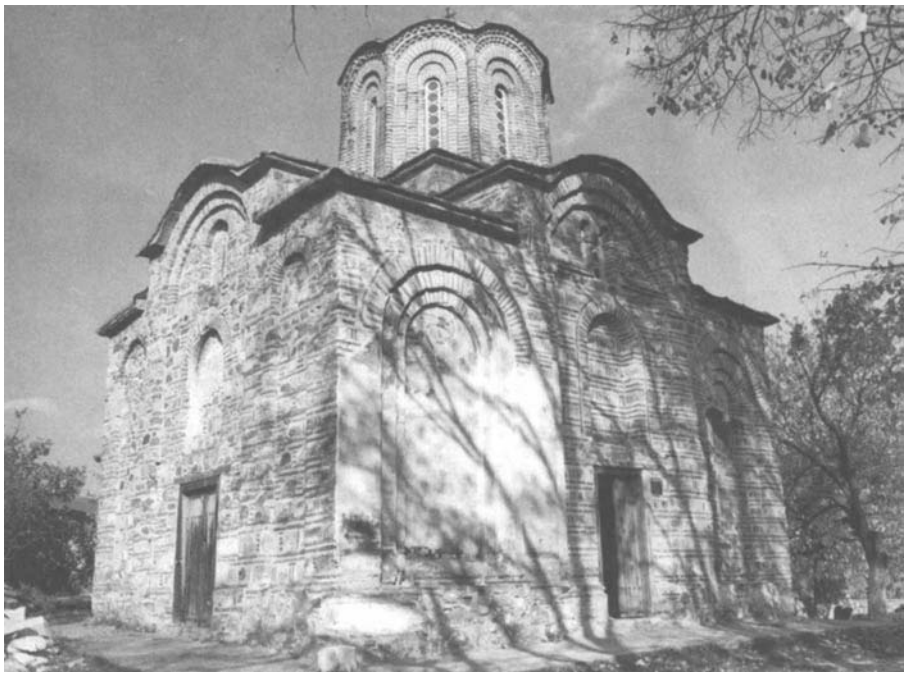

Figure 3.6
St. Nikita: west and south facades.

Figure 3.7
St. Nikita: apse.

Figure 3.8
St. Nikita: tambour.

Figure 3.9
St. Nikita: fresco.

The pentagonal apse (fig. 3.7) is broken up visually by double niches with blind brick arches, the tympanums of which are characterized by polychromy achieved by varied arrangements of bricks (rhomboids, cubes, and alternating horizontal and vertical bricks). All the cornices, with the exception of those of the tambour, are constructed of wavy, double-dentiled brick courses. The tambour is fabricated entirely of brick, and the corners are constructed in the form of semicircular pilasters without capitals (fig. 3.8). The recent reconstruction of the upper part of the tambour and the need for replacement of deteriorated mortar in the lower section are evident.

Frescoes

The fresco paintings in the interior of the church date from the time of King Milutin's invasion of Macedonia (1313–15) and were created by the well-known medieval fresco painters Michael and Eutychios. The wall frescoes and the scenes in the dome and the vaulted areas of the church were repainted in the post-Byzantine period (fifteenth century) and are of special importance to the history of medieval art in Macedonia. The fourteenth-century fresco paintings were largely preserved in the lower and middle areas of the church, but in most of the upper areas no paintings survived the early earthquakes. The fifteenth-century paintings on the dome and the upper portion of the tambour did survive.

The painting of frescoes on church domes and walls is a tradition established during earlier Byzantine and Balkan periods. Full-length figures of saints were painted on lower walls (fig. 3.9), and frescoes that depicted the great feasts, the Passion, and the miracles and parables of Christ were presented in the upper regions of the church. The two artists' obvious differences in painting technique make it clear that one worked on the north half of the church and the other on the south. They collaborated on the monumental composition *The Communion of the Apostles,* situated in the apsidal conch (fig. 3.10) and *The Dormition of the Holy Virgin,* on the west wall (fig. 3.11).

Structural system

The wall elements of the building are original and date from the fourteenth century. However, the upper levels and the roof of the church were reconstructed in 1977–78, and the appearance of the building has not changed since then. The structural system of the building consists of massive facade walls constructed of rough-hewn stone, polished stone, and brick. At the foundation level, the walls are 85 cm thick. The vaulted roof elements and the central dome over the naos rest on the walls and two rows of symmetrically placed columns. The massive walls, columns, and vaults are capable of carrying the compressive stresses in the structure caused by gravity loads.

The walls are constructed primarily of dressed limestone, sandstone, and layers of brick set in lime mortar. The recessed technique was used to create wide expansion joints, visible on the facade. The columns were fashioned in a similar way. The tambour and dome are constructed of brick.

Figure 3.10
St. Nikita: fresco.

Figure 3.11
St. Nikita: fresco.

The wall structure is characterized by the presence of timber belts, which consist of two 10 × 10 or 12 × 12 cm timber beams placed within the facade walls and connected transversely by smaller beams spaced 60–70 cm apart. The timber belts are incorporated into the wall mass and extend around the entire perimeter of the walls at two levels. As mentioned earlier, the invisible timber belts served to level the massive wall cross sections during the construction. Along with the timber ties visible within the church, the belts connect building elements, especially the walls, thus increasing the stability of the structure under seismic loads. This enables the individual wall elements to act synchronously and provides structural integrity to the church. However, because the timber elements are organic materials they tend to decay in the course of time and have ceased to function as elements that can sustain tensile forces. This is one of the reasons for the deterioration of the structural capacity of St. Nikita over time and for the damage resulting from recent earthquakes.

Previous conservation efforts and present condition of St. Nikita

During the earthquake that occurred in Skopje on July 26, 1963, the church structure was damaged, but it was repaired immediately after the earthquake. However, the repairs did not include seismic strengthening. In 1978–80 extensive structural repairs were carried out, and conservation work was performed on the upper interior areas, the dome, and the frescoes. The repairs involved removal of the couple roof areas and

reconstruction of the edge cornices, the upper zones of the perimeter walls, and the base of the tambour, using profiled stone cornices. The upper cornices of the tambour were erected in a wavy double-dentiled design. The vaulted upper areas of the cross arms remained round, while the space between the arms remained flat and inclined toward the perimeter walls. The entire building was reroofed and covered with lead sheathing 3–4 mm thick.

In general, the church building is in good condition and no urgent water-related problems have been noted. As a result of the recent replacement of the lead sheathing, the roof does not leak, and the effect of capillary moisture arising from the ground is negligible. Neither severe cracks nor extensive deformations of the walls have been observed. Because the building was constructed on stable soil, there are no indications of bulging of the walls or differential settlement of the structure.

Chemical analysis of masonry materials

Stone

Limestone, in both rough and surface dressed states, was used in construction of the church. In most cases, the limestone was quarried from surface mines that are still in use. For facade construction, tufa was often used, since it is easily cut and shaped, especially when moist. Travertine, dolomite, and granite were also used for wall construction, but to a lesser extent.

Brick

Brick was the principal masonry material used for the surfaces of structural elements such as walls, vaults, arches, and domes. Brick size varied depending on its use: for facade, wall mass, perimeter walls, tambour, cornices, blind niches, and so forth. In general, bricks were produced in a variety of lengths and widths, but always with a constant thickness of 3.0–3.2 cm. Brick manufacturing technology was well established during the Byzantine period, and a stable product was obtained that withstood damage from mechanical stress and weathering. Bricks found in many existing Byzantine structures have survived in surprisingly good condition.

Mortar

Lime mortars were used exclusively in the construction of churches for filling and pointing joints between masonry elements, for fresco wall plasters, and for finishing the surfaces of other interior walls. The composition of mortars and plasters for these purposes varied depending on the intended use. Particle size distributions and the lime-sand ratios were the principal variables, and often organic fibers or proteins were added to minimize cracking during drying and to increase strength. Crushed brick and clay were also often added, and this too resulted in a stronger mortar. Typical results of chemical analysis and particle size distribution of St. Nikita wall mortars are given in table 3.3.

Characteristic	Sample 1	Sample 2
Loss on ignition	22.01%	26.25%
Insoluble residue	39.90%	44.02%
CaO	22.24%	16.64%
MgO	11.88%	11.08%
$Al_2O_3 + Fe_2O_3$	1.72%	2.06%
Total	97.75%	100.05%
Crushed brick	(+)	(+)
Straw	(–)	(–)
Proteins	(+)	(+)
Binder-filler ratio	1:2	1:3

Table 3.3
Chemical composition of St. Nikita wall joint mortar

The river sand used had the following particle size distribution:

0.1–0.4 cm 65%
0.4–0.8 cm 15–20%
0.8–1.6 cm 15–20%

Mortars taken from fresco areas in the interior of the church and from fresco paintings on the south facade were analyzed chemically and by microscopy to identify the pigments used. Mortar compositions are shown in table 3.4.

The fresco mortars all contained detectable amounts of straw. Apparently, more dolomitic lime was used in the fourteenth- than fifteenth-century mortar. The loss on ignition varied from 45% to 48.69%. In all samples, carbonization was complete, and no free calcium hydroxide, hydroxyaluminates, or hydroxysilicates were present, indicating the absence of hydraulic mortars. Chlorides and nitrates were also present in small amounts.

The following fresco pigments were identified: azurite, malachite, yellow ocher, red ocher, sienna, hematite, green earth, lime, and charcoal. In the lower layers, lime was used as a binder, whereas tempera and calcium caseinate were the binders in the upper, pigmented layers.

Characteristic	Sample 1	Sample 2	Sample 3
Loss on ignition	45.15%	48.69%	45.00%
Insoluble residue	3.47%	1.40%	2.65%
CaO	38.10%	46.53%	42.61%
MgO	8.49%	2.90%	6.09%
$Al_2O_3 + Fe_2O_3$	0.96%	0.48%	1.35%
Total	96.17%	100.00%	97.70%
Binder-filler ratio	8.5:1	20.3:1	11.3:1
Straw	(+)	(+)	(+)
Free $Ca(OH)_2$	(–)	(–)	(–)

Table 3.4
Chemical composition of St. Nikita fresco mortars

Examination of fresco cross sections revealed that green and blue pigmented layers were applied over black layers. Dark blue was obtained by mixing green, gray, or orange pigment with the black; and the green color was attributed to a mixture of malachite and green earth.

Analysis of the seismic stability of St. Nikita

Preliminary analyses were carried out to define the mechanical and dynamic characteristics of the structural materials and the seismic parameters of the church of St. Nikita. The results of this study formed the basis for a detailed analysis, which in turn allowed for an estimate of the existing structure's seismic stability. The purpose of these calculations was to evaluate the ultimate bearing and deformability capacity of the church structure under several different seismic excitation conditions. A mathematical model normally used for analysis of masonry structures was used for the static analysis of the building. For the dynamic analysis, a single-degree-of-freedom system was assumed, and a trilinear hysteretic model developed at IZIIS was used in the analysis (Gavrilović 1982).

Mechanical characteristics of the church masonry were obtained experimentally. The mortar's compressive and tensile strengths, which are probably the most critical parameters, were found to be f_c = 1340 kPa and f_t = 60 kPa, respectively. The calculated bearing capacity of the masonry, expressed in terms of the base shear capacity coefficient, was K_{bc} = 0.17 for the state at which the first cracks in the structure appear. For the ultimate state, the base shear capacity coefficient was K_{bc} = 0.21, where $K_{bc} = S_{ui} / G$ (S_{ui} = ultimate seismic force and G = mass of the building).

Evaluation of the bearing capacity of the structure was calculated for the two types of seismic excitations that were considered to be highly probable at the location of St. Nikita. The first of these excitations would be similar to that caused by the 1976 earthquake at Friuli, Italy, and recorded at Breginj, Macedonia. The Breginj record is representative of a "local" earthquake (less than 40 km from the site). The 1979 earthquake in Montenegro, Yugoslavia, which was recorded at Petrovac, and the 1940 earthquake in El Centro, California, represent more distant (more than 40 km) earthquakes.

The dynamic analysis estimated that if St. Nikita were to be exposed to an El Centro–magnitude earthquake, the first cracks in the structure would appear at a ground acceleration of a_{max} = 0.14 g. At this point, the structure would no longer be in the elastic range. It was estimated that structural failure, which is defined as collapse of the entire structure, would occur at a_{max} = 0.20 g. For a Petrovac earthquake, calculations estimated that the elastic range would end when cracking occurred at a_{max} = 0.12 g, and failure took place at a_{max} = 0.20 g. The ductility or deformability of the St. Nikita church structure, calculated for the Petrovac- and El Centro–type earthquakes at various values of acceleration, is given in table 3.5.

On the basis of detailed analysis of the stability of the structure, it was concluded that at an expected acceleration level of a_{max} = 0.12–0.14 g, which corresponds to an earthquake with a return period

Table 3.5
Calculated ductility of St. Nikita for different earthquakes and input accelerations

	Ductility ($\mu = d_{max}/d_y$)			
Earthquake acceleration (g)	**0.12**	**0.20**	**0.29**	**0.36**
Petrovac	1.04	1.64	2.49	4.80
El Centro	1.01	1.53	2.22	2.58

of 100 years ($\mu < 1.5$), the building would suffer damage only to the secondary elements, and minimum deformations of its bearing structural elements would occur.

For expected earthquakes with $a_{max} = 0.20$ g, failure of some parts of the structure—such as the dome, tambour, cornices, and lintels—would be likely to occur, and severe structural damage to the bearing walls would take place ($1.5 < \mu < 2.5$). However, the building would still be repairable after an earthquake with a return period of 200 years.

For an earthquake with $a_{max} = 0.36$ g, which corresponds to an earthquake of the maximum severity expected in this area, the results indicate that total failure of the building would occur ($\mu > 2.5$). This was taken to correspond to an earthquake return period of 1000 years.

Note

1. The MCS (Mercalli-Cancani-Sieberg) scale is a measure of the relative damaging effects of earthquakes on structures and the environment.

This page intentionally left blank

Chapter 4

Proposed Strengthening Method and Preliminary Analysis of the Retrofitted St. Nikita Church

Designing structural repairs and strengthening methods that can enable historic buildings to survive seismic loading requires knowledge of the building site's seismicity parameters, the probable earthquake characteristics, and the location and maximum extent of damage that can be tolerated. The three principal safety criteria defined for historic structures are given in chapter 1 (see pages 1–2).

For each specific structure, design criteria are defined on the basis of the historic significance of the building, the seismic hazard, and the feasibility of incorporating suitable repair and strengthening measures.

Possible Methods for Repair and Strengthening of Historic Structures

The requirements for repair and strengthening methods to be implemented are directly related to the restoration and conservation ethics of the community, which ultimately has the responsibility for guiding the selection of structural measures used to assure the seismic safety of the structure. To arrive at an adequate repair-and-strengthening methodology, it is necessary to perform a detailed structural analysis of the building that takes into account the type and physical-mechanical characteristics of the masonry and other supporting elements.

Depending on the building's level of vulnerability, the repair-and-strengthening method should increase the strength of the existing structure or increase its ductile capacity—or, in certain cases, do both. It should be pointed out that historic structures are, in general, different in many ways from conventional, more modern structures, and this gives the design engineer fewer options in selecting an adequate repair method. If the load-carrying capacity of the existing support elements of the structure is not sufficient to receive and transfer the forces generated during an earthquake, new structural elements need to be inserted.

After a consideration of factors such as the existing state of St. Nikita, the causes of failures that have occurred in the past, the results of the analysis of the probable seismic stability of the church under the existing conditions, and the safety and design criteria mentioned above, the project team concluded that the principal areas of concern in strengthening the structural systems were the integrity of the

structural system at the floor and roof levels, the moment and shear resistance of the structure, and its ductile capacity.

Analysis of damaged massive structures has shown that one of the initial types of failure is wall separation and deterioration of the structural integrity resulting from the inability of the floor or roof structures to withstand the earthquake-generated tensile forces. Thus, the main strengthening goal should be to provide structural integrity, which can be achieved by inserting tie elements that enable the structure to perform as an entity. From an analysis of the failure mechanisms of certain walls, it is clear that the principal walls should have sufficient capacity to resist shear forces and moments, as well as have ductile capacity.

In general, the moment resistance of walls depends on their geometrical characteristics and on their capacity for withstanding tensile forces. Masonry itself has little tensile strength, and therefore strengthening is necessary. This can be achieved in one of two ways: (1) by increasing the tensile capacity of the masonry by using grouting to replace damaged mortar and fill existing wall cracks; or (2) by inserting reinforcements at the ends of the walls.

Historical masonry structures behave rigidly but tend to fail in shear—an effect that also depends on the tensile strength of the masonry. As mentioned previously, the load-carrying capacity of masonry in traditional Byzantine construction was increased by inserting wooden belt courses, starting at the roof level, at several levels in the walls, at the ends of the vaults, above window and door openings, down to the foundation. Two possible methods of strengthening are to replace timber belt courses with steel elements and to inject modern bonding compounds into voids and cracks.

In summary, the proposed methods for repair and strengthening are as follows:

- Strengthening the main structural system at the roof level with horizontal, steel-tie elements and partial injection inside the linear elements; replacing the traditional horizontal wooden ties with steel ties, which are coupled to the existing masonry with a grout; and grouting of masonry cracks. These methods are suitable for structures such as small, compact churches or those that have many load-carrying elements and are located in zones of low seismicity.
- To ensure seismic stability, it is at times necessary to augment horizontal elements with vertical elements to control tensile forces resulting from overturning moments. Vertical elements can be inserted at the ends of the walls or around the openings and should be grouted in place by injection. To achieve a higher bearing capacity in the case of anticipated axial stresses, prestressed vertical steel bars can be distributed uniformly along the length of the wall. The void space around the steel bar should be filled with a

high-strength grout that ensures connection with the existing masonry and avoids damage to the fresco mortar on the interior surface of the wall. Because of their flexibility, such vertical belt courses should be used for the columns of the tambour. Horizontal strengthening of the base of the tambour and the dome should also be provided.

- To increase the shear capacity of the masonry, a high-strength lime mortar grout should be used. The composition of the injection grout must be chosen carefully to ensure penetration and bonding of the steel belts and ties to the existing masonry. It is important that the grout be compatible with the fresco mortar.

Design of the St. Nikita Church Model

To verify the proposed concepts for the repair and seismic retrofitting of Byzantine churches, a scale model of St. Nikita was constructed and tested on the seismic simulation shaking table in the Earthquake Engineering Test Laboratory of IZIIS in Skopje, Macedonia. This section discusses the basic principles of model analysis and selection of the scaling factors. Details of the design and construction of the church model and the model testing protocol are discussed later in the chapter.

Model analysis and scaling factors

A dimensional system represents a set of physical quantities that is used for solving problems related to physics. For example, for addressing problems related to dynamics, a dimensional system is formulated in which all significant quantities (displacements, velocities, accelerations, forces) are derived from the three principal parameters: length (L), time (T), and mass (M).

The physical law referring to any phenomenon depending on n-quantities, $x_1, x_2, \ldots, x_n$, can be represented implicitly by equation 4.1.

$$f(x_1, x_2, \ldots, x_n) \tag{4.1}$$

The same equation can be rewritten in the form

$$f(\pi_1, \pi_2, \ldots, \pi_n) \tag{4.2}$$

where π_i is a nondimensional relation corresponding to x_i.

Buckingham's theorem

If a dimensional system with n quantities contains k main quantities, then each physical phenomenon can be represented by m independent π relations, where $m = n - k$. Hence, the above equation can be replaced by the reduced expression

$$F(\pi_1, \pi_2, \ldots, \pi_m) \tag{4.3}$$

in which only the important nondimensional relations are included when several quantities of the same dimension (the dimension that is already included in the general expression) are considered—for instance, length and displacement, inertial and elastic forces, stresses and elasticity modulus, and so forth.

Two systems are identical if all points of one system have identical counterparts in the other and if the physical quantities have constant relations with the corresponding points. The similitude condition can be expressed in the form

$$\phi_m(\pi_1, \pi_2, \ldots, \pi_k) = \phi_p(\pi_1, \pi_2, \ldots, \pi_k) \tag{4.4}$$

where the subscripts *m* and *p* represent two similar systems, for instance, a model and a prototype.

The first step in each model analysis is the definition of all the physical quantities relevant to the phenomenon under analysis. The fundamental basis of the dynamic analysis of structures is the differential equation of motion, which, for an oscillating, multiple-degree-of-freedom system, can be represented as

$$[m]\{\ddot{x}\} + [c]\{\dot{x}\} + [k]\{x\} = \{p(t)\} \tag{4.5}$$

where matrices [m], [c], and [k] represent the mass, damping, and stiffness of the system, respectively; vectors $\{\ddot{x}\}$, $\{\dot{x}\}$, and $\{x\}$ represent the response accelerations, velocities, and displacements, respectively; and vector $\{p(t)\}$ represents the external forces acting upon the system. If the elements of this matrix equation are analyzed, all the physical quantities necessary for the dynamic analysis will be obtained.

Table 4.1 shows how all quantities can be represented by three principal physical quantities: mass (M), length (L), and time (T). That is, all the problems related to dynamics of structures can be analyzed by use of the MLT dimensional system.

For determination of the nondimensional π products, three random quantities, *x*, *y*, and *z*, are selected. The product of these contains all the quantities of the MLT system that are used to determine the twelve nondimensional products by applying the following expression:

$$\pi_i = u_i / (x^{k1}\, y^{k2}\, z^{k3}) \tag{4.6}$$

This procedure is illustrated by the following example: Let the three random quantities in the analysis be length L (geometry of the system); specific density of the material used for construction, ρ, which is characteristic of the material; and stress, σ, which is the tangential stress at the base. Their product, expressed in terms of the MLT system, is given by

$$\begin{aligned} l^{k1}\, \rho^{k2}\, \sigma^{k3} &= [L]^{k1}\, [ML^{-3}]^{k2}\, [ML^{-1}\, T^{-2}]^{k3} \\ &= L^{k1-3k2-k3}\, T^{-2k3}\, M^{k2+k3} \end{aligned} \tag{4.7}$$

The nondimensional product, π, for force P is determined, according to equation 4.6, as follows:

Physical quantity	Indication	Dimensions
Length, displacement	l, x	L
Velocity	V	LT^{-1}
Acceleration	a, g	LT^{-2}
Time	t	T
Frequency	f	T^{-1}
Mass	m	M
Force	P, G	MLT^{-2}
Moment of force	M	ML^2T^{-2}
Stress	σ, τ	$ML^{-1}T^{-2}$
Mass density	ρ	ML^{-3}
Deformation	ε , γ	–
Modulus of elasticity, shear modulus	E, G	$ML^{-1}T^{-2}$
Poisson coefficient	ν	–
Damping coefficient	μ	–
Moment of inertia	I, F	L^4, L^2

Table 4.1
Physical quantities in model analysis of problems related to dynamics of structures

$$\pi_7 = P / (l^{k1}\, \rho^{k2}\, \sigma^{k3}) = MLT^{-2} / (L^{k1-3k2-k3}\, T^{-2k3}\, M^{k2+k3})$$
$$\pi_7 = L^{1-k1-3k2+k3}\, T^{-2+2k3}\, M^{1-k2-k3} \tag{4.8}$$

From the condition of nondimensionality of π_7, it follows that

$$1 - k1 + 3k2 + k3 = 0$$
$$-2 + 2k3 = 0$$
$$1 - k2 - k3 = 0$$

The following is obtained by solving this system of equations:

$$k1 = 2,\ k2 = 0,\ k3 = 1$$
$$\pi_7 = P / L^2\, \sigma \quad \text{i.e.,}\ P_m / L_m{}^2\, \sigma_m = P_p / L_p{}^2\, \sigma_p \tag{4.9}$$

Finally,

$$P_r = P_m / P_p = \{l_m / l_p\}^2 \{\sigma_m / \sigma_p\} = l_r{}^2\, \sigma_r \tag{4.10}$$

Using the same procedure, the scales of all model parameters expressed via the scales of the previously selected quantities (l_r, ρ_r, and σ_r) are shown in table 4.2.

Selection of scaling factors

The model used for determining the dynamic behavior of the church during seismic simulation was designed in accordance with the basic principles of model analysis. The model parameter scale was chosen based on the following criteria:

k1 = size of the seismic simulation shaking table (4.5 × 4.5 m)
k2 = total allowable height of the model (10 m)
k3 = total weight of the model (400 kN)
k4 = realistic simulation of nonlinear behavior
k5 = realistic simulation of failure mechanisms

Physical quantity	π value	Scale
Length, displacement	$\pi_1 = l$	l_r
Velocity	$\pi_2 = V / (\sigma / \rho)^{0.5}$	$V_r = (\sigma_r / \rho_r)^{0.5}$
Acceleration	$\pi_3 = al\rho / \sigma$	$a_r = \sigma_r / l_r \rho_r$
Time	$\pi_4 = t / l (\rho / \sigma)^{0.5}$	$t_r = l_r / (\rho_r / \sigma_r)^{0.5}$
Frequency	$\pi_5 = fl / (\sigma / \rho)^{0.5}$	$f_r = (\sigma_r / \rho_r)^{0.5} / l_r$
Mass	$\pi_6 = m / l^3 \rho$	$m_r = l_r^3 \rho_r$
Force	$\pi_7 = P / l^2 \sigma$	$P_r = l_r^2 \sigma_r$
Moment of force	$\pi_8 = M / l^3 \sigma$	$M_r = l_r^3 \sigma_r$
Stress	$\pi_9 = \sigma$	σ_r
Mass density	$\pi_{10} = \rho$	ρ_r
Deformation	$\pi_{11} = \varepsilon$	ε_r
Modulus of elasticity, shear modulus	$\pi_{12} = E / \sigma$	$E_r = \sigma_r$
Poisson coefficient	$\pi_{13} = \nu$	ν_r
Damping coefficient	$\pi_{14} = \mu$	μ_r
Moment of inertia	$\pi_{15} = I / l^4$	$I_r = l_r^4$

Table 4.2
Scaling factors for model parameters used in dynamic analysis

Geometrical scale

The geometrical scale of the model was determined considering the first three criteria. For an assumed scale of l_r = 1:2.75, the following dimensions of the model were obtained:

length: $b_m = 11.4 / 2.75 = 4.15$ m
width: $d_m = 7.7 / 2.75 = 2.80$ m
height: $H_m = 12.4 / 2.75 = 4.50$ m
mass: $G_m = 4670 / 2.75^3 = 210$ kN

Density

From condition k4 and considering that masonry is a nonhomogeneous material, it follows that the model must be constructed of the same materials as the prototype: stone, brick, and limestone. Hence, the scale of density is defined as $\rho_r = 1$.

Stress

Considering condition k5 and the fact that the failure mechanism depends mostly on the stress states of specific walls, the scale for normal stresses is $\sigma_r = 1$. In this case, the stress is given by

$$\sigma_r = m_r g_r / F_r = 1 / 2.75 \tag{4.11}$$

The required additional normal stresses are provided by application of a corresponding prestressed force in the vertical reinforcement bars placed at the ends of the walls and around the openings. During the construction of the model, these vertical steel bars were inserted in the walls, but a void was left around them to prevent contact with the adjacent masonry during testing of the unretrofitted model. As described later, this void space was filled with a grout during strengthening of the model.

Elasticity modulus

From the condition for realistic simulation of the failure mechanism, stress scale $\sigma_r = 1$, it follows that the scales of the elasticity modulus and the shear modulus are given by $E_r = 1$. For natural materials, similar values of E_m and E_p were easily obtained.

Mass

Starting with relation $m_r = lr^3 \sigma_r$, the following is obtained:

$$m_r = 1 / 2.75^3 (1) = 1 / 2.75^3 \tag{4.12}$$

Hence, to satisfy the geometrical and density scales, it follows that the mass of the model has to be $1 / (2.75)^3$ times the mass of the prototype.

Frequency

The natural frequencies are the principal dynamic characteristics of structures. Their relation to the excitation frequency content of the source has a significant effect upon the dynamic response of the structure and can induce either amplification or attenuation of the seismic effects. Resonance is the ultimate case of this phenomenon.

Starting with the relation

$$f_r = (\sigma_r / \rho_r)^{0.5} / l_r = \{1 / 2.75\}^1 = 2.75 \tag{4.13}$$

it follows that if the natural frequency of the prototype is $f_p = 4.8$ Hz, that of the model should be $f_m = 13.2$ Hz.

Using the ambient vibration technique, a value of $f_m = 11.0$ was obtained during tests of the model under laboratory conditions. This difference was probably due to the difficulty of using masonry materials that have exactly the same characteristics as those of the prototype.

Time

Time is a very important quantity in dynamic analysis, and all terms in the equation of motion (4.5) are functions of time. Time is inversely proportional to frequency, which in this case means that the time scale must be reduced; the scale of the input excitations should be reduced by a factor of 2.20.

Velocity

Velocity is a physical quantity that is used directly in the equation of motion (4.5). In this case, velocity is not measured during the tests but is given only for theoretical purposes—that is, for the generalization of the concept

$$V_r = (\sigma_r / \rho_r)^{0.5} = 1 \tag{4.14}$$

Acceleration

Starting with the expression $a_r = \sigma_r / 1_r \rho_r$, the scaling factor of $a_r = 2.75$ is obtained. Considering the scaling factors obtained for f_r and t_r, the acceleration values are reduced by a factor of 2.20 when interpreting the results of the model tests.

The structure that was modeled was characterized by a very low level of normal stress at the base. Therefore, gravitational forces were neglected, and $g_r = 1$.

Forces

Forces are important parameters in studies of the dynamics of structures. The dead weight of the structure, $Q_i = (m)(g)$, is used for obtaining the normal stresses and the inertial forces, $P_i = (m)(a)$. The force scaling factor is defined by the following expression:

$$P_r = l_r^2 \sigma_r = (1 / 2.75^2)(1) = 1 / 2.75^2 \tag{4.15}$$

Considering that ground acceleration cannot be simulated and that the model mass depends on volume (l_r^3), the following is obtained:

$$P_r = l_r^3 \tag{4.16}$$

Although gravity forces were neglected, an effective normal stress was achieved by prestressing the vertical reinforcement.

Moment of force

This quantity represents a product of force and length. Hence, its scaling factor can be derived directly as the product of the corresponding scaling factors:

$$M_r = P_r l_r = l_r^3 \sigma_r = 2.75^3 \tag{4.17}$$

Damping coefficient

The damping coefficient, μ, is a nondimensional quantity that is expressed as a percentage of the critical damping. The value of this coefficient depends on many factors (geometry, material, mass, stiffness) and is usually determined experimentally. In the case of a model designed in proportion to the prototype, a value of $\mu_r = 1$ was adopted.

Poisson coefficient

The Poisson coefficient, ν, is a nondimensional factor that is characteristic of a material. If $\nu_r = 1$, which is quite realistic for the materials under consideration, the sliding modulus will be $G_r = E_r = 1$.

Deformation

Deformations are nondimensional quantities used directly in the analysis. Their scaling factors can be selected arbitrarily and are independent of other parameters. For the model with neglected gravity forces, $\varepsilon_r = 1$ and $\varepsilon_m = \varepsilon_p$.

Area and moment of inertia

These two quantities are directly related to the geometrical scale and are not used in this analysis. They are given here for purely practical reasons, in that they are used as input data for the mathematical model and as an illustration of the direct determination of the design quantities.

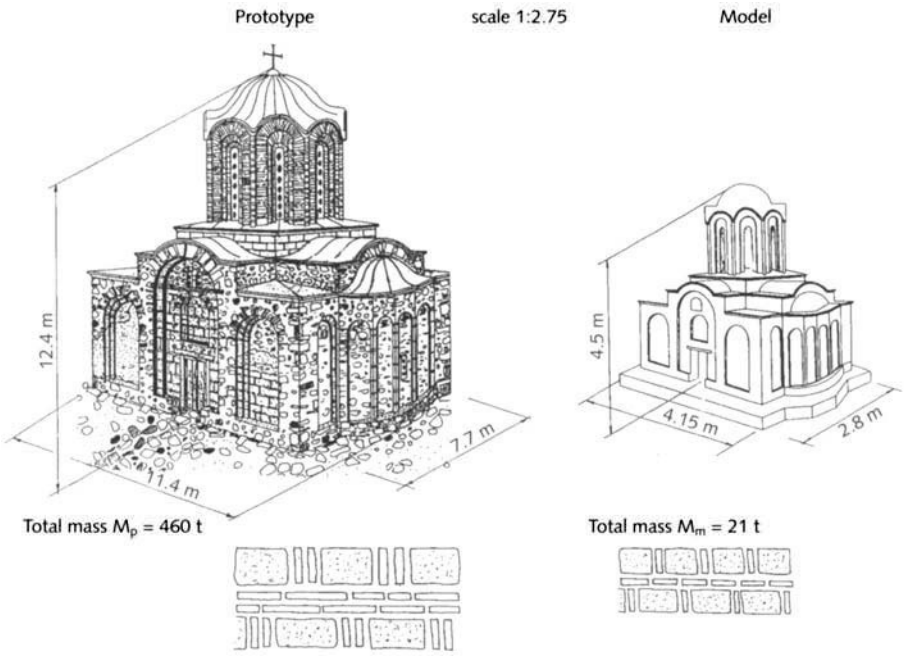

Figure 4.1
Size comparison of prototype St. Nikita and model church

$$F = l^2 \Rightarrow F_r = l_r^2 = 1 / 2.75^2; \quad F_m = (1 / 2.75^2)\, F_p \tag{4.18}$$

$$I = l^4 \Rightarrow I_r = I_r^4 = 1 / 2.75^4; \quad I_m = (1 / 2.75^4)\, I_p \tag{4.19}$$

A comparison of the principal characteristics of the prototype and the model is shown in figure 4.1 and table 4.3.

Model Construction

A model of the St. Nikita church prototype was constructed using the scaling parameters described in the previous section. The model was built to an approximate scale of 1:2.75. The structural elements of the model—walls, arches, vaults, tambour, and dome—were constructed with special care. A plan view and sections of the model are shown in figures 4.2 and 4.3, respectively. The model was constructed in compliance with the following general principles and criteria:

- The materials to be used for the construction of the model must be approximately the same as those of the prototype with respect to chemical, physical, and mechanical strength characteristics.
- The preparation, treatment, and incorporation of the construction materials for the model must be carried out in the same way as in the original church, that is, by hand.
- The traditional technologies used for constructing structures in the Byzantine period must be used. This refers especially to the *order* of construction of both the structural and nonstructural elements of the walls.

Table 4.3
Comparison of the principal properties of the prototype and model

Parameter	Units	Prototype (x_p)	Model (x_m)	Ratio (x_p / x_u)	Design scale
Total length by total width	m	11.4 x 7.70	4.15 x 2.80	2.75	2.75
Height	m	12.46	4.50	2.76	2.75
Volume	m^3	270	11.60	23.20	$2.75^3 = 20.8$
Bulk density	kN/m^3	17.29	17.80	0.97	1
Force	kN	4670	202	23.10	$2.75^2 = 7.56$
Tambour area	m^2	5.56	0.76	7.31	$2.75^2 = 7.56$
Wall area	m^2	30.30	3.90	7.76	$2.75^2 = 7.56$
Average s_0 at the tambour level	kN/m^2	87.00	89.00	0.98	1
Average s_0 for the walls	kN/m^2	116.00	110.00	1.05	1
Moment of force	kN sec^2/m^2	476	20.2	23.2	$2.75^3 = 20.8$
Modulus of elasticity (E)	kN/m^2	680,000	650,000	1.05	1
Compressive Strength (f_c)					
Mortar	MPa	1.34	0.55	2.40	1
Tufa	MPa	13.95	7.30	1.90	1
Brick	MPa	31.00	21.30	1.45	1
Shear strength					
Tufa	MPa	0.145	0.075	1.90	1
Mortar	MPa	0.102	–	–	1
Bending capacity					
Brick	MPa	5.0	4.70	1.06	1
Mortar	MPa	–	0.30	–	1
Frequency in north-south direction	Hz	4.8	11.2	0.42	1 / 2.75 = 0.36

- Repair and strengthening elements must be constructed and incorporated without adversely affecting the strength characteristics of the model.

Materials used in the model

Stone

Two types of stone were used. A limestone obtained from a quarry in the vicinity of the monastic complex in the village of Banjani was used for the interior face of the walls. Its chemical and mechanical characteristics were the same as or similar to those of the prototype. The sizes of the individual stone blocks did not exceed 12–15 cm. The second type of stone was a natural tufa limestone taken from the deposits in the vicinity of the village of Veljusa in the Strumica commune. This limestone was used on the external structure and had the same chemical, physical, and mechanical strength properties as those of the prototype. Most of the tufa was cut manually, but some blocks were mechanically dressed to the required size.

Brick

Bricks used for the construction of the walls, arches, vaults, tambour, and dome of the model church were prepared and fired in the facilities of

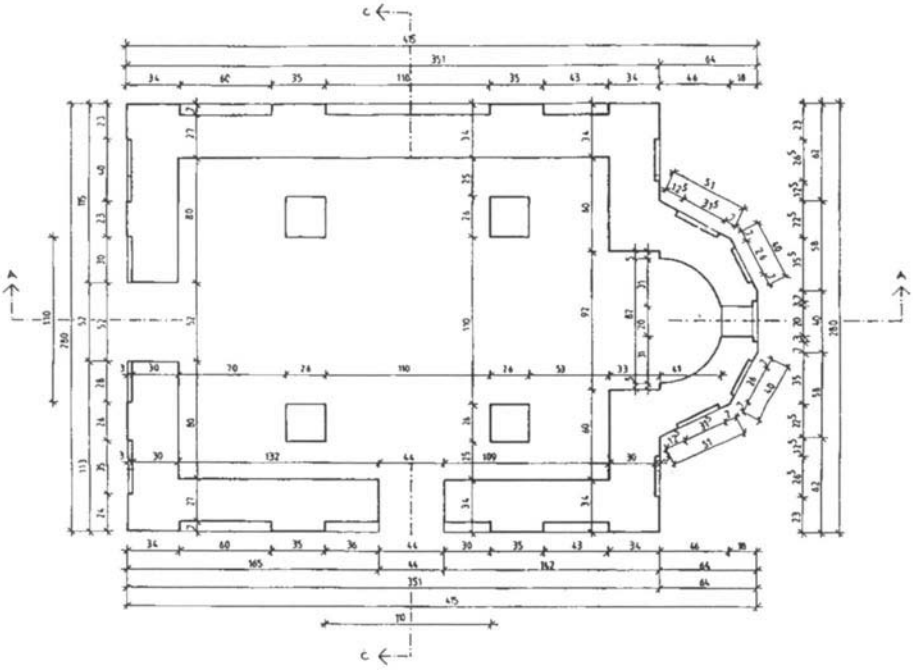

Figure 4.2
Dimensioned plan of model.

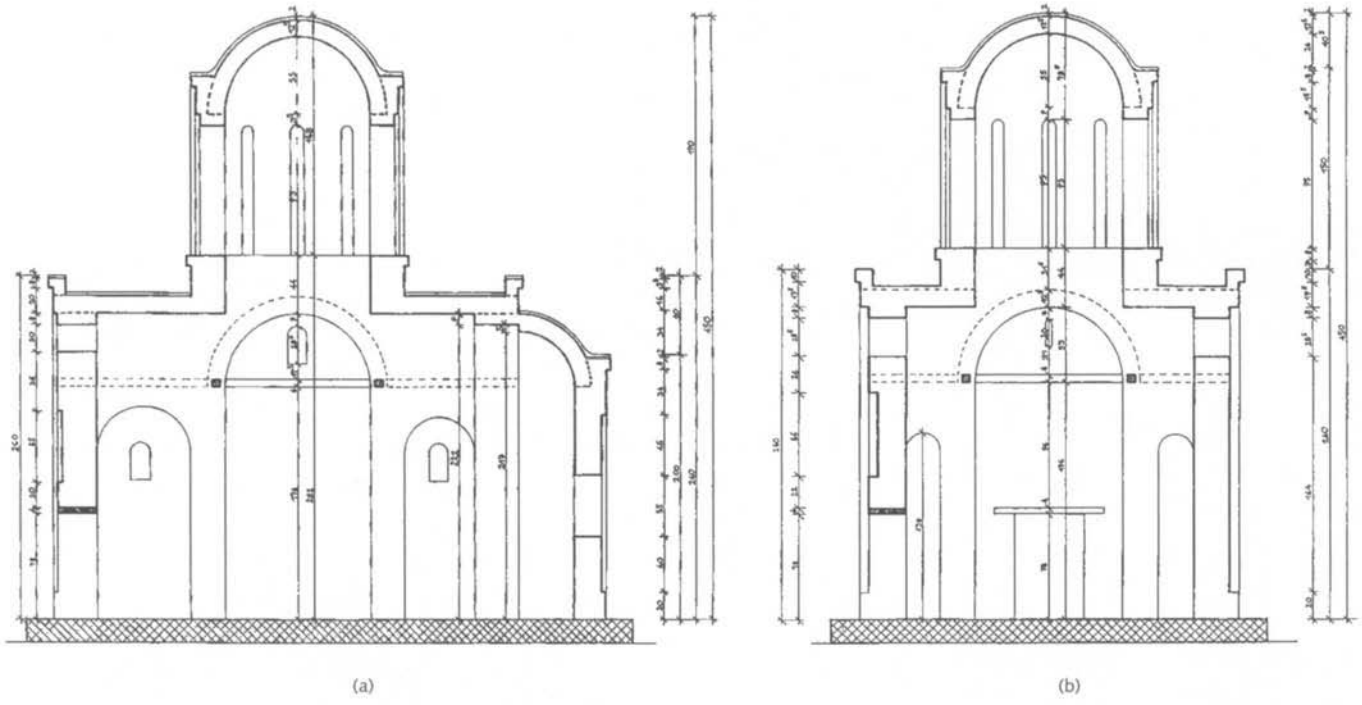

Figure 4.3
Elevations of model: (a) north-south, (b) east-west.

CI Elenica in Strumica, an organization experienced in the production of nonstandard sizes of bricks for conservation use in Macedonia. The brick size was 12 × 12 × 3 cm, and the composition, structure, and strength were about the same as those of the prototype bricks.

Lime mortar

Lime mortar was prepared in the traditional manner from slaked dolomitic lime, and the lime putty was aged for more than a year before use. For the preparation of mortar for construction, pointing, and plastering, the aged lime putty was mixed with river sand as the aggregate in a ratio of 1:2.5 (binder to filler). The grain size distribution was 65% at 0–4 mm, 15–20% at 4–8 mm, and 15–20% at 8–16 mm.

For the preparation of pointing mortar, the same ingredients were used, but the fraction of larger-grain sand (8–16 mm) was drastically reduced.

The interior wall plaster consisted of two layers of fresco-type mortar. Lime putty and sand were used; however, the binder-to-filler ratio was changed to 4:1, and chopped oakum was added as reinforcement. This composition was similar to that of the prototype church wall plaster. (Further details of the lime-mortar research, compositions tested, and mechanical properties are given in Gavrilović, Šumanov, et al. 1991, vol. 11.)

Wood

Fir was used for the construction of the interior timber ties.

Steel

The strengthening methodology required the use of 4-mm-thick steel plates for stress distribution at the ends of the ribbed steel reinforcement bars, which were 10, 14, and 16 mm in diameter. Their bearing capacities were σ_y = 400 MPa and σ_u = 500 MPa.

Figure 4.4
Model foundation during construction.

Figure 4.5
Model vault construction.

Building the model

The model was constructed on a reinforced concrete platform, which served as a foundation for the model. The platform, which measured 2.92 × 4.30 × 0.25 m, was bolted to the shaking table. The connection between the perimeter walls of the church and the concrete platform was provided by stone anchors, which were incorporated into the platform and protruded 3–4 cm from its surface. The anchors were added to prevent the model from sliding on the concrete platform during the test.

The walls of the model were constructed in accordance with typical Byzantine design: two faces of stone and brick separated by an infill of stone and brick rubble set in lime mortar. The wall thickness varied from 27 to 33 cm, and the horizontal mortar layers were 2.5 cm thick. Figure 4.4 shows the foundation level of the walls and the positioning of the vertical reinforcement bars. Removable plastic tubes were used to prevent contact of the bars with the wall during construction. The void space thus created was filled with grout during the strengthening phase.

The thickness of the arches, vaults, and dome was 12 cm, which was equal to the brick thickness (fig. 4.5). These elements, along with the blind niches, pilasters, and other interior and exterior architec-

Figure 4.6
Model under construction.

Figure 4.7
Model under construction.

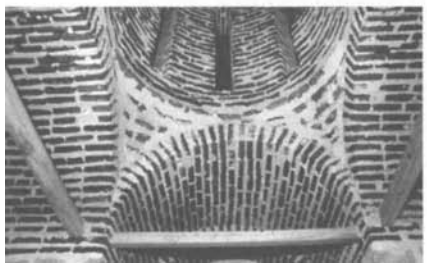

Figure 4.8 (near right)
Model interior showing timber ties, brick pendentives, and plastered walls.

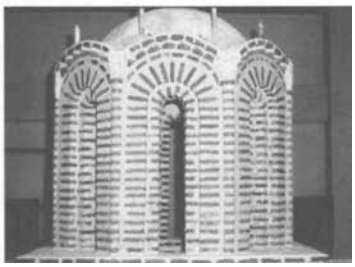

Figure 4.9 (far right)
Model tambour and dome.

Figure 4.10
Completed model.

tural elements, were simulated with regard to both appearance and the order and the continuity of construction. Figures 4.6 and 4.7 show the model at different stages of construction. Figure 4.8, an interior view, shows the timber ties at the vault level and the spherical, triangular pendentives that connect the vaults to the tambour above. A close-up of the tambour and dome is shown in figure 4.9, and a photograph of the completed model appears in figure 4.10.

After construction of the model was finished, the facades were pointed with lime mortar to a thickness of 1.5–2 cm. Half of the

church interior (the part south of the east-west axis) was plastered with two layers of fresco mortar, the first layer having a thickness of 1–1.5 cm and the second, finishing, layer having a thickness of about 0.5 cm. All roof areas were plastered with a layer of lime mortar 1–1.5 cm thick. After construction was completed, the model was aged for 45 days to allow the lime mortar to cure. After curing, the model was lifted, moved, and bolted to the shaking table.

Wall Element Tests

A series of static laboratory tests were conducted to determine the properties of the masonry materials used for construction of the model. In addition to the static testing of samples of materials, quasi-static tests of wall segments were also necessary to define the mechanical strength characteristics, bearing capacity, failure mechanisms, and other parameters of the masonry sections that affect the walls' dynamic behavior.

Three sections of the model walls were constructed and tested using the same materials and wall structures as those of the model. Two wall sections (WAC-1 and WAC-2) were subjected to axial compression tests, and a shear compression test was performed on the third section (WSC-3). All tests were performed up to failure of the wall section. The parameters recorded were the total force and the actuator displacement in the direction of the applied force.

Figure 4.11a shows the instrumentation locations and the loading pattern for the WAC-1 wall element. This element was subjected to axial compression by cyclic loading and unloading. The type of failure is shown in figure 4.11b. Figure 4.11c shows the P-Δ diagrams for the total axial shortening of the wall and side deformation. Important results of the WAC-1 test were

- occurrence of the first cracks (point 45) at $\sigma_0 = 270$ kPa
- tensile strength: $f_t = 35$ kPa
- initial sliding modulus: $g = \tau_u / \gamma = 165{,}000$ kPa
- maximum normal stress:
  $\sigma_0^{max} = 140 \text{ kN} / 0.243 \text{ m}^2 = 567$ kPa

The second (WAC-2) element was exposed to axial compression by a monotonic, gradual increase of the force amplitude up to the point of complete failure. The failure mechanism and the P-Δ diagrams for the shortening and lateral deformation of the element are given in figure 4.12b and c, respectively. The following results were obtained:

- Occurrence of the first crack (point 82) at $\sigma_0 = 257$ kPa
- Maximum normal stress at failure (compressive strength):
  $\sigma_0^{max} = f_c = 136 / 0.243 = 560$ kPa
- Initial modulus of elasticity:
  $E_0 = \sigma / (\Delta l / l) = 650{,}000$ kPa

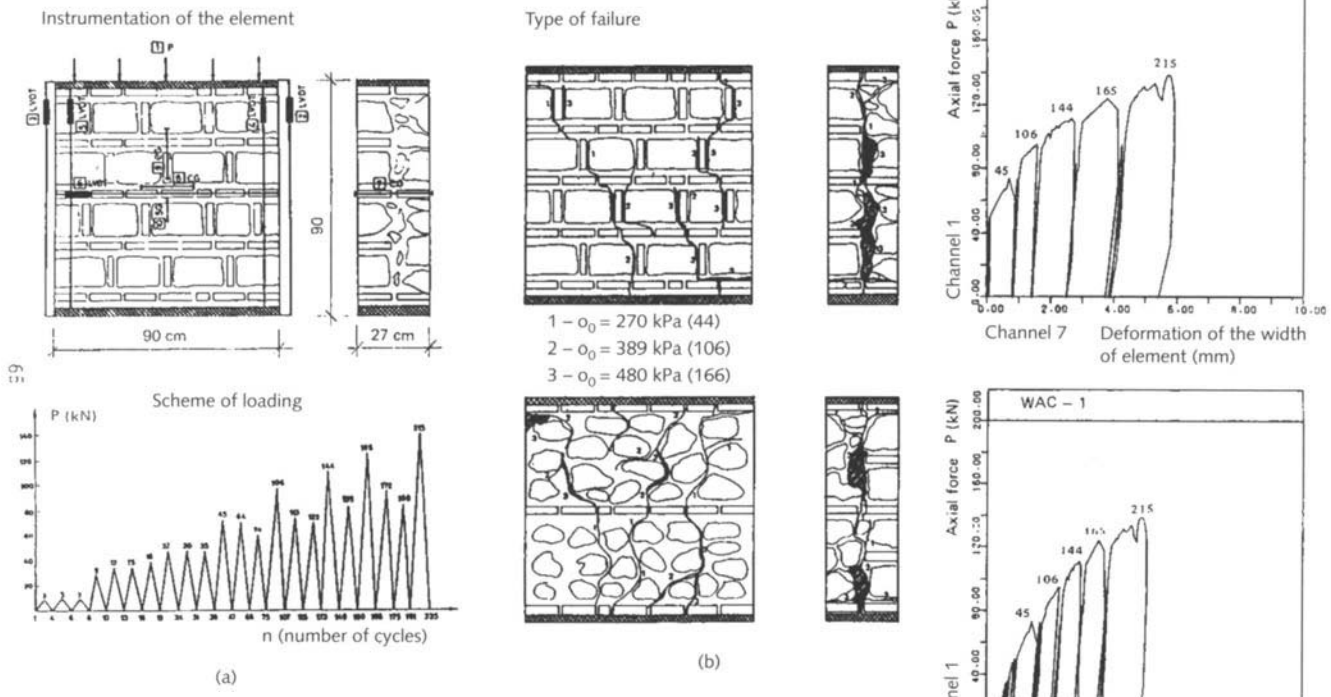

Figure 4.11 (above)
Wall section, test WAC-1, axial compression by cyclic loading: (a) instrumentation of the element, (b) type of failure, (c) P-Δ diagrams for total axial shortening of the wall and the side deformation.

Figure 4.12 (below)
Wall section, test WAC-2, axial compression by monotonic loading increases: (a) instrumentation of the element, (b) type of failure, (c) P-Δ diagrams for total axial shortening of the wall and the side deformation.

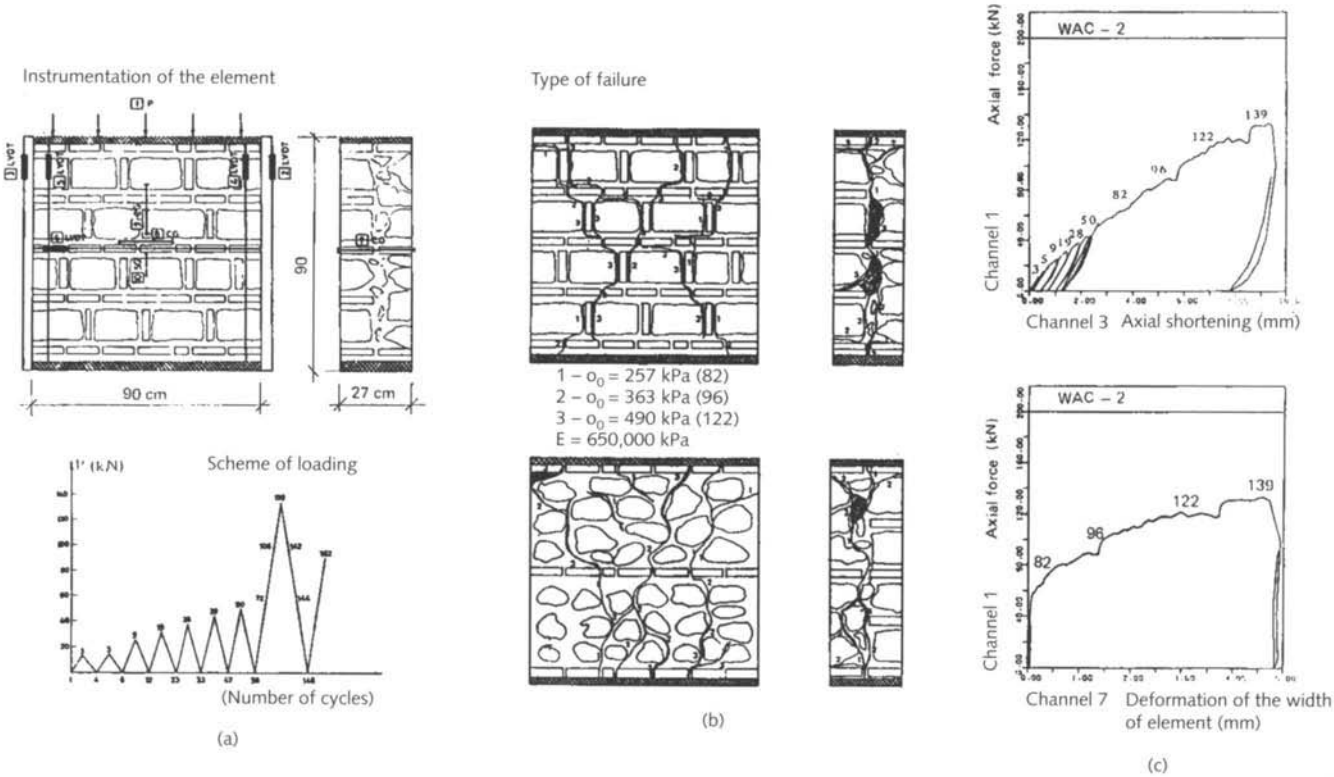

Both elements that were exposed to axial loads were characterized by occurrence of lateral cracks along the center of their width, which in both WAC-1 and WAC-2 resulted in loss of material and, in the case of WAC-2, total separation of the two faces of the wall. In the case of the third element, WSC-3, the force was applied monotonically at an angle of 45 degrees relative to the expansion joints of the wall up to total failure of the sample (fig. 4.13). Figure 4.13b shows the characteristic failure mechanism with the occurrence of diagonal cracks, and figure 4.13c shows the P-Δ diagrams for the deformations along the element diagonals, which yielded the sliding angle (distortion). In this test, the values of the tangential and normal stresses (τ_u and σ_0) are identical because of the angle of action of forces with respect to the planes of failure development.

- Maximum normal stress: $\sigma_0^{max} = \tau_u^{max} = 55$ kPa
- Tensile strength: $f_t = 35$ kPa
- Initial sliding modulus: $G = \tau_u / \gamma = 165{,}000$ kPa

These results were used as main input parameters for analysis of the model, not only from the aspect of application of seismic effect by a shaking table (for the repaired and the original model), but also for interpretation of the model's behavior.

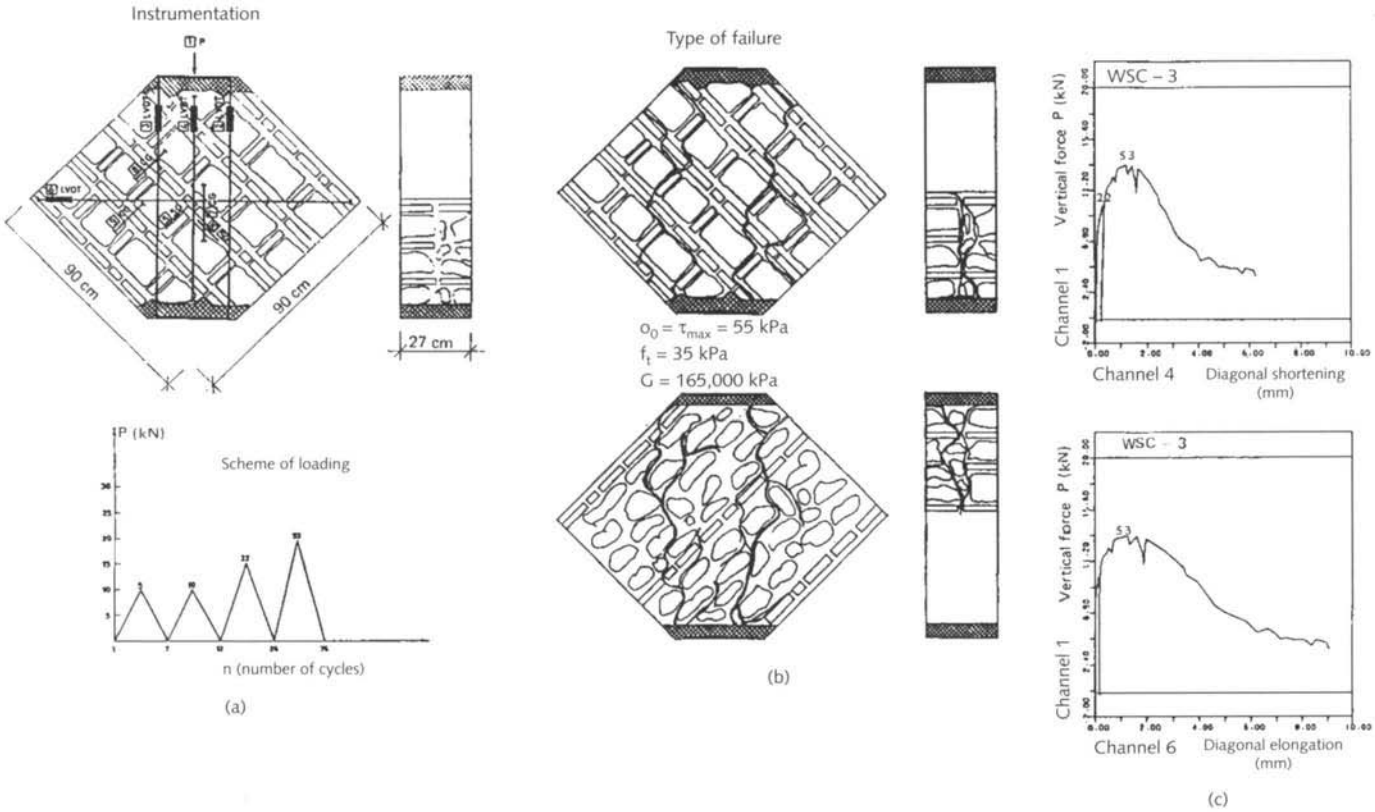

Figure 4.13
Wall section, test WSC-3, axial compression at a 45-degree angle: (a) instrumentation, (b) type of failure, (c) P-Δ diagrams for total axial shortening of the wall and the side deformation.

Chapter 5

Shaking-Table Tests of the St. Nikita Church Model

The biaxial shaking table at IZIIS was used to generate programmed motions that simulate known earthquake frequency-time spectra. The shaking table was controlled by a complex integral electro-hydraulic system that can control the programmed generation of translational vibrations in both horizontal and vertical directions (Larson 1972; Jurukovski and Mamucevski 1986). The control signal was generated by a digital computer with a subsystem for D/A, a noise generator, and a standard function generator. The model to be tested on this system was supported on a rigid body slab that was symmetrical about its center. The dimensions of the prestressed concrete slab were $5 \times 5 \times 0.8$ m, and its total mass was about 35 tons.

The shaking table was supported by four hydraulic actuators, two providing vertical motion and two operating horizontally. Simultaneous control of displacement, velocity, and acceleration of the shaking table was provided by three variable controllers. Preliminary processing in the time domain included conversion of data into engineering units, determination of time histories along the main stress directions, determination of maximum and minimum values, calculations of arithmetic media, and determination of amplitude distribution and standard deviations. Preliminary processing in the frequency domain included only determination and plotting of Fourier amplitude spectra. The spectral plots provided clear representations of the dynamic characteristics of the structure being tested and precise values of the natural frequencies of the model or the structural process spectra.

The model response was monitored by a thirty-two-channel, high-speed data acquisition system consisting of eleven accelerometers, seventeen displacement transducers, and four strain gauges. These instruments provided information on accelerations at different levels and points on the model, relative displacements, structural deformations, and strains at selected locations (fig. 5.1).

The shaking-table motion was controlled by an accelerometer and monitored by a displacement transducer, both of which were mounted on the table itself. Time histories of the displacement and acceleration of the table were considered to be the ground motion input. Response of the model at various levels and locations was obtained by measuring accelerations and displacements at the top of the dome and at a number of points along the height of the model, as well as at several points at level 1 (fig. 5.1).

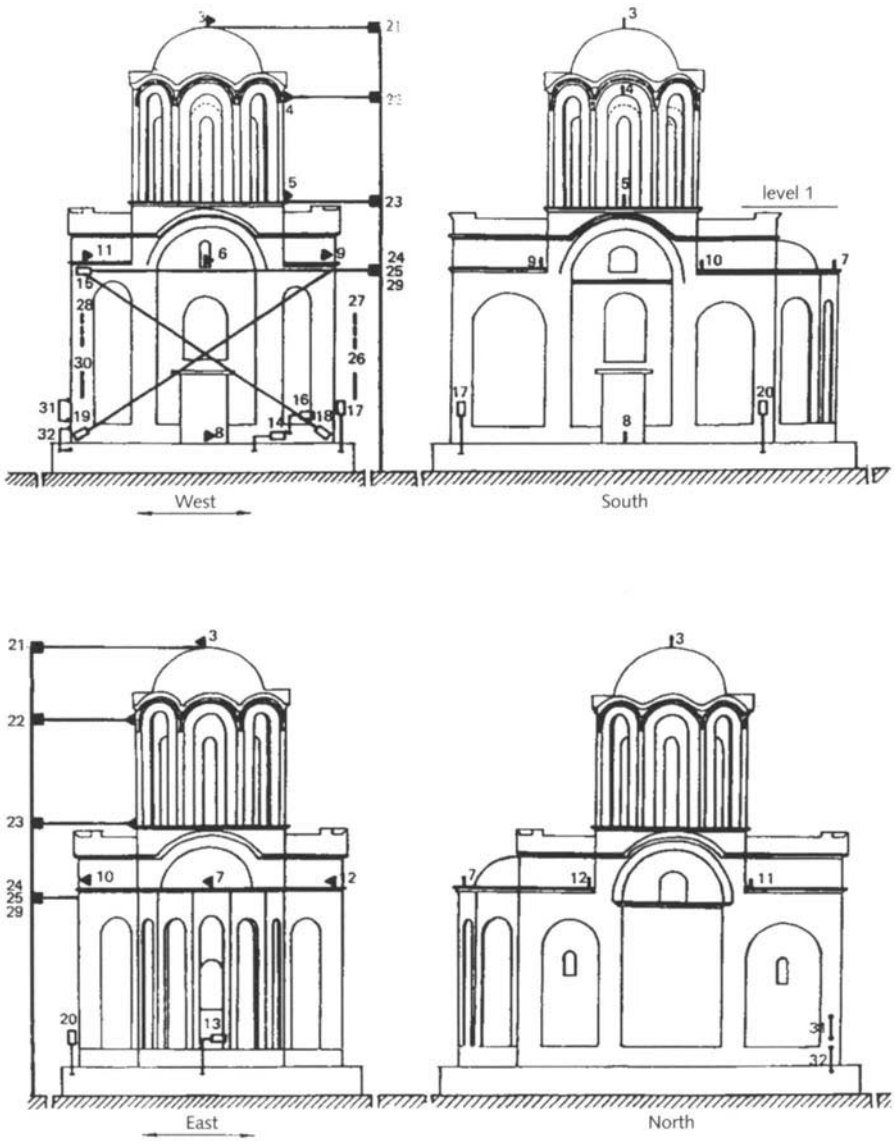

Figure 5.1
Location of model instrumentation.

Tests of the Original Church Model

The principal objectives of the shaking-table tests of the original model that simulated the existing state of the St. Nikita church were (1) to evaluate the vulnerability of the building to damage by earthquakes of increasing intensities and (2) to select the most appropriate procedures for repairing and strengthening the structure after earthquake damage. To achieve these goals a series of tests were performed in which the input earthquake excitations were gradually increased. The following parameters were monitored: the elasticity limit and the first occurrence of cracks, the progressive development of cracks, the modification of the dynamic characteristics and the phases of dynamic model behavior, and ultimately the failure mechanisms.

Ambient vibration measurements were carried out to check the dynamic properties of the original model before it was subjected to earthquake excitation and, later, on the strengthened model after repairs

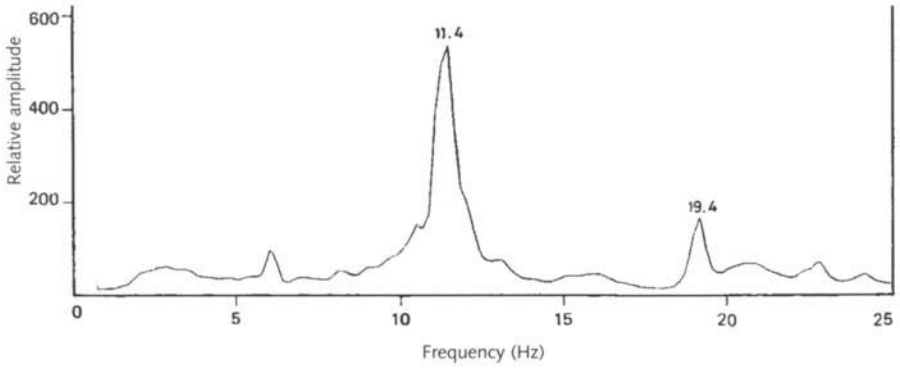

Figure 5.2
Ambient vibration spectrum of model.

had been performed. For these tests, the natural vibrations in the engineering building were used as the activation source. A Ranger seismometer was placed at the dome of the model, and the frequency spectrum was recorded in the range of 0–50 Hz. The Fourier amplitude spectrum clearly showed the dominant peak values corresponding to the natural frequencies of the model (fig. 5.2).

To obtain more precise measurements of the natural frequencies, mode shapes, and damping coefficients in both orthogonal directions of the model, forced vibration tests were performed on both the original and repaired models. For this purpose, a small electrodynamic shaker was placed at level 1 of the vaults. One accelerometer was placed at the top of the dome as a reference, and a second was placed successively at various locations around the models to obtain the vibration mode shapes.

Random excitation tests were also performed. This testing method is based on the use of a white noise input excitation when multifrequency components uniformly participate in the Fourier amplitude spectrum of input motion within the selected frequency range. This excitation was applied by shaking the original and strengthened church models in the north-south direction on the shaking table. The model responses showed the natural frequencies as dominant in Fourier amplitude spectra. In this case, a frequency range of 0–30 Hz was selected and was simulated by the shaking table.

The seismic simulation response tests were performed by applying the time history spectra of three different types of earthquakes: the earthquake at Friuli, Italy (1976), as registered in Breginj, Macedonia, which was taken to represent a local type of earthquake; the earthquakes at Petrovac, Montenegro (1979), and at El Centro, California (1949), served as distant earthquakes. Both the original and strengthened models were tested under the three types of earthquakes to predict the prototype behavior under different earthquake conditions. Table 5.1 shows the earthquake excitations with applied input acceleration levels. Figure 5.3 shows the scaled time histories of acceleration and the corresponding spectra of these excitations.

Detailed visual inspection of the models was performed after each excitation to define the initial cracking, the progress of crack development, the failure mechanisms, and the character of damage to the original model compared to that of the strengthened model. Documentation

Table 5.1
Input acceleration levels for selected earthquakes during seismic testing of the church model

	Type of earthquake		
Intensity	**El Centro**	**Petrovac**	**Breginj**
Linear tests (0.1 g)	0.05–0.1 g	0.04–0.1 g	0.07 g
Moderate intensity (0.3 g)	0.17–0.25 g	0.19–0.28 g	0.15–0.25 g
High intensity (0.4 g)	0.33–0.55 g	0.45 g	0.38–0.75 g

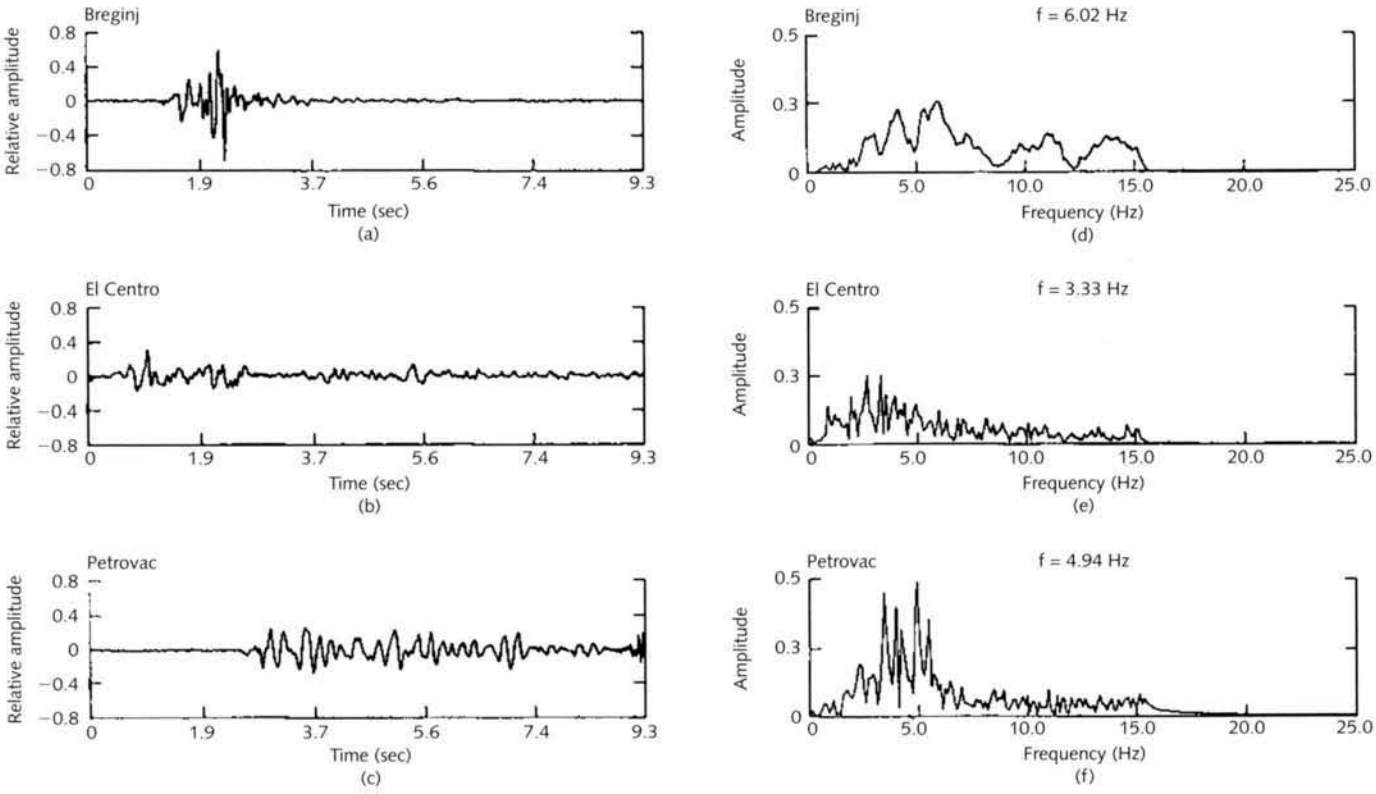

Figure 5.3
Scaled time histories of the amplitude as functions of time and frequencies for the Breginj, El Centro, and Petrovac earthquakes.

of the incremental damage to the structure after each excitation was carried out using both video and still photography.

Seismic response of the original model was investigated by applying the three different earthquake excitations at various intensity levels. Excitation was applied in the north-south direction of the model, and twelve tests were performed, starting at low intensity levels and increasing the excitation progressively. Table 5.2 presents the program of the seismic response tests together with maximum accelerations recorded at two characteristic levels of the model (at the top of the dome and at level 1, at the base of the tambour) and the relative displacements recorded at these levels.

The frequency content of the model's amplitude response, which was given by the Fourier amplitude acceleration spectrum for the top of the dome and for various input intensities of the Petrovac and El Centro earthquakes, is shown in figure 5.4. These spectra show that the fundamental mode is predominant and that the response of the church is governed by the fundamental mode, which is expected for structures of this type.

Table 5.2
Input and maximum accelerations and displacement responses for the original model tests

Test number and code	Input acceleration (g)	Maximum response				Damage
		Level 1		Top		
		Acceleration (g)	Displacement (mm)	Acceleration (g)	Displacement (mm)	
6 PET005N	0.02	0.02		0.04		None
7 ELC005N	0.02	0.02		0.04		
8 BRE003N	0.02	0.05		0.10		
9 PET012N	0.04	0.18	0.7	0.16	0.7	
10 ELC015N	0.04	0.05	0.8	0.11	0.7	
11 PET035N	0.10	0.22	1.9	0.49	2.2	
12 ELC045N	0.12	0.18	1.8	0.40	1.8	
13 BRE006N	0.08	0.17	0.9	0.41	2.3	
14 ELC085N	0.17	0.29	2.5	0.55	2.6	
15 PET075N	0.19	0.39	5.3	0.76	11.1	Cracks
16 BRE012N	0.17	0.22	1.8	0.52	4.5	
18 ELC130N	0.43					Failure

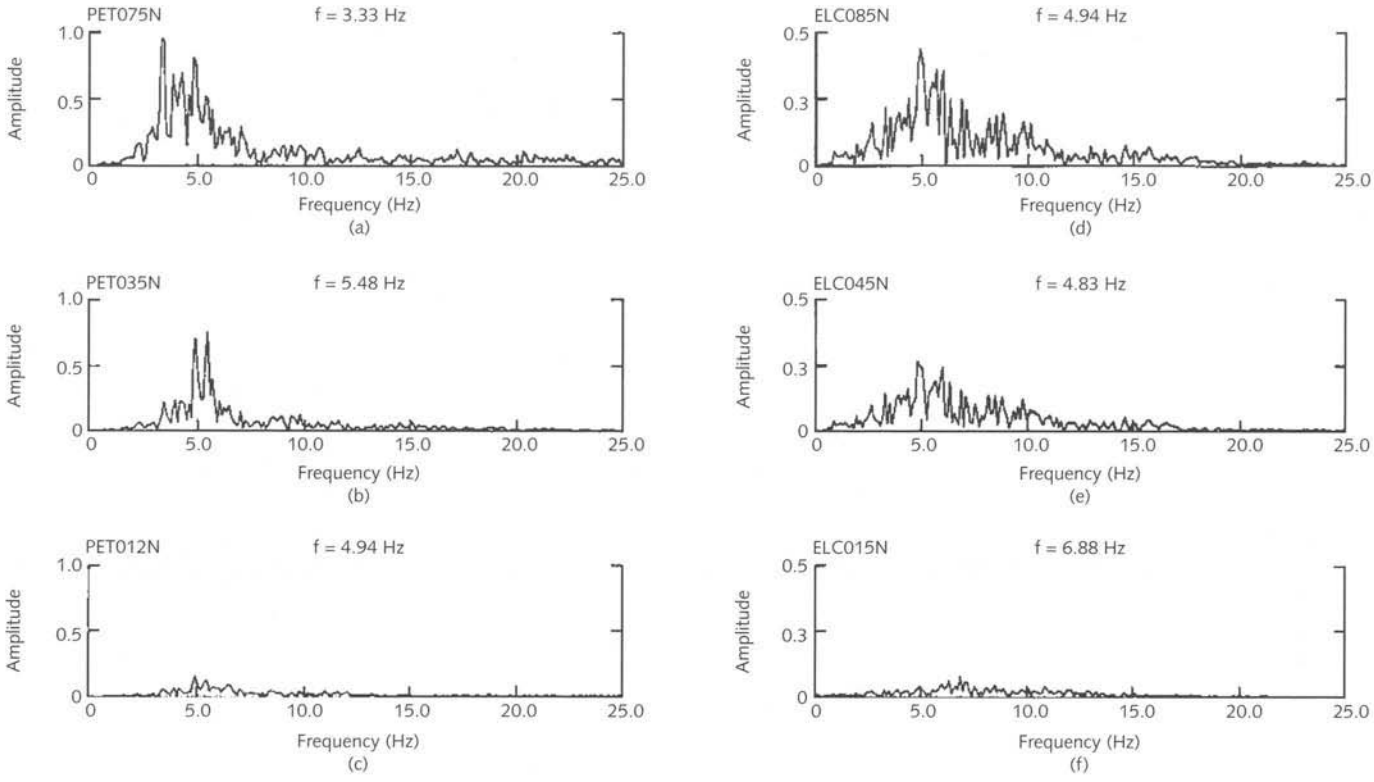

Figure 5.4
Amplitude-frequency responses at the top of the dome of the original model as functions of various input accelerations for the Petrovac and El Centro earthquakes. Frequencies at maximum amplitude are shown.

Comparison of the amplification at the top of the structure caused by earthquakes having relatively close input intensities (table 5.2) clearly showed that the Petrovac and El Centro earthquakes caused more intensive damage to the model than did the Breginj earthquake. Time histories of accelerations and relative displacements for the original model at different intensities of the three simulated earthquakes are presented in

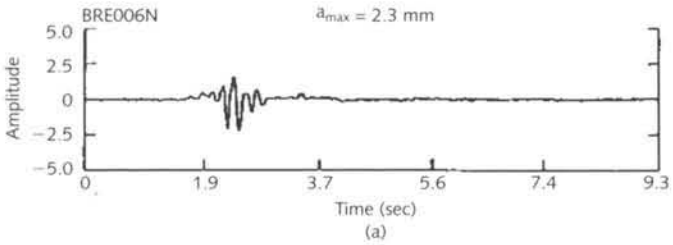

(a)

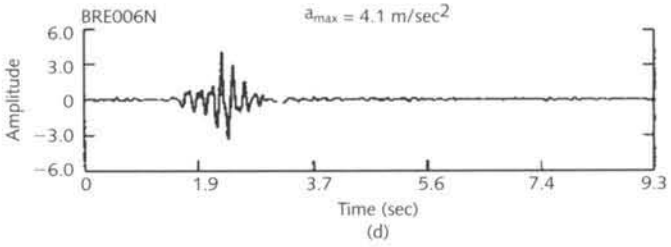

(d)

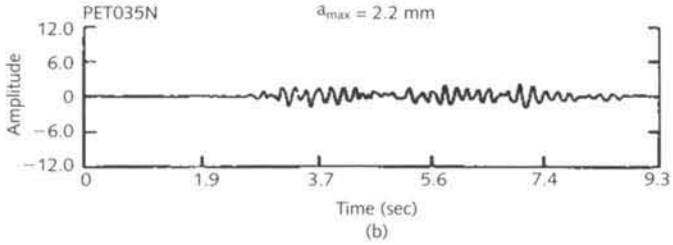

(b)

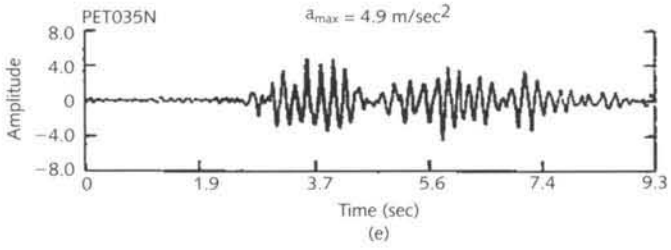

(e)

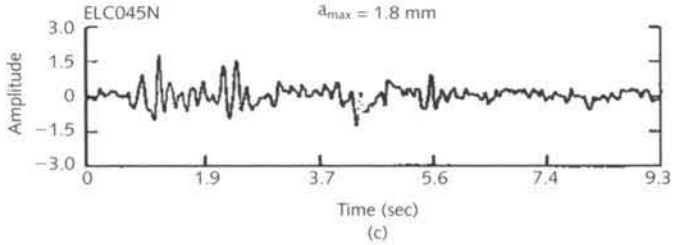

(c)

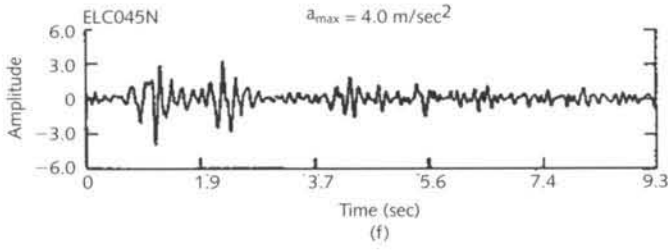

(f)

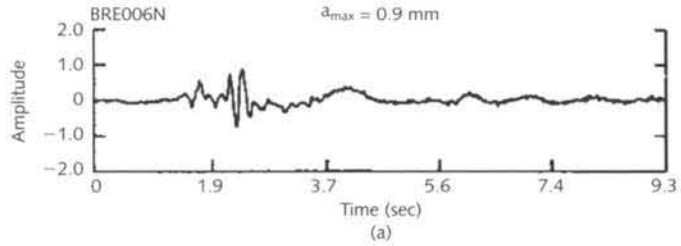

(a)

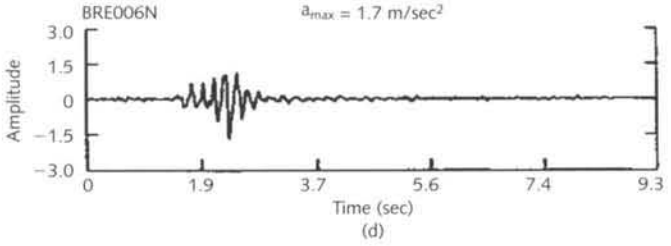

(d)

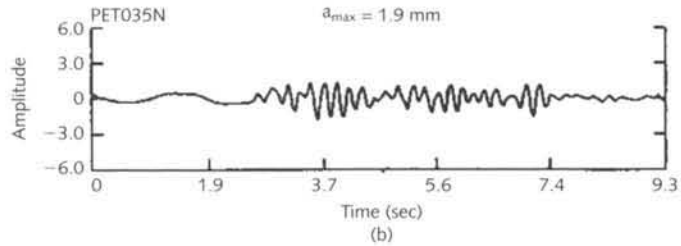

(b)

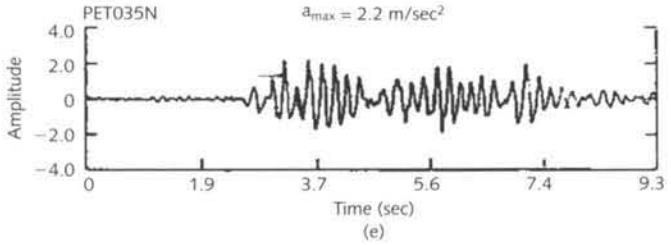

(e)

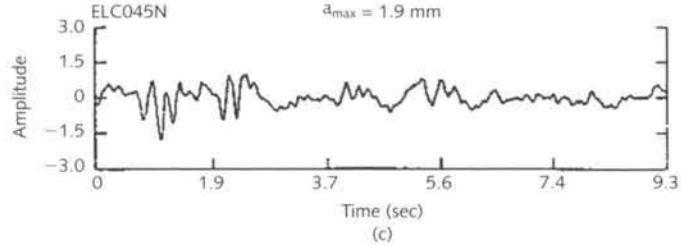

(c)

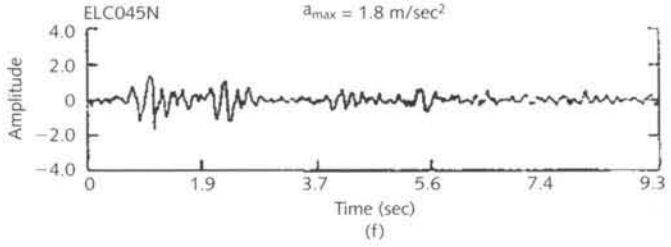

(f)

Figure 5.5 (opposite top)
Amplitude-time histories of original model response at various input accelerations for the Breginj, Petrovac, and El Centro earthquakes—top of the dome: (a–c) maximum displacement, (d–f) maximum acceleration.

Figure 5.6 (opposite bottom)
Amplitude-time histories of original model response at various input accelerations for the Breginj, Petrovac, and El Centro earthquakes—base of the tambour: (a–c) maximum displacement, (d–f) maximum acceleration.

figures 5.5 and 5.6. Records of shear force–displacement relationships for the top of the dome and for level 1 (base of tambour) are presented in figures 5.7 and 5.8. Shear forces were calculated as the product of the corresponding mass at the particular location in the structure (either the top or level 1) and the measured acceleration at that location.

During the seismic testing, intense vibration of the dome structure was first noticed during the Petrovac earthquake, and dome cracks occurred during test 15 (PET075N) at an intensity of 0.19 g, before any cracks were noticed on the lower part of the church model. The final test performed on the original model was test 18 (ELC130N), with an input acceleration of 0.43 g. This test caused many cracks

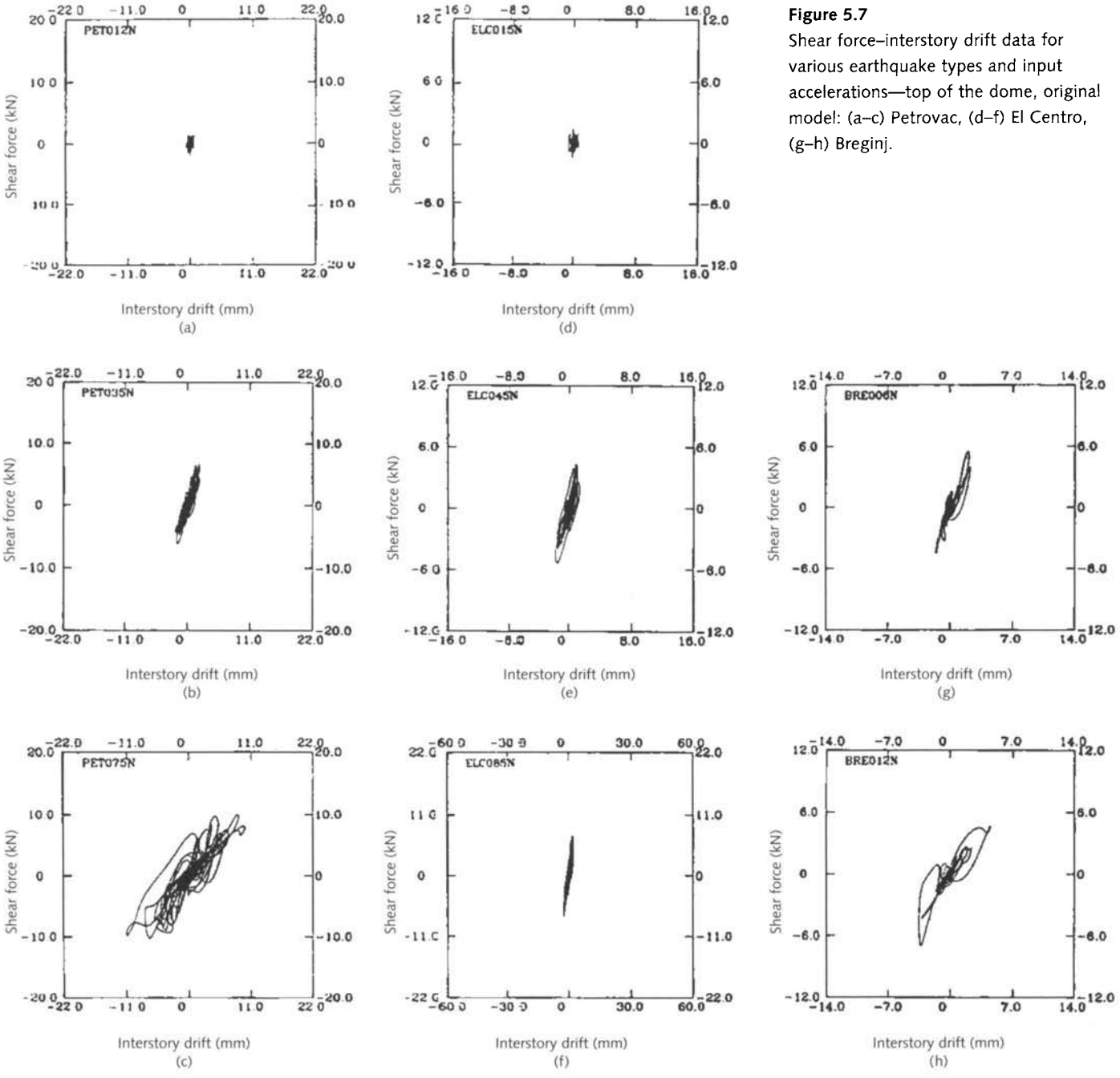

Figure 5.7
Shear force–interstory drift data for various earthquake types and input accelerations—top of the dome, original model: (a–c) Petrovac, (d–f) El Centro, (g–h) Breginj.

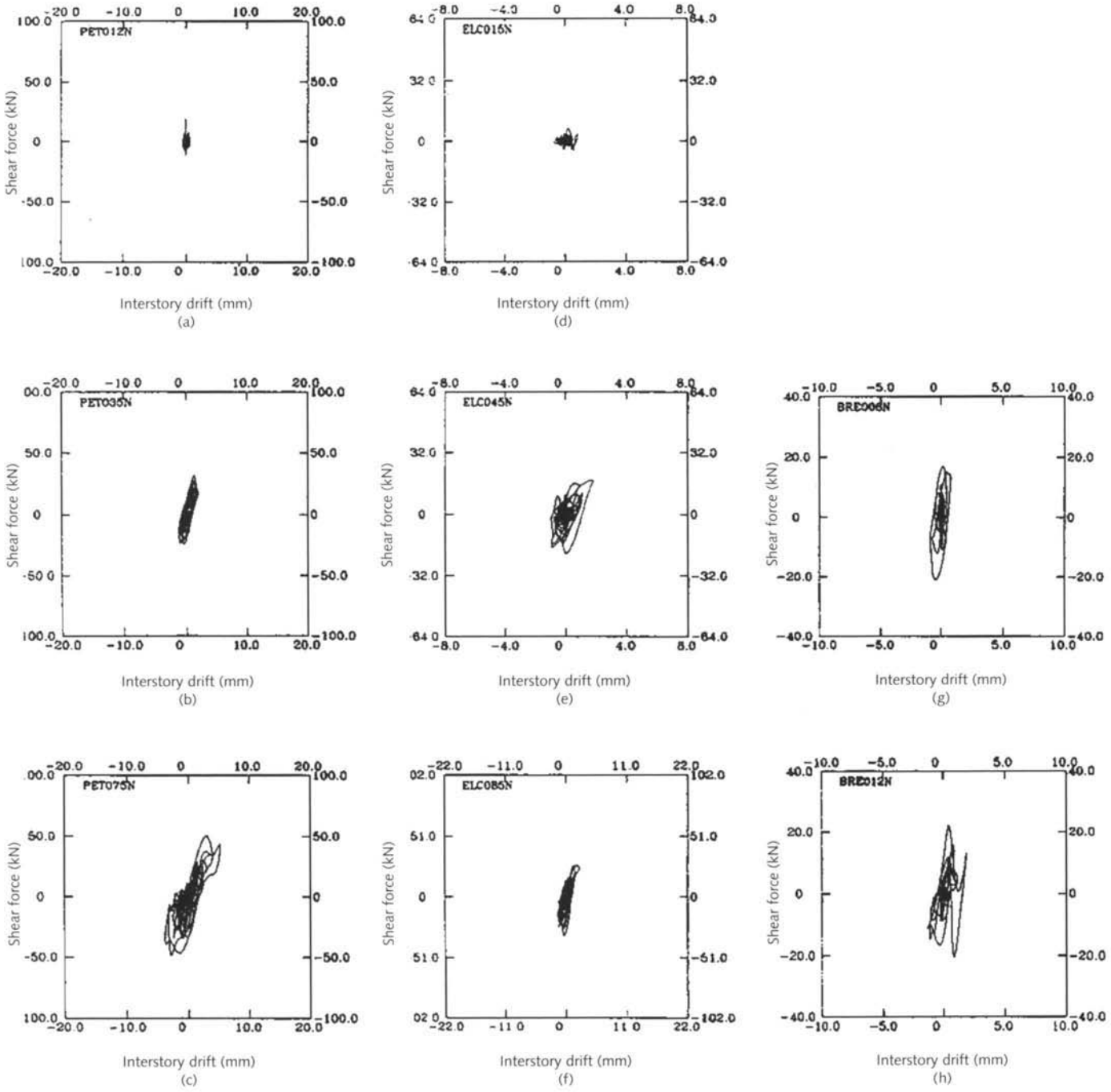

Figure 5.8
Shear force–interstory drift data for various earthquake types and input accelerations—level 1 (base of the tambour), original model: (a–c) Petrovac, (d–f) El Centro, (g–h) Breginj.

throughout the model and structural failure. Damage to the model after this test is shown in figures 5.9 and 5.10.

From an analysis of the time histories of acceleration and displacement and the force–relative displacement hysteretic relationships, it may be concluded that the structure behaved as a rigid body until it reached the elasticity limit at a_{max} (PGA) = 0.17 g (El Centro earthquake). The P-Δ hysteretic relationship showed the absence of cracks up to this point.

The first cracks occurred during the next excitation, the application of the Petrovac earthquake with a_{max} (PGA) = 0.20 g. Large

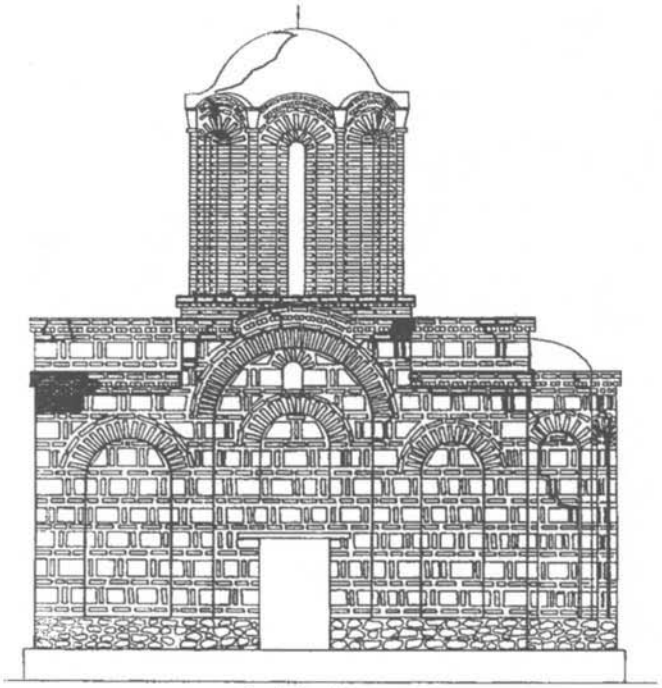
South facade

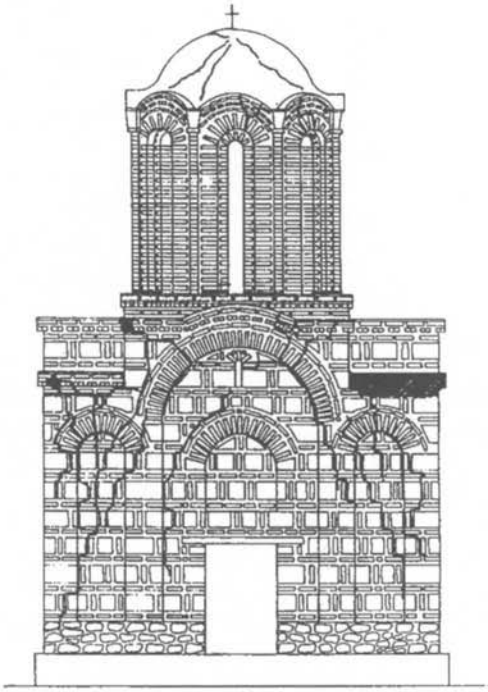
West facade

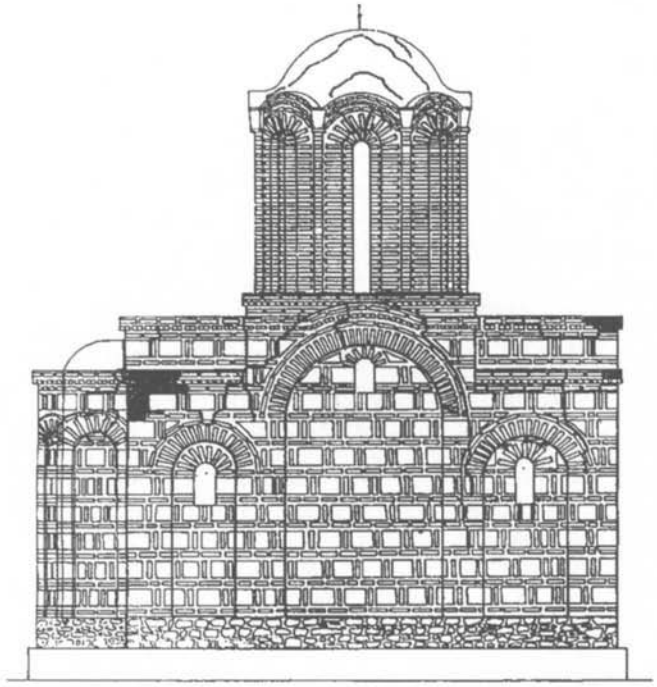
North facade

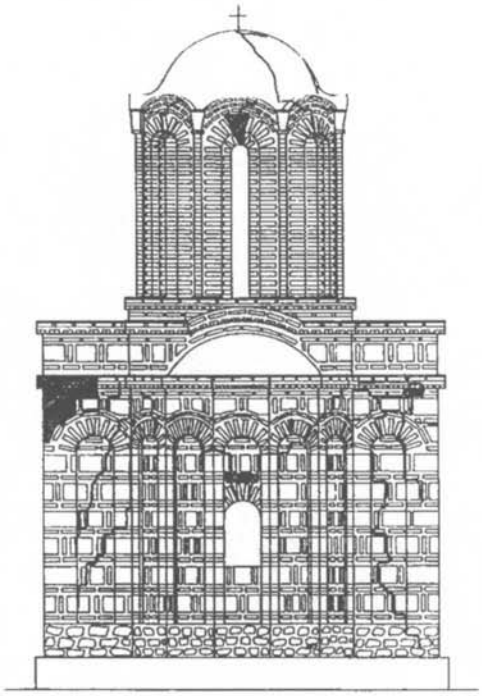
East facade

Figure 5.9 (above left, top and bottom) Damage to the original model: south and north facades.

Figure 5.10 (above right, top and bottom) Damage to the original model: west and east facades.

cracks occurred in the upper part of the model (tambour), with minimal crushing and loss of masonry from tambour arches, and fine cracks were observed in the bearing walls. The extent of the stresses, deformations, and damage can be estimated as a state of initial nonlinearity of the principal structure and large damage to the secondary parts of the model. Damage to the tambour was visible but not excessive, and cracks that were visible in the main structural system during the test were closed after the test.

After this loading phase, the El Centro earthquake excitation, with a_{max} (PGA) = 0.43 g, was applied, which resulted in major damage to the building. The principal failure mechanism was the loss of structural integrity and the development of cracks in the main vaults. Analysis of the damage progression showed that cracks in the dome and main vaults were followed by damage to the east and west bearing walls, which were in the plane of excitation. Damage to the altar structure was manifested by separation of the apse and the appearance of large diagonal cracks extending from the window to the cornices. Shear cracks and failure were not observed in the lower parts of the bearing walls. On the south and north facades, damage to the lintels, cornices, and other nonstructural elements was observed, but the walls themselves suffered minimal damage.

It should be noted, however, that at this acceleration level large cracks occurred in the tambour and the central dome, resulting from the separation of specific columns from the tambour, partial disintegration of the arches and dome, and the almost-vertical wall cracks. This severe damage was evidenced by the precipitous drop of the natural frequency (stiffness deterioration) from 11.0 Hz to 6.6 Hz.

Repair and Strengthening of the Damaged Model

From an analysis of the seismic stability of the prototype St. Nikita church and the results of the shaking-table tests on the model, it was concluded that the model did not exhibit the stability and resistance required for assuring the preservation of the church either for the "design" earthquake or for the maximum-severity earthquake. Therefore, damage to the model was repaired and the structure was strengthened in accordance with the proposed retrofitting techniques.

Strengthening elements used in retrofitting the church model consisted of horizontal and vertical belt courses formed by incorporating steel-bar reinforcements into the interior of the walls and filling the volume around the bars with an appropriate grout to establish continuity with the surrounding masonry. The function of the horizontal belts was to increase the synchronous performance of the perimeter walls and improve the resistance of the building to the expected dynamic loads.

Horizontal steel belt courses were inserted into the void spaces purposely built into the perimeter walls during construction at the levels +0.74 m and +1.74 m, and at a height of 2.6 m in the square base of the tambour, as shown in figure 5.11. Each of the two steel reinforcement bars was 10 mm in diameter. The ends were bolted to vertical, steel, stress-distribution plates, 10 mm thick, and the bars were prestressed to about 1 ton. The steel plates were visible on the exterior of the facade, but for use on the prototype church, they would be recessed below the surface and would not be visible. Ringlike belt courses were incorporated below the apsidal cornice and at the base of the dome. These belts were each made of four sections of 6 × 0.4 cm sheet steel. The horizontal belt at the tie level (fig. 5.12) was of special importance

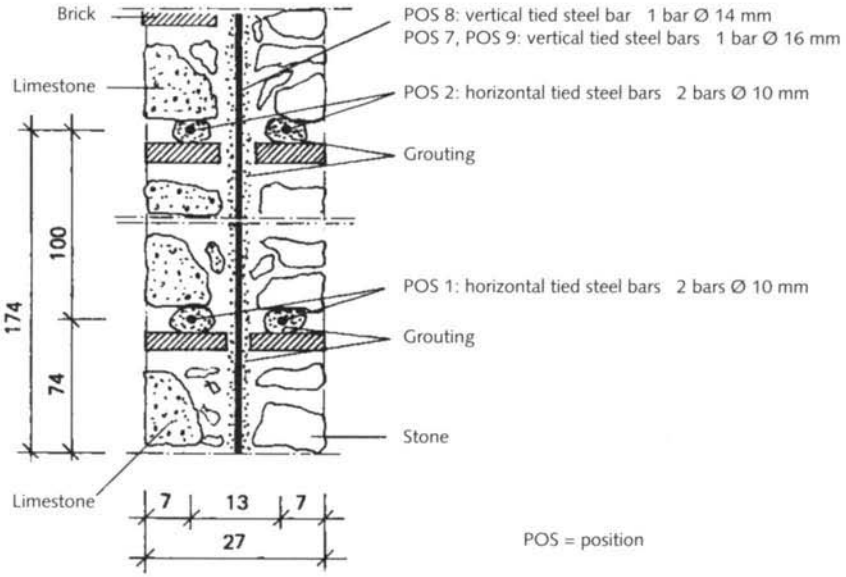

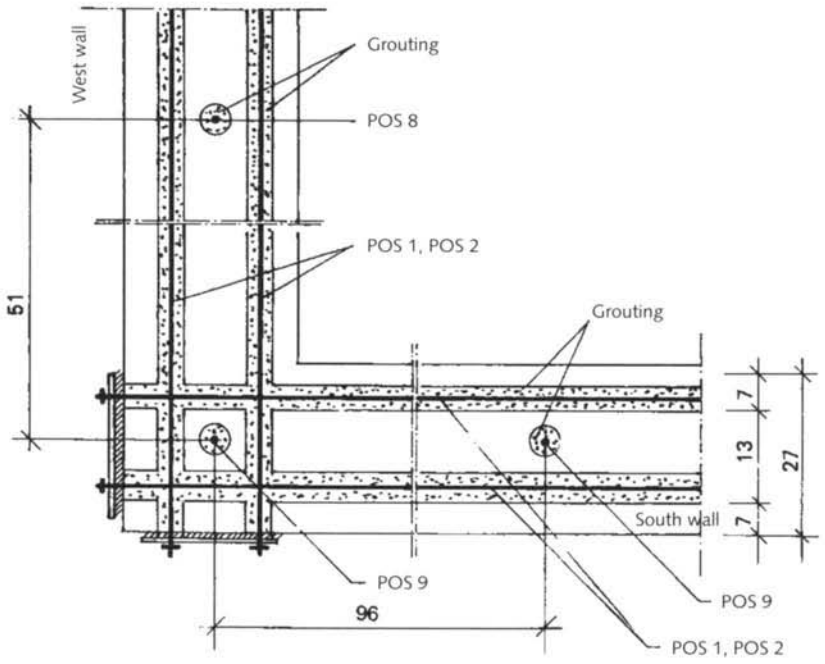

Figure 5.11
Details of horizontal belt courses.

because it increased the strength of the bearing walls and prevented the inclination of the vertical axis, which if allowed could lead to vault damage and collapse of the building.

Vertical belts were formed by incorporation of twelve 14 mm steel reinforcement bars at the ends of the walls and around openings (fig. 5.13). They were anchored into the reinforced concrete platform of the model and to horizontal steel plates on the roof. The bars were prestressed to 4–5 tons, which increased the normal stresses of the wall and also increased its tensile strength. Vertical bars, 10 mm in diameter, were incorporated into the eight tambour columns and prestressed to about

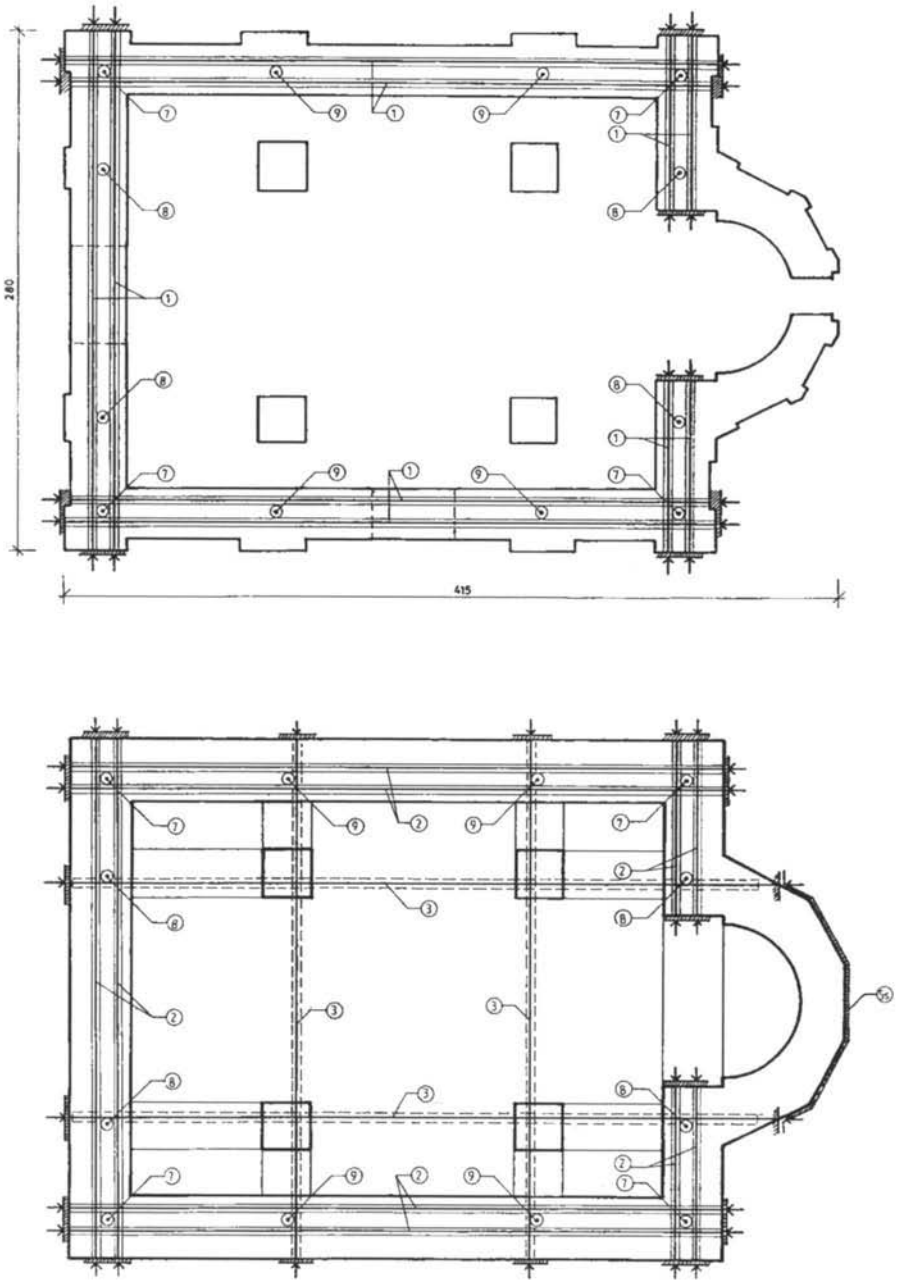

Figure 5.12
Location of belt courses, plan view. Numbers in circles represent positions of reinforcement bars.

1.5 tons. The vertical belts served to increase the ductility and bending resistance of the structure.

Two types of injection grout were used, one for the injection repair of cracks in the masonry and another for filling the volume around the reinforcement bars. These grouts differed in the grain size distribution of the aggregate and in the chemical composition of both the slaked lime matrix and the sand filler. Microsilica was added to the 1:1 lime-to-filler mix to decrease the setting time of the grout, and a phosphocasein was added to enhance plasticity and improve flow characteristics. Details of the development and testing of various grout compositions is given in Gavrilović, Šumanov, et al. (1991, vol. 11).

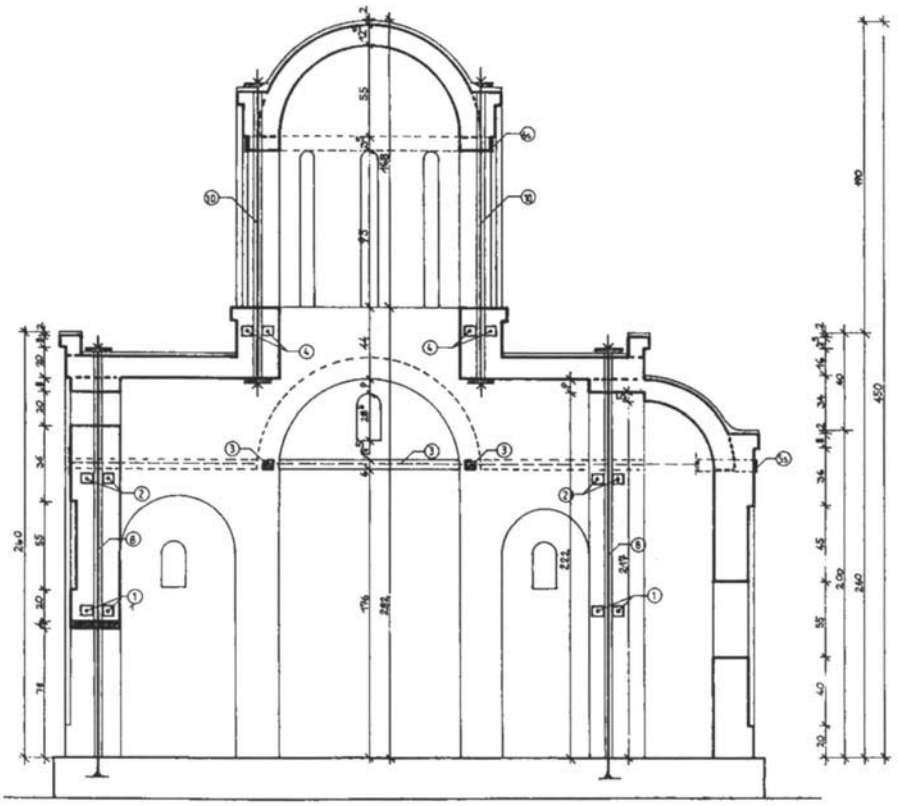

Figure 5.13
Location of belt courses, north-south elevation view. Numbers in circles represent positions of reinforcement bars.

The grouting procedure involved the removal of crushed and damaged material from cracks and voids and the insertion of the grout injection tubes. The cracked wall surfaces were sealed on the exterior with a fast-setting mortar before the pressurized grout injection. The cracks were injected with the appropriate grout at a pressure of 0.6–1.2 bars. The void spaces around the horizontal reinforcement bars in the bearing walls and the tambour (fig. 5.13, positions 1, 2, and 4) were injected with an alternate grout at the higher pressure of 1.2–1.6 bars. Placement of grout in the hollow surrounding the vertical belt courses (fig. 5.12, positions 7, 8, 9; and fig. 5.13, position 10) was done by free fall.

Tests of the Repaired and Strengthened Church Model

Following the repair and strengthening of the damaged church model, the dynamic characteristics of the model were redetermined by application of the ambient, forced, and random vibration measurement procedures used on the original model. A comparison of the natural frequencies and damping coefficients of the original and strengthened models is shown in table 5.3. It is apparent that the increase in stiffness of the model due to strengthening was negligible, as is indicated by the relatively constant natural frequency values.

The seismic response of the strengthened model was investigated by application of the same earthquake excitations that were used in the tests of the original church model. Tests were performed at the same

Table 5.3
Comparison of the natural frequencies and damping coefficients of the original and strengthened models

		Original model				Strengthened model			
		Frequency (Hz)		Damping coefficient (%)		Frequency (Hz)		Damping coefficient (%)	
Direction	Type of excitation	f_1	f_2	ξ_1	ξ_2	f_1	f_2	ξ_1	ξ_2
North-south	Ambient vibration	11.4	19.4	2.5	1.1	11.4	20.6	1.8	1.8
	Forced vibration	10.2	17.8	2.0	1.5	10.8	19.2	1.4	1.0
	Random excitation	9.2	–	–	–	11.2	–	4.5	–
East-west	Ambient vibration	14.0	23.2	3.0	1.8	15.8	23.2	1.7	0.7
	Forced vibration	13.6	20.8	2.8	3.1	15.2	22.2	3.3	1.1

input intensity levels to allow direct comparison of the response parameters for both models. However, owing to the higher strength of the strengthened model, a few additional tests were carried out at higher intensities of the input excitation. Table 5.4 lists the seismic tests performed.

The response of the strengthened model was substantially different from that of the original model. Although amplification of the response of the upper structure of the model was still observed, the displacements were considerably smaller and the elastic range was extended beyond that of the original model. The first cracks did not occur until test 25 (PET140S), at an intensity of 0.40 g. The maximum acceleration at the top of the dome during this test was 1.36 g; at level 1 it was 0.77 g. Relative displacement at the top of the dome was 21.1 mm; it was

Table 5.4
Input and maximum accelerations and displacement responses for the strengthened model tests

		Maximum response				
		Level 1		Top		
Test number and code	Input acceleration (g)	Acceleration (g)	Displacement (mm)	Acceleration (g)	Displacement (mm)	Damage
17 ELC085S	0.17	0.20	1.8	0.47	1.3	None
18 PET070S	0.19	0.27	2.7	0.48	1.7	
19 BRE012S	0.15	0.29	1.9	0.54	2.0	
21 ELC130S	0.25	0.50	7.8	0.79	15.8	
22 PET100S	0.28	0.53	7.5	0.80	9.8	
23 BRE020S	0.28	0.20	5.0	0.40	6.5	
25 PET140S	0.40	0.77	18.8	1.36	21.2	First cracks
26 ELC175S	0.30	0.65	15.2	1.10	18.3	
27 BRE027S	0.38	0.34	7.4	0.79	10.1	
29 ELC220S	0.41	0.87	17.7	1.49	28.3	
30 ELC280S	0.49	0.91	18.0	1.59	57.0	
33 BRE020S	0.28	0.20	5.0	0.40	6.5	Development
34 ELC150S	0.29	0.41	12.8	0.79	20.8	of cracks
35 BRE040S	0.55	0.33	8.5	0.55	12.8	
36 ELC280S	0.49	0.91	18.0	1.59	57.0	
37 BRE053S	0.75	0.64	8.0	0.50	17.1	
38 ELC320S	0.54	0.77	20.6	1.41	56.7	

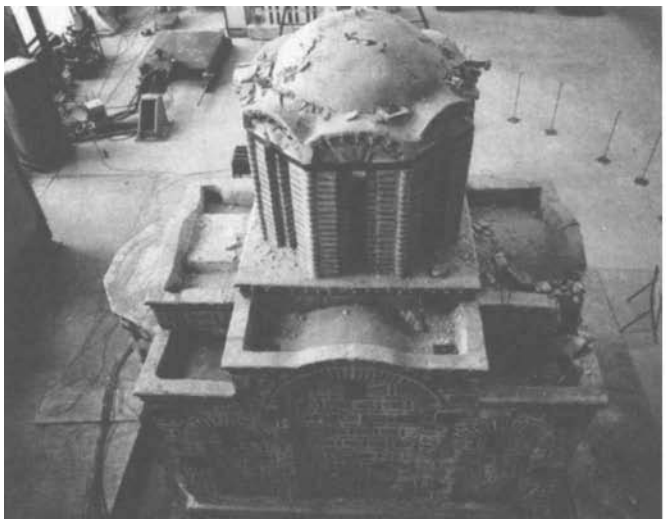

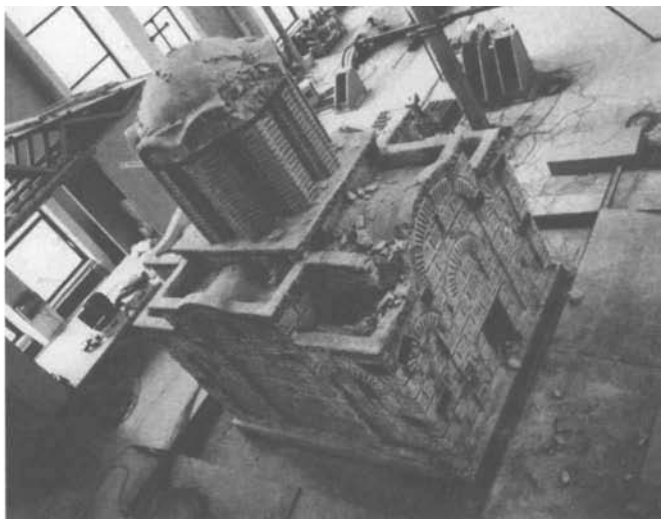

Figure 5.14
Damage to the retrofitted model after exposure to earthquake acceleration a_{max} = 0.54 g, north view.

Figure 5.15
Damage to the retrofitted model after exposure to earthquake acceleration a_{max} = 0.54 g, north-west view.

18.8 mm at level 1. Cracks appeared first in the dome structure and the west facade. Further testing at higher input intensities, 0.49–0.75 g, caused the progressive development of cracks. The response of the model was intense, especially during the El Centro and Petrovac earthquakes.

Shear-force distribution during tests of the strengthened model was regular up to intensities of 0.40 g. After cracks appeared, however, shear forces decreased as a result of the development of the ultimate failure pattern. Natural frequencies of the model were determined several times during the tests in order to obtain information on the stiffness decrease.

The final test performed on the model was ELC320S, which used the El Centro excitation for which a_{max} = 0.54 g. The model was heavily damaged during this test; the final damaged state of the model is shown in figures 5.14 and 5.15.

The structural responses of the strengthened model, when subjected to the El Centro (PGA = a_{max} = 0.17 g) and the Petrovac (PGA = a_{max} = 0.20 g) excitations were significantly different with respect to crack occurrence, maximum ground acceleration, and displacement values. With the gradual increase of acceleration level of the three earthquakes, up to a_{max} = 0.40 g (Petrovac), 0.30 g (El Centro), and 0.38 g (Breginj), it was concluded from the behavior of the repaired model that the nonlinear state started at about this level and that the linear elastic range was increased by about 100 percent over that of the original church model as a result of the retrofitting and repair operations.

Tests were carried out in which the El Centro earthquake excitation spectrum was applied and the input acceleration was gradually increased to a_{max} = 0.49 g in order to reach the stage of nonlinear behavior. This test was performed to obtain information that would allow the estimation of the expected damage levels for long-return-period earthquakes. It was found that at this acceleration level, cracks occurred in the load-carrying walls, tambour arches, and dome, and that the damage to nonstructural elements and the formation of small cracks in the load-

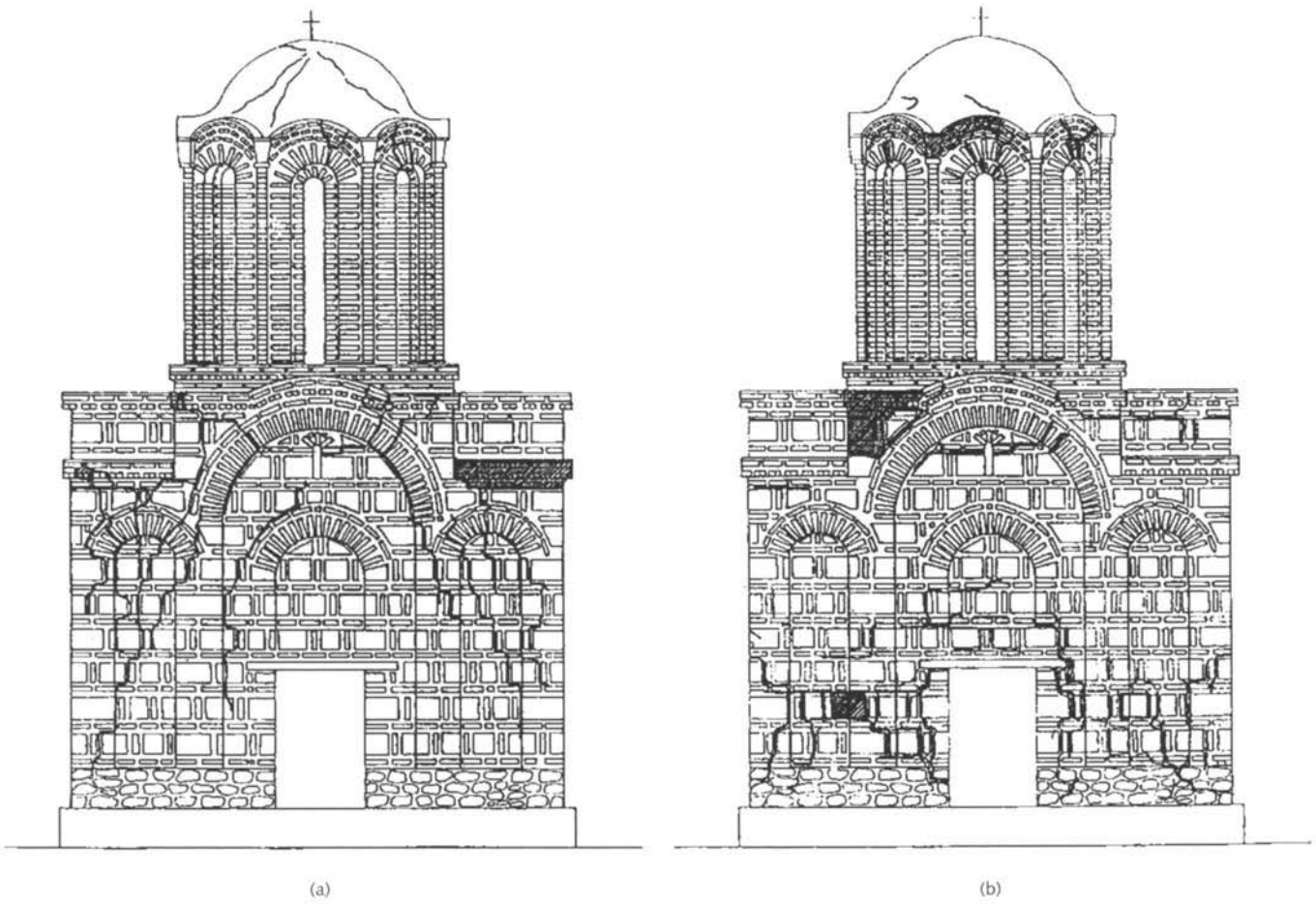

Figure 5.16
Comparison of damaged west facade areas of the model after final tests: (a) original model after application of El Centro earthquake at a_{max} = 0.43 g, (b) strengthened model after application of El Centro earthquake at a_{max} = 0.54 g.

carrying walls was inevitable. However, the structural stability of the entire building was not compromised.

When the Breginj earthquake excitation was applied and the acceleration was gradually increased to a_{max} = 0. 75 g, the failure mode and types of damage were not qualitatively changed, although further cracking did occur. In fact, this acceleration level corresponds to the maximum-severity earthquake for which the repair of the building was designed. On comparing the damage produced during the original model test at a_{max} = 0.40 g with that of the strengthened model at a_{max} = 0.75 g, it was shown that even at about twice the excitation level damage to the repaired model was considerably less than that sustained by the original model.

It was concluded also that there was a significant difference in the type of damage to the load-carrying walls of the structure. Separation and vertical cracking of the walls and vaults did not occur in the strengthened model, which points out the significant role of horizontal belts. The type and location of failure were changed, and the structure behaved like a higher-level "box system," which is characterized by the occurrence of diagonal cracks due to dominant shear stresses. This type of damage is shown schematically in figure 5.16, comparative drawings of the west facades of the original and strengthened church models after the specified tests.

To collect data about the nature of further damage produced by excitation at higher levels, the El Centro earthquake was applied at an input acceleration of $a_{max} = 0.54$ g. As expected, large cracks appeared in the structure, many of which were concentrated on the west wall. The overall stability of the building was not affected, however, due to the existence of ductile elements, and the damage produced was not beyond repair. If it is realized that this acceleration level is about 35% greater than that predicted for a maximum credible earthquake with a return period of 1000 years, the protection achieved justifies applying this basic seismic strengthening concept to existing buildings of this type.

In summary, a comparative analysis of the results obtained from the experimental tests of both models shows the following:

- The similarity between the dynamic characteristics of the two models indicates that only a minor increase in static stiffness resulted from the strengthening procedures.
- The response of the structures to acceleration levels up to $a_{max} = 0.20$ g shows that the linear elastic response of the original model was lost with the occurrence of the first cracks but that the strengthened model retained its elastic properties well past this level without the formation of cracks.
- At $a_{max} \approx 0.40$ g, the original model was severely damaged and close to failure, but at this same level, the strengthened model had just reached the nonlinear range and had started to exhibit minor cracking.
- Both the original and strengthened models showed amplification of acceleration of the principal structure with respect to the input excitation, and it was particularly high at the top of the dome.
- At the highest acceleration level at which tests were carried out, $a_{max} = 0.75$ g, the strengthened structure was well into the nonlinear range, but due to the ductile elements it was still stable and far from failure.
- Qualitatively different types of damage mechanisms were observed for the two models. The strengthened model did not exhibit the vertical cracking and separation of bearing walls observed in the original model, but the damage occurred at the lower zone of the structure in the form of diagonal cracks due to shear stresses in the east and west walls.
- The repair and strengthening procedures used were effective in increasing the bearing capacity and the allowable deformability of the structure and were implemented in accordance with the basic conservation principle of minimum intervention.
- The results of the tests on the church model are directly applicable to the stabilization of the prototype St. Nikita

church, but in view of the way in which the church was selected the information generated by the tests is also applicable to the analysis of many other churches of similar design and condition.

Chapter 6

Analytical Modeling of the Dynamic Behavior of Masonry Structures Exposed to Earthquake Motions

The materials used for construction of buildings generally satisfy the homogeneity, isotropy, and ideal elasticity conditions under all types of loads to which the structures are exposed during normal, everyday use. However, under seismic excitation conditions, the behavior of structures is specific because earthquakes result in loads that have essentially different characteristics than normal static loads. During strong earthquakes, the elastic limits of many construction materials are exceeded, resulting in nonlinear deformations of the structure and further modifications of its initial dynamic characteristics.

The behavior of masonry structures, and structures in general, during earthquakes can be estimated much more realistically by using a nonlinear dynamic analysis that, apart from other parameters, takes into account the nonlinearity of materials and the way that property changes affect the dynamic characteristics of structures over the course of time. Nonlinear dynamic analysis is, in fact, a method for determining the response of the mathematical model of the structural system when exposed to dynamic loads.

Dynamic Analysis of the Nonlinear Response of an Idealized Single-Degree-of-Freedom System

To obtain a structure's vibration characteristics, a simple model can be used to most adequately reflect the building's mechanical characteristics. The Byzantine churches that are the subject of this project can be represented as single-story structures, that is, structures with a single degree of freedom. A specific characteristic of single-dome churches is the behavior of the tambour-and-dome structure, which is considerably less stiff than the rest of the building. The tests performed on the model of the St. Nikita church demonstrated the vulnerability and high amplification in the response of the tambour structure, which leads to the conclusion that the tambour and the dome together behave as a separate structure and that this behavior depends on the vibrational response of the principal (lower) portion of the structure. Hence, it was assumed that the dynamic response of the tambour-and-dome structure could be obtained by analyzing a less-stiff, single-degree-of-freedom upper structure that is excited by the response of the principal structure at level 1 (fig. 6.1). In this way, the

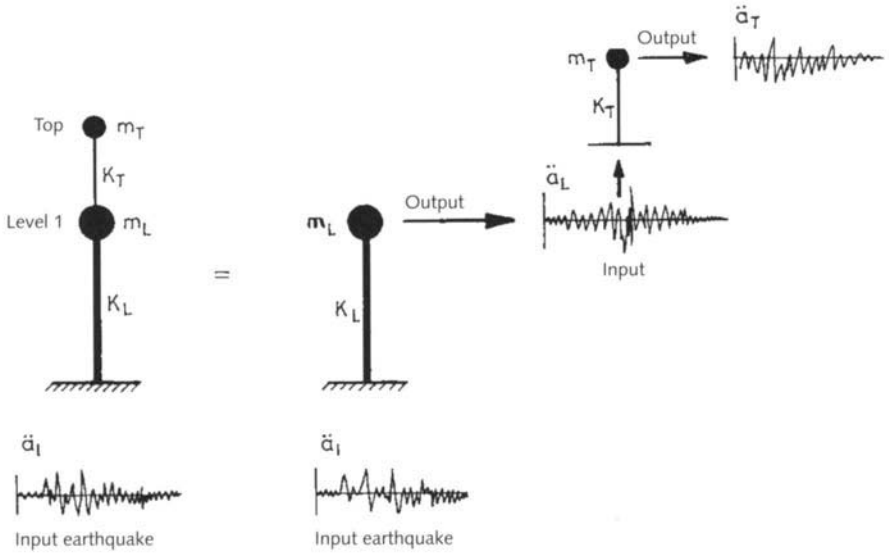

Figure 6.1
Premise of analytical model.

problem of modeling the church structure exposed to earthquake effects was reduced to a dynamic model of a single-degree-of-freedom system (fig. 6.2) exposed to a time-variable force acting at the base.

Dynamic Equations of Motions

The motion of the system presented in figure 6.2, the dynamic equilibrium at time *t*, is defined by

$$F_I(t) + F_D(t) + F_S(t) = P(t) \tag{6.1}$$

where

$F_I(t)$ = inertial force at time t$F_D(t)$ = damping force at time t
$F_S(t)$ = elastic force at time t$P(t)$ = force at the base (real-time history of the earthquake)

At time $(t + \Delta t)$, the force at the base is defined by

$$F_I(t + \Delta t) + F_D(t + \Delta t) + F_S(t + \Delta t) = P(t + \Delta t) \tag{6.2}$$

The incremental form of the equation of motion at time t is obtained by subtracting equation 6.1 from equation 6.2.

$$\Delta F_I(t) + \Delta F_D(t) + \Delta F_S(t) = \Delta P(t) \tag{6.3}$$

where

$$\Delta F_I(t) = F_I(t + \Delta t) - F_I(t) = m\,\Delta xt \tag{6.4}$$

$$\Delta F_D(t) = F_D(t + \Delta t) - F_D(t) = c\,\Delta xt \tag{6.5}$$

$$\Delta F_S(t) = F_S(t + \Delta t) - F_S(t) = k(t)\,\Delta xt \tag{6.6}$$

$$\Delta P(t) = P(t + \Delta t) - P(t) \tag{6.7}$$

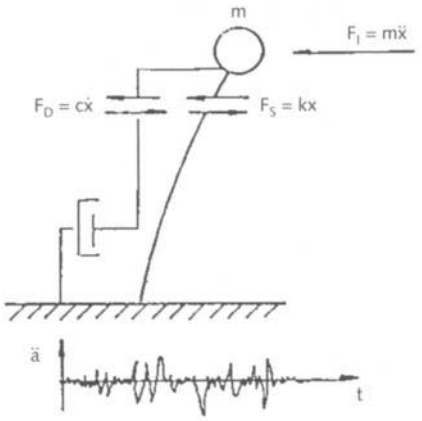

Figure 6.2
Single-degree-of-freedom model exposed to a time-variable force at the base.

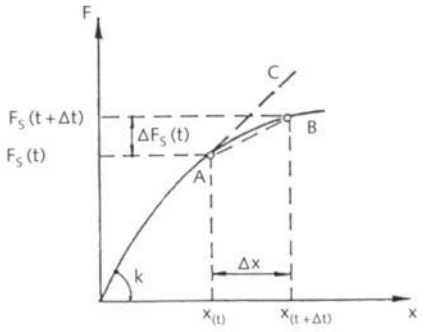

Figure 6.3
System stiffness characteristics.

During the motion of the system, the damping and stiffness characteristics are modified with time. However, in accordance with equation 6.4, the nonlinear dynamic analysis performed here takes into account only the modification of the stiffness characteristic of the system (fig. 6.3)—that is, K = K(t)—whereas the damping, *c*, is considered to be constant. Since defining the exact value of secant stiffness (the slope of straight line A-B) is a time-consuming process, the stiffness of the system, K(t), in nonlinear analyses is most commonly approximated by a tangent stiffness at time *t* (slope of straight line A-C), which is constant throughout the whole interval Δt:

$$K(t) = K_{tan} = F_S(t) / x^{(t)} \tag{6.8}$$

$$\Delta F_S(t) = K(t)\,\Delta t = K_{tan}\,\Delta t \tag{6.9}$$

By substitution of equations 6.4– 6.7, equation 6.3 acquires the following form:

$$m\,\Delta\ddot{x}t + c\,\Delta\dot{x}t + K_{tan}\,\Delta xt = P_{t+\Delta t} - (m\ddot{x}_t + c\dot{x}_t + F_S(t)) \tag{6.10}$$

The dynamic equations of motion are most commonly solved using the direct integration method and the numerical "step-by-step" procedure. Newmark's β method was used in its implicit form for integration of the equation of motion. A detailed description and flowchart of this commonly known method for obtaining the dynamic response quantities is given in Clough and Penzien (1975) and Bouwkamp and Rea (1970).

In the integration process, the values K* and Rt* are computed at each time interval (step), and the displacement increment is defined by Δxt = Rt*/K*. (See appendix B for a flowchart that defines the terms Rt* and K*, which are used in the analysis of a single-degree-of-freedom system.) Since Δxt is known, the response (x, ẋ, ẍ) at moment (t + Δt) is obtained and is used as an initial condition for the next step.

As previously stated, the main specificity of the method is the determination of the tangent stiffness and the elastic force $F_S(t)$, which depends on the way the stiffness modification of the system is modeled (the hysteretic model that is applied in the analysis). The tangent stiffness of the system is functionally dependent on the deformation extent. For each part of the hysteretic diagram, the stiffness is limited by envelope conditions, and the equivalent elastic force is obtained from and depends on the current stiffness and deformation of the system at a defined time, such as the start of the integration interval.

Models of Hysteretic Behavior

A structure exposed to random dynamic effects starts to exhibit hysteretic behavior at the moment when deformations of the structure exceed the elastic limit. The hysteretic behavior is defined by the force-deformation relationship for the entire time history of dynamic effects. This relationship represents, in fact, the nonlinear modification of the structural stiffness over the course of time.

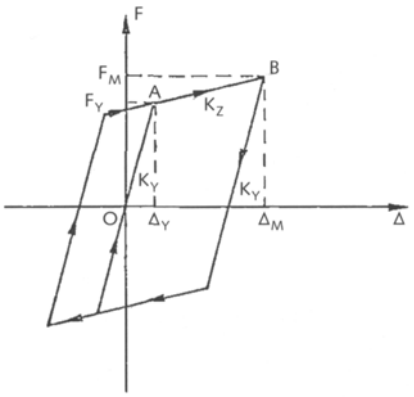

K_Y, Δ_Y, F_Y	Stiffness, deformation, and force at yielding point
K_Z	Stiffness after yielding point
Δ_M, F_M	Maximum force and corresponding displacement

Figure 6.4
Simple bilinear model diagram.

The experimentally obtained hysteretic diagrams are too complicated to be used as models in nonlinear analysis. Therefore, for practical computation, idealized hysteretic diagrams were defined that could be divided into three principal groups: (1) highly idealized, simplified models; (2) empirical models; and (3) models that describe individual phenomena pertaining to the behavior of structures. Two representative models, those classified in the first and third groups, are described here.

Bilinear hysteretic model

One of the most frequently applied models in dynamic analysis is the bilinear diagram shown in figure 6.4. It is characterized by an initial linear behavior region, line O-A, up to the yield point; and line A-B, which could have a random slope either positive or negative bilinear when line A-B has a positive or negative slope, respectively; or elastoplastic if line A-B has a zero slope.

For modeling performed using the bilinear diagram, the stiffness of the system during loading and unloading is assumed to be equal to the stiffness at the initial loading; that is, the stiffness degradation resulting from the reversible loading in the inelastic range is not taken into account. If one accepts this approximation, the bilinear diagram can be used for modeling masonry structures, as has been shown by the many examples described in the literature.

The response obtained by application of this model will depend to a large extent on the parameters selected for K_Y and K_Z, since the larger they are, the smaller the displacements. It is essential to note that with this model it is not possible to limit the force that is transferred through the element during cyclic loading, which is not always in agreement with the nature of the element's behavior.

Trilinear (IZIIS) model of stiffness degradation and pinching of the hysteretic loop

From an analysis of the actual behavior of structures and the diagrams obtained from experimental investigations of elements and models, it is clear that the hysteretic diagram should include pinching of the hysteretic loops, which is necessary to account for shear forces.

The IZIIS model (fig. 6.5) was originally proposed and developed by Gavrilović (1982) and was extended by Sendova (1988). It involves the stiffness degradation of structures under reversible loads and includes the pinching of the hysteretic loop due to the effect of shear forces. The two principal characteristics of the model are as follows:

- A delineated range, M-U, is identified in the hysteretic diagram. The model defines the stiffness modification and the behavior of the structure; that is, it describes the structure after it has reached the maximum deformation (Δ_M), which in other models is characterized as the ultimate or failed state. This provides the possibility of describing structures that have not yet failed, although they have suffered considerable damage. From diagrams obtained dur-

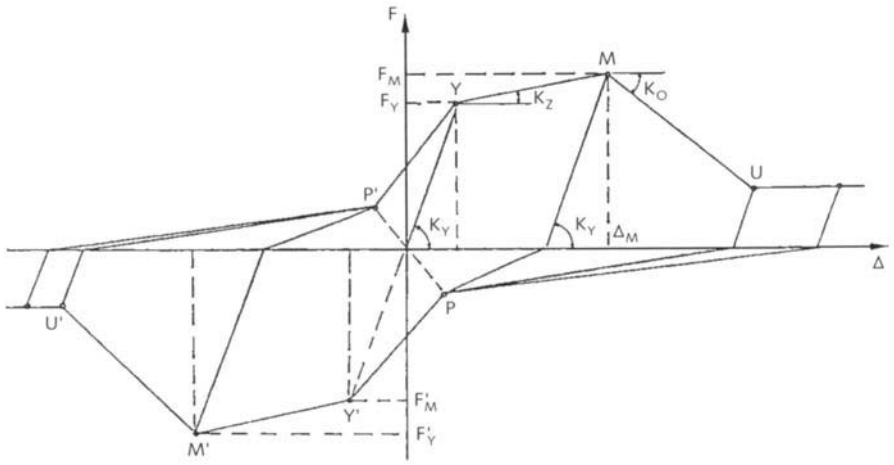

Figure 6.5
General trilinear IZIIS computer model.

ing experimental investigations, it is evident that failure of structures never occurs at zero force. In other words, even in the state of largest deformations, the structures are still capable of sustaining a certain force (F_u) as a result of friction in the masonry materials. Therefore, the model is defined in the range U-F (fig. 6.6), where the force remains constant ($F = F_u$), deformations can increase without limit with increasing force, and the stiffness is practically zero. This range represents structural failure.

- The model introduces the pinching of the hysteretic loop (point S in figure 6.6), which accounts for the stiffness variations under reversible loading that occur as a result of sliding and loss of adhesion between masonry materials. This feature allows the modeling of the shear effects.

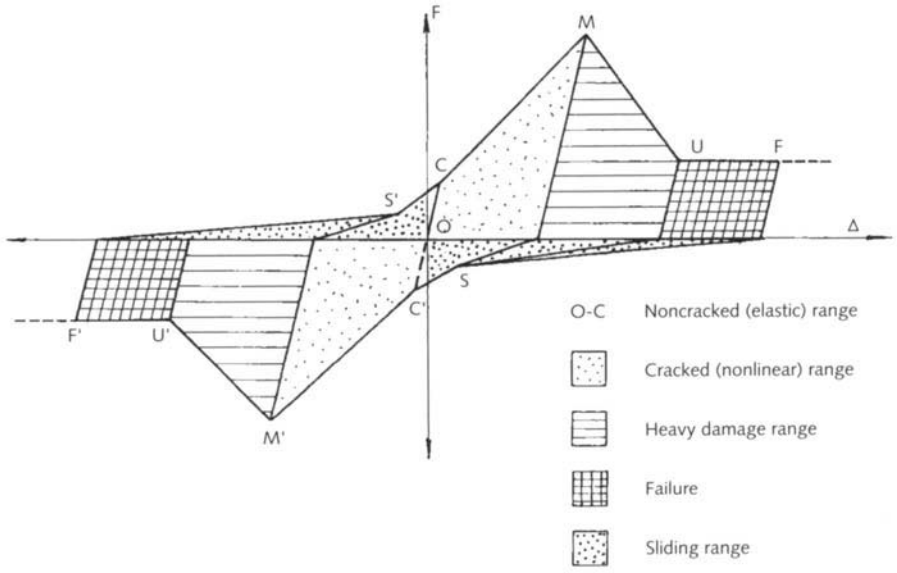

Figure 6.6
Adapted trilinear IZIIS model for masonry structures.

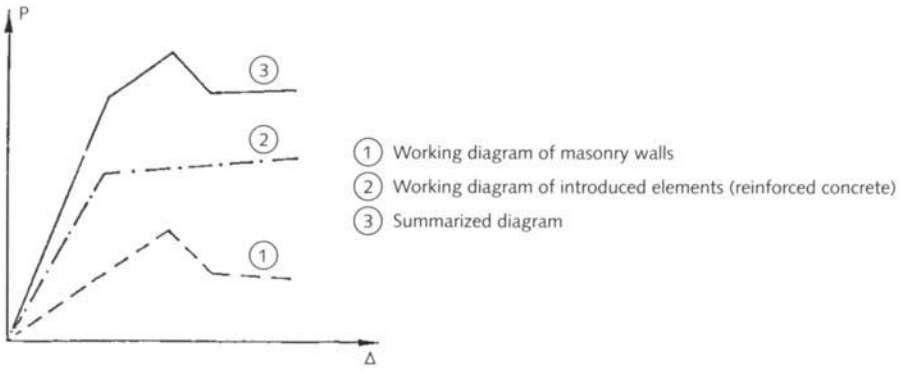

Figure 6.7
P-Δ diagram for strengthened, retrofitted structure.

The polygonal character of the P-D envelope curve permits the modeling of structures fabricated from different types of materials (fig. 6.7) and the identification of complex, experimentally measured hysteretic diagrams. This characteristic was used for describing the response of the church model.

The possibility of defining section Y-M by a negative slope (fig. 6.5) enables modeling of systems whose stiffness deteriorates immediately upon reaching the yield point, Y. Such systems are characterized by brittle, nonductile behavior, which is a characteristic of masonry structures.

The IZIIS-Gavrilović model (fig. 6.6) was adapted for the analysis of the dynamic behavior of masonry structures in the nonlinear range and was applied in the analyses performed in this study. An important characteristic of this analytical model is that the behavior of structures can be described successfully during all phases exhibited by the model being tested:

- noncracked (elastic) range,
- cracked (nonlinear) range,
- sliding range,
- heavily damaged range, and
- failure.

Due to the complexity and the wide applicability of the model for different types of structures and materials, there are no unique analytical expressions for definition of stiffness after points M and S. Therefore, they may be estimated or can be derived from experimentally recorded diagrams. In this case, the P-Δ diagrams for the principal lower and upper church structure regions obtained from the shaking-table tests were used. Figure 6.8 illustrates the method, based on the adapted IZIIS-Gavrilović model, for using the experimental results to obtain the envelope points. At the lower input acceleration levels it was possible to obtain the point, C, at which the first crack occurred and the stiffness at that point (fig. 6.8a). At higher input acceleration levels, where large linear deformations occurred, points U and S (fig. 6.8b) were defined as shown.

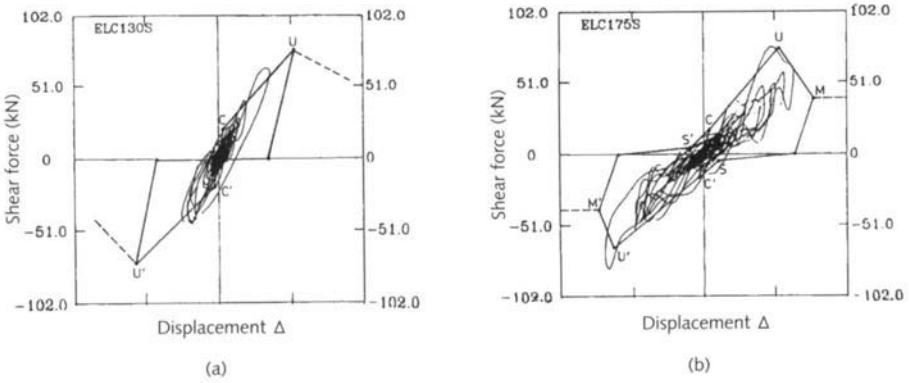

Figure 6.8
Determination of the experimental envelope points for the hysteretic IZIIS model: (a) low acceleration level, (b) high acceleration level.

IZIIS developed a computer program called SIEN that included a subroutine for computing stiffness and elastic force using the IZIIS model. In addition to information necessary for obtaining the dynamic response (input excitation, mass of the structure, and damping of the system), data are also required that describe the envelope of stiffness modification—the displacement and force at all points at which stiffness modification takes place (points C, M, U, and S in fig. 6.6). In this way, incorporation of subroutines for any other hysteretic model is easily implemented, and the principal dynamic-response algorithm remains unchanged.

This page intentionally left blank

Chapter 7

Analytical Studies and Correlation of the Behavior of the Two Models

The results obtained during the shaking-table tests of the St. Nikita church model can be expressed in terms of the relationship between the shear forces (product of the acceleration at a defined level and the mass) and the resulting relative deformations. Examples of these data for the original and strengthened models are shown in figure 7.1. These graphs refer to the principal structure of the model (level 1; fig. 7.1b, d) and to the tambour and top of the dome (fig. 7.1a, c), when the model was exposed separately to increasing intensities of the Petrovac earthquake. These diagrams show the degradation in stiffness of the model structure. It is apparent that there are two ranges of dynamic response for the original model: elastic behavior of the structure ($a_{max} < 0.12$ g), and nonlinear behavior ($0.12 < a_{max} < 0.20$ g). For the strengthened model, three dynamic response ranges were identified: the elastic range ($a_{max} < 0.20$ g), at which the model vibrates with the initial stiffness; the nonlinear range ($0.20 < a_{max} < 0.40$ g), at which the model stiffness deteriorates with the

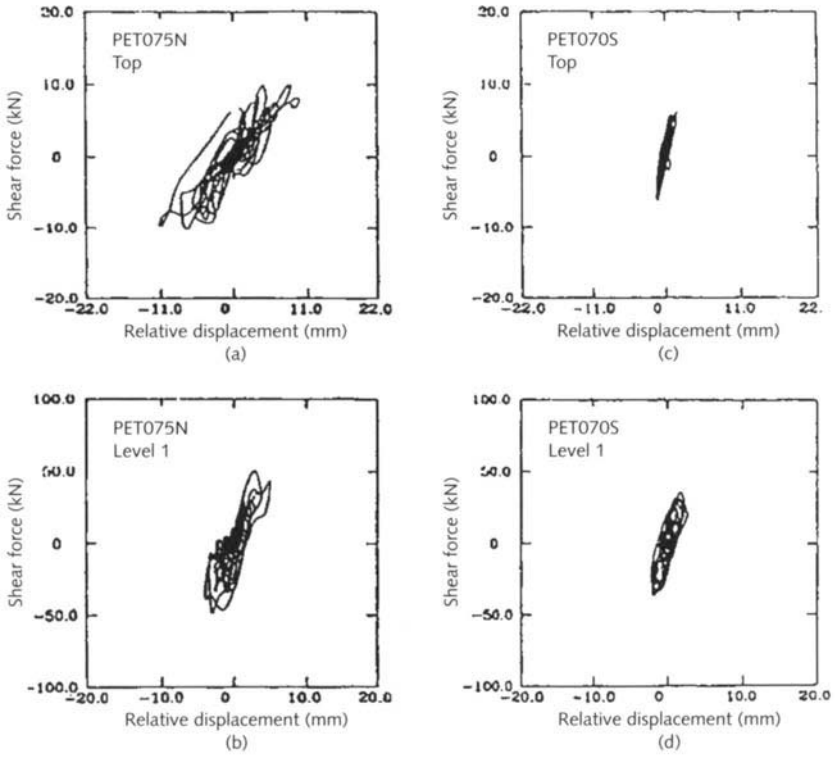

Figure 7.1
P-Δ data for original and strengthened models: (a, b) original model, (c, d) strengthened model.

occurrence of the first cracks; and the ultimate range ($a_{max} > 0.40$ g), where the stiffness has degraded seriously and large nonlinear deformations occur.

Original Model

Analytical modeling of the dynamic behavior in the linear range (input < 0.12 g)

For modeling the elastic dynamic response of the original model, the Structural Analysis Program (SAP90) for analysis of structures, which incorporates the finite-element method (Wilson 1990), was used.

Taking into account the complexity of the specific structural system, the materials used in the model, and other possibilities proposed by the SAP90 program, the team set out to define a mathematical finite-element model that would adequately represent the church model. A moderately dense net of 877 nodes and 442 elements was adopted; this encompassed the global geometrical characteristics of the church model without paying particular attention to the inhomogeneity of the construction materials.

The structure was modeled in such a way that the walls and the individual elements of the upper structure were designated as substructures and connected by application of the same deformations at common joints. The central columns of the lower structure, the columns of the tambour, and some connecting elements of the structure were modeled by two types of 86 FRAME elements (fig. 7.2a). These were three-dimensional prismatic elements for modeling of columns and beams—including biaxial bending, torsion, axial deformations, and biaxial shear deformations—the output quantities being given at the ends of the elements. The elements used for modeling the central columns were characterized by an area of 26 x 26 cm, an elasticity modulus of E = 55,000 kPa, and a density of $\rho = 19.8$ kN/m^3. For modeling the pendentives and the tambour, elements with a higher modulus of elasticity, E = 70,000 kPa and $\sigma = 17$ kN/m^3, were chosen because these parts were constructed exclusively of bricks and lime mortar.

The vaults, apse, and dome of the church were modeled by a total number of 259 SHELL elements, the formulation of which was a combination of membrane- and plate-bending behavior (fig. 7.2b). These elements were defined by four nodes and the following characteristics of the material: $\rho = 17$ kN/m^3 and E = 60,000 kPa.

The massive facade walls of the church were modeled by using SOLID elements for modeling three-dimensional solid structures. The eight-node brick elements represented were based on an isoparametric formulation including nine optional, incompatible bending modes. The walls were modeled using a total number of ninety-seven SOLID elements (fig. 7.2c)—the nodes of elements of the base being fixed—whereas the remaining elements had only three translational degrees of freedom.

For the structure modeled in this way, a static analysis was performed to determine the effect of dead weight (load 1) in order to

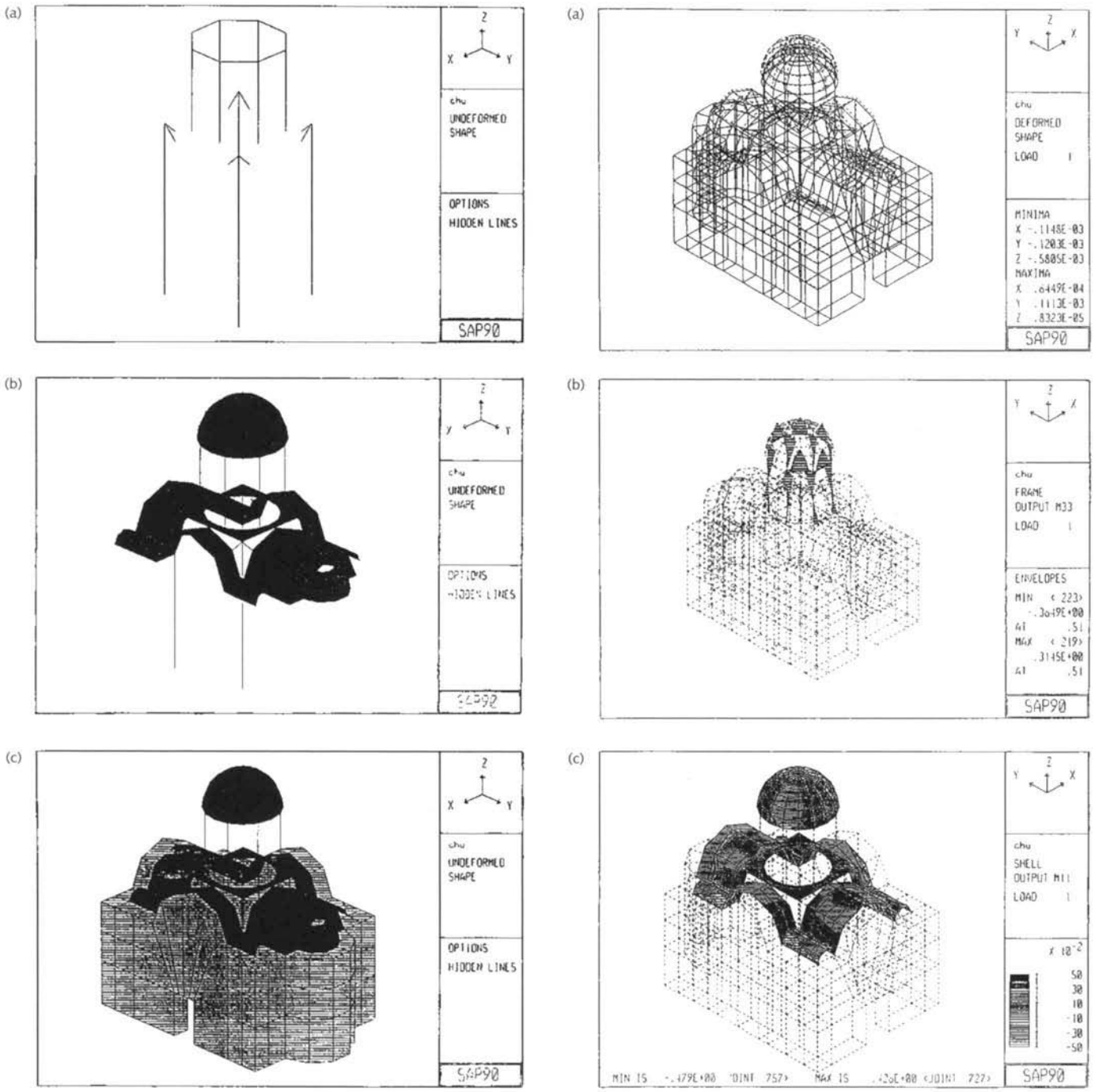

Figure 7.2 (above left, top to bottom) Finite-element modeling of the original model using the SAP90 computer program: (a) columns and beams; (b) vaults, apse, and dome; (c) facade walls.

Figure 7.3 (above right, top to bottom) Results of a static analysis to determine the effects of dead weight.

control the input data through the quantities obtained for axial stresses at the base of the walls. The deformed state and the results obtained for quantities regarding the model elements are presented in figures 7.3 and 7.4. It was concluded that this computer package was capable of generating a complete definition of the stress-strain state of the structure under static loads.

The principal dynamic characteristics, natural frequencies, and mode shapes of the church model structure were investigated. The results are presented in the CHU.EIG output and shown in figure 7.5.

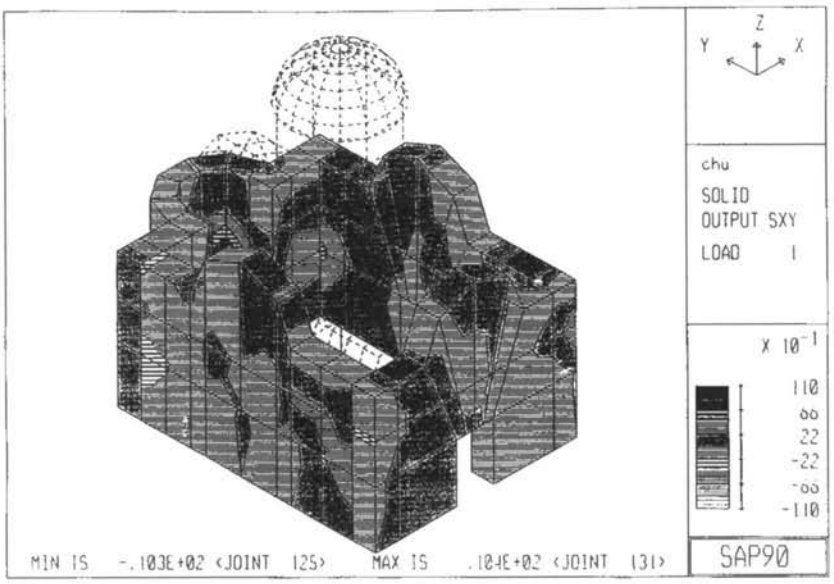

(a)

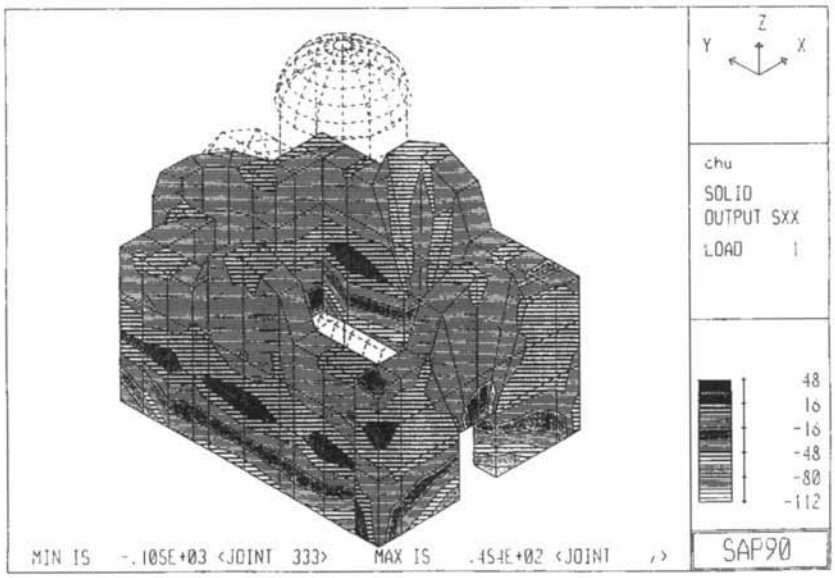

Figure 7.4
Results of a solid static analysis to determine the effects of dead weight.

Although not exclusively in one direction, mode shapes 5 and 8 can be considered as second mode shapes in the north-south (fig. 7.6a) and east-west (fig. 7.6b) directions, with frequencies of $f_2^{N\text{-}S}$ = 27.4 Hz and $f_2^{E\text{-}W}$ = 28.9 Hz. The calculated mode shapes indicate a greater flexibility in the upper part of the model structure compared to the lower level in both orthogonal directions.

A linear dynamic analysis of the model was performed using the scaled acceleration time histories of the Petrovac and El Centro earthquakes (identical to those used in the church model tests) as input excitations. The SAP90 computer program was used to obtain results in the form of time histories of displacement, velocity, and acceleration at each of the defined nodes.

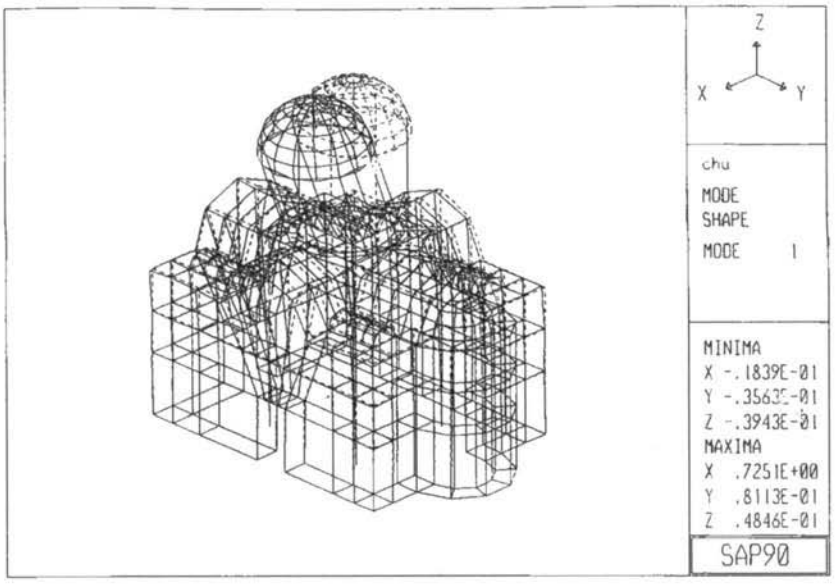

(a)

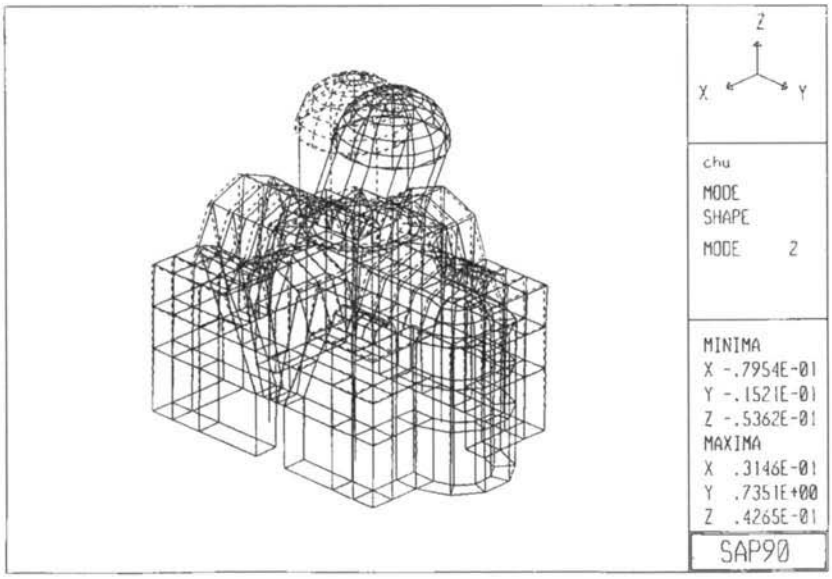

(b)

Figure 7.5
Computed dynamic mode shapes and natural frequencies.

For the linear analysis of a system with two masses, the model structure was idealized as a system with two degrees of freedom and was analyzed by applying the IZIIS hysteretic model only in the linear range O-C (fig. 6.6). The masses were assumed to be concentrated at two locations, the level at the dome and the level at the vaults (level 1), where the accelerometers and linear potentiometers were located. In this way a direct comparison between the calculated and experimental results was possible. The mass of the upper part of the structure was computed as the sum of the dome mass and half the mass of the tambour columns. The mass of the lower part (level 1) was computed as a sum of half the mass of the tambour columns, the mass of the tambour base, the mass of the main vaults, and half the mass of the massive facade walls. Stiffness

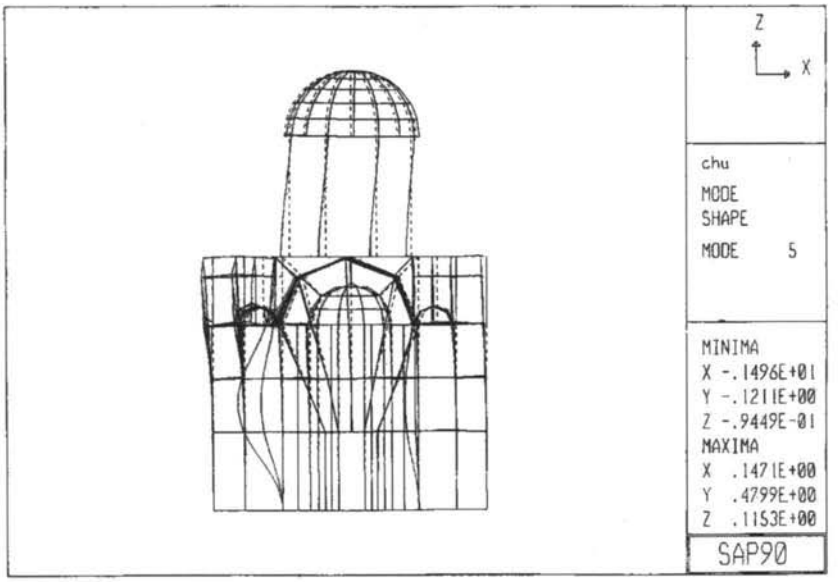

(a)

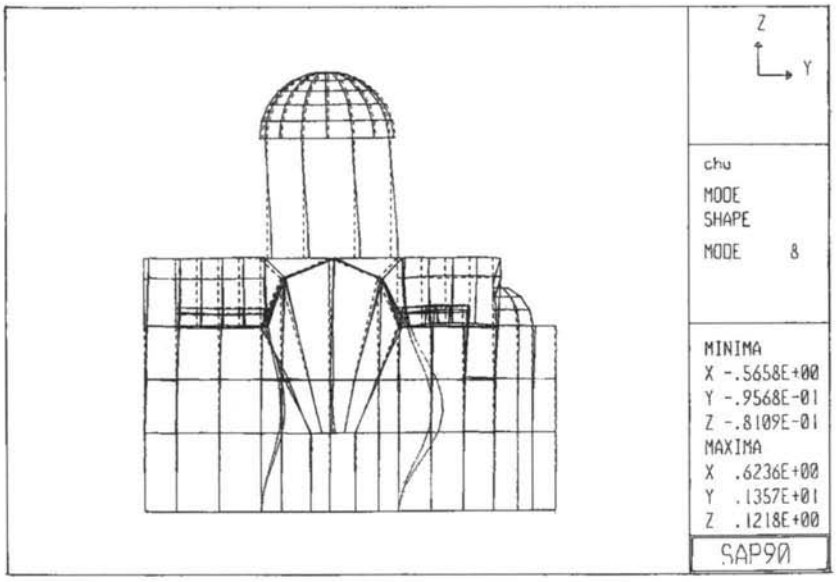

(b)

Figure 7.6
Mode shapes: (a) north-south direction, (b) east-west direction.

was defined for each mass on the basis of the predominant periods of the system, which were recorded during the ambient vibration measurements of the original model in the north-south direction, f_1 = 11.4 Hz and f_2 = 19.4 Hz, respectively for each mass, by using the simple relation that applies to the dynamics of structures:

$$k = \omega^2 m = 2\pi f m \tag{7.1}$$

The scaled acceleration time histories of the Petrovac and El Centro earthquakes used as input excitation were the same as those used for the seismic shaking-table tests of the church model. In this way, all necessary input parameters were obtained for analyzing the structure using the SEIN computer program. The computed masses and elastic stiffness values are given in table 7.1.

Table 7.1
Parameters of the linear response of the original model

	Linear range input: $a_{max} < 0.12$ g		
	m(kNsec²/cm)	K_e (kN/cm)	Damping ξ (%)
Top of dome	0.015	190	5
Level 1	0.141	725	8

The elastic response of the church model during earthquake simulation was determined using this mathematical model. Although displacements and accelerations were measured directly during the test, the damping parameter was not measured but was selected to obtain the best fit between the analytically and experimentally determined absolute displacement values. This procedure was applied for the initial accelerations of 0.04 g (tests PET012N and ELC015N). Relatively good agreement was obtained between the analytical and experimental results for the time histories of displacements and accelerations at level 1 and at the dome, respectively (appendix C, figs. C.1a, c and C.2a, c), considering the very small (about 1 mm) measured displacements.

The frequency contents obtained analytically and experimentally using the Fourier transformation are shown in appendix C, figure C.1b, d and figure C.2b, d. A good correlation was shown for the Petrovac earthquake. But for the El Centro earthquake the frequency content dominated in the experimental response, whereas the analytically predicted response had the natural frequency dominating. Under such low excitations (0.04 g) the model behaves as a rigid body, in synchronization with the shaking table.

It may be concluded that under differing earthquake excitations, the model behaved differently due to the dissimilar frequency contents of the excitations. On the other hand, the programmed test sequence of the experiment was such that differing types of earthquakes were alternately applied, and it is known that the behavior during a given earthquake and defined level is not independent of what has been used to excite the model previously. Such was the case with tests PET075N and ELC085N (table 5.2), which were performed using almost the same maximum accelerations. A considerable nonlinear response was obtained during the PET075N test, while during test ELC085N the model behaved in the linear range. Hence, the use of the same mathematical model for modeling the dynamic response to different earthquakes could yield different correlations with experimentally obtained results.

Analytical modeling of the dynamic response in the nonlinear range (input 0.12–2.0 g)

The characteristic behavior of the church model was nonlinear at the higher acceleration levels. The first visible cracks in the tambour structure occurred during test PET075N at an intensity of $a_{max} = 0.19$ g. The nonlinear dynamic response of the model was obtained by using the IZIIS trilinear model.

The stiffness and damping parameters necessary for the analysis were obtained from the analytical and recorded responses of the

Table 7.2
Parameters of the nonlinear response of the original model

	Nonlinear input acceleration range: a_{max} = 0.12–0.20 g										
	F_c (kN) (Cbs)	D_c (cm) D/H (%)	K_c (kN/cm)	F_u (kN) (Cbs)	D_u (cm) D/H (%)	K_u (kN/cm)	F_m (kN) (Cbs)	D_m (cm) D/H (%)	K_m (kN/cm)	F_s (kN) (Cbs)	D_s (cm) D/H (%)
Top of dome		0.03 (0.1)	80	6.5 (0.25)	0.3 (0.15)	15	2 (0.1)	1.1 (0.5)	–5.6	1.5 (0.05)	0.006 (0.003)
Level 1	9 (0.06)	0.015 (0.06)	600	27 (0.2)	0.3 (0.12)	63	10 (0.06)	0.6 (0.25)	–56	7 (0.04)	0.008 (0.003)

model structure and from the recorded hysteretic diagrams. Table 7.2 lists the values of elastic force and displacement and corresponding stiffness values for all the characteristic envelope points of the diagram. Shown also are the corresponding computed base shear coefficients and indices of displacement obtained as a ratio between the relative displacement and the story height.

The computed nonlinear dynamic responses for level 1 and for the top of the dome, in the form of time histories of displacements and accelerations, are compared with the recorded experimental curves in appendix C, figure C.3. It is evident that the analytical response correlates well with the recorded response in form, except that the maximum displacement values are somewhat lower than the recorded ones, especially for the upper structure. There is also a good correlation between the experimental and analytical values of the Fourier acceleration amplitude-versus-frequency content data (appendix C, fig. C.4a, b), in that stiffness degradation of the church model is evident, as shown by a drop in the predominant frequency from about 5 Hz to 3 Hz.

Correlation between the analytical and experimental results

The dynamic characteristics of the original model in terms of the analytical and experimental values of the natural frequencies in both directions are given in table 7.3, and the corresponding mode shapes are shown in figure 7.7. It is evident that the recorded value of the first natural frequency (f_1) correlates well with that obtained using the SAP90 computer program. However, the higher value obtained for the second frequency computed by SAP90 (f_2) results from the incorporation of effects from other directions.

With regard to the mode shapes, the SAP90 computer program gives much lower values for the mode shape of the upper part of the structure. This results from the type of element chosen for modeling the massive walls (SOLID), for which the program anticipates translation only in the three directions as a degree of freedom.

The results obtained by application of the IZIIS mathematical model that assumed two masses—the dome and the principal structure—

Direction	Type of excitation	Type of analysis	Natural frequencies (Hz) f_1	f_2
North-south	Ambient vibration		11.4	19.4
	Forced vibration		10.2	17.8
	Random excitation		9.0	–
		SAP90	12.7	27.4
East-west	Ambient vibration		14.0	23.2
	Forced vibration		13.6	20.8
		SAP90	13.0	8.7

Table 7.3
Comparison of measured and computed natural frequencies of the original model

correlated well with the recorded values of maximum response in both the linear and nonlinear ranges of church model behavior (table 7.4). This method of estimating the dynamic response of a structure is relatively fast and simple and is frequently of great value when conducting practical analyses.

Strengthened Model

Linear and nonlinear response parameters

Results of the experimental tests on the strengthened church model are given in figures 7.8 and 7.9. The shear force was plotted against the relative deformation at level 1 and at the top of the dome during the Petrovac and El Centro earthquake simulation excitations. These graphs, particularly for the El Centro earthquake (figs. 7.8b, 7.9b), show three distinct ranges of church model response: elastic behavior up to input $a_{max} < 0.20$ g, where the model vibrates without damage and without changes in initial stiffness; the nonlinear range of behavior up to input $a_{max} < 0.40$ g, where stiffness degradation results from the formation of invisible microcracks; and the ultimate range, with input of $a_{max} > 0.40$ g, where considerable stiffness degradation and the occurrence of large nonlinear deformations were observed.

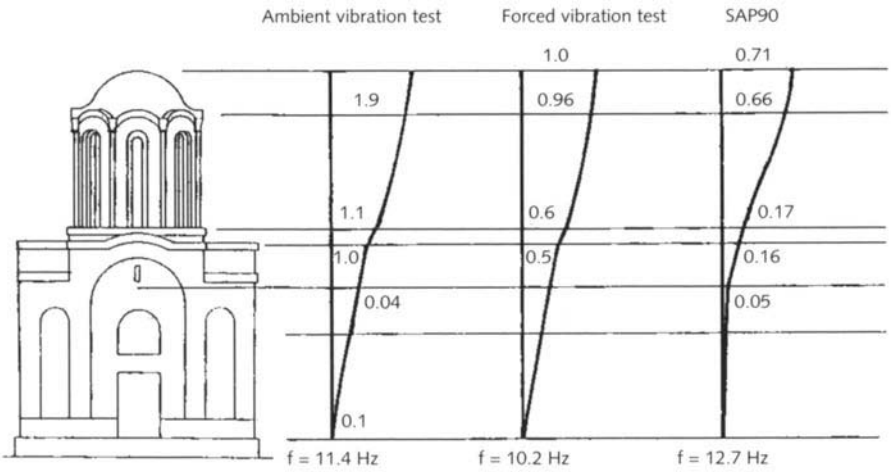

Figure 7.7
Calculated and measured first mode shapes of translation-vibration in the N-S direction for the original model.

Table 7.4
Dynamic response of the original model: Experimental and computed results (maximum) using SAP90 and IZIIS programs

			Experimental results				Analytical results									
			1 = level 1 2 = top of dome				SAP90 model 1 = level 1; 2 = top of dome				IZIIS model 1 = level 1; 2 = top of dome					
Range	Test	Input acceleration (a_{max}) (g)	a-1 (g)	a-2 (g)	d-1 (cm)	d-2 (cm)	a-1 (g)	a-2 (g)	d-1 (cm)	d-2 (cm)	a-1 (g)	a-2 (g)	d-1 (cm)	d-2 (cm)	duct 1	duct 2
Linear	PET012		0.05	0.09	0.07	0.07	0.05	0.12	0.01	0.026	0.04	0.09				
	(0.04)				0.15	0.18							0.12	0.14		
	ELC015		0.05	0.11	0.08	0.07	0.05	0.13	0.008	0.020	0.045	0.10				
	(0.04)			0.16	0.18									0.17	0.16	
	PET035		0.20	0.49	0.19	0.22	0.13	0.30	0.025	0.065	0.10	0.22				
	(0.10)			0.32	0.40								0.30	0.35		
	ELC045		0.18	0.40	0.18	0.18	0.15	0.39	0.024	0.060	0.11	0.25				
	(0.12)				0.42	0.58							0.43	0.48		
Nonlinear	PET075		0.39	0.76	0.53	1.11					0.22	0.45	0.42	0.50	1.40	1.67
	(0.19)															

Note: A second value for a given test indicates the absolute displacement; all values are for the maximum response.

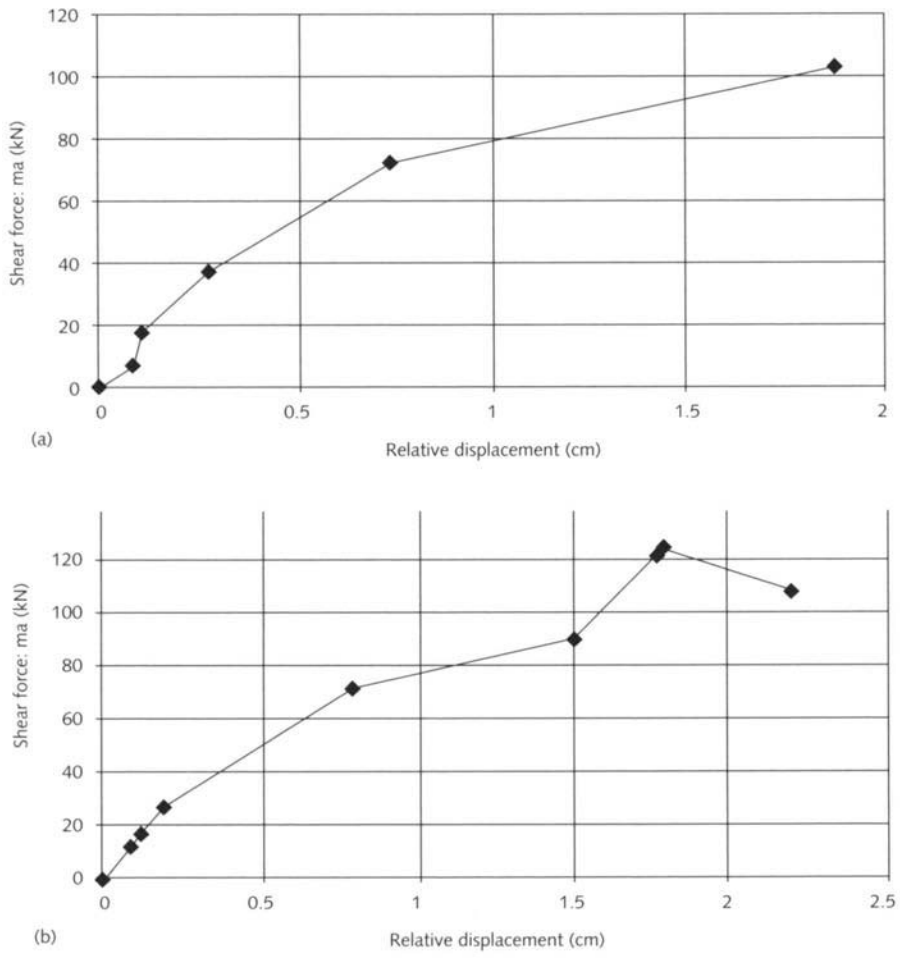

Figure 7.8
Shear force versus relative displacement at level 1 of the strengthened model: (a) Petrovac, (b) El Centro.

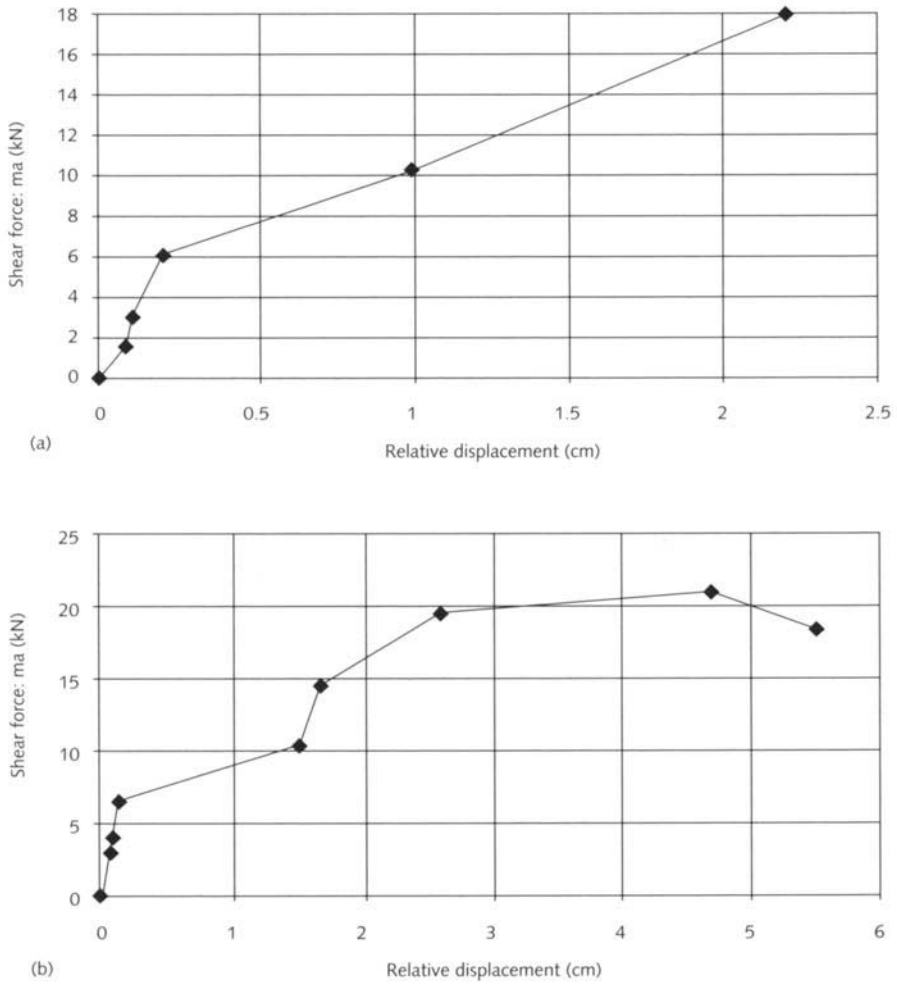

Figure 7.9
Shear force versus relative displacement at the top of the dome of the strengthened model: (a) Petrovac, (b) El Centro.

Analytical modeling of the dynamic behavior in the linear range (input < 0.20 g)

The SAP90 computer program was used for modeling the elastic response of the strengthened church model, which included modeling of the strengthening elements. As described earlier, the damaged model was repaired and strengthened by incorporating horizontal and vertical steel ties in the walls and upper structure and by filling the void volume around the ties with an appropriate grout. In the SAP90 computer program these elements were modeled as FRAME elements that exhibited only axial stiffness and the corresponding characteristics of the material.

The geometry of the model was described by a total number of 877 nodes and 557 elements. A total of 201 FRAME elements were used to model the central columns in the lower part of the walls and the upper part of the structure, the columns of the tambour, and all the new vertical and horizontal strengthening elements. A total of 259 SHELL elements were used to model the vaults, apse, and dome, and the massive facade walls were modeled by a total number of 197 SOLID elements.

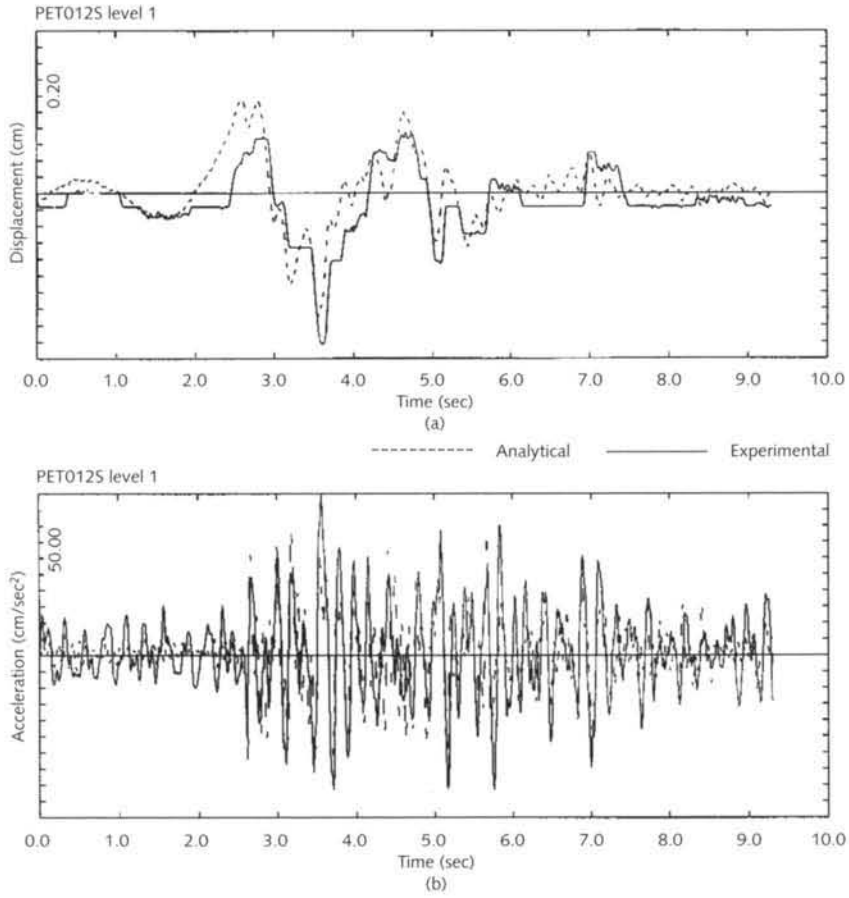

Figure 7.10
Time histories for level 1 (PET012S): (a) displacement, (b) acceleration.

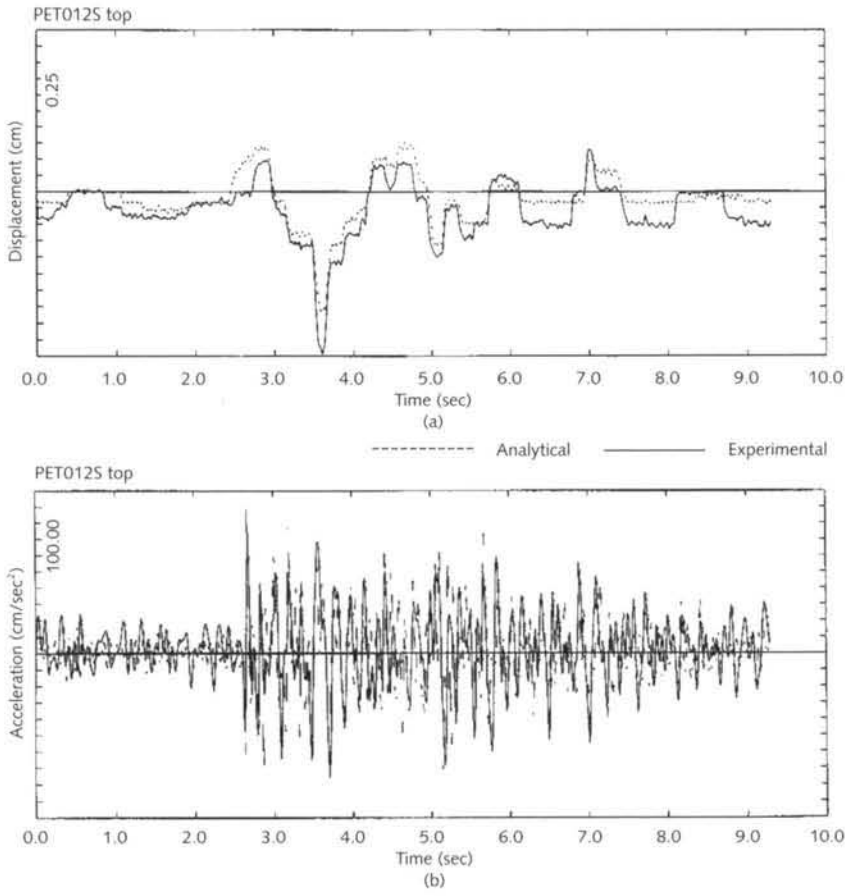

Figure 7.11
Time histories for top of dome (PET012S): (a) displacement, (b) acceleration.

A linear dynamic analysis of the strengthened model was performed in a way similar to that used for the original model. The input excitations used were the same scaled acceleration time histories of the Petrovac and El Centro earthquakes used for the original model.

At the lower input excitations, the calculated response obtained for the strengthened church model was similar to that of the original model. Displacements at the top were insignificantly lower, but the displacements at level 1 were almost identical to those in the original church model. However, these values, when compared to the response of the original model, were considerably smaller, which was probably due to the characteristics of the types of strengthening elements used for modeling the lower part of the structure.

The church model structure was idealized again as a system with two masses and was subjected to a linear analysis in the same way as the original model. The same stiffness characteristics as those for the original model were used for the analysis of the strengthened model (table 7.1). The linear dynamic responses of the strengthened model during accelerations of 0.04 g and 0.19 g were computed using the mathematical model, and a best-fit optimal damping of 6% was obtained by comparing the time histories of the church model's experimental displacement with the analytical response. As an example, the calculated and experimental displacements, accelerations, and Fourier spectra under Petrovac earthquake excitation with input acceleration of 0.04 g for both level 1 and the top of the dome are shown in figures 7.10–7.12. The experimental results for the same parameters at an input acceleration of 0.19 g are shown in figures 7.13–7.15.

A very good correlation was noted between the analytical and experimental data on displacements, accelerations, and frequency contents of acceleration. It should be pointed out, however, that apart from the input earthquake frequencies, the natural frequency of the church model differed from the frequency content of the analytically obtained response, which was not the case for the experimental data. Under such low excitations, the church model responded as a rigid body and followed the movement of the shaking table. It is important to note that the good correlation between the experimental and analytical responses of the church model under the Petrovac excitation of a_{max} = 0.19 g, using the linear mathematical model, indicates that the strengthened model had a considerably higher elasticity limit than the original model.

Analytical modeling of the dynamic behavior in the nonlinear range (input 0.20–0.40 g)

The strengthened church model exhibited nonlinear behavior when subjected to the higher accelerations characteristic of the ELC130S and PET00S tests, in which a_{max} = 0.20–0.40 g. The first visible cracks in the arches of the tambour and the dome occurred within this range. The nonlinear response of the model was computed using the IZIIS model, and the stiffness and damping parameters were defined based on the analytically recorded response and the hysteretic diagrams. The computed

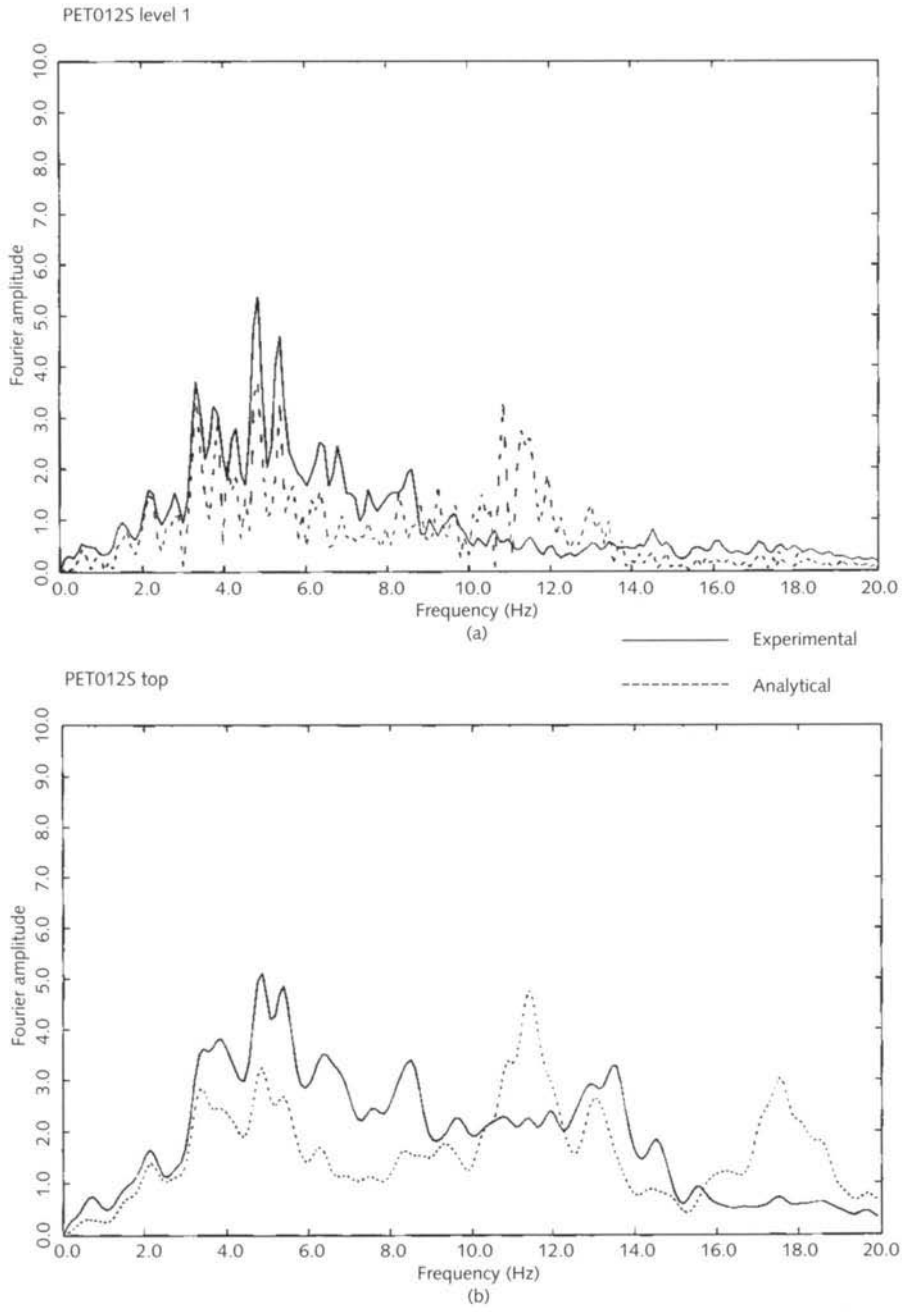

Figure 7.12
Frequency content of experimentally and analytically obtained accelerations (PET012S): (a) level 1, (b) top of the dome.

values of displacements, forces, stiffness, base shear coefficients, and displacement indices are given in table 7.5

Extensive charts that show the nonlinear dynamic responses of the model under the El Centro (a_{max} = 0.25 g) and Petrovac (a_{max} = 0.28 g) earthquakes—in the form of time histories of acceleration and displacement, the Fourier analysis of acceleration, and the nonlinear hysteretic diagrams—are given in Gavrilović, Šumanov, et al. (1991, vol. 12). A good correlation was found between the analytical and recorded acceleration and displacement values, particularly for level 1. The dominant frequencies ranged from 3 to 5 Hz for both earthquakes, which resulted from the "softening," or stiffness degradation, of the system.

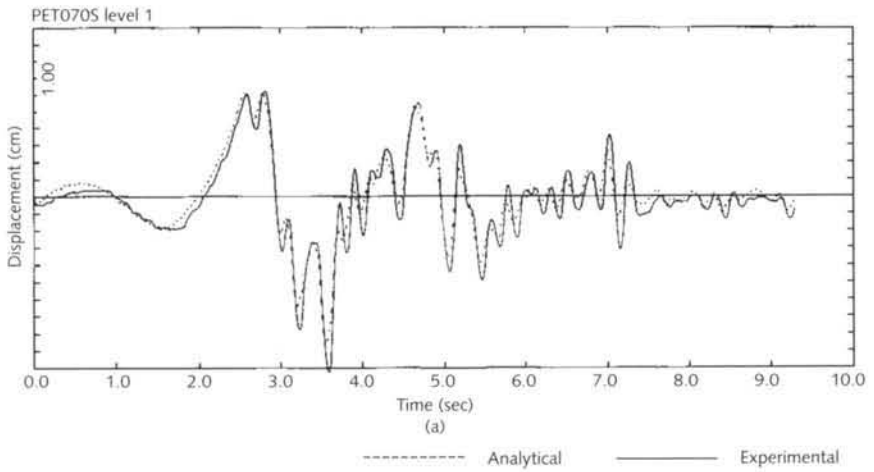

Figure 7.13
Time histories for level 1 (PET070S): (a) displacement, (b) acceleration.

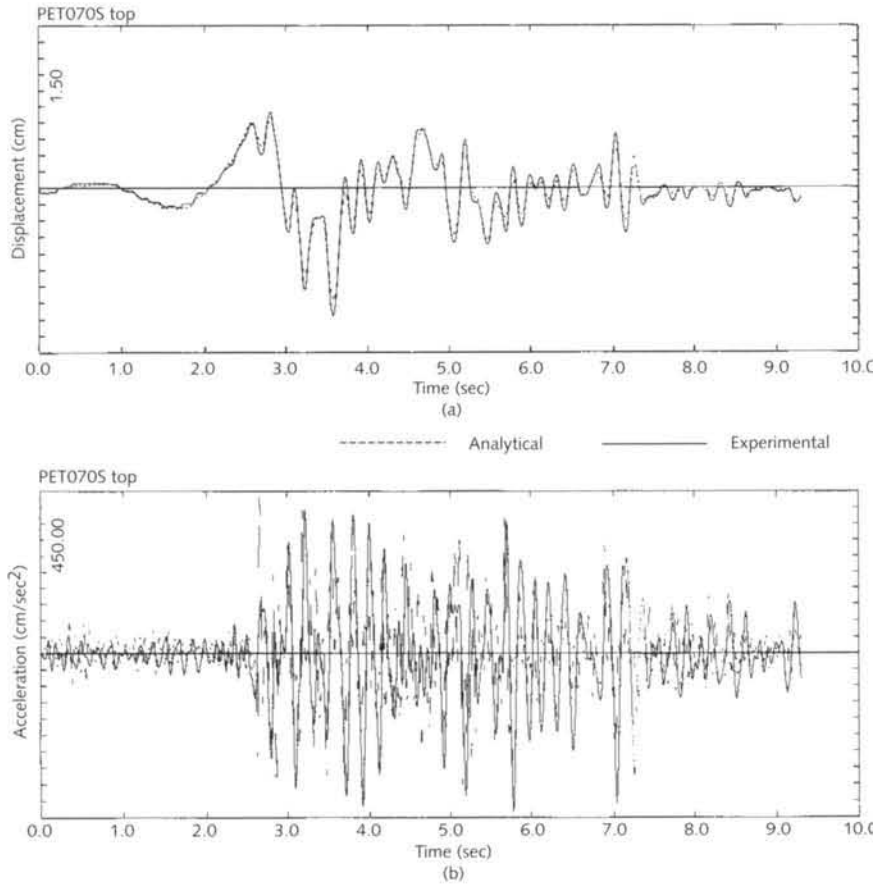

Figure 7.14
Time histories for the top of the dome (PET070S): (a) displacement, (b) acceleration.

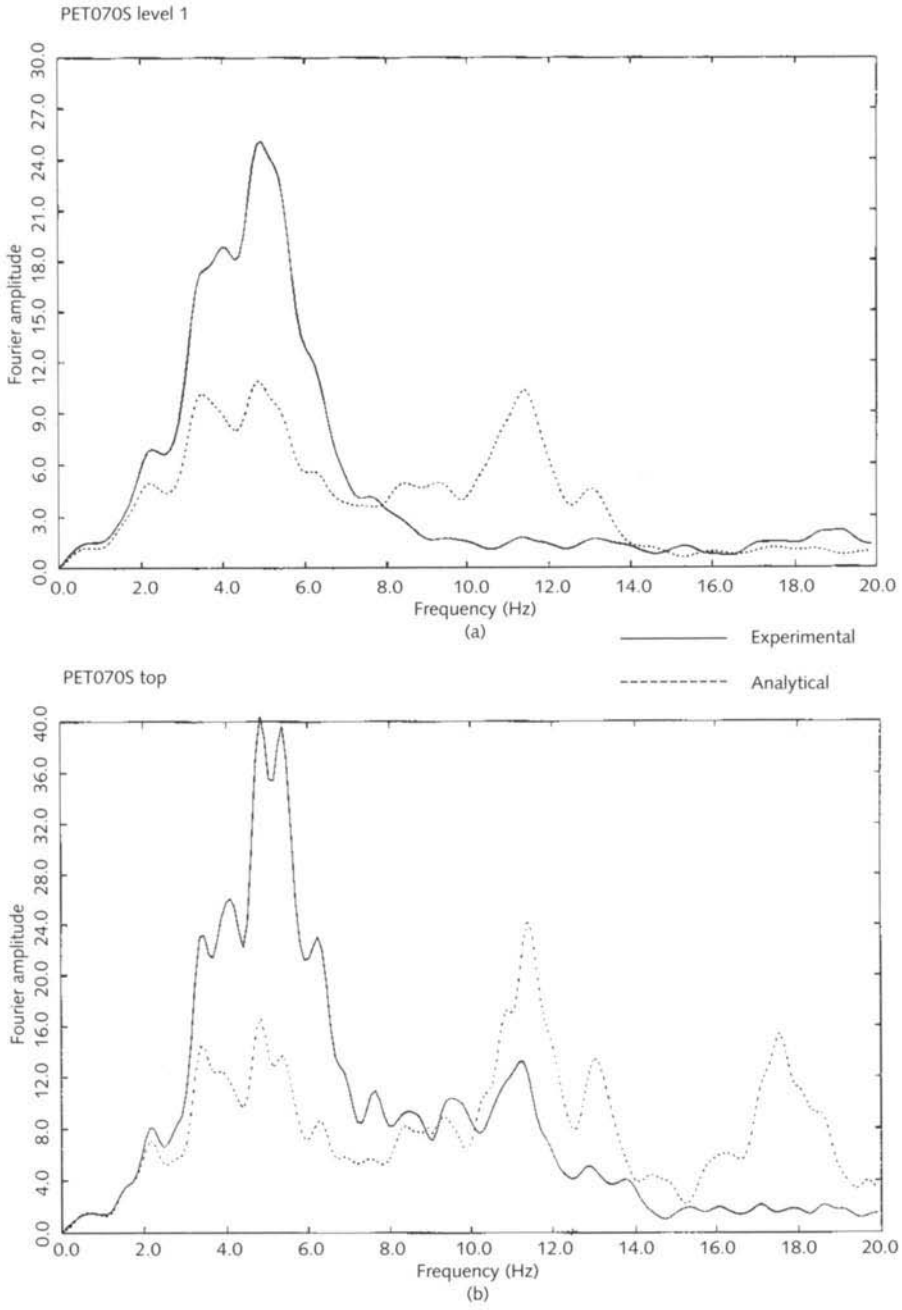

Figure 7.15
Frequency content of experimentally and analytically obtained accelerations (PET070S): (a) level 1, (b) top of the dome.

Larger deviations of the maximum displacements were obtained for the top of the dome under the El Centro earthquake excitation, which was also the case for the frequency content. Analysis of the hysteretic diagrams showed that pinching of the hysteretic loop occurred for the lower structure, whereas almost no pinching was obtained for the upper structure, where bending was the dominant mode.

Analytical modeling of the dynamic behavior in the ultimate range (input > 0.40 g)

At input accelerations greater than 0.40 g, plastic deformations occurred, particularly in the upper part of the structure. For this reason, the model response in this and the postultimate range was analyzed by application

Table 7.5
Parameters for the nonlinear response of the strengthened model

Nonlinear input acceleration range: a_{max} = 0.20–0.40 g								
	F_c (kN) (Cbs)	D_c (cm) D/H (%)	K_c (kN/cm)	F_u (kN) (Cbs)	D_u (cm) D/H (%)	K_u (kN/cm)	F_s (kN) (Cbs)	D_s (cm) D/H (%)
Top of dome	3.5 (0.13)	0.035 (0.017)	100	14 (0.54)	0.4 (0.2)	28	8 (0.3)	0.3 (0.015)
Level 1	10 (0.06)	0.02 (0.008)	500	65 (0.42)	0.45 (0.19)	128	15 (0.07)	0.01 (0.004)

of the IZIIS trilinear hysteretic model. As in the previous cases, the parameters of the strengthened model were based on the analysis of the recorded response under test PET140S. The mathematical model was then applied in the analyses of the El Centro earthquake excitations (ELC220S, ELC280S, and ELC320S). The values of the necessary parameters are given in table 7.6.

Analysis of the nonlinear dynamic response of the principal structure (level 1) showed a good correlation between the analytical and the recorded data, but this was not the case for the upper structure, especially the top of the dome. Due to the large deformation of the tambour arches after test PET140S, it was necessary to decrease the initial stiffness of the upper structure in order to achieve a good response correlation in the subsequent test, ELC220S. The initial stiffness value and the other needed parameters were obtained from the response at the top of the dome under each of the subsequent tests performed separately. Table 7.7 shows the values of the parameters of tests ELC220S, ELC280S, and ELC320S for the upper part of the model structure, for which the best correlation between the analytical and recorded responses was achieved.

The detailed results of the analysis, presented as hysteretic F-Δ diagrams and time histories of displacement and acceleration response, as well as the Fourier response spectra of acceleration, are given in Gavrilović, Šumanov, et al. (1991, vol. 12). The values of the damping coefficients ranged from 6% to 9%. Comparison of the analytical and recorded responses of the model structure points to a good correlation, especially for tests PET140S and ELC220S.

Table 7.6
Parameters for the ultimate response of the strengthened model

Ultimate input acceleration range: a_{max} = 0.40–0.60 g											
	F_c (kN) (Cbs)	D_c (cm) D/H (%)	K_c (kN/cm)	F_u (kN) (Cbs)	D_u (cm) D/H (%)	K_u (kN/cm)	F_m (kN) (Cbs)	D_m (cm) D/H (%)	K_m (kN/cm)	F_s (kN) (Cbs)	D_s (cm) D/H (%)
Top of dome	12 (0.46)	0.45 (0.23)	27	15 (0.58)	1.1 (0.56)	4.6	15 (0.58)	2.6 (1.33)	0	9 (0.35)	0.05 (0.024)
Level 1	60 (0.38)	0.55 (0.24)	109	65 (0.42)	1.0 (0.43)	11	55 (0.35)	2.5 (1.1)	–6.7	11 (0.07)	0.01 (0.004)

Table 7.7
Modified parameters for the ultimate response of the strengthened model, top of the dome

Ultimate input acceleration range: a_{max} = 0.40–0.60 g											
Test	F_c (kN) (Cbs)	D_c (cm) D/H (%)	K_c (kN/cm)	F_u (kN) (Cbs)	D_u (cm) D/H (%)	K_u (kN/cm)	F_m (kN) (Cbs)	D_m (cm) D/H (%)	K_m (kN/cm)	F_s (kN) (Cbs)	D_s (cm) D/H (%)
ELC220S	8.0 (0.30)	0.45 (0.23)	18	14.0 (0.53)	2.5 (1.27)	2.9	10.0 (0.37)	5.5 (2.8)	−1.3	5.0 (0.19)	0.05 (0.025)
ELC280S	6.0 (0.22)	0.45 (0.23)	13.3	12.0 (0.45)	2.5 (1.27)	2.9	8.0 (0.30)	5.5 (2.8)	−1.3	3.0 (0.11)	0.15 (0.08)
ELC320S	2.0 (0.08)	0.45 (0.23)	4.4	9.0 (0.34)	3.0 (1.5)	2.7	6.4 (0.24)	4.5 (2.3)	−1.6	1.0 (0.04)	0.15 (0.008)

The shape of the time histories of acceleration obtained in all the tests indicates the important contribution of the low frequencies, which was also observed in the Fourier acceleration spectra. As the stiffness degradation of the system increases, participation of the higher periods (lower frequencies) increases. Frequencies of 2–4 Hz dominate in the Fourier spectra in tests PET140S and ELC220S, whereas the dominating frequencies in the final tests, ELC280S and ELC320S, are 1–3 Hz. The increased transition of the system to a lower frequency range is shown in the analytical response by the increased softening of the system due to stiffness degradation under reloading and pinching of the hysteretic loop (characteristics of the IZIIS model).

Degradation of the initial stiffness resulted from cracks that occurred during previous tests. For level 1, the initial stiffness of 500 kN/cm, corresponding to deformations of about 0.1% of the story height, dropped to 109 kN/cm for deformations of about 2% (see table 7.6). The initial stiffness of the top of the dome, 100 kN/cm, dropped to 27 kN/cm (see table 7.6) and to 4.4 kN/cm in the final tests.

The modeling response was described by the initial stiffness values. For deformations of about 2–5% of the story height, the K_u stiffness was taken as 15% of the initial stiffness. The stiffness in the plastic phase was considered zero for the top of the dome and negative for level 1. The pinching point was also defined by the coordinates of about $0.2F_u$ and $0.01\ D_u$. The coordinate in the diagram at which maximum force was achieved (i.e., prior to stiffness degradation) was taken as the yielding point; it was 4% for level 1 and 5.6% for the top of the dome. The ultimate deformation, OM, was $2.5\ D_u$, which corresponded to a ductility of 2.5%.

Correlation between the analytical and experimental results

Dynamic characteristics of the model

The experimental and analytical values of the fundamental frequencies of the strengthened model are shown in table 7.8. A very good correlation is evident between the first natural frequencies obtained experimentally

and analytically by using the SAP90 computer program. For the second frequencies, SAP90 yielded higher values due to the effects from other directions. With regard to the mode shapes, lower values were obtained than those for the original model. The SAP90 computer program yielded lower values than the experimental data for the principal structure, which probably resulted from the characteristics of the type of elements (SOLID) used for modeling of the facade walls.

Dynamic response of the model

Table 7.9 shows the experimental and analytical values obtained for the maximum accelerations and displacements (relative and absolute) at level 1 and at the top of the dome, using both the SAP90 computer program and the IZIIS model.

Lower displacement values were obtained for the principal structure of the strengthened model when analyzed by the SAP90 computer program, particularly at the higher input acceleration levels, since the linear response was closely connected with mode shapes. Although this computer package provides far greater possibilities for static analysis than for dynamic, it can still be applied to obtain basic information and approximate solutions for the dynamic response of such specific and complex structures.

The analytical results obtained by applying the mathematical model, based on a system with two masses and the use of the IZIIS hysteretic model in the form of maximal displacements and accelerations, show values similar to the experimental data for all three characteristic ranges of behavior of the church model structure (table 7.9). The analysis of these ranges and the results given in the preceding section lead to the following conclusions:

- Under low excitation accelerations, <0.20 g, which corresponds to an acceleration of 0.09 g for the prototype church, the model behaved in the linear range and the dynamic behavior of the structure could be described by a linear mathematical model. Stiffness values were determined from the results of the test of the model; the initial stiffness was 190 kN/cm for the top of the dome and 725 kN/cm at level 1 (see table 7.1). These values were used to obtain the

Table 7.8
Comparison of the computed and experimental values of the natural frequencies of the strengthened model

Direction	Type of excitation	Type of analysis	Natural frequency (Hz) f_1	f_2
North-south	Ambient vibration		11.4	20.6
	Forced vibration		10.8	19.2
	Random excitation		11.2	–
		SAP90	14.1	28.9
East-west	Ambient vibration		15.8	23.2
	Forced vibration		15.2	22.2
		SAP90	14.6	29.5

Table 7.9
Summary of the experimental and dynamic results for the strengthened church model

			Experimental results 1 = level 1 2 = top of dome				SAP90 model 1 = level 1 2 = top of dome				IZIIS model 1 = level 1 2 = top of dome					
Range	Tests	Input acceleration (a_{max}) (g)	a-1 (g)	a-2 (g)	d-1 (cm)	d-2 (cm)	a-1 (g)	a-2 (g)	d-1 (cm)	d-2 (cm)	a-1 (g)	a-2 (g)	d-1 (cm)	d-2 (cm)	duct 1	duct 2
Linear	PET012S	0.04	0.05	0.09	0.07	0.05	0.04	0.10	0.01	0.026	0.04	0.09				
					0.18	0.25							0.12	0.18		
	ELC015S	0.05	0.07	0.14	0.07	0.06	0.05	0.13	0.008	0.020	0.045	0.10				
					0.12	0.15							0.17	0.16		
	PET035S	0.10	0.13	0.20	0.10	0.10	0.10	0.25	0.025	0.065	0.10	0.22				
					0.39	0.45							0.30	0.45		
	ELC045S	0.10	0.12	0.27	0.10	0.08	0.15	0.39	0.024	0.060	0.09	0.20				
					0.33	0.36							0.34	0.38		
	ELC085S	0.18	0.19	0.46	0.18	0.13	0.15	0.39	0.024	0.060	0.16	0.36				
					0.67	0.70							0.61	0.68		
	PET070S	0.19	0.24	0.45	0.27	0.17	0.19	0.47	0.024	0.060	0.20	0.45				
					1.00	1.00							0.90	1.10		
Nonlinear	ELC130S	0.25	0.49	0.72	0.78	1.48					0.33	0.59	0.31	0.22	0.69	0.55
	PET100S	0.28	0.50	0.75	0.72	0.80					0.35	0.70	0.36	0.27	0.67	0.80
Ultimate	PET140S	0.42	0.71	1.20	1.90	2.00					0.55	1.05	1.6	1.10	1.60	1.00
	ELC220S	0.41	0.81	1.41	1.68	2.58					0.60	1.10	1.40	2.60	1.20	1.46
	ELC280S	0.48	0.90	1.52	1.80	4.70					0.60	1.20	1.52	4.40	1.76	1.52
	ELC320S	0.52	0.64	1.11	1.96	5.50					0.61	0.78	1.62	4.45	1.80	1.62

Note: A second value for a given test indicates the absolute displacement; all values are for the maximum response.

results in table 7.9, in the form of maximum absolute displacements and accelerations. A high level of correlation was evident. Negligible deviations in the time histories resulted from minor differences in material properties and procedures during such complex experiments.

- At excitation acceleration levels of $0.20 < a_{max} < 0.40$ g, visible and invisible cracks occurred in the church model structure. These cracks resulted in stiffness deterioration, which gave rise to nonlinear deformations. This state was modeled analytically by an IZIIS hysteretic model that had the following characteristics: initial stiffness, K_c = 100 kN/cm for the top of the dome, and K_c = 500 kN/cm for level 1; a very low deformation level of 0.1%; a stiffness, K_u, that is about 25–30% of the original model stiffness; deformations of D_u = 2% of the story height; and the point of pinching of the hysteretic loop with coordinates $F_u/4$, $D_u/25$. As to their shape, the analytically computed time histories of acceleration and displacement obtained for the church model correlated well with the experimen-

tal data, with the exception of the values for tests ELC130S and PET100S (table 7.9).

- At excitation acceleration levels greater than 0.40 g, large, nonlinear deformations of the tambour arches occurred and substantial cracks developed in the walls. For this reason, the initial stiffness obtained by identification of the analytical and recorded responses was about 25% of the initial stiffness during the nonlinear behavior region and held for deformation levels of about 2%, whereas the K_u stiffness amounted to 10–20% of the initial stiffness for deformation levels of up to 5%. The stiffness after point U (fig. 6.6) was negative, while the maximum deformation was 2.5 times larger than the D_u deformation. Pinching of the hysteretic loop that was found to be characteristic of the principal structure (level 1) was defined by coordinates 0.2 F_u and 0.01 D_u, indicating that shear forces exerted a dominant influence. The maximum analytical values for tests PET140S, ELC220S, ELC280S, and ELC320S, shown in table 7.9, were obtained using these defined parameters. A high level of correlation was observed when these values were compared with those obtained experimentally. It should be pointed out, however, that the initial stiffness of the upper structure deteriorated with each successive test due to the large plastic deformations of the tambour and the dome structure. The damping coefficient in all analyses was taken as 6–9%.

The Bearing and Deformability Capacities of the Model Structures at the Design and Maximum Levels of Expected Ground Motion

On the basis of the results obtained from the nonlinear analysis of the original and strengthened church models by application of the IZIIS hysteretic model, the following bearing capacities and deformabilities of the models were obtained:

- The bearing capacity of the original model, expressed in terms of the base shear coefficient, is $C_{bs} = 0.20$ for the state of occurrence of the first cracks, whereas that for the strengthened model is $C_{bs} = 0.29$.
- The analytically obtained ductility of the structure under different seismic excitations (tables 7.4 and 7.9) is shown in table 7.10.

These results show that for an input acceleration $a_{max} < 0.20$ g, corresponding to a return period of 100 years, the structure of the original model suffered some nonlinear deformations, whereas the strengthened model remained completely undamaged (ductility < 1).

Table 7.10
Analytical ductility ($\mu = D_{max}/D_y$) for different input accelerations

	a_{max} input ≤ 0.2 g		a_{max} input = 0.2–0.4 g		a_{max} input = 0.4–0.6 g	
Model	Level 1	Top	Level 1	Top	Level 1	Top
Original	1.4	1.7	–	–	Failure	Failure
Strengthened	0.7	0.6	1.4	1.2	1.6	1.8

At input accelerations between $a_{max} = 0.20$ and $a_{max} = 0.40$ g, corresponding to a return period of 200 years, failure of part of the dome, the tambour, and the cornices, as well as the appearance of large cracks in the bearing walls, was observed in the original model, whereas the effects in the strengthened model were characterized by the occurrence of the first nonlinear deformations of secondary elements (ductility < 1.5).

At input accelerations between $a_{max} = 0.40$ and $a_{max} = 0.60$ g, corresponding to an earthquake of the maximum expected severity with a return period of 1000 years, the original model suffered complete failure, whereas the strengthened model exhibited severe damage to the upper structure (the dome and the tambour) and the bearing walls, but the ultimate bearing capacity was not exceeded (ductility $1.5 < \mu < 2$).

It may be concluded that the analytical modeling of all phases of the dynamic behavior of the original and strengthened church models correlated well with the results obtained experimentally.

Capacity Analysis of Masonry Buildings

Although the IZIIS hysteretic model with stiffness degradation and pinching of the loops could successfully describe all phases of the nonlinear dynamic behavior of the church model structure, there are still no unique analytical expressions for definition of all the model parameters. However, in practice, the analysis of such structures under dynamic loads requires simpler methods that permit a rapid and effective way of answering the question of how a specific structure will behave during a specified earthquake event.

Bearing capacity and deformability are the principal initial parameters that must be known in order to define the behavior of the structure, and these factors are also necessary for defining the remaining parameters used in the hysteretic model. The following methodology allows definition of the bearing capacity of the structure in the form of an ultimate story shear force that is compared to the equivalent seismic force and yields the factor of safety against failure.

Depending on the degree of exactness and the complexity of the analysis, the dynamic effects of ground motion acting upon the structure can be expressed in three different ways:

- as a static equivalent horizontal load *independent* of the dynamic characteristics of the structure;
- as a static equivalent horizontal load *dependent* on the dynamic characteristics of the structure; or

- by means of a dynamic analysis in which a recorded or synthetic accelerogram is used.

In the case of masonry buildings of limited height and plan dimensions, and for practical engineering reasons and building code requirements, the horizontal seismic action is usually given in terms of "base shear," which represents the resultant of the inertial forces distributed along the height of the structure and acting horizontally in both principal directions of the structure. The total horizontal seismic force is

$$S = K\,G \tag{7.1}$$

where K is the total seismic (base shear) coefficient and G is the total mass of the structure. The total seismic coefficient is defined as

$$K = K_s\,K_d\,K_p \tag{7.2}$$

where

K_s = seismic intensity coefficient
K_d = dynamic coefficient
K_p = ductility and damping coefficient

Seismic intensity coefficient, K_s

The seismic intensity coefficient is given by

$$K_s = a_{max}\,B_{max}/g\,\mu \tag{7.3}$$

where

a_{max} = maximum expected ground acceleration
B_{max} = maximum value of the representative response spectrum
$g = 9.81$ m / sec^2 (acceleration of gravity)
$\mu = 4$ (the equivalent nominal ductility factor)

The values of a_{max} are obtained from seismic investigations of the site; for the needs of this analysis, the values of a_{max} for different return periods are taken from table 3.1.

Coefficient B is given by

$$B = 1.4 / T; \quad 2.0 > B > 0.94 \therefore B_{max} = 2.0 \tag{7.4}$$

Substituting the values, the seismic intensity coefficient becomes

$$K_s = 2.0\,(a_{max}) / (9.81 \times 4.0) = a_{max} / 19.62 \tag{7.5}$$

Ductility and damping coefficient, K_p

The ductility and damping coefficient depends on the type of structure. For brittle, nonductile stone-wall structures, $K_p = 2.2$–3.0.

Dynamic coefficient, K_d

The dynamic coefficient represents the dynamic amplification factor and depends on the fundamental period of the structure and soil characteristics. It is computed from the spectral curve of the dynamic coefficient,

which equals 1.0 for periods smaller than 0.5. The fundamental period of masonry structures of ordinary height does not exceed a value of 0.5. Accordingly, the total seismic force is

$$S = (a_{max} / 19.62)\ (2.2)\ (1.0)\ (G) = 0.112\ (a_{max})\ (G) \qquad (7.6)$$

and the distribution of seismic forces per story is given by

$$S_i = S\ (G_i H_i / \sum_{i=1}^{n} G_i H_i) \qquad (7.7)$$

where

S_i = horizontal seismic shear force at the *i*th story
G_i = mass of the *i*th story
H_i = height of the *i*th story from the foundation level
n = number of stories

The story seismic force, S_i, is distributed according to the stiffness of the walls

$$S_j = S_i\ (K_j / \sum_{j=1}^{m} K_j) \qquad (7.8)$$

where

S_j = equivalent shear force at the *j*th wall
K_j = stiffness of the *j*th wall
m = number of walls at the *i*th story

Chapter 8

Mathematical Model of the Byzantine Church Structure

The principal bearing structure of a masonry church building consists of walls in both orthogonal directions, and therefore modeling of the structure is reduced to modeling the shear walls. In the analysis, the walls are usually treated as vertical cantilevers fixed at the base and interconnected by floor structures, which are assumed to have the role of rigid horizontal diaphragms that transfer the horizontal loads to other walls, depending on their stiffness. The assumption about the vertical cantilevers holds when the individual walls are interconnected by flexible floor structures and the wall openings are small, so the simple cantilever behavior of the wall as a whole is not disturbed.

However, when the floor structures are rigid, the wall element is modeled as fixed at the top and the bottom. If the openings in the walls are larger, the weak points with regard to earthquake effects are the piers of the walls (narrow wall segments between openings) or the lintel "beams," so rather than modeling the wall as a whole it becomes necessary to model the individual wall elements.

Rigid floor structures are not usually found in historic churches. Instead, a system of arches, vaults, and pendentives spans the horizontal spaces. The massive facade walls most frequently have openings in the form of doors and mono- or multiforia or are otherwise weakened by niches and pilasters. The interior walls always have large openings separated by the central columns, which support the upper part of the structure. Individual exterior walls and interior wall elements behave in different ways, which complicates the behavior of the building systems to the extent that precise mathematical modeling and analyses are virtually impossible given the present level of knowledge of the problem.

The mathematical model proposed here assumes the facade walls are vertical cantilevers fixed at the base. If data exist that confirm the presence of horizontal belt courses in individual walls of specific structures, the walls can be modeled as fixed at both ends.

Analysis of Structural Walls

Wall stiffness

Horizontal seismic forces are distributed through the individual walls in proportion to their stiffness, assuming that all the walls of the particular

story behave similarly. The stiffness of the wall depends on its geometry, the elastic moduli and shear moduli characteristic of the construction materials, and the nature and condition of the supports at the top and the base of the wall.

Using relations from the theory of structures regarding stiffness coefficients for both fixed and cantilever elements with included shear effects,

$$K_{fixed} = (G / 1.2\ h)\ (A / 1 + 0.83\ G / E\ [h/d]^2) \tag{8.1}$$

$$K_{cantilever} = (G / 1.2\ h)\ (A / 1 + 3.33\ G / E\ [h/d]^2) \tag{8.2}$$

where

K = initial, elastic stiffness of the wall
A = horizontal cross-sectional area of the wall
h = height of the wall
d = length of the wall
E = elastic modulus
G = shear modulus

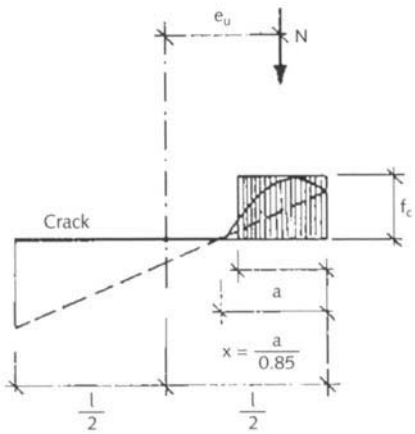

Figure 8.1
Idealized stress distribution in plain masonry.

Flexural capacity

Plain masonry

When defining the flexural capacity of a wall under the simultaneous effects of horizontal and vertical loads, it is usually assumed that the masonry has no tensile bearing capacity. In that case, the cracks occur in the tensile part and extend further up to the compressed part of the wall.

Assuming that the actual diagram can be idealized as a rectangular distribution of pressure(fig. 8.1), the ultimate moment, or shear force, can be computed from the equivalent vertical forces:

$$N = (f_c)\ (t)\ (a) \tag{8.3}$$

From the condition that $\Sigma M = 0$, the ultimate moment is given by

$$M_u = (\sigma_0\ t\ d^2 / 2)\ (1 - \sigma_0 / f_c) \tag{8.4}$$

that is, the ultimate shear force that can be sustained by the cross section

$$Q_u|^M{}_{fixed} = 2\ M_u / h \tag{8.5}$$

$$Q_u|^M{}_{cantilever} = M_u / h \tag{8.6}$$

where

$Q_u|^M$ = ultimate shear force due to bending
M_u = flexural capacity of the wall
σ_0 = average compressive stress due to vertical load
N = applied vertical force
f_c = compressive strength of material

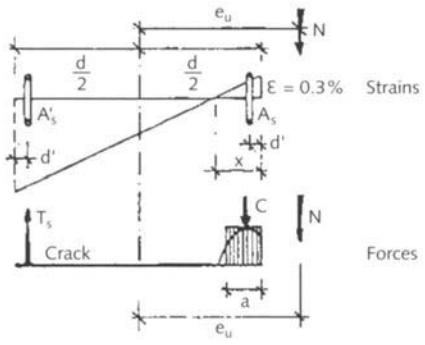

Figure 8.2
Flexural capacity of a wall can be increased by reinforcement.

t = thickness of the wall
d = length of the wall
h = height of the wall

Confined masonry

To increase the bending resistance of the wall elements, vertical belt courses are often incorporated at the ends of the wall, and along with the horizontal belt courses they form the so-called confined wall. In this case, the flexural capacity is increased by the value of the additional moment due to the reinforcement at the wall ends (fig. 8.2)

$$M_u = (\sigma_0 \, t \, d^2 / 2) \, (1 - \sigma_0 / f_c) + A_s \, F_{s,y} \, (d - 2d') \qquad (8.7)$$

where

A_s = cross section of the reinforcement at the ends of the wall
$F_{s,y}$ = stress at reinforcement yield
d' = distance from the reinforcement to the end of the wall

Shear capacity

Plain masonry

Considering an ultimate shear state of a wall element and applying the relations for the principal normal stresses occurring in the element, the following expression is obtained for the main tensile stresses, f_t:

$$f_t = -\sigma_0 / 2 \pm \sqrt{(\sigma_0)^2 + (4\tau_u)^2} \qquad (8.8)$$

That is, the average ultimate shear stresses are given by

$$\tau_u = f_t / \zeta \sqrt{\sigma_0 / f_t + 1} \qquad (8.9)$$

The ultimate shear capacity of the wall can be defined by multiplying the average ultimate shear stress by the area of the horizontal cross section of the wall

$$Q_u l^s = (A \, f_t / \zeta) \sqrt{\sigma_0 / (f_t + 1)} = (d \, t \, f_t / \zeta) \sqrt{\sigma_0 / (f_t + 1)} \qquad (8.10)$$

where

$Q_u l^S$ = ultimate transverse shear force (shear capacity)
τ_u = average ultimate shear stress
σ_0 = average compressive stress under vertical load
f_t = characteristic tensile strength of the wall
A = area of the horizontal cross section of the wall (d t)
ζ = coefficient of distribution of shear stresses depending on the wall geometry (height/length ratio) and the load eccentricity. (The value of this coefficient varies from 1.54 for slender walls [h / d > 1.5] to 1.0 for wide walls [h / d < 1.0].)

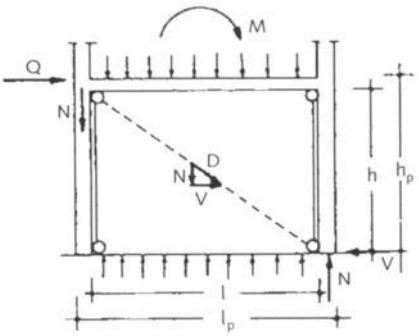

Figure 8.3
Shear mechanism in confined masonry.

Confined masonry

The shear capacity of a confined masonry panel is defined by the occurrence of a diagonal crack due to tension along the diagonal (fig. 8.3) and is computed using the following formula:

$$Q_u^s = t\ d\ f_t\ [h / 2d + \sqrt{(h / 2d)^2 + \sigma_0 / f_t + 1}] \qquad (8.11)$$

Calculation Procedure

The steps required for an earthquake capacity analysis of a structure are as follows:

1. Compute the masses of the structure concentrated at specific levels and define the geometry of the bearing walls and the corresponding vertical loads.
2. Adopt values for the physical-mechanical characteristics of masonry: elastic and shear moduli, ultimate compressive strength (f_c), and ultimate tensile strength (f_t).
3. Define the total seismic force at the base—the story horizontal seismic forces in both orthogonal directions (S, S_i)—in accordance with the procedure described in chapter 7, in the section entitled "Capacity Analysis of Masonry Buildings."
4. Compute the stiffness of the individual walls (K) by adopting an adequate mathematical model.
5. Distribute the story horizontal force (S_i) through the individual walls (S_j), in proportion to their stiffness, in each of the walls' main directions.
6. Define the bearing capacity of the horizontal section of each wall under bending and shear forces as the ultimate shear force, the lower value of which is used (Q_{uj}).
7. Compare the ultimate shear force to the distributed horizontal seismic force for each wall, and express their ratio as a safety factor ($F_j = Q_{uj} / S_j$).
8. Define the story Q-Δ diagram by summing up the Q-Δ diagrams for all the walls in the considered direction.
9. Compare the story ultimate force to the total horizontal force obtained by the base shear coefficient; the story safety factor against failure is given by $F_u = Q_u^{story} / S$.

Interpretation of the results obtained in this way allows consideration of both the individual behavior of each wall and the behavior of the structure as a whole, which leads to identification of the critical or weak points in the structure (walls). Adequate measures can then be taken to minimize these weaknesses.

The MASAN computer program was developed to carry out the procedure described above. The input parameters for this program were the geometry of the walls, the characteristics of the materials, and

the previously computed base shear coefficient. The output parameters were the safety factors—both separate ones for each wall and one for the entire structure. This computer program was used to analyze the St. Nikita church model as well as the structures of the three other churches selected for detailed study.

Results from the MASAN Program for the Original St. Nikita Model

Input data for analysis of the structure of the original model were prepared, the masses corresponding to the dome and vaults levels were computed, and the geometry and vertical loads in the walls in the north-south direction were calculated. The base shear coefficient was computed based on local soil condition data for the site of the church of St. Nikita and the scale to which the model was constructed. Its value was found to be $C_{bs} = 0.70$.

The results of the quasi-static tests of the three wall elements (E = 600,000 kPa, G = 140,000 kPa, f_c = 500 kPa, f_t = 35 kPa) were taken as the mechanical characteristics of the material constituting the model and were used for computation of the directional stiffness and the bearing capacity of the individual walls.

The walls were modeled as vertical cantilevers fixed at the base, and the vertical load for each wall taken separately was computed as a sum of its mass, the vertical load, and the value of the tensile force that was applied to the vertical steel bars. The latter was required for modeling the compressive stresses under vertical loads.

Values of the initial story stiffness at both levels were obtained based on the stiffness of the individual walls, the shear and bending bearing capacities for each wall taken separately, and the safety factor, F_N, obtained as a ratio between the applied seismic force on the wall and the ultimate shear force. The results obtained for F_N for each wall indicated that the east-west walls used for modeling the tambour would not have sufficient bearing capacity ($F_N < 1.0$) to resist excitation from a maximum-severity seismic event.

Satisfactory results were obtained for the initial-story stiffness values (K_1 = 784; K_2 = 111 kN/cm), which correlated well with stiffness values obtained from the ambient vibration measurements that were taken as initial stiffness values in the analysis of the dynamic response of the model. The values obtained for the story safety factors against failure under the conditions of a maximum-severity seismic event pointed to an insufficiency in the north-south direction. From an analysis of the story ultimate shear forces, Q_2 = 7 kN and Q_1 = 74 kN, and the base shear coefficients, $(C_{bs})_2 = 0.27$ and $(C_{bs})_1 = 0.47$, the level of seismic effect that the structure would have sufficient capacity to withstand was determined. The results indicated that the upper structure of the model would fail at $a_{max} = 0.27$ g and that failure of the principal structure would occur at $a_{max} = 0.47$ g. These computed results correlated well with the experimental results obtained from the shaking-table tests of the model. The results indicated the necessity of adding seismic

strengthening to the structure to increase the shear and bending bearing capacities of the west and east walls of the church.

Results for the Strengthened Church Model

After the series of shaking-table tests that resulted in damage to the church model, the structure was repaired and strengthened. Cracks were repaired by grout injection under pressure and replacement of damaged mortar and loose bricks. Strengthening was carried out by incorporating horizontal steel ties in the facade walls, in the base of the tambour, and in the base of the dome. Vertical steel ties were inserted at the ends of the walls and around the openings to increase the bending resistance. An earthquake capacity analysis of the strengthened church model was performed using the MASAN program for a maximum base shear coefficient of $C_{bs} = 0.70$. In this case, the walls were modeled as being fixed at the base and at the top. The new input data were concerned with the reinforcements used for the vertical belt courses: bars 10 mm in diameter in the tambour; 14 mm bars in each of the west and the east walls; and 16 mm bars in the interior walls, W3 and W4. For computing the bearing capacity of the walls, the relations referring to confined masonry were used. The remaining input parameters remained unchanged.

The computed results indicated an increased bearing capacity for each wall taken separately and a safety factor against failure of $F_N > 1.0$. A higher bearing capacity, and therefore an increased safety factor ($F_N > 1.0$), was also obtained for the structure as a whole, and this was confirmed by the results of the experimental shaking-table tests of the strengthened church model.

Bearing Capacity of the Church Model Structure

The structures of the original and strengthened model were analyzed using the appropriate mathematical models. The ultimate shear and bending forces for each wall, and for the structure as a whole, were determined based on the computed masses, horizontal seismic forces, and stiffness characteristics. Finally, the safety factor was computed as the ratio between the ultimate force and the base shear force in the analyzed direction. The results for the original church model are presented in table 8.1 and those for the strengthened model in table 8.2.

The values of C_{bs} for corresponding return periods are

- 100 years: $C_{bs} = 0.28$
- 200 years: $C_{bs} = 0.44$
- 1000 years: $C_{bs} = 0.68$
- 10,000 years (maximum): $C_{bs} = 0.70$

Table 8.1
Original church model: Analytical results for $(C_{bs})_{max} = 0.70$ (corresponding to a return period of 10,000 years)

Level	K (kN/cm)	$Q(C_{bs})$	$F\ [Q/(C_{bs})_{max}]$
Top of dome	111	7 (0.27)	0.41
Level 1	784	74 (0.47)	0.68

Table 8.2
Strengthened church model: Analytical results for $(C_{bs})_{max} = 0.70$ (corresponding to a return period of 10,000 years)

Level	K (kN/cm)	$Q(C_{bs})$	$F\ [Q/(C_{bs})_{max}]$
Top of dome	111	26 (1.0)	1.94
Level 1	784	144 (0.92)	1.49

The bearing capacity of the upper part of the original church model structure, expressed in terms of the base shear force, is $C_{bs} = 0.27$. This corresponds to a return period of 100 years for the prototype, whereas the value computed for the principal structure is $C_{bs} = 0.47$, which corresponds to a return period of 200 years. The computed safety factor for the maximum expected seismic effect ($C_{bs} = 0.70$) was $F_N = 0.41$ and $F_N = 0.68$ for the upper (top/dome) and lower (principal structure) parts, respectively. For the strengthened model, in which the walls in the analyzed direction were modeled as confined masonry, the safety factors for the maximum seismic effects were substantially greater than 1; that is,1.94 for the top of the dome and 1.49 for level 1.

Overall, the earthquake capacity analysis yielded results on the bearing characteristics of the church model structure that correlate well with the results obtained experimentally.

This page intentionally left blank

Chapter 9

Capacity Analysis of Existing Byzantine Church Structures

Computer analyses of the present state of the structures of the four churches selected for detailed study—St. Nikita, Banjani; St. Bogorodica Zahumska, Trpejca; St. Nikola, Psača; and St. Bogorodica, Matejče—were performed using the MASAN computer program. The analyses were directed toward determination of the bearing capacities of the churches and the need for strengthening the structures during potential restoration and conservation efforts. For these analyses, maximum acceleration values corresponding to a return period of 1000 years, which were obtained from detailed geophysical studies of the churches' local terrain, were used to define the base shear coefficients.

Given the values of initial stiffness, K, and ultimate shear force, Q, the analysis of the results obtained by dynamic analysis of the behavior of the St. Nikita church model defined the envelope points of the Q-D relationship necessary for the dynamic response analysis using the hysteretic IZIIS model (fig. 6.6). These points were as follows:

Point C: $K_c = K$; $Q_c = 25–30\%\ Q$; $D_c = 0.2\%\ H$
Point U: $D_u = 1.5–2\%\ H$; $Q_u = Q$
Point M: $D_m = 2.5–3.5\%\ H$; $Q_m = 20–30\%\ Q$
Point F: $Q_f = 10–15\%\ Q$
Point S: $D_S = 0.05–0.1\%\ H$; $Q_S = 5–10\%\ Q$

Response analyses were performed at these envelope points for each church under the Petrovac and El Centro earthquakes at the maximum accelerations corresponding to the minimal "design" and maximum earthquake severity, the values of which are given separately for each church in the sections that follow.

A structural analysis of the church of St. Gjorgji, Kurbinovo, was also performed. This church had been exposed to the MCS = 5.2 earthquake that occurred in Bitola, Macedonia, on September 1, 1994.

Analysis of St. Nikita, Banjani

The existing structural system of the church of St. Nikita in the village of Banjani consists of massive facade walls constructed of roughly hewn stones, dressed stones, and bricks. At the foundation level, the walls are 85 cm thick. The vaulted roof elements and the central dome over the naos

rest on these walls and on two rows of symmetrically placed columns. In general, the building is in good condition and the roof does not leak. Further details of the structure of St. Nikita are shown in figure 3.4.

The walls were modeled as single-story, rectangular cantilevers that were fixed at the base. The structure as a whole was modeled as a single-degree-of-freedom system, with a mass concentrated at the level of the main vaults. It was analyzed for a base shear coefficient of $C_{bs} = 0.38$, which corresponds to an earthquake with a return period of 1000 years. Mechanical characteristics of the masonry building materials used in the analysis were obtained from laboratory tests of samples taken from the prototype structure. Analytical results were obtained for both orthogonal directions using the MASAN computer program. This showed that the facade walls did not have high enough shear and bending bearing capacities to resist the maximum seismic effect, and this resulted in a safety factor of less than 1 for the entire structure. This is especially the case for the transverse direction ($F_u = 0.66$). In the longitudinal direction, this factor was higher ($F_u = 0.84$), owing to the larger size of the bearing walls, but it was still below the minimum acceptable value of $F_u = 1$. Therefore, it was deemed necessary to strengthen the existing St. Nikita structure by incorporating seismic retrofitting elements to increase bending resistance and tensile strength.

The structure of St. Nikita was also analyzed in both orthogonal directions using the IZIIS hysteretic model at three levels (0.12 g, 0.20 g, and 0.34 g) of the maximum input accelerations of the Petrovac and El Centro earthquakes. The results, in the form of Q-D relationships, are presented in appendix D. The results showed that the structure would suffer severe damage even when subjected to the design earthquake ($\mu > 1.5$), and complete failure of the structure would be likely under the maximum-severity earthquake. Hence, strengthening the structure to increase its deformability capacity is necessary to avoid serious damage or destruction in the future.

Analysis of St. Bogorodica Zahumska, Trpejca

This church (fig. 9.1a) is situated on a small plateau south of the village of Trpejca on the coast of Lake Ohrid. Figure 9.1b shows a plan and elevation of St. Bogorodica Zahumska, and a detailed description of its architectural, structural, and material characteristics is given in Gavrilović, Šumanov, et al. (1991, vol. 12).

Structurally, two rows of timber ties were used in the walls, one at the height of the capitals of the columns (lower zone) and the other at the height where the vaults of the cross arms merge (the upper zone). The principal structural system of the church has suffered considerable damage in the past. The southeast column in the central part of the building—the naos—is considerably damaged and deformed, and the northeast column is also badly damaged. The southeast column is inclined from its original vertical position as a result of seismic effects. This has resulted in an eccentricity in the transfer of the axial forces,

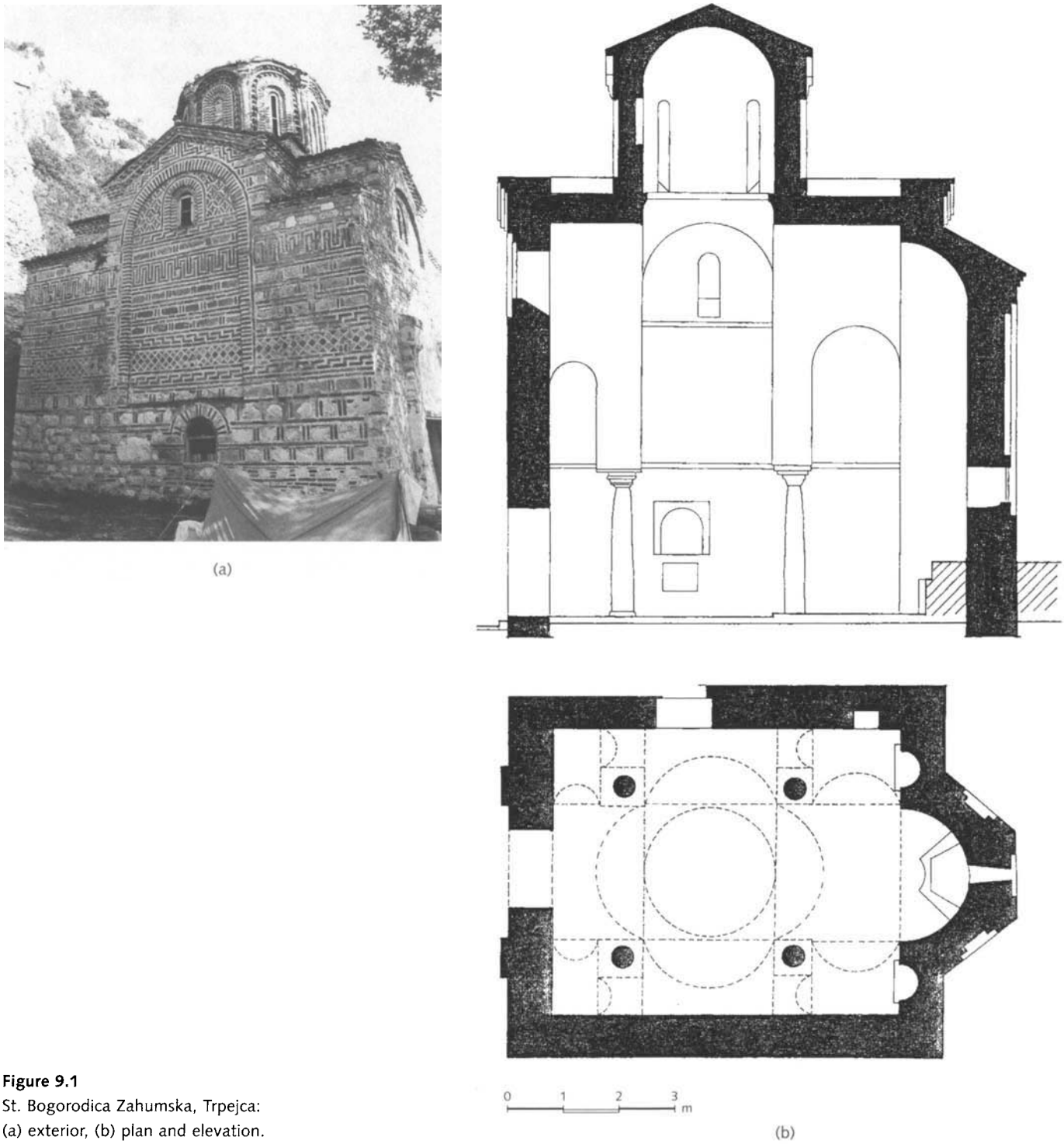

Figure 9.1
St. Bogorodica Zahumska, Trpejca:
(a) exterior, (b) plan and elevation.

resulting in ongoing additional bending and cracking of the column, especially at the base and capital. Neither extensive deformations nor large cracks are present in the facade walls, but fine vertical cracks were observed in the walls to the left and right of the apse. This is typical of buildings of this architectural style. The cracks and the separations in the interior most likely resulted from thrust forces due to secondary effects.

The existing structure was modeled as a single-degree-of-freedom building with a single mass concentrated at the main vault level.

The walls were modeled as rectangular cantilevers fixed at the base (each direction taken separately), and vertical loads were computed by static analysis. This analysis was performed for a base shear coefficient of $C_{bs} = 0.38$, a value obtained from the results of the investigations of local soil conditions. In view of both the absence of direct observational data and the similarity of this church to St. Nikita, Banjani, in terms of proportion and period of construction, the input parameters used for the mechanical characteristics of St. Nikita were used here as well.

The results of the analysis indicated that the facade walls, particularly the west wall, had relatively low bearing capacities and that the computed safety factors were less than 1.0 in both the east-west ($F_u = 0.86$) and the north-south ($F_u = 0.68$) directions. The instability of the existing structure is due mainly to the observed damage. The inadequate bearing capacity of the building when it is subjected to the maximum seismic effects points to the necessity of taking immediate measures to repair and restore the church and to institute measures to seismically strengthen the structure to increase its resistance.

Using the calculated results of the initial stiffness, K, and bearing capacity, Q, the parameters necessary for conducting a dynamic response analysis were specified, using the IZIIS hysteretic model for three levels of input acceleration: $a_{max} = 0.20$ g, 0.27 g, and 0.34 g, corresponding to return periods of 100, 200, and 1000 years, respectively. Ductility values resulting from the dynamic response analysis pointed to the great vulnerability of the church structure under very minor earthquake excitations and hence noncompliance with the safety criteria. This analysis also showed the necessity for seismic strengthening of the church during the restoration process.

Analysis of St. Nikola, Psača

The church of St. Nikola in the village of Psača is a structure with an inscribed cross in a rectangular plan with a narthex in the western part, a three-sided apse, and a former dome in the naos and narthex (fig. 9.2). The structure of the church consists of massive facade walls constructed of roughly dressed stone and brick. The walls and two symmetrical rows of columns support the vaulted roof elements and the dome above the exonarthex.

In general, the present state of the building is not considered to be satisfactory. Paved areas adjacent to the church and drainage channels on the south, east, and north sides are in poor condition. This has resulted in capillary moisture rise and rain- and snow-water damage to both the interior and exterior walls up to a height of about 1 meter. Stone blocks in the upper zone sustained damage from roof leaks. Damage at the level of the supports and the vaulted structures was particularly noticeable and timber belts are missing at the first naos level. Further details of the structure are given in Gavrilović, Šumanov, et al. (1991, vol. 12).

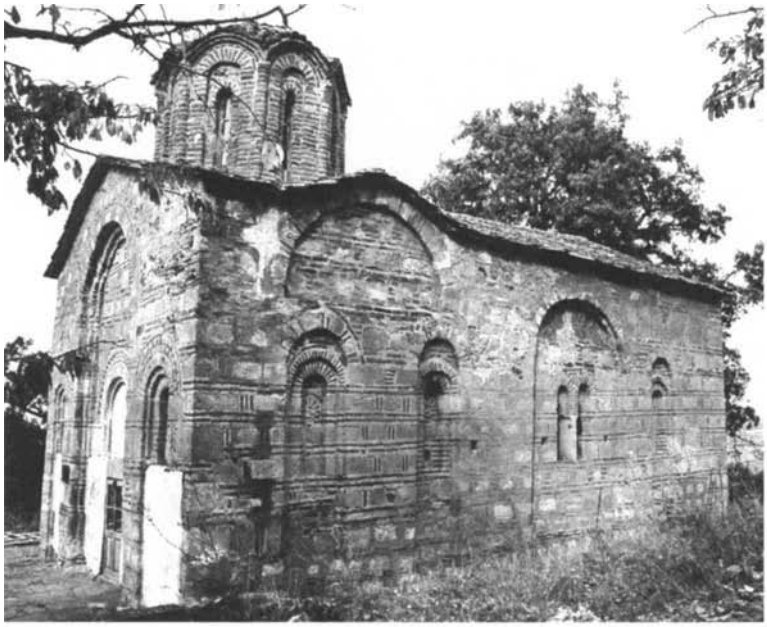

(a)

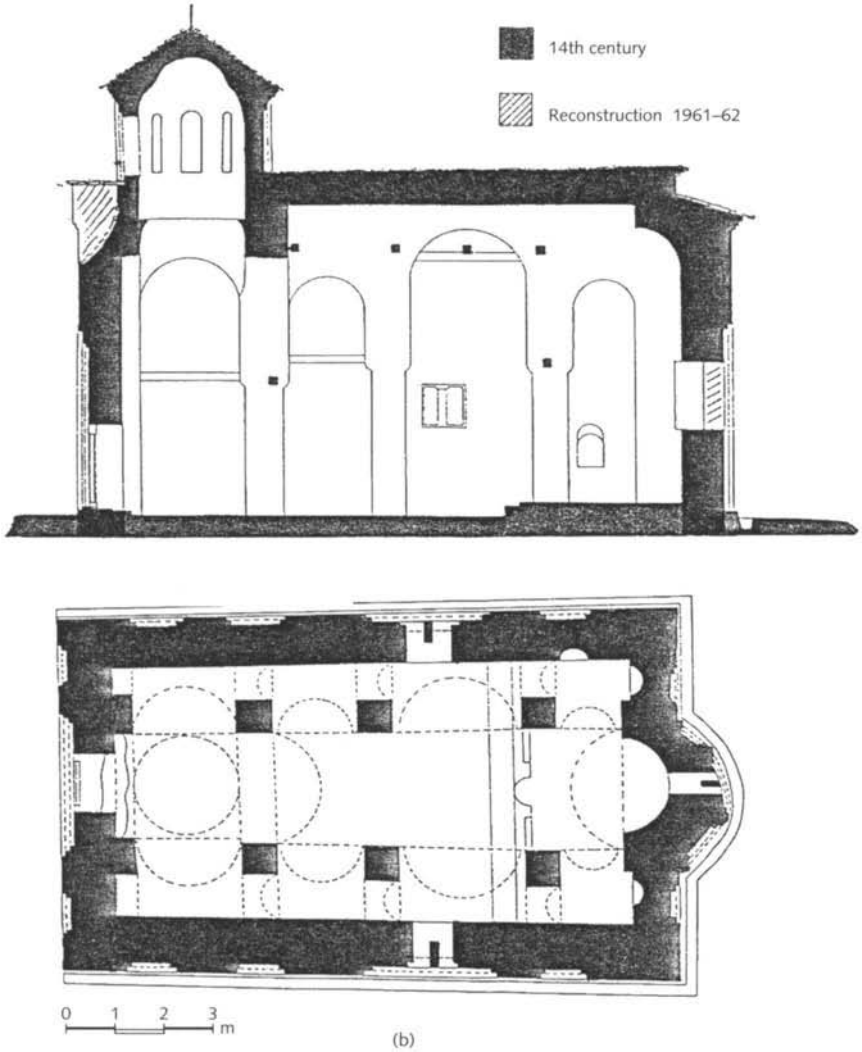

(b)

Figure 9.2
St. Nikola, Psača: (a) exterior, (b) plan and elevation.

The structure was modeled as a single-degree-of-freedom system with a mass concentrated at the level of the principal vaults. The analysis was performed in both orthogonal directions, the walls being modeled as rectangular cantilevers fixed at the base. Five walls (two facades and three interior walls) were analyzed in the longitudinal direction, and four other walls (two facades and two interior walls) were analyzed in the vertical direction. The base shear coefficients were calculated from the results of local geophysical studies, and the analysis was performed for $C_{bs} = 0.23$, which corresponded to a return period of 1000 years. Input parameters for the physical-mechanical characteristics of the masonry materials were the same as those used for St. Nikita because of the similar heights of the structures and the similar values of σ_0.

Owing to the relatively low seismicity of the region, the structure as a whole showed an acceptable estimated bearing capacity ($F_u > 1.0$). The bearing capacity in the transverse direction was $F_u = 1.04$, whereas in the longitudinal direction a higher value, $F_u = 1.8$, was obtained due to the greater length of the walls in this direction. Nevertheless, to protect this structure, it would be necessary to replace the timber ties in the wall mass because evidence exists that these are missing in some locations (they may have decayed or been removed during previous conservation work). Replacement of these ties would increase the strength and therefore the stability of the structure under dynamic seismic loading.

A dynamic response analysis of St. Nikola was performed using the IZIIS model at three input acceleration levels: 0.14 g, 0.19 g, and 0.21 g. It was evident that the structure had a satisfactory bearing capacity ($Q > Q_{max}$) in both orthogonal directions. However, at low seismicities a relatively high vulnerability was observed in the north-south direction, which showed a $\mu > 1.6$ for a return period of 100 years. These results confirmed the need to strengthen the structure, which would provide the ductility required for compliance with the safety criteria.

Analysis of St. Bogorodica, Matejče

The church of St. Bogorodica (fig. 9.3a) is situated on a plateau on the slopes of Crna Gora, a mountain located north of the village of Matejče. One of the reasons for selecting this church as a representative subject for this project was the extensive reconstruction and conservation activities initiated around 1930 and continued in 1970. A plan and elevation of this church are shown in figure 9.3b.

Generally, the present state of the structure is relatively satisfactory from both the structural and conservation points of view, with the exception of the permanent penetration of capillary moisture through the perimeter walls and the church floor. Part of the reconstruction of the church included incorporating reinforced concrete elements, columns, and belt courses within the massive masonry structure, which was originally constructed of stone and brick set in lime mortar. Complete reconstruction of the vaults and domes was performed in

(a)

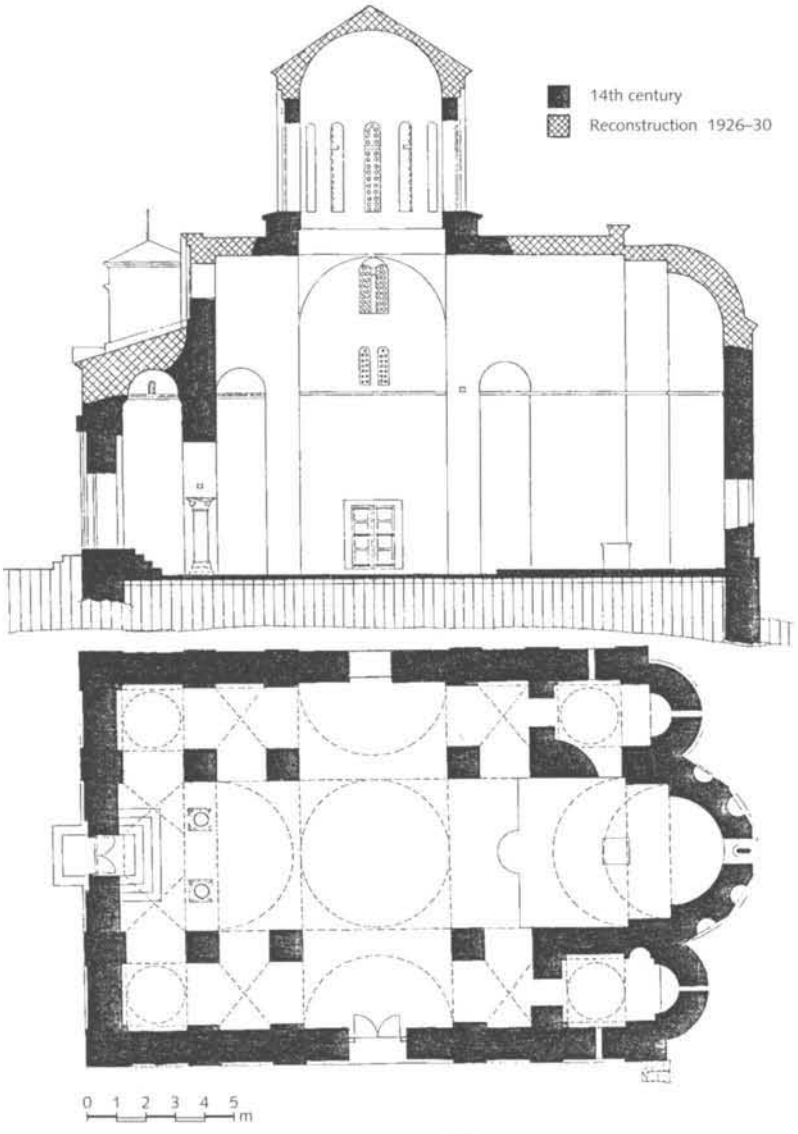

(b)

Figure 9.3
St. Bogorodica, Matejče: (a) exterior, (b) plan and elevation.

1930. These changes have led to a disturbance of the basic structural concept and structure of the church.

The structural system of the building as a whole consists of massive facade walls, 80 cm thick, which are constructed of roughly dressed limestone. The walls and two rows of symmetrically placed columns support the vaulted roof elements, the central dome over the naos, and the four peripheral domes, which characterize the design of the church. On the basis of the generally stable behavior of the structure, it may be concluded that it was constructed on stable soil. The foundation extends well below the ground surface level, and apparently this has prevented excessive differential settlement of the structure.

Horizontal cornices on the tambours of the domes were in place until the 1970s, when extensive reconstruction and conservation of the monument occurred. Static and seismic analyses of the structure were performed in 1978. The effects of vertical and horizontal forces were estimated from the computed stresses in the bearing elements of the structure. Visual inspection of the structure led to the conclusion that the masonry materials were of satisfactory quality, which was evidenced by the fresh appearance and compactness of the facades. Hence, the compression resistance of masonry was taken to be 2000 kPa.

During reconstruction, the following structural strengthening measures were installed:

- **Horizontal rings.** Horizontal concrete rings were placed at the connection between the cornice and the dome structure as well as between the cornice and the vault structure (the base of the tambour). The proportions of the rings used for the central dome were 20 × 30 cm, and those used for the four smaller domes were 20 × 20 cm. These were cast in parts; each ring was 1.5 m long and made of cast reinforced concrete, which had a crushing strength of 20 MPa.
- **Horizontal belt courses.** Horizontal belt courses installed in the west, south, and north walls were constructed of 40 × 25 cm reinforced concrete. Those used for the east wall were 25 × 25 cm.
- **Vertical belt courses.** Four vertical belt courses were constructed of 40 × 40 cm reinforced concrete (crushing strength 25 MPa) and were reinforced by four lengths of 20 mm (diameter) rebar—two on the south wall and two on the north. The belts were cast in parts, each of which was 1.5–2 m long. The rebar was joined by overlapping, using wire and a length of 40 mm rebar. The columns were constructed in the core of the wall, after which the facade wall structure was restored.
- **Steel ties.** A system of steel ties was constructed at the base of the vaults and was anchored to the facade walls

and the columns in the interior. The steel ties were located 6.25 m from the floor.

- **Crack repair.** Outer facade cracks were repaired with a cement-lime-sand mortar (1:3:6). The interior fresco surfaces were repaired by priming and then injecting a casein-type lime mortar before the frescoes were conserved. The horizontal and the wavy cornices of the facade walls and the double wavy dome cornices were reconstructed during this restoration. All roof areas of the church, domes, and apses were sheathed with sheet lead.

Results of the analysis of the bearing capacity of the structure in both orthogonal directions showed a base shear coefficient of Cbs = 0.36, which indicated a return period of 1000 years. The walls were modeled as fixed at the base and top because of the presence of horizontal belt courses in the facade walls below the cornice structure. In the transverse direction, the structure was modeled as consisting of six walls (two facade and four internal walls), and the reinforcements in the vertical belt courses were included for the two central walls. In the longitudinal direction, the structure was modeled with four walls. The following values were chosen as input parameters for the mechanical characteristics of the masonry materials: f_t = 130 kPa; f_c = 2,000 kPa; E = 10^6 kPa; and G = 360,000 kPa. Based on the results of the capacity-analysis approach, it was concluded that each individual wall, and the structure as a whole, would have sufficient bearing capacity to resist the postulated seismic effect. In the transverse direction, the ultimate bearing capacity was F_u = 1.1, whereas in the longitudinal direction it was higher, F_u = 1.90, due to the size of the walls.

The structural masonry bearing elements—walls, vaults, and domes—have been preserved in their original form so that the structure as a whole is stable. At the time of observation, there were no signs of extensive structural deformations or cracks. Nevertheless, it is important to note that the newly incorporated reinforced concrete elements, consisting of a material whose physical properties are different from those of the remaining original materials, can have an adverse effect on the original structure and especially on the fresco paintings. The possible effects of this change need to be explored further.

A dynamic response analysis of the church was performed using the IZIIS model and the Petrovac and El Centro earthquakes for input acceleration levels of 0.14 g, 0.23 g, and 0.32 g, which correspond to return periods of 100, 200, and 1000 years, respectively. The computed ductility values for the existing church structure, which is situated in an area of high seismicity, satisfy the required safety criteria. Ductility values of $\mu < 1.0$; μ = 1.0–1.2; and μ = 1.2–1.5 were obtained for return periods of 100, 200, and 1000 years, respectively. These results confirm the fact that the church structure has adequate bearing and deformability capacities.

Analysis of St. Gjorgji, Kurbinovo

This was not among the four representative churches selected for detailed analysis. It was nonetheless analyzed, because it is situated in an area affected by the earthquake that occurred in Bitola, Macedonia, on September 1, 1994, while this study was in progress.

No historical data exist that specify the construction date or founder of St. Gjorgji, but an inscription on one of the frescoes indicates that the decoration of the church began in April 1191. This structure is one of the rare examples of a Macedonian Byzantine church that contains almost all of the original fresco paintings in a well-preserved state (figs. 2.19 and 2.20). (A few of the frescoes—those located in the first zone of the north wall and in the upper areas occupied by paintings of the prophets—were destroyed during the reconstruction of the flat timber ceiling in the nineteenth century.)

The church (fig. 9.4) is a single-nave structure with a spacious semicircular internal and external apse in the east and a couple roof without a vault. The structural system of single-nave churches is usually characterized by massive perimeter walls and large apses, but some do have vaults.

In 1958, and again in 1981–83, conservation activities were carried out that involved reconstruction of the roof and repair of the

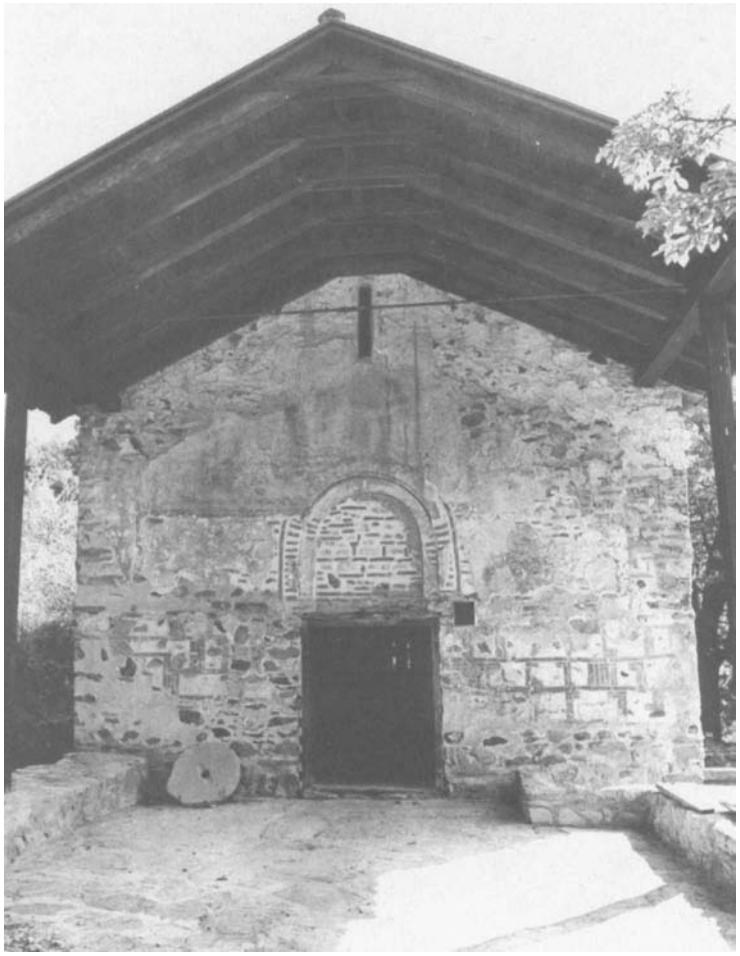

Figure 9.4
St. Gjorgji, Kurbinovo: west facade entrance.

exterior facade frescoes. During repair of the roof structure, two 25 × 25 cm concrete belt courses, reinforced by four lengths of 14 mm rebar, were incorporated into the longitudinal walls. The existing wooden beams were strengthened on the upper side by 24 mm steel ties, which were anchored into the concrete belt courses. The belts were encased in lime mortar and were embedded in the facade wall masonry.

For protection of the facade fresco paintings on the exterior west wall, a pitched wooden canopy was constructed at the roof height and was supported by two wooden columns in which 24 cm steel ties were anchored. A short canopy, without any supporting columns or diagonal bracings, was constructed for protection of the frescoes on the south wall.

Following a detailed inspection of the church after the Bitola earthquake and an examination of photographs taken in 1991, it was concluded that the church had not suffered any significant damage. A widening of an existing vertical crack in the south facade wall was observed, and in the church interior, small cracks were noticed at the junctions between the west and the south and north walls, which produced a negligible loss of lime mortar from the upper part of the cracks. The roof structure was undamaged, and it was concluded that the behavior of the structure as a whole was satisfactory. However, the cracks along the intersections of the west wall with the south and north walls indicated a lack of synchronized movement of the walls.

For the analysis of bearing capacity, the church structure was assumed to be a single-degree-of-freedom system with four bearing walls (two each in the vertical and longitudinal directions), which were modeled as rectangular cantilevers fixed at the base. In accordance with the available data on the seismicity of the terrain, the base shear coefficient, $C_{bs} = 0.25$, was computed for a return period of 1000 years. In the absence of specific data for this church, the results of previous studies performed on materials of similar structures were used as input parameters for the mechanical characteristics of the masonry.

The results of the analysis showed that the structure as a whole had an adequate bearing capacity in both directions analyzed ($F_u > 1.0$), which was confirmed by the actual behavior of the structure during the last earthquake (Bitola). Nevertheless, the existing cracks in the south facade wall should be repaired, and the timber belts at the first two levels should be augmented by steel ties. The voids around the steel ties should be filled with a lime mortar grout. These changes should result in the synchronized movement of the walls during any future seismic excitations.

An analysis of the dynamic response of this church was also performed. Using the IZIIS model, the response of the church to three input acceleration levels, 0.15 g, 0.20 g, and 0.25 g, corresponding to return periods of 100, 200, and 1000 years, respectively, was obtained based on the story stiffness, K, and bearing capacity, Q. The results showed that the church structure had sufficient bearing and deformability capacity to be in compliance with the safety criteria. Nevertheless, it was recommended that the timber ties be replaced or augmented by steel ties at a height of 1.3 m from the foundation level, as suggested previously.

This page intentionally left blank

Chapter 10

Implementation of Methods for Repair and Strengthening of Byzantine Church Structures

As mentioned earlier, it is possible to define methods for the strengthening of historic structures based on their characteristics and artistic-historical value and by taking into account their expected structural response to anticipated earthquakes. Any modification of historic monuments in the Republic of Macedonia should be done in compliance with the recommendations defined at the International Seminar on Modern Principles in Conservation and Restoration of Urban and Rural Cultural Heritage in Seismic-Prone Regions, held in Skopje in 1988. The recommendations formulated at this meeting are as follows:

- It is necessary to review the existing documentation on the building prior to any intervention or decisions regarding methods and materials to be used for repair.
- The authenticity of the building should be preserved, and new architectural structural elements should be distinguished from the original structure.
- Interventions should be held to a minimum. For each intervention, the historical, aesthetic, and physical integrity of the building should be considered. Each building should be analyzed from archaeological and historical viewpoints to collect information on elements of cultural and historic importance for future restoration, repair, and strengthening. A decision should be made on the selection of repair and strengthening methods based on structural and architectural elements, such as architectural shape and materials and technologies used in the original construction of the building.
- During repair and strengthening, maximum care should be taken to preserve the authenticity of the original materials; the original structural systems and elements and their inherent qualities should be used to the greatest possible extent. Any materials used for repair and strengthening should have physical, chemical, mechanical, and deformability characteristics identical or very similar to those used in the original building. These materials should have slightly greater strength characteristics than

the original (referring to masonry binders) to withstand possible dynamic effects without additional damage to the existing binding materials.

- Existing elements of the prototype structure, such as timber belts and ties, should be retained and reused, if possible. In many cases the timber belts have decayed, so the existing void spaces should be the designated location for the new strengthening elements. This modification could be accomplished with minimum destruction of existing building fabric.
- If possible, materials, building elements, and systems used should be replaceable so that the interventions are reversible.
- The design of structures to sustain dynamic or seismic loads should take into account the site's seismicity and the importance of the structure. Three seismic-related criteria apply: (1) In light earthquakes, the dynamic behavior of the structure should be such that no damage occurs to either structural or nonstructural elements. (2) In the case of stronger earthquakes (the design earthquake), damage to the main structural system should not occur, although slight deformations of nonstructural elements would be permitted. (3) The maximum-severity earthquake expected should not affect the stability of the principal structural system. More severe deformations of the nonstructural and structural elements are allowed only if the elements of the whole structure do not suffer irreparable damage.

Repair and strengthening of buildings to withstand stronger future dynamic loads can be implemented by following these criteria and principles and by defining safety criteria that will allow repairable damage to the load-carrying structural elements and considerable damage to the nonstructural elements.

Possible Methods and Techniques for Repair and Strengthening of Historic Byzantine Churches

The repair and strengthening methods used should be designed to increase the strength and ductile capacity of the existing structure to the extent required by the anticipated vulnerability level. In certain cases, implementation of repair and strengthening measures can lead to synergistic effects that need to be considered as well. It should be reiterated that these historic church structures differ from most other (more modern) structures, so few options in the way of adequate repair methods are open to the design engineer. If the load-bearing capacity of the existing structural elements is not sufficient to sustain and transfer the forces generated during an earthquake, new structural elements should be inserted.

Analysis of damaged massive structures and the results of the experimental shaking-table tests performed on the original church model have shown that the initial type of failure is wall separation and loss of structural integrity due to the inability of the floor or the roof structure to sustain the tensile forces. The main strengthening concept is the improvement of structural continuity, and this can be achieved by incorporating ties that will enable the structure to perform as an entity. Analysis of the failure mechanisms of walls leads to the conclusion that resistance to shear forces and moments and improvement of ductile capacity are the factors that need to be considered.

In general, apart from being dependent on geometrical characteristics, the moment resistance of walls depends also on the capacity of the wall to withstand tensile forces. Hence, a need arises to increase the low tensile strength of the existing masonry, which could be done in two ways: by using the grouting method to repair voids in the existing masonry or by inserting steel reinforcement bars in and at the ends of the walls.

The church structures considered in this study generally behave rigidly, and shear effects, which depend upon the tensile capacity of masonry, predominate. In traditional Byzantine construction, the load-carrying capacity of the masonry was increased by incorporating wooden belt courses at various levels: at the roof, in the ends of vaults, above the openings, and down to the foundation. To strengthen the system, two methods can be used: replacing the timber belt courses with steel belts and injecting the masonry with modern bonding compounds.

Accordingly, the proposed repair and strengthening methods are as follows:

- Strengthen the principal structural system with strong horizontal elements at the roof level; replace the traditional wooden ties with steel ties; establish contact between the strengthening elements and the existing masonry with a strong bonding material; and insert grout in cracks. These methods are suitable for small, compact churches and for structures located in zones of low seismicity that have many load-carrying walls.
- To sustain tensile forces due to overturning moments and to maintain seismic stability, insert vertical elements at the ends of the walls and around openings. Complete the process by partial injection of grout along horizontal strengthening elements.
- The two preceding strengthening concepts represent modified traditional conservation methods. A third, more modern way of providing seismic stability is to use seismic base isolation methods. One such technique has been implemented in the construction of new buildings and bridges and in several more modern historic structures. The method consists of installing "isolating dampers"

between the foundation and the base of the structure that modify the structural response. Although this method is costly and its applicability to a structure with limited foundation strength or stability presents technological problems, it should not be completely rejected from consideration, especially in the case of small, compact buildings containing valuable murals or architectural features, for which any extensive conventional intervention would involve the risk of irreversible damage (Naeim and Kelly 1999).

Repair and Strengthening of Historic Monuments in Accordance with the Experimentally Verified Methodology

The investigations performed during this project resulted in the development and experimental verification of a method for the repair and strengthening of churches dating from the late Byzantine period in Macedonia. In the following sections, the principles and techniques derived from this study are applied to the general seismic strengthening of churches of this period, and specific applications of the technology to the four selected Byzantine churches are detailed.

Horizontal belt courses in perimeter walls

To provide integrity and to ensure the synchronous behavior of bearing walls, it is recommended that steel ties be inserted at locations that previously contained timber belt courses. Steel ties serve to increase the bearing capacity of masonry and enable the structure to respond to seismic excitation without sustaining substantial damage. The existence and location of timber ties can be determined visually, from available documentation, or by using instruments that measure the propagation velocity of sound waves in the walls of the structure.

If it is found that the timber belts have decayed and voids exist or that the belts are no longer continuous along the perimeter of the wall, the belt regions should be cleaned and steel ties with a minimum diameter of 14 mm inserted. At the ends of the wall where the ties protrude, the facade masonry (stone or brick) should be removed, after marking the stones and bricks so that they can be replaced in their original positions. Steel stress-distribution plates must be bolted to the ends of the ties before accurate prestressing is accomplished. However, before this, voids around the ties are filled with a grout consisting of lime mortar containing additives that improve fluidity, accelerate curing to reduce the time required for attaining maximum strength, and improve adhesion to the existing masonry. After replacement of the facade stones and bricks, no evidence of the ties remains visible.

If the timber belts still exist inside the wall and can successfully perform their function of connecting the bearing walls, systematic injection of these masonry regions is performed using modern bonding compounds, such as epoxies or polyesters.

Vertical belt courses in perimeter walls

This strengthening method involves incorporating vertical elements at the ends of walls and adjacent to wall penetrations (windows and doors), to increase the moment resistance and ductility of the structure and to resist the tensile forces produced by overturning moments generated during dynamic vibrations.

Vertical strengthening elements are incorporated at the corners of the building and at the intersections of adjacent walls, where firm connections are generally required in masonry construction. After removal of minimal sections of the roof, drilling equipment is used to bore the vertical holes in the walls in which steel tie bars are to be incorporated. The lower ends of the tie bars are anchored to the existing foundation at the bottom of the hole. If the stresses in the ground and the safety criteria are not adequate, the foundation strength needs to be upgraded by increasing the foundation's contact area with the ground. To attach the upper end of the tie bar, a row of stone and brick is removed from the wall and a steel stress-distribution plate is inserted to anchor the tie, which is prestressed. Here again, the void space around the bar is filled with grout.

It should be pointed out, however, that vertical belt courses are to be used only at those locations where the wall does not possess sufficient bearing capacity to resist overturning moments, which is the case for slender walls (height >> thickness) where bending effects are dominant. In the case of walls with large bases, moderate heights, and dominating shear effects, vertical belt courses are not required and their installation should be avoided.

Details of strengthening of the tambour and dome structures

Data collected during the investigations of the state of existing churches reveal that almost none of the churches have original domes. Domes and tambours were the structures most frequently damaged or completely destroyed by earthquakes. Almost without exception, the domes and the tambours were repaired on several occasions and were often completely reconstructed. Therefore, before making decisions regarding strengthening these parts of the church structure, the originality and the degree of damage should always be taken into account.

When reconstructing or rebuilding the tambour and dome structures is deemed necessary, the design of strengthening elements, such as horizontal belt courses at the base of the tambour and base of the dome, or vertical ties in the columns of the tambour adjacent to the openings, need to be considered carefully. In the case of architectural elements that have a high degree of authenticity, decisions regarding strengthening measures will vary from case to case, and only minimal interventions should be considered.

The procedure for placement of horizontal belt courses at these locations is similar to that described above for the perimeter walls. The facade masonry is removed from the base of the dome after the stones and bricks have been labeled. A circular steel tie is constructed in several parts; these are then interconnected by steel plates and installed

around the dome base. The dimensions of this circular tie are determined by the geometry of the dome. Grout is systematically injected into the masonry after replacement of the facade stone and bricks. Vertical ties are inserted into the masonry adjacent to the tambour openings and are anchored below the roof and in the vaults.

Special attention needs to be paid to the selection of the appropriate lime-based mortar, which should contain additives that will provide high strength, good adhesion, and effective penetration into the existing masonry. It is important, too, that the augmented mortar be compatible with, and not have an adverse effect on, the existing fresco mortar.

Injection, grouting, and rebuilding

In the process of developing a strengthening methodology, in addition to structural strengthening, repair and restoration of damaged masonry elements needs to be a primary focus. This process includes injection of cracks, pointing, grouting, and even rebuilding of certain parts of the walls that have sustained extensive damage.

As mentioned above, in regions where horizontal or vertical belt courses are incorporated, the void volumes around steel ties are filled with a lime-based grout that contains special additives to improve the interaction with the existing surrounding masonry. In this way, the grouting process forms a spatial belt course of an amorphous shape.

On the external wall facades where steel ties are installed, it is recommended that systematic grout injections be performed along the length of the belt courses. Special mixtures of lime mortar with additives are injected under low pressure through previously placed metal tubes. In the case of general injection, the mixture needs to be fluid enough to penetrate the masonry pores under very low pressure. When cured, the grout serves to improve the mechanical characteristics of the existing masonry. For heavily damaged parts of walls that require more complicated repairs, rebuilding should include the use of lime mortar with additives that decrease the curing time, so that the ultimate strength characteristics of the repaired masonry, including the bricks and stones that were removed and replaced, are reached as quickly as possible.

Strengthening of the Structures of Three Representative Churches

The methods selected for the repair and strengthening of Byzantine churches depend on conservation requirements, restoration ethics, and the structural measures needed to achieve the seismic safety of the structure. To define an adequate repair-and-strengthening design for a church structure, it is necessary to perform a detailed structural analysis of the building. This includes specification of the type and physical-mechanical characteristics of the masonry and other details of the structure, such as plastered walls, ceilings, roofs, floors, and so on. In many cases, these data are not available; however, data obtained from investigations of

similar structures can be used in lieu of mechanical and chemical analyses of the specific building.

In this section, measures used for strengthening the church model are applied hypothetically to the selected representative churches, assuming that incorporation of individual strengthening elements would be carried out in the manner described earlier in this chapter. The bearing and deformability capacities of a structure are the principal parameters used to define the behavior of the building. These factors are required for the definition of the other parameters needed for implementation of the IZIIS hysteretic model. This model, together with the tools that were developed for the linear and nonlinear dynamic analysis of the model church, can then be used to estimate the performance of the strengthened church structure under earthquake excitation conditions.

Details of the strengthening methods and the capacity and dynamic response analyses that were carried out for all the representative churches are given in Gavrilović, Šumanov, et al. (1991, vol. 12). Brief examples of the calculations are shown here for a single earthquake return period.

An earthquake capacity analysis for a base shear coefficient, C_{bs}, corresponding to an earthquake with a return period of 1000 years, was performed for the strengthened structures of three of the representative churches. A dynamic response analysis was also performed by defining the parameters for the IZIIS hysteretic model in accordance with the results of the analytical modeling of the strengthened church model:

- Point C: $K_c = K$ (K is the initial stiffness computed using the MASAN program.)

  Q_c = 25–30% Q (Q is the bearing capacity computed using the MASAN program.)

  D_c = 0.2–0.3% H (H is the story height.)
- Point U: D_u = 1.5–2% H

  $Q_u = Q$
- Point M: D_m = 3–3.5% H

  $Q_m = Q$
- Point F: D_f = 5–5.5% H

  Q_f = 10–15% Q (Q_f is the friction force.)
- Point S: D_S = 0.05–0.1% H

  Q_S = 5–10% Q

The output results are given in the form of Q-D relationships, and the required ductility ($\mu = D_{max} / D_y$) is given separately for each church. For St. Nikita, the parameters for the IZIIS model calculations for the original and strengthened models are given in figure 10.1.

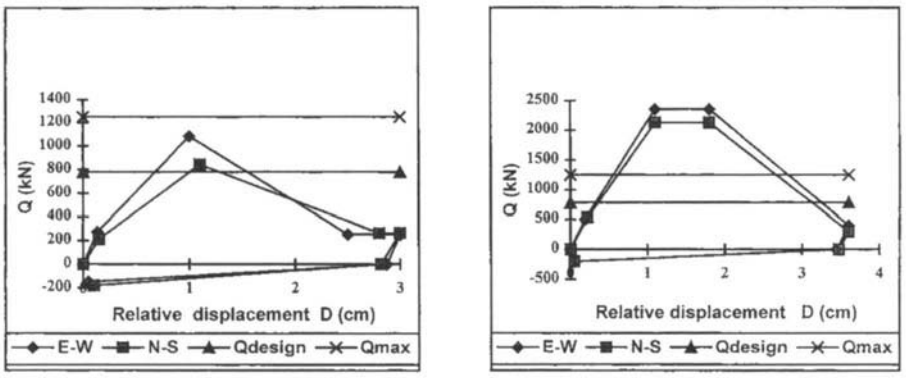

Figure 10.1
Input parameters for the hysteretic model analysis of St. Nikita: (a) original, (b) hypothetically strengthened.

St. Nikita, Banjani

The strengthening methods listed below were defined based on the analysis of the existing structure of St. Nikita. This method assumed the following:

1. Horizontal steel ties would be incorporated into the facade walls at two levels:
   - two 20 mm steel ties at the lintel levels, 2.5 m above the ground level, along the length of the south, north, and west walls and at the east wall up to the apsidal area; and
   - four 20 mm steel ties at the level of the existing visible wooden ties in the interior of the church and at the base of the vaults along the length of the perimeter wall (POS[1] 3), one 20 mm steel tie anchored into the opposite walls and placed along the side of each of the timber beams at POS 4, and a circular or polygonal 20 mm tie incorporated at POS 5.
2. In addition to the horizontal ties, three 20 mm vertical steel ties would be incorporated at the connections between two adjacent walls, and three 20 mm ties at each corner, POS 1.
3. The upper part of the structure would be strengthened using several elements:
   - two 20 mm horizontal steel ties added at the base of the tambour (POS 6);
   - three 20 mm circular steel ties (in four parts) incorporated in the base of the dome at a height of 10.5 m, and one 20 mm tie added below the roof (POS 8); and
   - two 20 mm circular steel ties positioned beside each of the eight columns of the tambour (POS 7).

Strengthening was assumed to have been carried out below ground level in the foundation area. Because data on the depth and the proportions of the foundation were not available, the following assumptions were made in the calculations:

- The width of the foundation footing equals the width of the walls.
- The structure is founded in soil with $\sigma_{ultimate} = 350$ kN/m^2.
- The control of stresses is performed according to well-known relations.

Calculation of the safety factor for the maximum earthquake effect yielded a value >1.1; therefore, the existing foundation structure satisfied the safety criteria.

An analysis of the bearing capacity of the church was performed for both orthogonal directions. The walls were modeled as fixed at both ends, and the reinforced perimeter walls were considered to be confined masonry.

The results of the capacity analysis (table 10.1) showed that each of the individual walls and the strengthened structure as a whole had a sufficient bearing capacity ($F_{E\text{-}W} = 1.83$ and $F_{N\text{-}S} = 1.65$) to withstand the maximum expected earthquake excitation ($C_{bs} = 0.39$), unlike the existing structure, which has an insufficient bearing capacity, particularly in the transverse north-south direction.

A dynamic response analysis of the strengthened structure was performed using the IZIIS hysteretic model in both orthogonal directions and at three input acceleration levels (0.12 g, 0.20 g, and 0.34 g) for both Petrovac and El Centro earthquake spectra. The output data are presented in two forms. In terms of required ductility values for earthquakes corresponding to return periods of 100, 200, and 1000 years, the computed values are shown in table 10.2. The results, in the form of Q-D diagrams,

Table 10.1
Earthquake capacity analysis of the representative church structures calculated for the existing state and for the defined strengthened state

Church	Force (kN)	Height (H) (m)	Maximum seismic force (S) (kN)	Base shear coefficient (C_{bs})	State of church building	Direction	Stiffness (K) (kN/cm)	Q (kN)	F (Q/S)
St. Nikita, Banjani	3378	7.20	1284	0.38	Existing	East-west	1991	1084	0.84
						North-south	1425	843	0.66
					Strengthened	East-west	2938	2354	1.83
						North-south	2367	2124	1.65
St. Bogorodica Zahumska, Trpejca	2400	7.70	912	0.38	Existing	East-west	1263	787	0.86
						North-south	968	624	0.68
					Strengthened	East-west	2068	2036	2.23
						North-south	1722	1763	1.93
St. Nikola, Psača	4230	7.25	973	0.23	Existing	East-west	4860	1794	1.84
						North-south	1435	1011	1.04
					Strengthened	East-west	5980	1926	1.98
						North-south	2541	1535	1.58
St. Bogorodica, Matejče	11,000	11.80	3960	0.36	Existing	East-west	12,573	7517	1.90
						North-south	9636	4492	1.13
St. Gjorgji, Kurbinovo	2107	5.40	527	0.25	Existing	East-west	4538	1332	2.34
						North-south	2605	921	1.75

Table 10.2
Required ductility values ($\mu = D_{max}/D_y$) for the existing and strengthened St. Nikita church

	Existing structure						Strengthened structure							
	North-south			East-west			North-south				East-west			
Acceleration	**0.12 g**	**0.20 g**	**0.34 g**	**0.12 g**	**0.20 g**	**0.34 g**	**0.12 g**	**0.20 g**	**0.34 g**	**0.39 g**	**0.12 g**	**0.20 g**	**0.34 g**	**0.39 g**
Petrovac	0.80	1.90	4.20	0.55	1.40	4.10	0.60	1.14	1.40	3.56	0.55	1.00	1.31	2.59
El Centro	0.52	1.00	3.00	0.32	0.79	3.60	0.54	1.11	1.40	1.60	0.40	0.98	1.30	1.50

are shown in figures 10.2a–c through 10.5a–c. It can be seen that, unlike the existing church, the strengthened church structure had a satisfactory ductility capacity and was in compliance with the safety criteria.

An analysis was also performed on the strengthened St. Nikita church structure under the condition of the maximum-severity earthquake expected, one with a return period of 10,000 years. The aim of this calculation was to demonstrate the applicability of the IZIIS model in the range of extreme nonlinearity. The Q-D diagrams for an input acceleration of 0.39 g (part d, figs. 10.2–10.5) showed that, despite the expected stiffness and strength degradation, the dissipation of hysteretic energy was still possible. These diagrams describe the performance of the structure immediately before failure, when the remaining strength of the building is due mostly to friction.

St. Bogorodica Zahumska, Trpejca

Based on the analysis of the existing structure of St. Bogorodica Zahumska, in the village of Trpejca, it was concluded that the structure did not have sufficient bending and shear-bearing capacity to resist the destructive effects of the design earthquake.

Before strengthening the church, it would be necessary to carry out a number of repairs: remove local damage to the southeast and southwest columns by supporting the surrounding structure; bring the columns into a vertical position to provide contact with the vaults; and replace all deteriorated wooden ties.

The procedure for strengthening the existing structure was assumed to be the following:

1. Horizontal steel ties would be incorporated into the perimeter walls to augment the existing timber beams inside the church:
   - two 18 mm steel ties incorporated at a height of 2.95 m (the level of the first timber ties) along the entire length of the perimeter walls, and one 18 mm steel tie along each of the timber ties; and
   - four 18 mm steel ties incorporated at a height of 5 m within the perimeter walls, and one 18 mm tie along each timber beam.

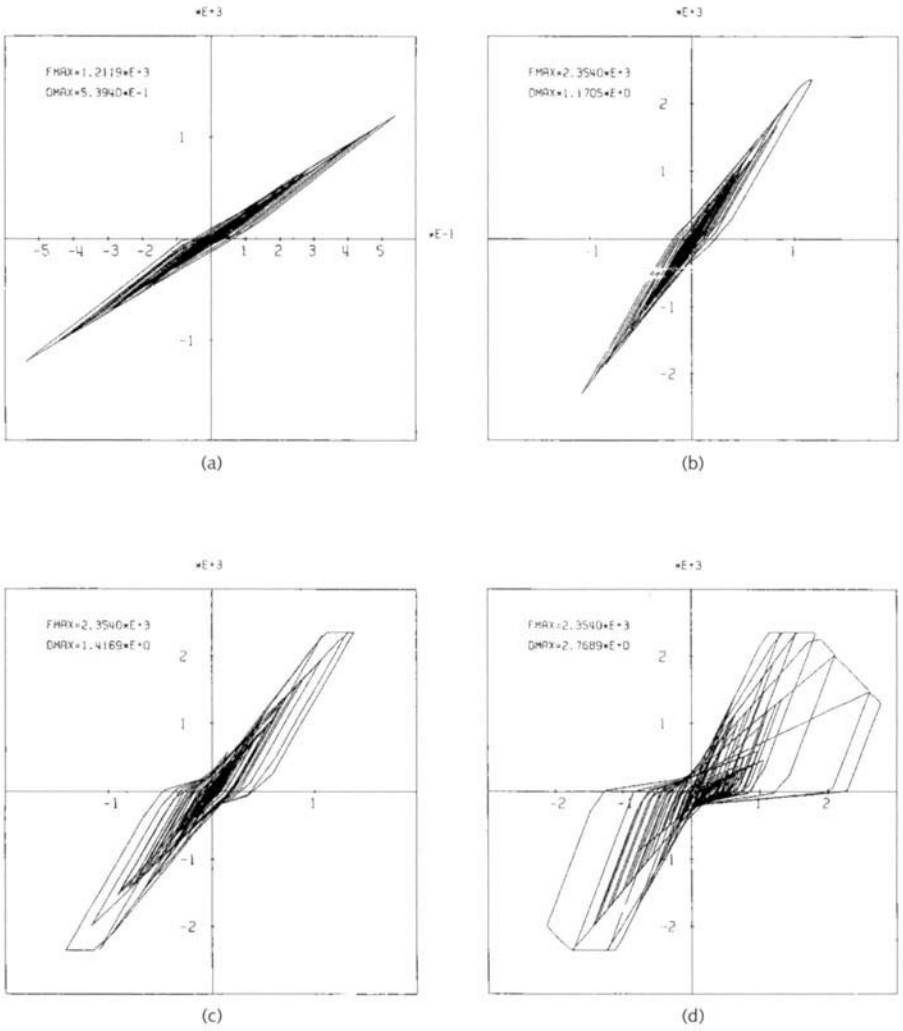

Figure 10.2
Q-D diagrams for the strengthened St. Nikita, Petrovac excitation, east-west direction: (a) a = 0.12 g, (b) a = 0.20 g, (c) a = 0.34 g, (d) a = 0.39 g.

2. Three 18 mm steel ties would be incorporated in each corner of two adjacent walls.
3. The upper part of the structure would be strengthened by installation of the following:
   - two 18 mm horizontal steel ties at the base of the tambour, at a height of 8.7 m;
   - three 18 mm circular steel ties in four parts, at a height of 10 m, at the base of the dome; and
   - two 18 mm vertical steel ties at each side of the four openings.

Stresses in the soil were calculated, and the results showed that the existing foundation structure satisfied the safety requirements for the maximum-severity earthquake with a safety factor of 1.2.

The MASAN computer program was used for analysis of the bearing capacity and the stability of the strengthened structure in both orthogonal directions under the maximum expected earthquake excitation. The walls were modeled as confined masonry fixed at both ends

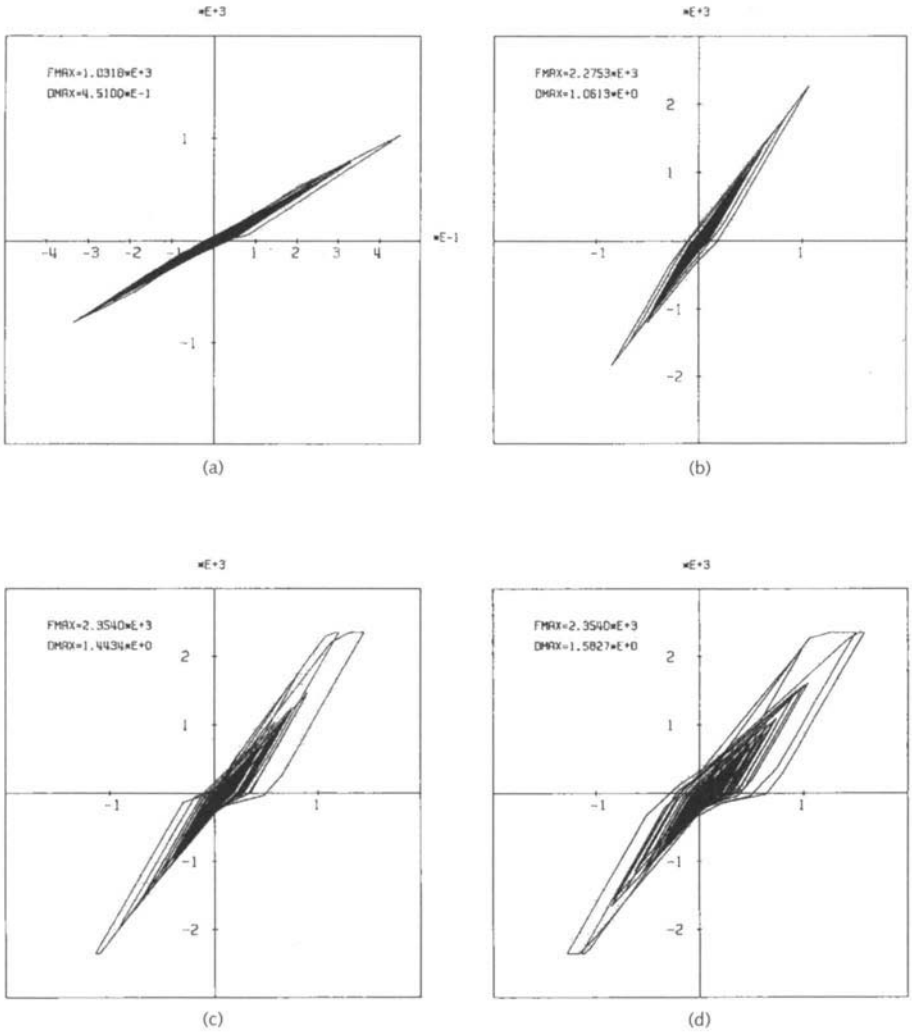

Figure 10.3
Q-D diagrams for the strengthened St. Nikita, El Centro excitation, east-west direction: (a) a = 0.12 g, (b) a = 0.20 g, (c) a = 0.34 g, (d) a = 0.39 g.

with the assumed amount of vertical reinforcement at the ends of the walls. The results of the analysis (table 10.1) showed that each of the individual walls and the structure as a whole had an adequate bearing capacity, with both safety factors against failure being greater than 1 ($F_{E\text{-}W}$ = 2.2 and $F_{N\text{-}S}$ = 1.9) at Cbs = 0.39.

The results of the dynamic analysis at three levels of input acceleration (0.20 g, 0.27 g, 0.34 g), corresponding to return periods of 100, 200, and 1000 years, respectively, showed that under conditions of high seismicity, the dynamic behavior of the strengthened structure complied with the safety criteria. The IZIIS hysteretic model was used to obtain the Q-D diagrams, a ductility of μ = 1.0–1.2 was obtained for the "design" earthquake, and $\mu < 1.5$ was obtained for the maximum-severity earthquake (table 10.2).

St. Nikola, Psača

On the basis of the analysis of the church of St. Nikola, Psača, presented in chapter 9, it was concluded that certain repair measures would be necessary to protect this building, including replacement of those timber ties

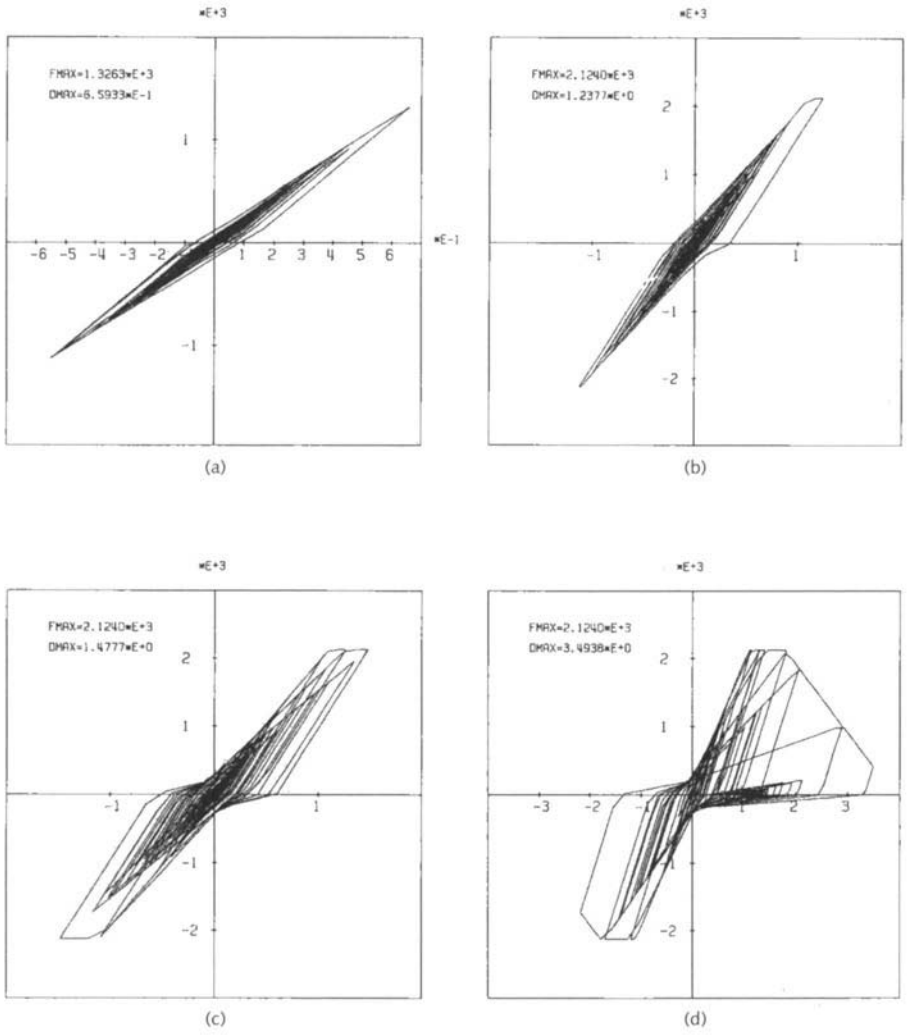

Figure 10.4
Q-D diagrams for the strengthened St. Nikita, Petrovac excitation, north-south direction: (a) a = 0.12 g, (b) a = 0.20 g, (c) a = 0.34 g, (d) a = 0.39 g.

within the wall mass and the interior of the church that have deteriorated or were removed during previous interventions. Replacement of the missing or ineffective timber ties with steel ties would constitute an important segment of the overall seismic strengthening of the structure. Steel ties would be incorporated as follows:

- two 18 mm steel ties placed along the length of each of the perimeter walls at the level of the lintels, 2.9 m above the ground level, and one 18 mm steel tie incorporated along side each of the existing timber ties in both longitudinal and transverse directions;
- four 18 mm steel ties along the length of each perimeter wall at a height of 5.6 m above the ground level, and one 18 mm tie alongside each of the existing transverse timber ties;
- two 18 mm steel ties at each of four locations around the base of the tambour, and three 18 mm sheet steel ties,

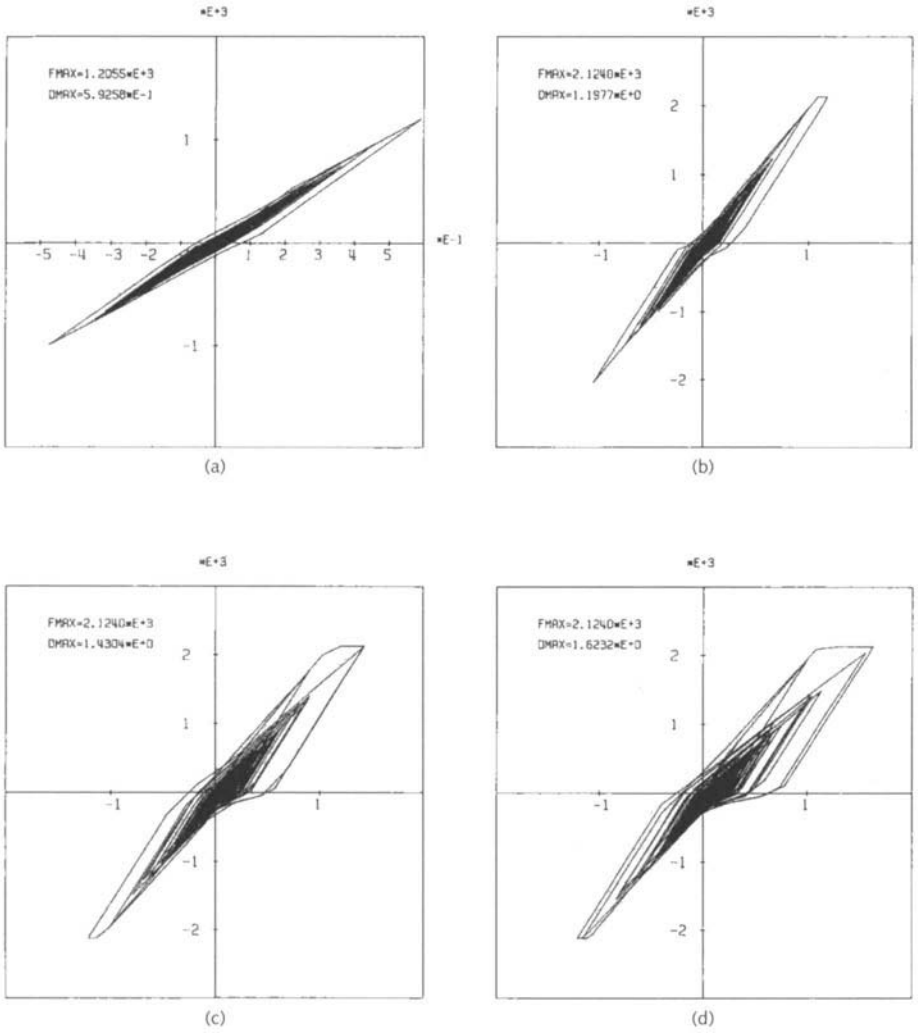

Figure 10.5
Q-D diagrams for the strengthened St. Nikita, El Centro excitation, north-south direction: (a) a = 0.12 g, (b) a = 0.20 g, (c) a = 0.34 g, (d) a = 0.39 g.

each in four parts, at the base of the dome at a height of 9 m; and

- one 4 mm vertical steel tie at each side of the eight openings in the tambour structure.

Analysis of the bearing capacity and stability of such a hypothetically strengthened structure was performed for the maximum-severity seismic event expected, C_{bs} = 0.23. The walls were modeled as being fixed at both ends and as plain masonry. Results of the capacity analysis (see table 10.1) showed retrofitting resulting in an increase in the bearing capacity of the structure, particularly in the transverse direction. The safety factor against failure increased from $F_{N\text{-}S}$ = 1.04 to $F_{N\text{-}S}$ = 1.58 for the maximum earthquake excitation.

The results of the dynamic-response analysis, obtained by application of the IZIIS hysteretic model, are presented in the form of Q-D diagrams and ductility values for three levels of input acceleration (0.14 g, 0.19 g, 0.21 g), corresponding to return periods of 100, 200, and 1000 years. Although the analysis of the existing structure showed

that the church was in satisfactory condition, the dynamic behavior of the strengthened structure in the transverse (north-south) direction was improved. Analysis also showed that, at a = 0.21 g, the ductility decreased from $\mu = 1.6$ to $\mu = 1.34$ under the Petrovac earthquake excitation. The behavior of the hypothetically strengthened structure is in compliance with the established safety criteria.

Note

1. POS (position) indicates the locations where strengthening elements were added to the church model (see figs. 5.11–5.13).

This page intentionally left blank

Chapter 11

Summary, Conclusions, and Recommendations

A procedure for the conservation, repair, and seismic strengthening of a typical late Byzantine church in Macedonia has been demonstrated successfully by the dynamic testing of a scale model of a prototype fourteenth-century church—St. Nikita, in the village of Banjani—on the seismic simulation shaking table at IZIIS. The procedure was designed to provide protection to churches during exposure to the maximum-intensity earthquake expected in the region, with an estimated return period of 1000 years.

The methodology satisfies the seismic stability criteria established for the churches and adheres to the basic, universally accepted conservation principles of maintaining authenticity, restricting interventions to those that have minimum impact on the architectural and historical aspects of the structure, and providing maximum protection to church buildings and their occupants during earthquakes. The procedures developed and tested during this study should be generally applicable to the strengthening of similar church structures that still exist throughout the high-seismicity areas of the Mediterranean basin, the Middle East, and the adjacent regions of Asia.

The bearing capacity and deformability of the structural system of the scale model of the church were bolstered by the seismic strengthening techniques to the levels specified by the design safety criteria established at the beginning of the study. This was shown by the results of mechanical property measurements of the church model structure before and after repairs and by the retrofitting of the model that was damaged during the shaking-table tests.

A trilinear hysteretic analytical method, the IZIIS model, was used for the dynamic analysis of the church model before damage was incurred and after the damage was repaired and the structure seismically strengthened. The IZIIS model was shown to be applicable in all characteristic phases of church model behavior, including the elastic state; the inelastic, or nonlinear, state; and the state of severe damage that could lead to complete failure. The IZIIS model was also applied to the analysis of several hypothetically strengthened Macedonian churches, and it was shown that the methodology developed in this study, when applied to these churches, would provide ample protection from the serious structural damage that would result from exposure to the expected earthquakes.

It is recommended that a demonstration case study be initiated that would apply the methodology developed and tested in this project to the retrofitting of one of the more vulnerable churches identified during the program. It is also proposed that strong motion instrumentation be installed in the St. Nikita church in order to obtain actual earthquake records on historic monuments, because no records of this kind are available on a world scale today.

Following completion of the work on this project, activities continued on a separate program to investigate the possibility of applying seismic base isolation as a retrofitting technology. Base isolation is one of the more advanced and promising methods for protecting historic monuments from devastating earthquakes. The strengthened St. Nikita church model was used in this project, and a test of the base isolation methodology was demonstrated successfully on the IZIIS shaking table (Gavrilović and Sendova 2001).

Appendix A
List of Churches Surveyed

Table A.1 lists the churches visited and evaluated during this project. Documentation of the detailed results of this portion of the study is given in Gavrilović, Šumanov, et al. (1991, vols. 2–6; see the volume column).

Table A.1
List of churches surveyed

Church name	Location (village)	Description	Century constructed	Volume[a]
St. Andreja	Matka	Triconch, single dome, inscribed cross	14th	5
St. Arhangel Mihail	Radožda	Single dome, cave-type	13th–14th	6
St. Arhangel Mihail	Štip	Single dome	14th	6
St. Arhangel Mihail	Lesnovo	Single dome, inscribed cross	14th	4
St. Arhangel Mihail	Varoš	Single nave, single dome	12th–13th	5
St. Atanasie	Lešok	Freestanding cross, dome missing	13th–14th	6
St. Atanasie	Varoš	Single dome, single nave, inscribed cross	14th	4
St. Bogorodica	Drenovo	Three naves, basilica	13th–14th	4
St. Bogorodica	Matejče	Quincunx, three naves, inscribed cross	13th–14th	2
St. Bogorodica	Ohrid	Single nave, semibarrel vault	14th	3
St. Bogorodica	Osogovo Monastery, Kriva Palenka	Single dome	14th	4
St. Bogorodica	Sušica	Single nave, vaulted roof	NA	6
St. Bogorodica	Treskavec Monastery, Dabnica	Tri-dome	13th	4
St. Bogorodica	Varoš	Single nave	14th	5
St. Bogorodica Čelnica	Ohrid	Single nave	14th	4
St. Bogorodica Eleusa	Veljusa	Tetraconch	11th	3
St. Bogorodica Perivlepta	Ohrid	Single dome, inscribed cross	13th	4
St. Bogorodica Zahumska	Trpejca	Single dome, inscribed cross	14th	2
St. Dimitrija	Markov Monastery, Sušica	Single dome, inscribed cross	14th	6
St. Dimitrija	Ohrid	Single nave, couple roof	14th	3
St. Dimitrija	Titov Veles	Single nave with steeple	14th	6
St. Dimitrija	Varoš	Single nave, single dome	13th	5
SS. Elena and Konstantin	Ohrid	Small church, couple roof	11th–14th	4
St. Gjorgji	Begnište	Single nave, single dome	14th	5

Table A.1 *continued*

Church name	Location (village)	Description	Century constructed	Volume[a]
St. Gjorgji	Gorni Kozjak	Single dome, inscribed cross	11th–12th	6
St. Gjorgji	Kurbinovo	Single nave, couple roof	12th	5
St. Gjorgji	Rečica	Single nave, barrel mount, couple roof	14th	3
St. Gjorgji	Staro Nagoričane	Quincunx, basilica	11th	4
St. Jovan	Štip	Single nave	14th	6
St. Jovan Kaneo	Ohrid	Single dome, inscribed cross	13th	3
St. Kliment Mal	Ohrid	Single nave	14th	3
St. Leontije	Vodoča	Single dome	11th–14th	6
St. Nikita	Banjani	Single dome, inscribed cross	14th	2
St. Nikola	Čelopek	Single nave	14th	6
St. Nikola	Ljuboten	Single nave, inscribed cross	14th	5
St. Nikola	Manastir	Three naves, basilica, barrel vault	13th–16th	4
St. Nikola	Psača	Single dome, inscribed cross, couple roof	14th	2
St. Nikola	Radišani	Single nave	14th	5
St. Nikola	Šiševo	Single nave, barrel vault	14th	5
St. Nikola	Varoš	Single nave, barrel vault	12th–13th	5
St. Nikola Bolnicki	Ohrid	Single nave	14th	4
St. Nikola Čudotvorec	Ohrid	Single nave, couple roof	13th	5
St. Pantelejmon	Gorno Nerezi	Quincunx, inscribed cross	12th	6
St. Pantelejmon	Ohrid	Single dome, triconch	9th–14th	4
St. Sofia	Ohrid	Three naves, basilica	11th	4
St. Spas	Kučevište	Single dome, inscribed cross	14th	5
St. Spas	Štip	Single nave, couple roof	14th	6
St. Spas	Zrze	Single nave	14th	5
St. Stefan	Konče	Single dome, inscribed cross	14th	4
St. Vrači Mali	Ohrid	Single nave, couple roof	14th	3

[a] Refer to listed volume of Gavrilovič, Šumanov, et al. (1991) for detailed description.

Appendix B

Single-Degree-of-Freedom Analysis Flowchart

The dynamic equations of motion are most commonly solved by the direct integration method, using the numerical step-by-step process. Newmark's β-method was used in its implicit form for integration of the equation of motion. In lieu of a detailed description of this widely used method, the flowchart for obtaining the quantities of the dynamic response is presented in figure B.1.

At each time interval (step) in the integration process, the values K^* and Rt^* are computed and the displacement increment, $\Delta xt = Rt^*/K^*$, is defined. With Δxt known, the response ($\ddot{x}, \dot{x}, x$) at moment $t + \Delta t$ is obtained and used as an initial condition in the next step. The principal specificity of the method is the determination of the tangent stiffness and the elastic force, F_S (t), which depends on the way the stiffness modification of the system is modeled, that is, the hysteretic model that is applied in the analysis. The tangent stiffness of the system is functionally dependent on the extent of the deformations. For each part of the hysteretic diagram, the stiffness is limited by envelope conditions. The equivalent elastic force is obtained (fig. B.1) and depends on the stiffness and deformation of the system at a specifically defined time (beginning of the integration interval).

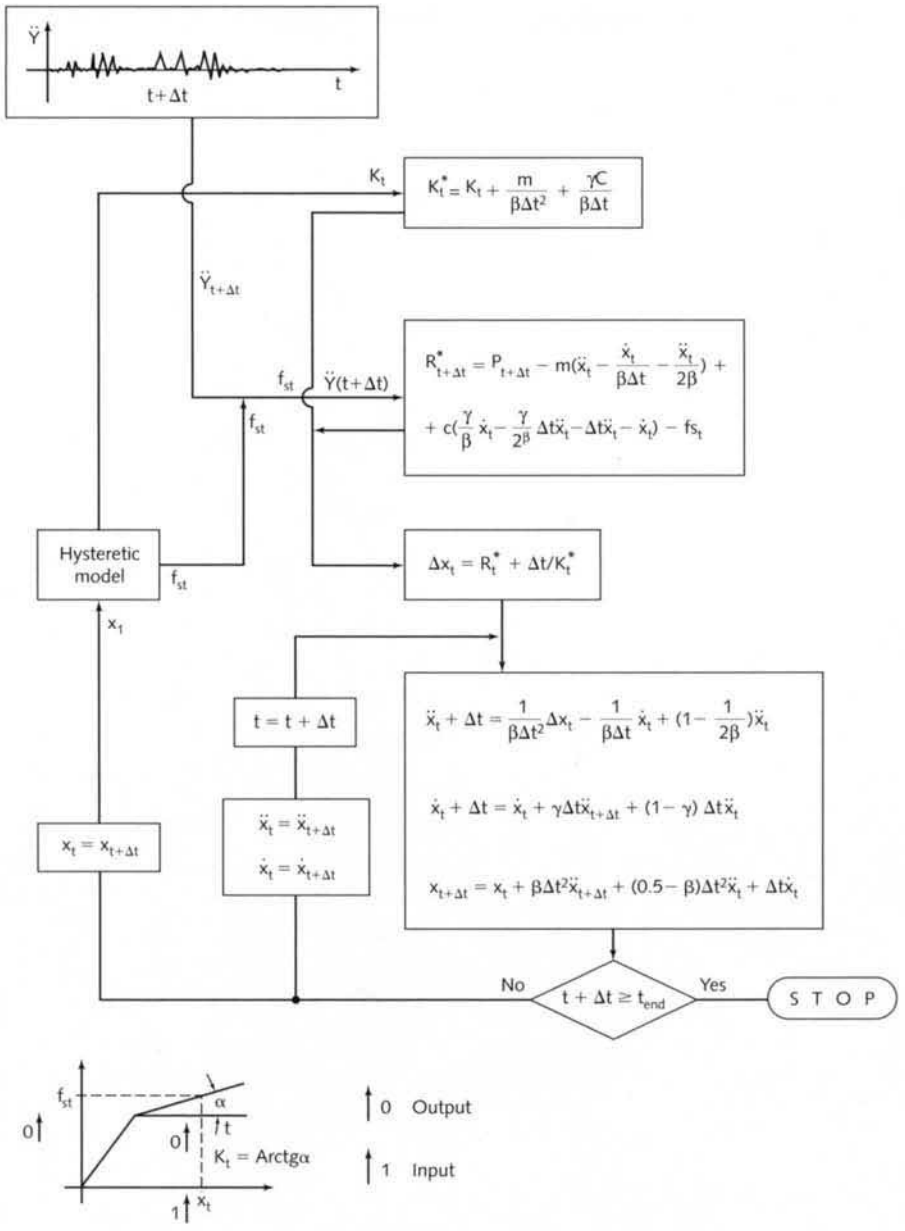

Figure B.1
Analysis of a single-degree-of-freedom system.

Appendix C

Experimental and Analytical Displacement and Acceleration Time History

Figures C.1–C.4 show comparisons between actual experimental data and calculated time histories of the displacements and accelerations of the original model during exposure to the Petrovac and El Centro earthquake excitations. Data are given for level 1 and the top of the dome at two input acceleration levels. Complete data for all sensor locations on the model and for all input acceleration levels tested can be found in Gavrilović, Šumanov, et al. (1991, vol. 12).

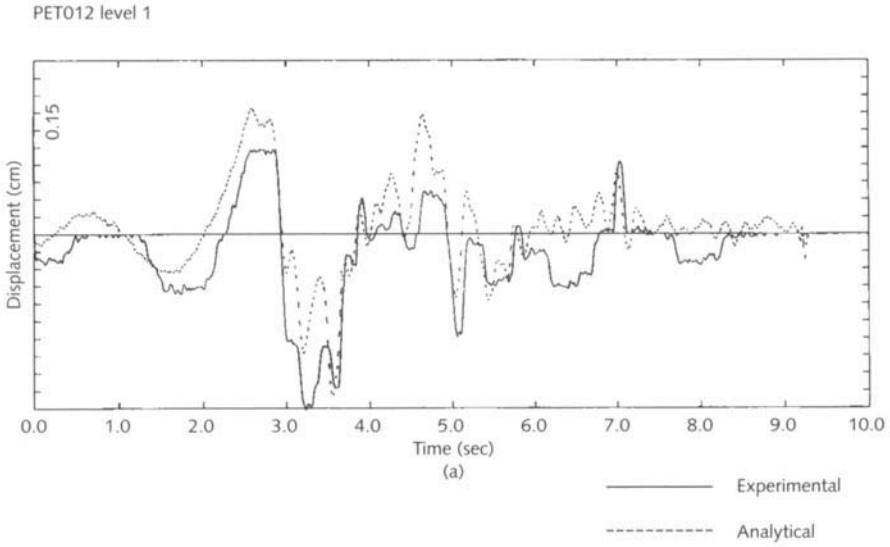

Figure C.1a
Displacement time history for level 1 (PET012N).

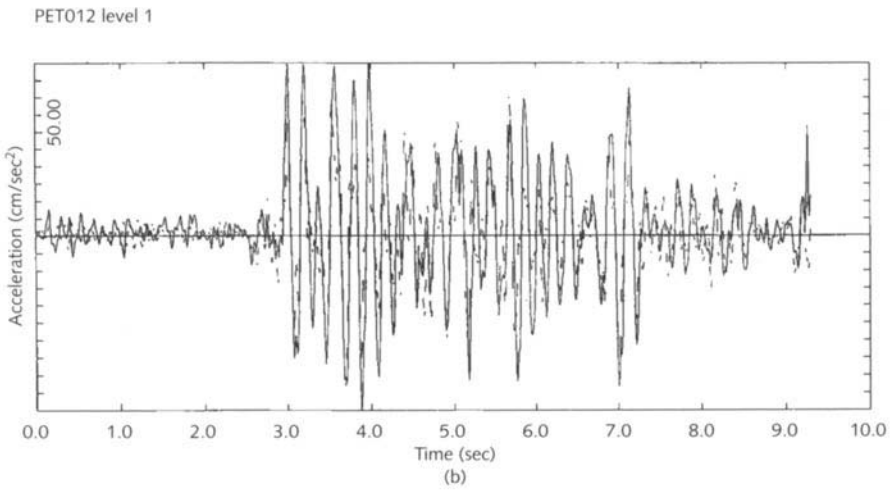

Figure C.1b
Acceleration time history for level 1 (PET012N).

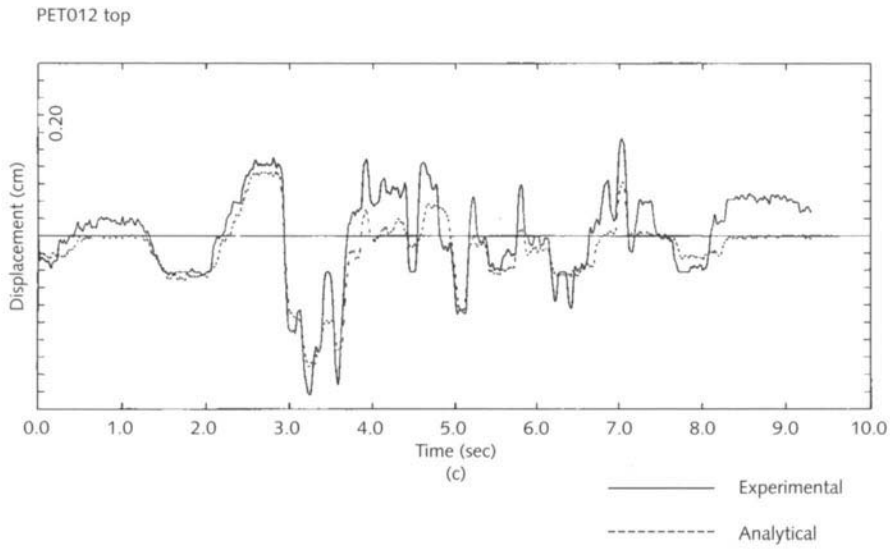

Figure C.1c
Displacement time history for top of the dome (PET012N).

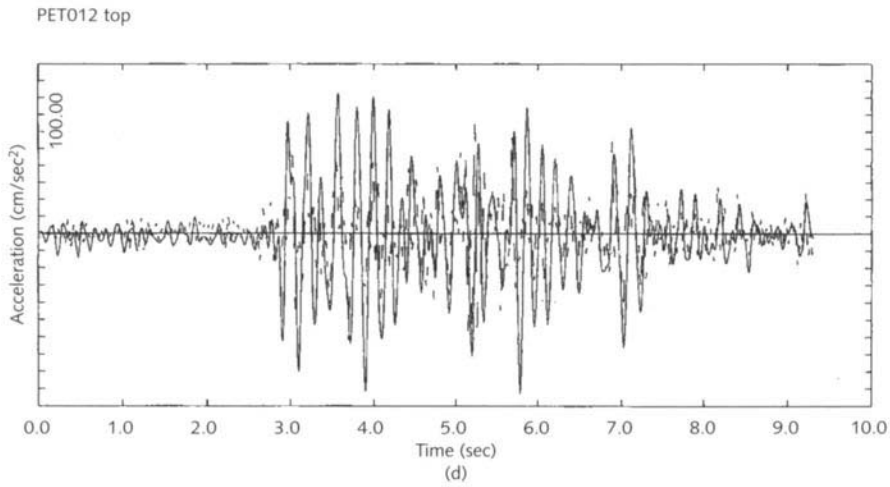

Figure C.1d
Acceleration time history for top of the dome (PET012N).

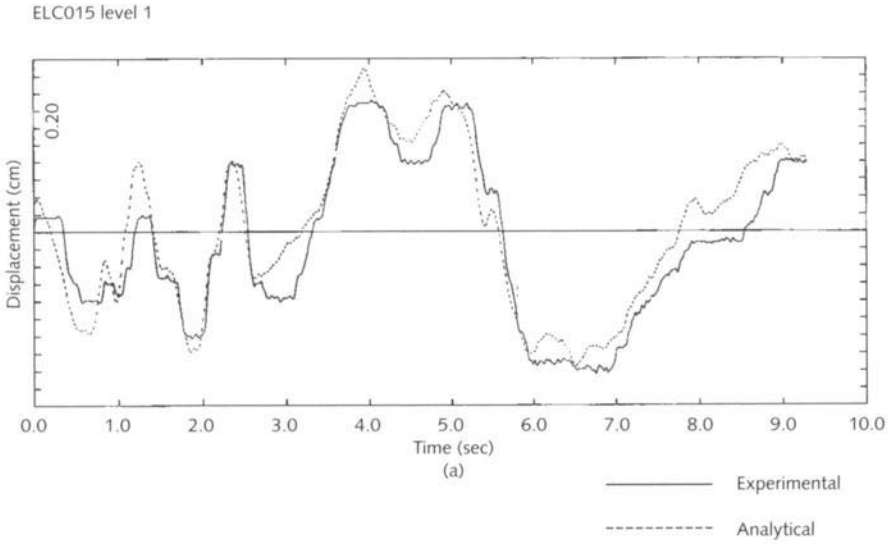

Figure C.2a
Displacement time history for level 1 (ELC015N).

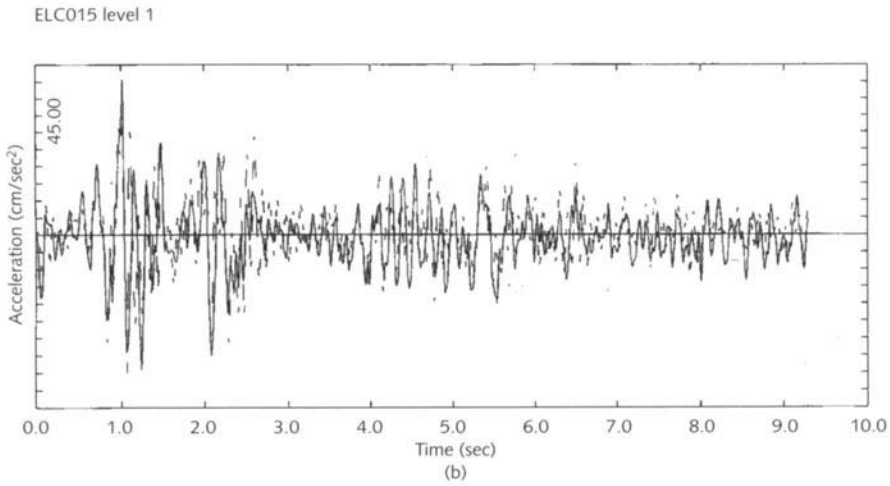

Figure C.2b
Acceleration time history for level 1 (ELC015N).

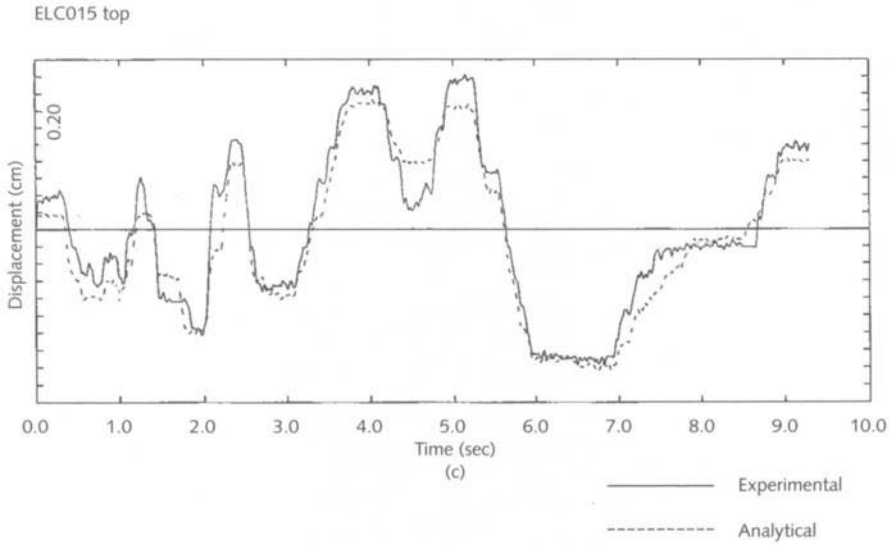

Figure C.2c
Displacement time history for top of the dome (ELC015N).

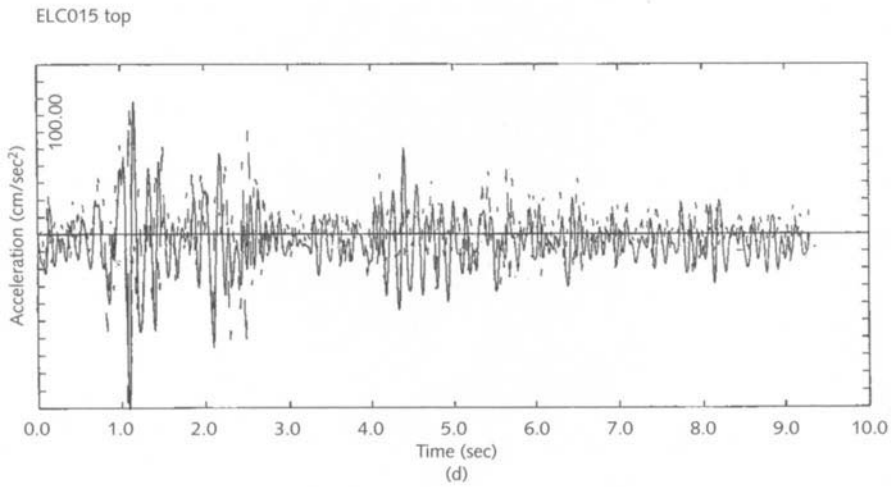

Figure C.2d
Acceleration time history for top of the dome (ELC015N).

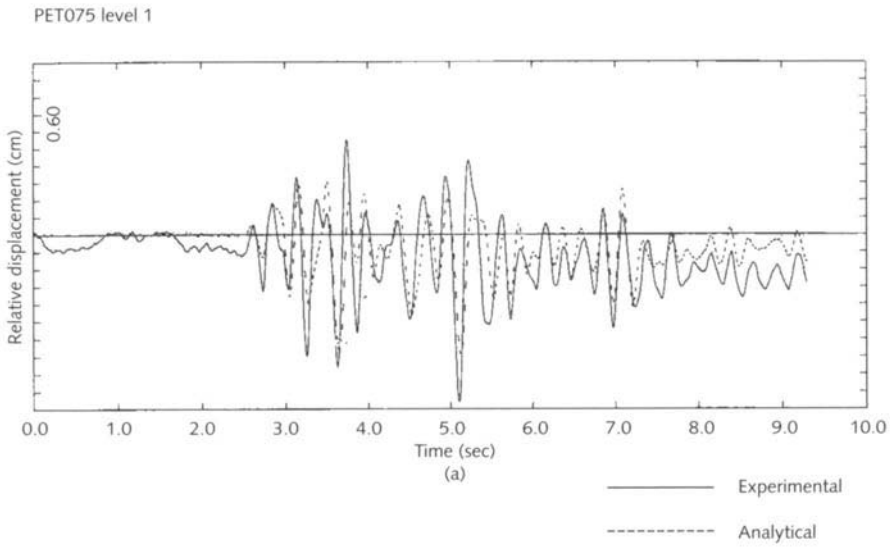

Figure C.3a
Displacement time history for level 1 (PET075N).

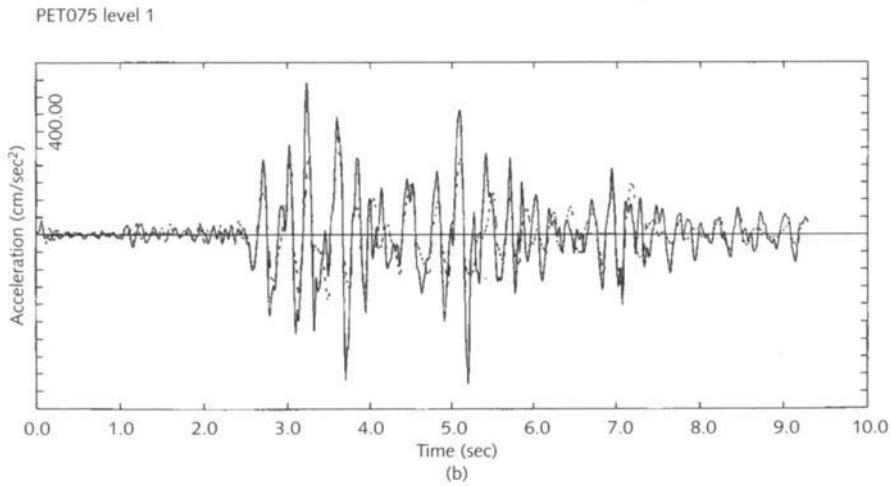

Figure C.3b
Acceleration time history for level 1 (PET075N).

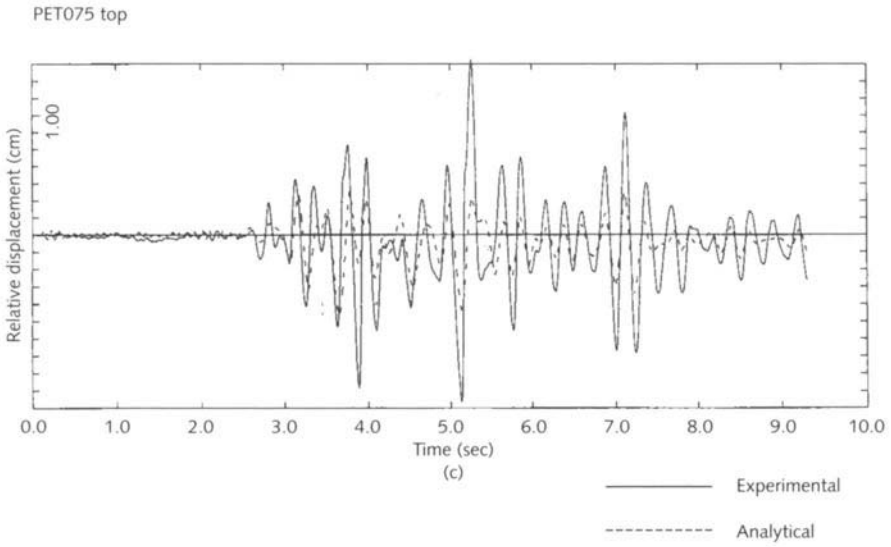

Figure C.3c
Displacement time history for top of the dome (PET075N).

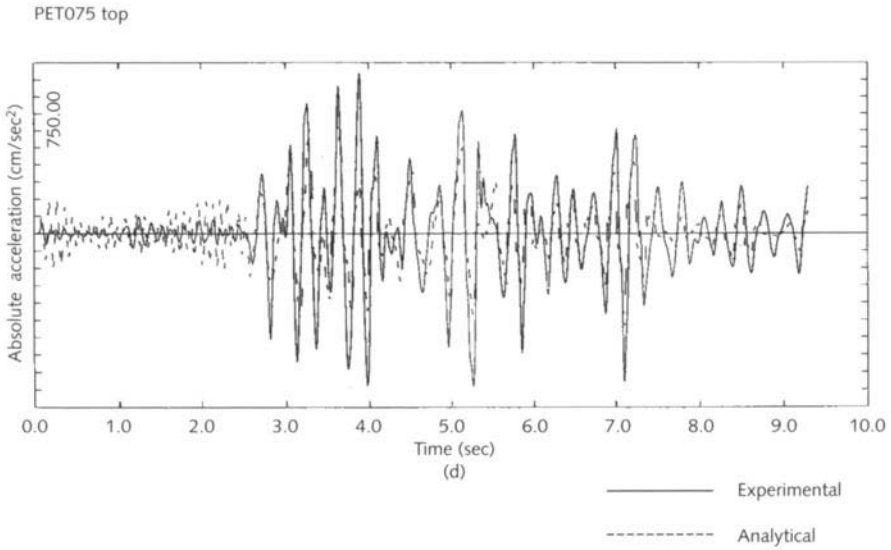

Figure C.3d
Acceleration time history for top of the dome (PET075N).

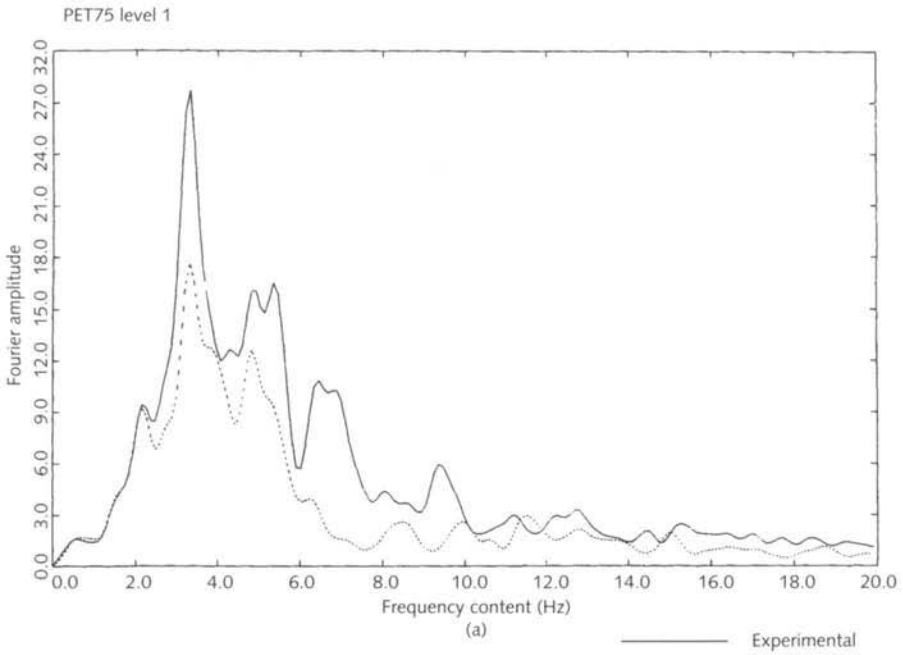

Figure C.4a
Frequency content for level 1 (PET075N).

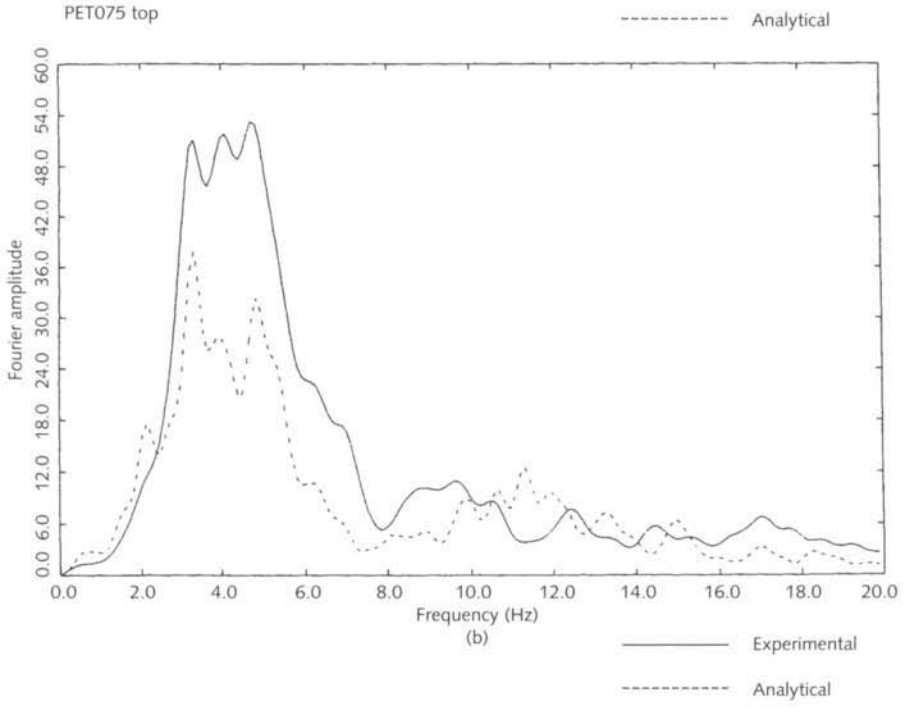

Figure C.4b
Frequency content for top of the dome (PET075N).

Appendix D

Results of Dynamic Response Analysis of the Existing St. Nikita Church Using the IZIIS Hysteretic Model

Figures D.1–D.4 show the analytically derived dynamic response of the real St. Nikita church, in its current condition, to a postulated excitation by the El Centro and Petrovac earthquakes. The responses are given in the form of Q-D diagrams for both orthogonal directions and at three a_{max} levels. The IZIIS hysteretic model was used in this analysis.

Figure D.1 (top row)
Q-D diagrams, north-south direction, El Centro earthquake: (a) a_{max} = 0.12 g, (b) a_{max} = 0.20 g, (c) a_{max} = 0.34 g.

Figure D.2 (bottom row)
Q-D diagrams, east-west direction, El Centro earthquake: (a) a_{max} = 0.12 g, (b) a_{max} = 0.20 g, (c) a_{max} = 0.34 g.

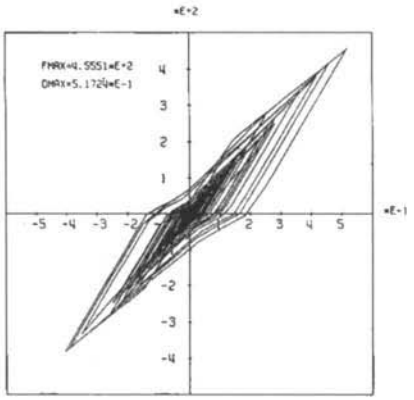

(a)

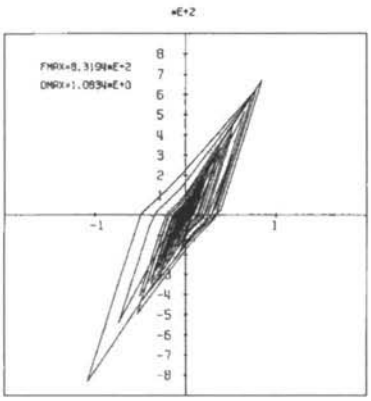

(b)

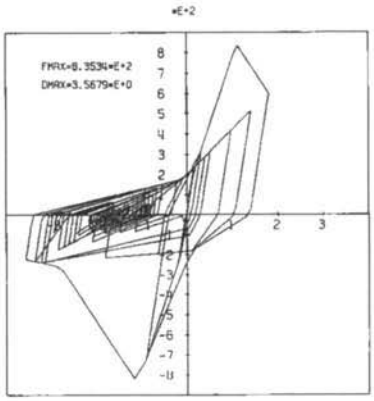

(c)

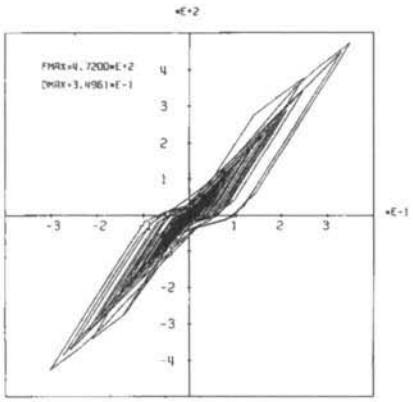

(a)

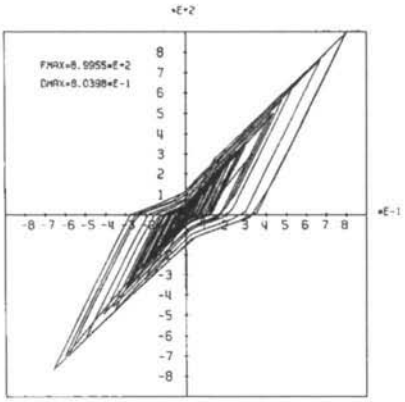

(b)

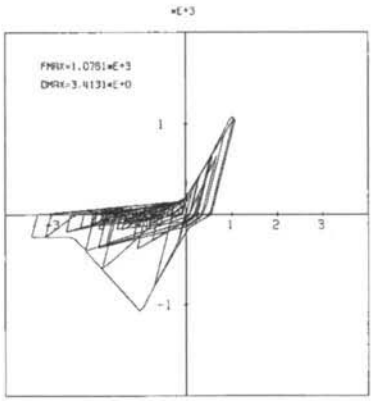

(c)

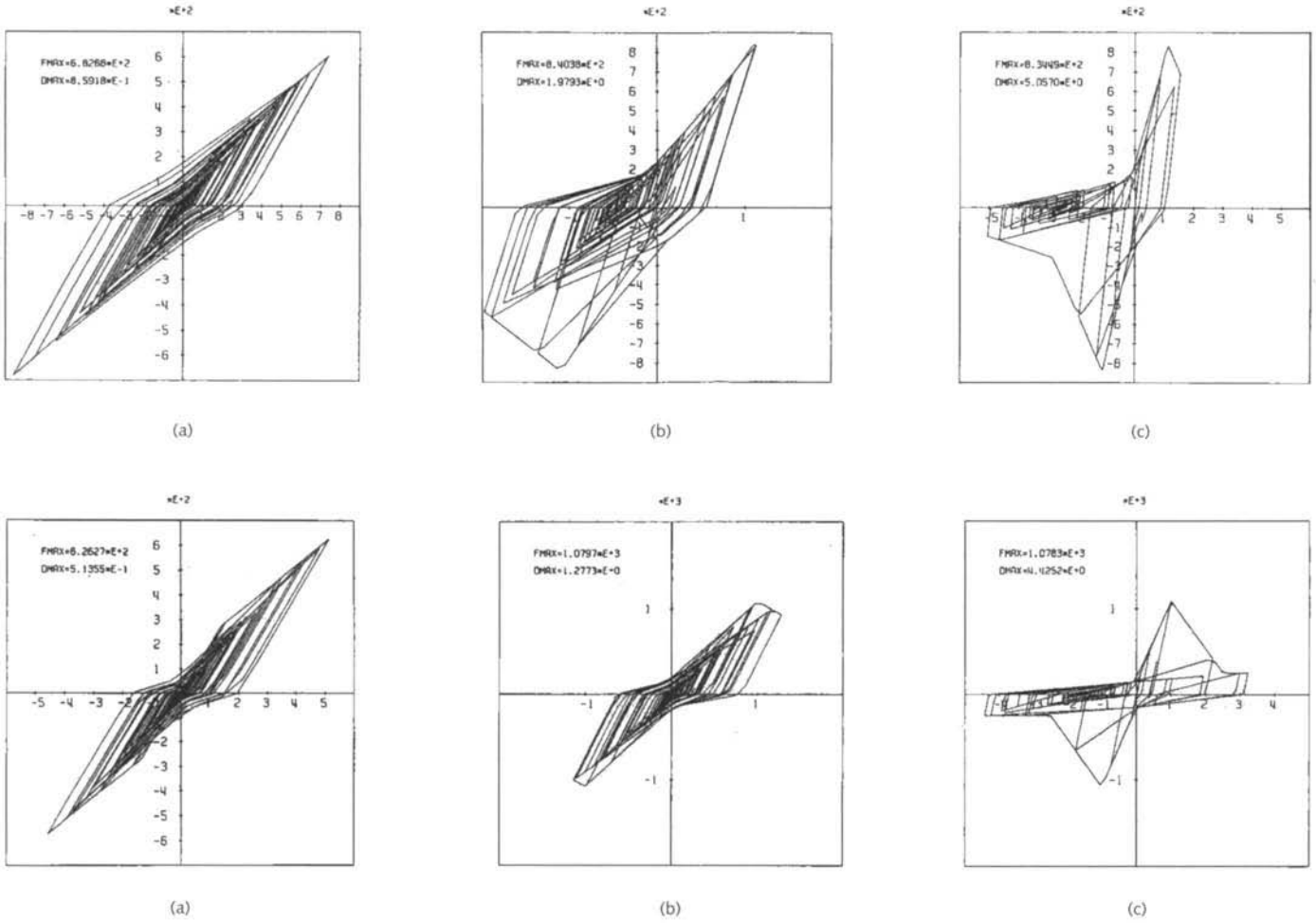

Figure D.3 (top row)
Q-D diagrams, north-south direction, Petrovac earthquake: (a) a_{max} = 0.12 g, (b) a_{max} = 0.20 g, (c) a_{max} = 0.34 g.

Figure D.4 (bottom row)
Q-D diagrams, east-west direction, Petrovac earthquake: (a) a_{max} = 0.12 g, (b) a_{max} = 0.20 g, (c) a_{max} = 0.34 g.

References

Bošković, D. J.
1947 *The Fundamentals of Medieval Architecture.* Belgrade.

Bouwkamp, J. G., and D. Rea
1970 Dynamic testing and formulation of mathematical models. In *Earthquake Engineering*, 151–165, ed. R. L. Wiegel. Englewood Cliffs, New Jersey: Prentice-Hall.

Clough, R. W., and J. Penzien
1975 *Dynamics of Structures.* New York: McGraw-Hill.

Djurić, V. J.
1974 *Byzantine Frescoes in Yugoslavia* (in Macedonian). Belgrade.

Feilden, B. M.
1982 *Conservation of Historic Buildings.* London and Boston: Butterworth Scientific.

Feilden, B. M.
1987 *Between Two Earthquakes: Cultural Property in Seismic Zones.* Marina del Rey, Calif.: Getty Conservation Institute; Rome: ICCROM.

Foutch, D. A.
1976 A study of the vibrational characteristics of two multistory buildings, EERL 76-03. Pasadena: California Institute of Technology, Earthquake Engineering Research Laboratory.

Gavrilović, P.
1982 Shear resistance of reinforced concrete structures during non-linear dynamic behavior under cyclic and dynamic excitation. PhD dissertation, University of Belgrade.

Gavrilović, P., V. Sendova and W. S. Ginell
1999 Seismic Strengthening and Repair of Byzantine Churches. *Journal of Earthquake Engineering* 3, no. 2: 199–235.

Gavrilović, P., and V. Sendova
2001 Protection of Byzantine churches against earthquakes using seismic isolation. Report IZIIS 2001-59. Skopje, Republic of Macedonia: IZIIS.

Gavrilović, P., L. Šumanov, et al.
1991 *Study for Seismic Strengthening, Conservation, and Restoration of Churches Dating from the Byzantine Period (Ninth to Fourteenth Century) in Macedonia,* 12 vols. Skopje, Yugoslavia: IZIIS.

Vol. 1: Study of architectural structural systems, and strengthening of the monuments. Report IZIIS 500-76-91/1.

Vol. 2: Existing state of representative selected monuments (nos. 1–4). Report IZIIS 500-76-91/2.

Vol. 3: Existing state of the monuments (nos. 5–11). Report IZIIS 500-76-91/3.

Vol. 4: Existing state of the monuments (nos. 12–25). Report IZIIS 500-76-91/4.

Vol. 5: Existing state of the monuments (nos. 26–38). Report IZIIS 500-76-91/5.

Vol. 6: Existing state of the monuments (nos. 39–50). Report IZIIS 500-76-91/6.

Vol. 7: Determination of seismic hazard parameters for the sites of the selected monuments. Report IZIIS 92-71/7.

Vol. 8: Ambient vibration testing of selected monuments. Report IZIIS 92-71/8.

Vol. 9: Shaking table test of models. Report IZIIIS 92-71/9.

Vol. 10: Study for repair and strengthening of St. Nikita church on the basis of investigation of existing state, experimental field works, and shaking table tests. Report IZIIS 92-71/10.

Vol. 11: Study of lime mortars and lime-based mixtures for repair, grouting, and injection of churches dating from the Byzantine period in Macedonia. Report IZIIS 94-68/1.

Vol. 12: Study for definition and implementation of the methodology for repair and strengthening of Byzantine churches in Macedonia on the basis of the performed experimental and analytical investigations of structural behavior. Report IZIIS 94-68/2.

Hadžievski, D.
1976 *Seismicity of the Territory of Macedonia* (in Macedonian). Skopje, Yugoslavia: IZIIS Seismological Observatory.

Hoddinott, R. F.
1963 *Early Byzantine Churches in Macedonia and Southern Serbia: A Study of the Origins and the Initial Development of East Christian Art*. London: Macmillan; New York: St. Martin's Press.

Jurukovski, D., and D. Mamucevski
1986 Biaxial system for earthquake simulations with three variable controls. *Proceedings of the 8th European Conference on Earthquake Engineering* (Sept. 7–12, 1986), vol. 4, 7.1/1–8. Lisbon: Laboratório Nacional de Engenharia Civil.

Jurukovski, D., and S. Percinkov
1977 Dynamic forced vibration study of the tower-type building no. 2 at Karadjordje Square in Zemun. Report LDI 77/2. Skopje, Yugoslavia: IZIIS.

Larson, R. L.
1972 *Programming and Control of Large Vibration Tables in Uniaxial and Biaxial Motions*. Minneapolis: MTS Systems Corporation.

Mango, C. A.
1974 *Byzantine Architecture*. New York: Harry N. Abrams.

Naeim, F., and Kelly, J. M.
1999 *Design of Seismic Isolated Structures: From Theory to Practice*. New York: John Wiley.

Sendova, V.
1988 Shear resistance of reinforced concrete structures under seismic excitations. MS thesis, IZIIS, Skopje, Yugoslavia.

US/ICOMOS
1999 ICOMOS charters and other international doctrinal documents. *US/ICOMOS Scientific Journal* 1, no. 1.

Wilson, E. L.
1990 *Structural Analysis Program: SAP90*. Berkeley: University of California.

Additional Reading

Alessi, A., P. P. Diotallevi, D. Jurukovski, M. Petkovski, Lj. Taskov, and F. Zarri. Shaking table test of reduced scale model of brick masonry building. In *Proceedings of the Ninth European Conference on Earthquake Engineering.* Moscow: Kucherenko Tsniisk of the USSR Gosstroy, 1990.

Benedetti, D., and M. L. Casella. Shear behaviour of layered stone masonry walls under different strengthening conditions. *L'Industria delle Construzioni*, no. 123 (1982): 26–32.

Benedetti, D., and A. Castoldi. Dynamic and static experimental analysis of stone masonry buildings. In *Proceedings of the Seventh European Conference on Earthquake Engineering*, vol. 5, 179–188. Athens: Technical Chamber of Greece, 1982–1985.

Gavrilović, P. Repair and strengthening of earthquake damaged buildings. National report to WG-E, UNDP; UNIDO Project RER/79-015, 1979.

———. The restoration of monuments in Pagan: Survey and selection of monuments for dynamic testing and study for repair and strengthening with assessment of the record of Pagan region. UNESCO Report, Project BUR 78/023. Pagan, Burma, and Skopje, Yugoslavia: IZIIS, 1982.

———. Methods and techniques for repair and strengthening of historical monuments and old urban nuclei in seismically active regions. In *Proceedings of Protection of Patrimony in Seismic Risk Zones: Analysis and Intervention,* eds. Ferruccio Ferrigni and Bruno Helly. Strasbourg: Conseil de l'Europe; Ravello: Centre Universitaire Européen pour les Biens Culturels; Rome: FORMEZ, Centro di Formazione e Studi, 1990.

Gavrilović, P., Lj. Taskov, and D. Jurukovski. Methods for repair and strengthening of the national monuments in Pagan, Burma, vols. I–V and appendix. UNESCO/UNDP Project BUR 78/023. Report IZIIS 83-30/1-6. Skopje, Yugoslavia: IZIIS, 1983.

Hidalgo, P. A., R. L. Mayes, H. D. McNiven, and R. W. Clough. Cyclic loading tests of masonry single piers. Volume 3, Height to width ratio of 0.5. Earthquake Engineering Research Center Report UCB/EERC 79-12. Berkeley: University of California, 1979.

Isaacson, B. de St. Q., and M. de St. Q. Isaacson. *Dimensional Methods in Engineering and Physics: Reference Sets and the Possibilities of Their Extension.* New York: Wiley, 1975.

Jurukovski, D., et al. Basic and applied research study for seismic modeling of mixed, reinforced concrete-masonry buildings. Volume 4: Shaking table test of reduced scale model strengthened by R.C. (reinforced concrete) central core. Report IZIIS 91–92. Skopje, Yugoslavia: IZIIS, 1991.

Jurukovski, D., J. Petrovski, Lj. Taskov, and S. Percinkov. Dynamic testing of brick masonry structure in Preska Settlement, Ljubljana, and formulation of mathematical model. Report IZIIS 78-62. Skopje, Yugoslavia: IZIIS, 1978.

Krstevska, L., L. Taskov, and P. Gavrilović. Dynamic characteristics of historical monuments dating from the Byzantine period in Macedonia. In *Proceedings of the 10th European Conference on Earthquake Engineering*, vol. 2, 987–991. Rotterdam and Brookfield, Vt.: A. A. Balkema, 1995.

Mayes, R. L., and R. W. Clough. State-of-the-art in seismic shear strength of masonry: An evaluation and review. Earthquake Engineering Research Center Report UCB/EERC 75-21. Berkeley: University of California, 1975.

Penzien, J., J. G. Bouwkamp, R. W. Clough, and D. Rea. Feasibility study: Large scale earthquake simulator facility. Earthquake Engineering Research Center Report UCB/ EERC 67-01. Berkeley: University of California, 1967.

Petrovski, J., K. Talaganov, and S. Galbov. Research in the field of seismic design of masonry structures: Definition of soil-structure interaction parameters from the dynamic response of embedded foundation. Report IZIIS 78-47. Skopje, Yugoslavia: IZIIS, 1978.

Pichard, P. The restoration of Pagan, Burma. UNESCO Technical Report FMR/CC/CH/76/116; RP/1975-76/3.411.6. Paris: UNESCO, 1976.

Taskov, Lj., P. Gavrilović, and, D. Jurukovski. Methods for repair and strengthening of the national monuments in Pagan, Burma. Volume IV: Dynamic properties of selected structures. Report IZIIS 83-30/4. Skopje, Yugoslavia: IZIIS, 1983.

Wilson, E. L., J. P. Hollings, and H. H. Dovey. Three dimensional analysis of building systems. Earthquake Engineering Research Center Report UCB/EERC 75-13. Berkeley: University of California, 1975.

Glossary

aisle One of several east-west walkways of a basilica that extend the length of the church and run parallel to the nave.

apse Semicylindrical or polygonal extension on the east end of a church.

archivolt The architectural member that outlines an arch or other curved opening in a wall.

barrel vault Semicylindrical, arched roof structure.

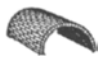

basilica Type of church having aisles, apse, nave, bema, and (often) narthex.

bema Area in the crossing of a church that is a few steps above the floor of the nave and is located behind the altar and in front of the apse.

biforium Arch-top niche containing two subniches.

calotte A dome or caplike architectural member such as a cupola or half-cupola (semicalotte).

concha Semidome vaulting of an apse.

corbel A stepped stone or timber projection from the face of a wall, usually used as a support for a horizontal beam.

cornice Horizontal or other upper, molded architectural member that projects from and crowns a wall or gable.

dentil Series of small rectangular or triangular blocks under a cornice, which gives it a toothlike appearance.

diaconicon A sacristy to the right, or south, side of the apse or altar.

facade The exterior face or architectural front of a church or other building.

gabled roof A roof that is triangular in cross section with a gable at one or both ends (also called a *couple roof*).

groin vault Semicylindrical intersecting roof structures without ribs.

lintel Horizontal architectural member that spans an opening in a wall above a doorway or window. Used to provide support for the superstructure above the opening.

monoforium Arch-top niche containing one subniche.

naos Area under the dome of a cruciform church at the intersection of the transept and nave.

narthex Western entry area within the church leading to the nave and aisles or to the naos.

nave High, central aisle of a basilica.

niche A recess in a wall.

pendentive Transition region between the upper cylinder (tambour) that supports the dome and the square, lower support structure. Usually has the shape of a semispherical triangle.

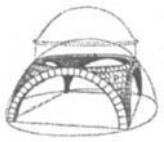

pilaster A vertical, rectangular projection from a wall serving as a support column or pier. Usually has a capital and a base.

porch Covered exterior entrance to a building. Has a separate roof.

portico Covered walkway parallel to a building wall. Supported by a row of columns on the outside.

prothesis A chapel to the left, or north, side of the apse or altar.

quincunx A church structure surmounted by five domes, one in the center and one in each of the four corners.

ribbed vault Intersecting, arched roof structures with ribs at intersections.

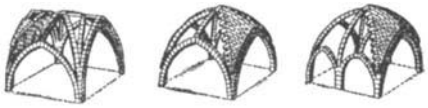

squinch Arch, lintel, or corbel across a square corner that supports an octagonal drum or tambour.

tambour A cylindrical or polygonal drum base for a dome.

trachyte Light-colored, volcanic rock having a rough fractured texture (potassium feldspar + biotite, amphibole, or pyroxene).

transept Transverse portion of a cruciform church.

triforium Arch-top niche containing three subniches.

Turkish tiles Semicylindrical roof tiles made of terracotta.

tympanum Recessed face of a pediment bounded by the upper and lower cornices; a triangular space.

vestibule Narthex.

Index

Note: Page numbers followed by the letters *f* and *t* refer to figures and tables, respectively.

acceleration, in model analysis, 41*t*, 43
ambient vibration tests, 25–26
  on original church model, 54–55, 55*f*
apse(s)
  of basilica-type churches, 8, 9*f*
  niches on, 17, 17*f*
  of single-dome or quincunx churches, 10, 10*f*
  of single-nave churches, 10, 13*f*
  of St. Nikita, Banjani, 26, 30, 30*f*
    model of, mathematical modeling of, 80, 81*f*
arches, of Byzantine churches, 13, 14
  decorative, 16
  of St. Nikita model, 48
area, in model analysis, 44
authenticity
  preservation of, xii, 123
  of selected churches, 22

base isolation, 125–26, 140
basilica-type churches, 7, 7*f*, 8, 9*f*
  combination with quincunx type, 10, 11*f*
bearing capacity
  analysis prior to repair and strengthening, 129
  methodology for definition of, 100–102
  of model structures, 99, 108–9, 109*t*
  of St. Nikita, Banjani, 34
biforia, 17*f*, 18
bilinear hysteretic model, 74, 74*f*
Bitola earthquake (1994), 120
bitumen
  adverse effects of, 21
  use in conservation efforts, 20–21
bonding materials. See grouting
Breginj earthquake (1976), 34
  time history spectra of, 56*f*
  use in seismic simulation response tests
    of original church model, 55, 57*t*, 58*f*–60*f*
    of strengthened church model, 68
brick, use in Byzantine churches, 12
  combined with limestone, 16
  combined with tufa stone, 18
  ornamentation created with, 16, 16*f*
  St. Nikita, Banjani, 30, 32
    scale model of, 46–47
Buckingham's theorem, 39–41
Bulgaria, 5
Burra Charter, 20
Byzantine churches. *See also specific churches*
  architecture of, 6
  authenticity of, 22
  damage to, causes and level of, 19–21
  dynamic characteristics of, 25–26, 26*t*
  fresco paintings in, 6–7, 15, 15*f*
  materials used in, xi, 12
  mathematical model of, formulating, 25
  repair and strengthening of
    detailed methodology for, 126–28
    possible methods for, 37–39, 124–26
  selection for detailed investigation, 22–23
  structural characteristics of, 12–15
  surface characteristics of, 15–18
  surveyed, list of, 141*t*–142*t*
  types of, 7–10, 7*f*, 8*f*
Byzantine Empire, 5

calottes, 14
capacity analysis. *See also* bearing capacity; deformability capacity; shear capacity
  of existing Byzantine churches, 111–21

of masonry structures, 100–102
MASAN computer program used in, 106–7
steps required for, 106
of St. Bogorodica, Matejče, 116–19, 131*t*
of St. Bogorodica Zahumska, Trpejca, 112–14, 131*t*, 133–34
of St. Gjorgji, Kurbinovo, 120–21, 131*t*
of St. Nikita, Banjani, 111–12, 131–32, 131*t*
original model of, 107–8
strengthened model of, 108
of St. Nikola, Psača, 114–16, 131*t*, 136–37
cement
Roman, 13
use in conservation efforts, 20–21
cement mortar, incompatibility with lime mortar, 21
CI Elenica, Strumica, 47
cloisonné surface, 13
columns, of Byzantine churches, 12
St. Nikita, Banjani, 30
scale model, mathematical modeling of, 80, 81*f*
The Communion of the Apostles (fresco), 30, 31*f*
conches, 14. *See also* tetraconch churches; triconch churches
conservation. *See* repair and strengthening
cornices, of St. Nikita, Banjani, 30, 32
corrosion, use of iron reinforcements and, 21
cracks
first occurrence of, monitoring in shaking-table tests, 54
grouting of, 3, 128
cross, inscribed, 10

damage, causes and level of, 19–21
damping characteristics, determining, 25
damping coefficient. *See also* ductility and damping coefficient
in model analysis, 41*t*, 44
of original vs. strengthened model, 66*t*
data acquisition system, in shaking-table tests, 53
dead weight effect, static analysis of, 80–81, 81*f*, 82*f*
deformability capacity
analysis prior to repair and strengthening, 129
of model structures, 100
deformation, in model analysis, 41*t*, 44
demonstration case study, recommendation for, 140
density, scale of, 42
differential equation of motion, 40
dimensional system, 39
dolomite, use in Byzantine churches, 32
dome(s)
of Byzantine churches
behavior during earthquakes, 71
repairs to, 25
strengthening of, 127–28
of original church model, 48, 49, 49*f*
mathematical modeling of, 80, 81*f*
during seismic simulation testing, 59, 61*f*, 62
of St. Nikita, Banjani, 30
strengthening of, 130
of strengthened church model, during seismic simulation testing, 67, 67*f*
The Dormition of the Holy Virgin (fresco), 30, 31*f*
drainage channels, 20
ductility
improving, xi, 2, 124
of St. Nikita, Banjani, 35*t*
model structures, 100, 100*t*
strengthened structure, 132, 132*t*
ductility and damping coefficient (K_p), 101
dynamic analysis
differential equation of motion and, 40
nonlinear, 71–77
of original church model
in linear range, 80–85
in nonlinear range, 85–86
of single-degree-of-freedom system, 71–72, 72*f*, 143, 144*f*
of St. Bogorodica Zahumska, Trpejca, 134
of St. Nikita, Banjani, 131–32, 132*t*, 133*f*–136*f*
of St. Nikola, Psača, 136
of strengthened church model
in linear range, 89–91
in nonlinear range, 91–94
in ultimate range, 94–96, 95*t*, 96*t*
use of IZIIS hysteretic model for, 139
dynamic characteristics
ambient vibration method for determining, 25–26
monitoring in shaking-table tests, 54
dynamic coefficient (K_d), 101, 102
dynamic equations of motion, 72–73

El Centro earthquake (1940), 34
dynamic analysis of St. Nikita based on magnitude of, 34, 35*t*
time history spectra of, 56*f*
use in mathematical modeling of dynamic response, 84–85
use in seismic simulation response tests
of original church model, 55, 57, 57*f*–60*f*, 57*t*, 60, 62
of strengthened church model, 67, 69, 87*f*, 88*f*
elastic response
of original church model, 80–85, 85*t*
of strengthened church model, 89–90, 90*f*, 92*f*–94*f*
elasticity limit, monitoring in shaking-table tests, 54
elasticity modulus, in model analysis, 41*t*, 43
ethics, restoration, 2
Eutychios (fresco painter), 30

facades of Byzantine churches
finishing of, 15–17, 16*f*, 17*f*
St. Nikita, Banjani, 28
scale model of, 49
failure
initial modes of, 2, 38, 125
mechanism of, monitoring in shaking-table tests, 54
Feilden, Sir Bernard, 20
floors, of Byzantine churches, 15
forced vibration tests, 25
on original church model, 55
forces, in model analysis, 41*t*, 44
foundation, strengthening of, 130–31
Fourier amplitude spectra, in shaking-table tests, 53, 55
frequency. *See also* natural vibration frequencies
in model analysis, 41*t*, 43
in shaking-table tests, 53
fresco(es), in Byzantine churches, 6–7, 15, 15*f*
damage to, causes of, 21
St. Nikita, Banjani, 6, 30, 30*f*, 31*f*
fresco mortars
compatibility of grouting with, importance of, 39
composition of, 33, 33*t*
fresco pigments, 33–34
Friuli earthquake (1976). *See* Breginj earthquake

geometrical scale, 42
Getty Conservation Institute (GCI), xii
granite, use in Byzantine churches, 32
gravity forces, in model analysis, 44
grouting
composition of, 64
of cracks, 3, 128
injection of, 39, 128
procedure for, 65
in strengthened church model, 64–65
in voids around belts and ties, 125, 126, 128
and tensile capacity of masonry, increase in, 38

historic buildings. *See also* Byzantine churches
basic conservation principles for, 1
in Macedonia, materials and structural elements of, xi
repair and strengthening of, possible methods for, 37–39, 123–24
structural analysis of, 2
horizontal elements
flexural capacity of, 105
use in retrofitting of Byzantine churches, 3, 125
at base of tambour and dome, 127–28
in perimeter walls, 126
St. Bogorodica Zahumska, Trpejca, 132
St. Nikita, Banjani, 38, 130
St. Nikola, Psača, 135
use in strengthened church model, 62–63, 63*f*–65*f*
importance of, 68
hysteretic models, 73–77
bilinear, 74, 74*f*
trilinear, 74–77, 75f–77*f*. *See also* IZIIS hysteretic model

inscribed cross, 10
Institute of Earthquake Engineering and Engineering Seismology (IZIIS), xii
model of hysteretic behavior. *See* IZIIS hysteretic model
shaking table at, 53
International Seminar on Modern Principles in Conservation and Restoration of Urban and Rural Cultural Heritage in Seismic-Prone Regions, Skopje, 1988, 123
interventions
minimizing, 123
reversible, 124

iron reinforcements, corrosion resulting from, 21
isolating dampers, 125–26
IZIIS. *See* Institute of Earthquake Engineering and Engineering Seismology
IZIIS hysteretic model, 74–77, 75*f*
  applicability in range of extreme nonlinearity, 132
  correlation with experimental results, 96–98, 98*t*
  defining parameters for, 129, 130*f*
  use in capacity analysis, 112, 114, 116, 119
  use in dynamic analysis, 139
    in linear range (system with two masses), 83–84, 86–87
    in nonlinear range, 85, 92
    of strengthened St. Bogorodica Zahumska structure, 134
    of strengthened St. Nikita structure, 131–32
    of strengthened St. Nikola structure, 136
    in ultimate range, 94–95

K_d (dynamic coefficient), 101–2
K_p (ductility and damping coefficient), 101
K_s (seismic intensity coefficient), 101

lime mortar
  incompatibility with cement mortar, 21
  selection of, for repair and strengthening, 128
  and shear capacity of masonry, increase in, 39
  use in Byzantine churches, 32
  use in scale model, 48
limestone
  combined with brick, 16
  use in Byzantine churches, 12, 14
    St. Nikita, Banjani, 30, 32
  use in scale model, 46

Macedonia
  archaeological sites in, 5
  historic buildings in, materials and structural elements of, xi
  history of, 5
  seismic characteristics of area of, 23–25, 24*f*
MASAN computer program, 106–7
  analysis of existing Byzantine churches, 111, 112, 133
  analysis of original church model, 107–8
  analysis of strengthened church model, 108
masonry
  bonding of, improving, 3, 128
  chemical analysis of materials, 32–34
  confined
    flexural capacity of, 105
    shear capacity of, 106, 106*f*
  plain
    flexural capacity of, 104
    idealized stress distribution in, 104*f*
    shear capacity of, 105–6
  shear capacity of, 105–6
    increasing, 39
  tensile strength of, increasing, 2, 38, 125
masonry structures
  capacity analysis of, 100–102
    steps required for, 106
  seismic behavior of, analytical modeling of, 71–77
  static testing of, 50–52, 51*f*, 52*f*
mass
  of existing structure, determining, 25
  of model, 41*t*, 43
materials. *See also* brick; stone
  elastic limits of, during strong earthquakes, 71
  inappropriate for conservation and repair, 21
  used in Byzantine churches, xi, 12
  used in scale model, 46–49
  used in St. Nikita, Banjani, 30
mathematical model
  in analysis of structural walls, 103–6
  formulating, 25
  in modeling of elastic response
    of original church model, 80–85
    of strengthened church model, 89–91
  in modeling of nonlinear response
    of original church model, 85–86
    of strengthened church model, 91–94
Michael (fresco painter), 30
Milutin (Serbian king), 26, 30
mode shapes
  of scale model
    comparison of measured and computed values, 87*f*
    computation of, 81–82, 83*f*, 84*f*
  of St. Nikita, Banjani, 26*f*
model (St. Nikita, Banjani), 49*f*. *See also* strengthened model
  ambient vibration measurements of, 54–55, 55*f*

analytical studies of, 80–87
linear (elastic) response, 80–85, 85*t*
nonlinear response, 85–86, 86*t*
arches of, 48
bearing capacity of, 99, 108–9, 109*t*
capacity analysis of, 107–8
comparison with prototype, 45*f*, 46*t*
construction of, 45–46, 48–50, 48f–49*f*
correlation between computed and experimental results for, 86–87, 87*f*, 87*t*, 88*t*
damping coefficient of, comparison with strengthened model, 66*t*
deformability capacity of, 100
design of, 39–45
dimensioned plan of, 47*f*
dome of, 48, 49, 49*f*
ductility of, 100, 100*t*
elevations of, 47*f*
finite-element modeling of, 80, 81*f*
forced vibration tests on, 55
materials used in, 46–49
natural vibration frequencies of, comparison with strengthened model, 66*t*
random excitation tests on, 55
repair and strengthening of, 62–65, 63*f*–65*f*
seismic simulation response tests on, 55–56, 56*f*–61*f*, 56*t*, 57*t*
shaking-table tests of, 53–70
comparative analysis with tests of strengthened model, 68–70, 68*f*
damage caused by, 59–62, 61*f*
objectives of, 54–62
relationship between shear forces and resulting deformations, 79, 79*f*
tambour of, 49, 49*f*
timber ties in, 48, 49, 49*f*
vaults of, 48, 48*f*
wall element tests on, 50–52, 51*f*, 52*f*
walls of, 48
model analysis, 39–41
physical quantities in, 41*t*
scaling factors in, 41–45
model instrumentation
location of, 54*f*
use in shaking-table tests, 53
moment of force, 41*t*, 44
moment of inertia, 41*t*, 44
moment resistance of walls, 2, 38, 125
mortar(s)
fresco, composition of, 33, 33*t*
multicolored, 17
portland cement, adverse effects of, 21
used in Byzantine churches, 12
St. Nikita, Banjani, 32–33, 33*t*
motion
differential equation of, 40
dynamic equations of, 72–73

natural vibration frequencies
determining, 25
of original model
computation of, 81, 83*f*
measured vs. computed values, 87*t*
vs. strengthened model, 66*t*
of strengthened model
measured vs. computed values, 97, 97*t*
vs. original model, 66*t*
niches, in Byzantine church facades, 17
St. Nikita, Banjani, 28–29
nonlinear dynamic analysis, 71–77
of original church model, 85–86
of strengthened church model, 91–94

Ohrid. *See also specific churches*
seismic characteristics of area of, 23, 24*f*
original model (St. Nikita, Banjani). *See* model
Ottoman Empire, 5

pendetives
of Byzantine churches, surface characteristics of, 17*f*, 18
of scale model, mathematical modeling of, 80, 81*f*
Petrovac earthquake (1979), 34
dynamic analysis of St. Nikita based on magnitude of, 34, 35*t*
time history spectra of, 56*f*
use in mathematical modeling of dynamic response, 84–85
use in seismic simulation response tests
of original church model, 55, 57, 57*f*–60*f*, 57*t*, 60–61
of strengthened church model, 67, 88*f*, 89*f*
plasters, in Byzantine churches
composition of, 32
scale model of, 48
Poisson coefficient, in model analysis, 41*t*, 44
polychromatic effect, of Byzantine church facades, 13, 14*f*, 16–17, 16*f*, 17*f*

in St. Nikita, Banjani, 28, 29*f*, 30
portland cement mortar, adverse effects of, 21
prototype structure tests, 25

quincunx churches, 8, 8*f*, 10, 11*f*
combination with basilica type, 10, 11*f*

Radoviš, seismic characteristics of area of, 24*f*, 25
random excitation tests, on original church model, 55
reinforced-concrete elements, incorporation into original church structure, 21
repair and strengthening
of church model, 62–65, 63*f*–65*f*. *See also* strengthened model
detailed methodology for, 126–28
possible methods for, 37–39, 124–26
previous efforts, 20–21
problems with, 21
at St. Nikita, Banjani, 20, 31–32
recommendations for, 123–24
seismic-related criteria for, 124
of St. Nikita, Banjani, proposed methods for, 38–39, 130–32
Republic Institute for the Protection of Cultural Monuments (RZZSK), xii
retrofitting. *See* repair and strengthening; seismic retrofitting
Roman cement, 13
Roman Empire, disintegration of, 5
Roman walls, 12–13
roofs, of Byzantine churches, 12
St. Nikita, Banjani, 30, 32
RZZSK. *See* Republic Institute for the Protection of Cultural Monuments

St. Andreja, Matka, 141*t*
previous conservation efforts at, 20
south and east facades, 7*f*
St. Arhangel Mihail, Lesnovo, 141*t*
degree of authenticity of, 22
St. Arhangel Mihail, Radožda, 141*t*
damage to, 19
St. Bogorodica, Drenovo, 141*t*
naves of, 8
St. Bogorodica, Matejče, 141*t*
capacity analysis of, 116–19, 131*t*
degree of authenticity of, 22
dynamic characteristics of, 26*t*
exterior of, 117*f*
north and west facades of, 8*f*
plan and elevation of, 117*f*
previous conservation efforts at, 21
quincunx plan and elevation of, 11*f*
seismic hazard parameters for, 24*t*
selection for detailed investigation, 22, 23
tambours of, 10
St. Bogorodica, Osogovo Monastery, Kriva Palenka, 141*t*
previous conservation efforts at, 21
tambour of, 18
St. Bogorodica, Treskavec Monastery, Dabnica, 141*t*
damage to, 19, 20
frescoes in, 7
St. Bogorodica Eleusa, Veljusa, 141*t*
apse of, 17
floor of, 15
frescoes in, 6
previous conservation efforts at, 20
south and east facades of, 7*f*
St. Bogorodica Perivlepta, Ohrid, 141*t*
degree of authenticity of, 22
frescoes in, 15*f*
St. Bogorodica Zahumska, Trpejca, 141*t*
capacity analysis of, 112–14, 131*t*, 133–34
damage to, 19, 20
degree of authenticity of, 22, 23
dynamic characteristics of, 26*t*
exterior of, 113*f*
plan and elevation of, 113*f*
polychromy in, 17, 17*f*
repairs needed for, 132
seismic hazard parameters for, 24*t*
selection for detailed investigation, 22
strengthening methods for, 132–33
west facade of, 17*f*
St. Catherine of Sinai, Crete, 6
St. Dimitrija, Markov Monastery, Sušica, 141*t*
apse of, 17, 17*f*
degree of authenticity of, 22
east facade and apse of, 10*f*
frescoes in, 6
previous conservation efforts at, 20
tambour of, 18
St. Dimitrija, Ohrid, 141*t*
damage to, 19
St. Gjorgji, Gorni Kozjak, 142*t*

pendentive and interior of tambour of, 17*f*
St. Gjorgji, Kurbinovo, 142*t*
capacity analysis of, 120–21, 131*t*
frescoes in, 6, 15*f*
west facade entrance of, 120*f*
St. Gjorgji, Rečica, 142*t*
degree of authenticity of, 22
St. Gjorgji, Staro Nagoričane, 10, 142*t*
basilica plan and elevation of, 9*f*
previous conservation efforts at, 20
south facade of, 11*f*
St. Jovan Kaneo, Ohrid, 12*f*, 142*t*
previous conservation efforts at, 20
St. Kliment Mal, Ohrid, 142*t*
damage to, 19
St. Leontije, Vodoča, 142*t*
degree of authenticity of, 22
frescoes in, 6
north facade of, 14*f*
polychromy in walls of, 13, 14*f*
previous conservation efforts at, 21
tambour and dome of, 14*f*
St. Nikita, Banjani, 26–35, 27*f*, 142*t*
apse of, 26, 30, 30*f*
architecture of, 27–30
authenticity of, 23
bearing capacity of, evaluation of, 34
calculated mode shapes for, 26*f*
capacity analysis of, 111–12, 131–32, 131*t*
construction date of, 26–27
cornices of, 30, 32
deterioration of
principal areas of concern, 37–38
reasons for, 31
ductility for different earthquakes, 35*t*
dynamic characteristics of, 26*t*
earthquake damage to, 30, 31
elevation views of, 27, 29*f*
frescoes in, 6, 30, 30*f*, 31*f*
pigments used in, 33–34
materials used in construction of, 30
chemical analysis of, 32–34, 33*t*
model of. *See* model; strengthened model
motion instrumentation in, proposal for, 140
niches in, 28–29
north facade window of, 29*f*
plan of, 28*f*
polychromy in, 28, 29*f*, 30
present condition of, 32
previous conservation efforts at, 20, 31–32
repair and strengthening of, proposed methods for, 38–39, 130–32
roof of, 30, 32
seismic hazard parameters for, 24*t*
seismic stability of, analysis of, 34–35
selection for detailed investigation, 22, 26
south and east facades of, 27*f*
strengthened structure, dynamic response analysis of, 131–32, 132*t*, 133*f*–136*f*
structural system of, 30–31
tambour of, 27, 28*f*, 30, 30*f*, 32
timber belts and ties in, 31
tests to determine presence of, 26
walls of, 26, 30
west and south facades of, 29*f*
St. Nikola, Ljuboten, 142*t*
degree of authenticity of, 22
St. Nikola, Manastir, 142*t*
damage to, 19
St. Nikola, Psača, 142*t*
capacity analysis of, 114–16, 131*t*, 136–37
degree of authenticity of, 23
dynamic characteristics of, 26*t*
exterior of, 115*f*
plan and elevation of, 115*f*
previous conservation efforts at, 20
repair measures necessary in, 134–35
selection for detailed investigation, 22
strengthening methods for, 135–36
St. Nikola, Radišani, 142*t*
degree of authenticity of, 22
previous conservation efforts at, 21
St. Nikola, Šiševo
seismic hazard parameters for, 24*t*
single-nave plan and elevation of, 12*f*
south and west facades of, 8*f*
tambour of, 18
St. Nikola, Varos, 142*t*
exterior fresco in, 17*f*
polychromy in, 17, 17*f*
St. Pantelejmon, Gorno Nerezi, 142*t*
frescoes in, 6
previous conservation efforts at, 20, 21
SS. Elena and Konstantin, Ohrid, 141*t*

frescoes in, 15*f*
St. Sofia, Ohrid, 142*t*
biforium of, 17*f*
east facade and apse of, 9*f*
floor of, 15
frescoes in, 6
interior timber ties of, 14*f*
naves of, 8
north facade of, 7*f*
previous conservation efforts at, 20
west facade of, 7*f*
St. Spas, Kučevište, 142*t*
apse of, 17
St. Stefan, Konče, 142*t*
east and south facades of, 14f
previous conservation efforts at, 20, 21
St. Vrači Mali, Ohrid, 142*t*
apse of, 13*f*
single-nave plan and elevation of, 13*f*
salt crystallization damage, 21
Samoil (Macedonian king), 5
sandstone, use in Byzantine churches, 12
St. Nikita, Banjani, 30
SAP90. *See* Structural Analysis Program
scaling factors, selection of, 41–45, 42*t*
seismic base isolation, 125–26, 140
seismic hazard parameters, 23–25, 24*f*, 24*t*
seismic intensity coefficient (K_s), 101
seismic retrofitting. *See also* repair and strengthening
approaches to, 2–3
design criteria, xi
based on earthquake characteristics, 1–2
objectives of, 2
seismic simulation response tests. *See* shaking-table tests
seismometer, Ranger, 55
Serbia, 5
shaking-table tests
of original church model, 53–70
comparative analysis with strengthened church model, 68–70, 68*f*
damage caused by, 59–62, 61*f*
objectives of, 54–62
relationship between shear forces and resulting deformations, 79, 79*f*
of strengthened church model, 65–69, 66*t*
comparative analysis with original church model, 68–70, 68*f*
damage caused by, 67*f*
relationship between shear forces and resulting deformations, 79, 79*f*
shear capacity, of masonry
confined, 106, 106*f*
increasing, 39
plain, 105–6
SIEN computer program, 77
single-degree-of-freedom system, dynamic analysis of, 71–72, 72*f*, 143, 144*f*
single-dome churches, 8, 10
behavior during earthquakes, 71
single-nave churches, 8, 8*f*, 10, 12*f*, 13*f*
Skopje, seismic characteristics of area of, 23, 24*f*
Skopska Crna Gora, 26
Slavic tribes, 6
soil conditions, considering in seismic retrofitting, xi
steel, use in St. Nikita model, 48
steel ties
incorporation of, 127
in St. Bogorodica Zahumska, Trpejca, 132–33
in St. Nikita, Banjani, 38, 130
in St. Nikola, Psača, 135
replacing timber ties with, 3, 38, 126
use in strengthened church model, 62–63, 63*f*–65*f*
Stobi, basilica excavated in, 6
stone
use in Byzantine churches, 12, 14
bricks combined with, 16, 18
multicolored, 17, 17*f*
St. Nikita, Banjani, 32
use in scale model, 46
strengthened model (St. Nikita, Banjani)
analytical studies of, 87–96
linear (elastic) response, 89–91, 90f, 92*f*–94*f*
nonlinear response, 91–94, 95*t*
ultimate response, 94–96, 95*t*, 96*t*
bearing capacity of, 99, 108–9, 109*t*
capacity analysis of, 108
construction of, 62–65, 63*f*–65*f*
correlation between analytical and experimental data for, 91, 92–94, 96–99, 97*t*, 98*t*
damping coefficient of, comparison with original model, 66*t*
deformability capacity of, 100
ductility of, 100, 100*t*
natural vibration frequencies of, comparison with original model, 66*t*

seismic simulation tests on, 65–69, 66*t*
comparative analysis with tests of original model, 68–70, 68*f*
damage after, 67*f*
relationship between shear forces and resulting deformations, 79, 79*f*
strengthening. *See* repair and strengthening
stress, in model analysis, 41*t*, 42
structural analysis, 2, 128. *See also* capacity analysis
Structural Analysis Program (SAP90)
correlation with experimental results, 96–97, 98*t*
finite-element modeling using, 80, 81*f*
in modeling of elastic response
of original church model, 80–85
of strengthened church model, 89–91
structural continuity, improvement of, 125
structural integrity
deterioration under earthquake conditions, 2, 38, 125
loss during seismic simulation testing of model, 62
Strumica, seismic characteristics of area of, 24*f*, 25
Study of the Seismic Strengthening, Conservation, and Restoration of Churches Dating from the Byzantine Period in Macedonia, xii

tambour(s)
behavior during earthquakes, 71
of conched churches, 10
repairs to, 25
of scale model, 49, 49*f*
damage after seismic simulation testing, 61, 62
mathematical modeling of, 80, 81*f*
of single-dome or quincunx churches, 10
of St. Nikita, Banjani, 27, 28*f*, 30, 30*f*, 32
strengthening of, 130
strengthening of, 127–28, 130
vertical belts for, 39
surface characteristics of, 17*f*, 18
vulnerability of, 71
tensile strength, of masonry, 2
increasing, 2, 38, 125
tetraconch churches, 7*f*, 8–10
timber belts, in Byzantine churches, 15, 38
flexural capacity of, 105
replacing with steel ties, 3, 38, 126
retaining and reusing in conservation efforts, 124
in St. Nikita, Banjani, 31
tests to determine presence of, 26
timber ties, in Byzantine churches
determining existence and location of, 126
replacing with steel ties, 3, 125
retaining and reusing in conservation efforts, 124
in St. Nikita, Banjani, 31
scale model of, 48, 49, 49*f*
visible, 14, 14*f*
time
in model analysis, 41*t*, 43
in shaking-table tests, 53
travertine, use in Byzantine churches, 32
triconch churches, 7, 7*f*, 8–10
triforia, 18
trilinear hysteretic model. *See* IZIIS hysteretic model
tufa, use in Byzantine churches, 12
combined with bricks, 18
St. Nikita, Banjani, 32
scale model of, 46

vaults
of Byzantine churches, 13–14
St. Nikita, Banjani, 30
of church model, 48, 48*f*
damage during seismic simulation testing, 62
mathematical modeling of, 80, 81*f*
velocity, in model analysis, 41*t*, 43
Venice Charter, 20
vertical elements
flexural capacity of, 105
use in retrofitting of Byzantine churches, 3, 125
adjacent to tambour openings, 128
in perimeter walls, 127
St. Bogorodica Zahumska, Trpejca, 133
St. Nikita, Banjani, 38–39, 130
St. Nikola, Psača, 135
use in strengthened church model, 63–64, 65*f*
vibration mode shapes, determining, 25
vulnerability level, anticipated, repair and strengthening methods based on, 124

walls
Byzantine, 3, 12, 13
strengthening methods for, 3
of church model, 48
after seismic simulation tests, 62
mathematical modeling of, 80, 81*f*
static laboratory tests on, 50–52, 51*f*, 52*f*
failure mechanisms of, analysis of, 125
flexural capacity of, 104–5
increasing, 105, 105*f*
mathematical modeling of, 103–6
moment resistance of, 2, 38, 125
Roman, 12–13
separation of, as initial mode of failure, 2, 38, 125
shear capacity of, 105–6
of St. Nikita, Banjani, 26, 30
stiffness of, defining, 103–4
windows, of Byzantine churches, 17*f*, 18
St. Nikita, Banjani, 29*f*
wood. *See also* timber belts; timber ties
use in church model, 48

About the Authors

Predrag Gavrilović, Ph.D., is a professor at the Institute of Earthquake Engineering and Engineering Seismology, University "SS. Cyril and Methodius," Skopje, Republic of Macedonia. His forty years of research and teaching have focused on the earthquake resistance of buildings and the repair and strengthening of damaged structures, including structural conservation of monuments and historic buildings and towns, resulting in the publication of more than 150 technical papers and articles in international journals and scientific publications. He has been a consultant to agencies of the United Nations, as well as other international foundations and organizations, and has worked as project manager and participant in many international projects in the field of post-earthquake reconstruction as well as in the repair and conservation of monuments and historic complexes.

William S. Ginell, Ph.D., is a materials scientist with extensive experience in industry. In 1943, after graduating from the Polytechnic Institute of Brooklyn with a bachelor's degree in chemistry, he became part of the secret research team at Columbia University working to develop the atomic bomb. After the war, he received his Ph.D. in physical chemistry from the University of Wisconsin and spent nine years at the Brookhaven National Laboratory on Long Island, New York, followed by twenty-six years working for aerospace firms in California. In 1984 he joined the Getty Conservation Institute and helped to design the laboratories at the GCI's Marina del Rey facility, becoming senior conservation research scientist at the GCI in Los Angeles and project director of the Getty Seismic Adobe Project. Since his retirement from the Getty in 2003, he has worked as a consultant in Los Angeles.

Veronika Zelenkovska Sendova, Ph.D., graduated from the Civil Engineering Faculty, Skopje, Republic of Macedonia, and earned her master's degree and doctorate from the Institute of Earthquake Engineering and Engineering Seismology, University "SS. Cyril and Methodius," Skopje, where she works in the field of earthquake engineering, specializing in the analysis, repair, strengthening, and seismic protection of historical structures. As an active member of national and international professional organizations, she has emphasized the role of the structural engineer in the protection of cultural heritage in both legislation and everyday practice.

Lazar Šumanov, Ph.D., is a retired engineer, architectural advisor, and conservator. He received his doctorate in architectural conservation from the University of York and has worked for more than thirty-five years in the field of protection and conservation of cultural heritage in the Republic of Macedonia. Currently he is president of the Macedonia National Committee of the International Council on Monuments and Sites (ICOMOS). He has been involved in various activities related to the theoretical and physical treatment of architectural heritage with a special interest in the documentation and conservation of Byzantine churches, Ottoman architecture, and vernacular architecture of stone, wood, and earth. Over the past twenty years he has focused on the relationship of architectural heritage to natural and human-caused disasters, investigating, designing, conducting, publishing, and lecturing on a range of projects.